Geoscience Canada

Journal of the Geological Association of Canada
Journal de l'Association Géologique du Canada

Iron Formations - Unique Witnesses to Secular Planetary Change

Okanangan Gold - Tiny Tell-Tale Nuggets Talk Tectonics

Problematic Past Penetrations - The Challenges of Legacy Oil Wells in Ontario

Canadian Geoscience Diplomacy -Retrospective Views and Future Prognosis

Brandon 2024 GAC-MAC-PEG - At the Heart of the Continent

2023 Volume 50

Publisher/Éditeur
Geological Association of Canada
Alexander Murray Bld., Rm ER4063
Memorial University of Newfoundland
St. John's, NL, Canada, A1B 3X5
Tel: (709) 864-7660
Fax: (709) 864-2532
gac@mun.ca
www.gac.ca

Print Edition: ISSN 0315-0941
Online Edition: ISSN 1911-4850

Volume 50

A journal published quarterly by the Geological Association of Canada, incorporating the Proceedings.
Une revue trimestrielle publiée par l'Association géologique du Canada et qui en diffuse les actes.

Those wishing to submit material for publication in Geoscience Canada should refer to the Instructions to Authors on the journal's website, www.geosciencecanada.ca

AUTHORS PLEASE NOTE:
Please use the web address http://journals.hil.unb.ca/index.php/GC/index for submissions; please do not submit articles directly to the editor.

The Mission of the Geological Association of Canada is to facilitate the scientific wellbeing and professional development of its members, the learned discussion of geoscience in Canada, and the advancement, dissemination and wise use of geosciences in public, professional and academic life. Articles in Geoscience Canada are freely available one year after their publication date, unless authors have arranged for immediate open access. Opinions expressed and interpretations presented are those of the authors and do not necessarily reflect those of the editors, publishers and other contributors. Your comments are welcome.

Cover Image: The 2.5 billion-year-old banded iron formations in Karijini National Park, Western Australia. Photo courtesy of Stefan Lalonde.

GAC MEDALLIST SERIES

Logan Medallist 8. Trace Elements in Iron Formation as a Window into Biogeochemical Evolution Accompanying the Oxygenation of Earth's Atmosphere

Kurt O. Konhauser[1], Andreas Kappler[2], Stefan V. Lalonde[3] and Leslie J. Robbins[4]

[1]Department of Earth and Atmospheric Sciences, University of Alberta Edmonton, Alberta, T6G 2E3, Canada
Email: kurtk@ualberta.ca

[2]Geomicrobiology, Department of Geosciences, University of Tübingen Tübingen, 72076, Germany

[3]European Institute for Marine Studies, CNRS-UMR6538 Laboratoire Domaines Océaniques, Technopôle Brest-Iroise Plouzané, 29280, France

[4]Department of Geology, University of Regina Regina, Saskatchewan, S4S 0A2, Canada

SUMMARY
Iron formations exemplify a type of sedimentary rock found in numerous Archean and Proterozoic supracrustal successions. They serve as a valuable chemical record of Precambrian seawater chemistry and post-depositional iron cycling. These formations accumulated on the seafloor for over two billion years during the early history of our planet, offering a unique opportunity to study environmental changes that occurred during Earth's evolution. Among these changes, one of the most significant events was the shift from an anoxic planet to one where oxygen (O_2) became consistently present in both the marine water column and atmosphere. This progression towards global oxygenation was closely linked to the emergence of aerobic microbial metabolisms, which profoundly impacted continental weathering processes, nutrient supply to the oceans, and ultimately, the diversification of the biosphere and complex life forms. In this review, we synthesize two decades of research into the temporal fluctuations of trace element concentrations in iron formations. Our aim is to shed light on the complex mechanisms that contributed to the oxygenation of Earth's surface environments.

RÉSUMÉ
Les formations de fer sont un exemple de roche sédimentaire que l'on trouve dans de nombreuses séquences supracrustales de l'Archéen et du Protérozoïque. Elles représentent un enregistrement chimique précieux de la composition de l'eau de mer du Précambrien et du cycle du fer post-dépôt. Ces formations se sont accumulées sur le fond marin pendant plus de deux milliards d'années au début de l'histoire de notre planète, offrant une occasion unique d'étudier les changements environnementaux survenus au cours de l'évolution de la Terre. Parmi ces changements, l'un des événements les plus significatifs a été la transition d'une planète anoxique à une planète où l'oxygène (O_2) est devenu constamment présent à la fois dans la colonne d'eau marine et dans l'atmosphère. Cette progression vers l'oxygénation globale était étroitement liée à l'émergence de métabolismes microbiens aérobiques, qui ont profondément influencé les processus d'altération continentale, l'apport de nutriments aux océans et, finalement, la diversification de la biosphère et des formes de vie complexes. Dans cette revue, nous synthétisons deux décennies de recherche sur les fluctuations temporelles des concentrations en éléments traces dans les formations de fer. Notre objectif est de faire la lumière sur les mécanismes complexes qui ont contribué à l'oxygénation des environnements de la surface de la Terre.

Traduit par la Traductrice

INTRODUCTION
The study of ancient sediments, such as iron formations (IF), has generated important insights into the complex interplay

Geoscience Canada, v. 50, https://doi.org/10.12789/geocanj.2023.50.201 pages 239–258

between life and Earth's surface environments throughout geologic history (e.g. Konhauser et al. 2017). Uniquely, most IF are chemical sediments, characterized by high iron (15–40 wt.% Fe) and silica (40–60 wt.% SiO_2) content that were deposited from seawater during the Precambrian. Notably, the Nuvvuagittuq Supracrustal Belt in northern Quebec and the Isua Supracrustal Belt in West Greenland, which date back over 3.75 billion years, contain perhaps the earliest IF and associated sedimentary rocks (Mloszewska et al. 2012; Czaja et al. 2013). The period between 2.7 and 1.9 Ga witnessed the highest abundance of IF. Indeed, Isley and Abbott (1999) estimated that during those 800 million years, perhaps as much as 60% of the global volume of preserved IF was deposited. This timeframe coincides with a significant transition in Earth's oceans and atmosphere towards a partially oxygenated state (Lyons et al. 2014). Iron formations then essentially disappear from the rock record for nearly 1.2 billion years. This gap has been explained by a shift to fully oxic or sulphidic deep-ocean conditions. The earlier suggestion of oxic deep-ocean conditions after ca. 1.88 Ga (Holland 1984) was challenged by the proposal that deep-ocean conditions were predominantly euxinic (anoxic and sulphidic) until full ocean ventilation during the late Neoproterozoic or earliest Phanerozoic (e.g. Canfield 1998). Iron formations reappear again briefly in the Neoproterozoic when oceans returned to a ferruginous state during the ice-covered Sturtian glaciation (Hoffman et al. 1998), with rare instances documented in the early Phanerozoic (e.g. Li et al. 2018).

Classically, IF have been categorized into three main types: Algoma-type, Superior-type and Rapitan-type, based primarily on their depositional environment (Gross 1980). Algoma-type IF are typically found interlayered with, or genetically linked to, volcanic rocks. These volcanic rocks range from ultramafic–mafic to felsic compositions and are commonly accompanied by volcaniclastic greywacke and shale in greenstone belts. In many cases, Algoma-type IF are spatially associated with volcanogenic massive sulphide (VMS) deposits (Bekker et al. 2010). The prevailing belief is that Algoma-type IF precipitated near volcanic arcs and spreading centres through exhalative hydrothermal processes associated with submarine volcanism (Gross 1980). In contrast, Superior-type IF developed in sediment-dominated settings, specifically on the passive margins of continental shelves. Unlike the Algoma-type IF, they lack direct stratigraphic connections with volcanic rocks. Superior-type IF are believed to have been deposited on the outer shelf, but they are often interbedded with, or transition into, carbonate rocks and black shale suggesting their deposition moved landwards with changing sea level (Trendall 2002). Superior-type IF can be laterally extensive (Fig. 1A), with estimates suggesting original aerial extents may have exceeded 100,000 km^2 (Bekker et al. 2010). In terms of mass, the largest Superior-type IF contain over 10^{14} tonnes (10^{17} kg) of iron (Isley 1995), and today serve as a significant source of iron for global iron and steel production (Hagemann et al. 2016). Rapitan-type IF are associated with Neoproterozoic Snowball Earth conditions and are thought to be deposited as a by-product of global-scale glacial activity (Hoffman et al. 1998). Named after the ca. 715 Ma

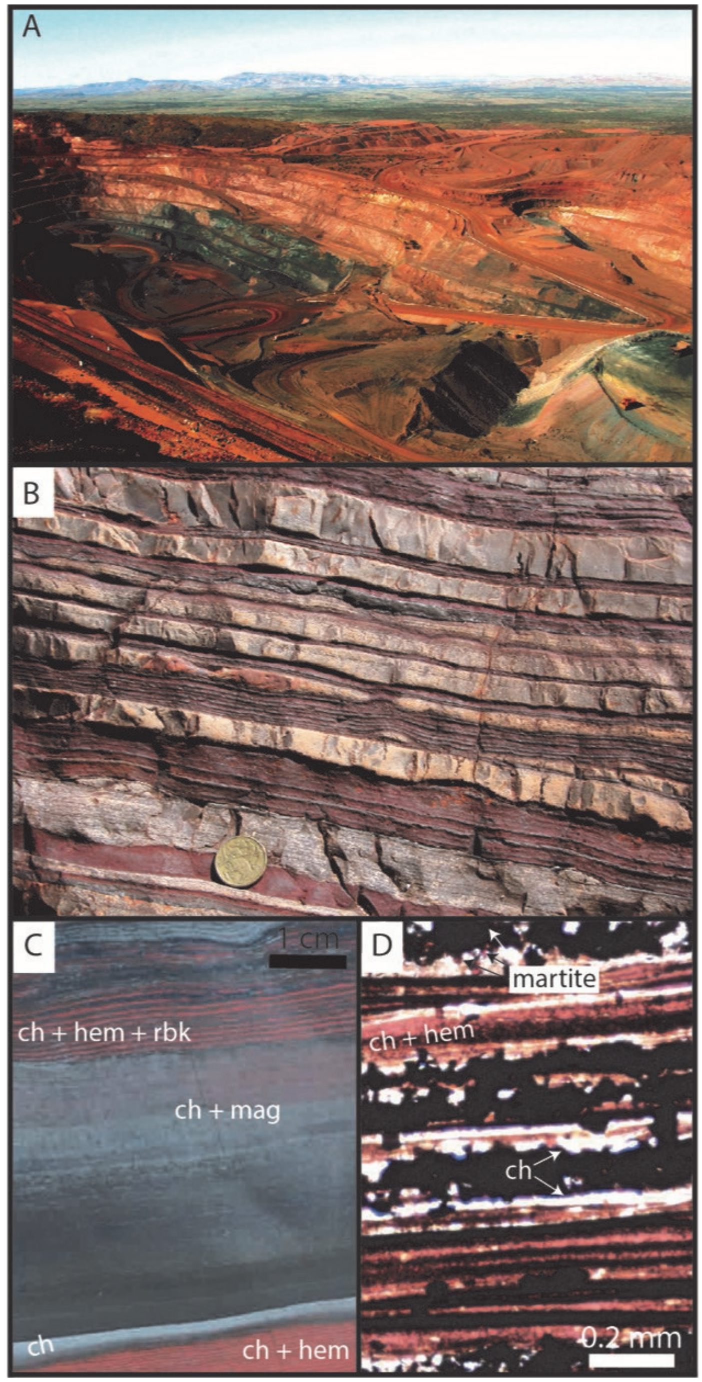

Figure 1. Representative images of Paleoproterozoic iron formations (IF). (A) Aerial overview of the 2.48 Ga Dales Gorge Member along the southern ridge at Tom Price, Western Australia. Photo credit: Mark Barley. (B) Section of banding in the 2.45 Ga Joffre Member, Western Australia. (C) This core from the Joffre Member displays pale grey micro- and mesobands of alternating chert and magnetite, dark grey magnetite mesobands and reddish and bluish (1 mm thin) microbands of chert–hematite–riebeckite. (D) Coarse- and fine-grained magnetite microbands with chert and very fine hematite. The latter likely is a product of secondary magnetite oxidation. Note the single grains of martite upper left. ch = chert, hem = hematite, mag = magnetite, rbk = riebeckite.

Rapitan Iron Formation in northern Canada, a major feature of these IF is their interbedding with glacial diamictite (e.g. Smith 2018). In a model developed by Klein and Beukes

(1993), the authors proposed that as a result of global ice cover, dissolved Fe(II) built up in concentration within the water column, and then during glacial melting, seawater became exposed to O_2 leading to Fe(II) oxidation. Lechte and Wallace (2016) also proposed that some of those IF were deposited below the ice shelf through an ice pump mechanism where cold oxygenated glacial fluids mixed with ferruginous seawater.

For the purposes of discussing IF in the context of Earth's oxygenation, we focus below only on Superior-type IFs.

One of their notable characteristics is alternating iron-rich and silica-rich layers (Fig. 1B) which give the sediments the name banded iron formation (BIF). The layers range from macrobands (metre-thick) to the mesobands (centimetre-thick) by which they are typically defined to microbands (millimetre and sub-millimetre layers; Fig. 1C-D). The latter have been linked to episodic hydrothermal input and hypothesized to represent an annual depositional process (e.g. Trendall and Blockley 1970; Morris 1993) driven by the metabolic activity of microbial plankton (Posth et al. 2008; Schad et al. 2019a). There is, however, another Superior-type iron formation called granular iron formation (GIF). What differentiates GIF from BIF is that the former was deposited in a coastal marine environment subject to riverine input of clastic sediment (i.e. mud, silt and sand). Many of the granules appear to have been derived by sedimentary re-working of iron-rich clay, mudstone, arenite, and even stromatolites (e.g. Simonson and Goode 1989), while others are composed of concentric cortices of hematite that were likely precipitated where Fe(II)-rich waters met more oxygenated shallow seawater (e.g. Dorland 1999). By contrast, BIF typically lack evidence of wave action. For simplicity, we will from herein simply use the abbreviation IF.

The iron-rich layers of IF consist of minerals such as hematite (Fe_2O_3), magnetite (Fe_3O_4), iron-bearing carbonate minerals like siderite ($FeCO_3$) and dolomite–ankerite ($(Ca,Mg)CO_3$ or $Ca(Fe,Mg,Mn)(CO_3)_2$), as well as various Fe(II)–/Fe(III)-silicates. In contrast, the silica-rich layers are mainly comprised of microcrystalline silica (Klein 2005). It is widely recognized that none of the minerals observed in IF are of primary origin, indicating that the minerals initially deposited on the seafloor did not endure. Instead, the mineral assemblages observed in IF today are the result of multiple post-depositional alteration events that occurred during diagenesis (low-temperature transformations during burial in sedimentary basins) and metamorphism (high-temperature changes induced by deep burial as well as tectonic and magmatic events). Additionally, research has shown that the mineral compositions preserved in IF differ along a gradient from deeper water settings near hydrothermal sources of Fe(II) to more distal, shallower environments. For instance, in the Mesoarchean Witwatersrand IF in South Africa, this variation manifests as a transition from hematite-dominated facies in the most distal settings to magnetite and siderite proximal to the paleoshore. This transition reflects an increasing input of organic matter that facilitated the diagenetic and metamorphic reduction of Fe(III) (Smith et al. 2013).

The iron oxides found in IF are believed to have originated from an initial ferric oxyhydroxide phase, such as ferrihydrite ($Fe(OH)_3$). This phase was biologically precipitated from seawater in the well lit upper layers of the ocean. Precipitation occurred through the oxidation of dissolved ferrous iron (Fe^{2+}), with concentrations estimated to range from 0.03 to 0.5 millimolar (mM) (Holland 1973; Morris 1993), although concentrations exceeding 1.0 mM have also been proposed (Derry 2015; Jiang and Tosca 2019). Recent research suggests that in the presence of dissolved silica, which could have reached concentrations as high as 2 mM during the Archean eon (Siever 1992; Maliva et al. 2005), the initial precipitate in the water column could have been a gel-like substance composed of ferric oxyhydroxide and silica (Konhauser et al. 2007a; Fischer and Knoll 2009; Percak-Dennett et al. 2011).

Conversely, the mineral greenalite ($Fe_3Si_2O_5(OH)_4$) has been identified in several IF and interpreted as a relict primary mineral phase formed in the ancient water column (Rasmussen et al. 2017, 2021a; Johnston et al. 2018). Initially, greenalite was proposed by Konhauser et al. (2007b) as a primary precipitate in the ancient oceans, but crucially having formed below the photic zone in deep (> 100 m) waters and thus in the absence of an oxidant such as light or O_2. Such an interpretation would be consistent with greenalite nanoparticles forming during hydrothermal venting in environments that were distal to the deposition of Superior-type IF (e.g. Tosca and Tutolo 2023). By contrast, in the photic zone, ferrihydrite would have formed. The controversy over whether ferrihydrite versus greenalite was the primary precipitate then comes down to whether one thinks that there was a photosynthetic component to the marine biosphere at that time. From our perspective, in the run up to the Great Oxidation Event (GOE), the shallow marine environments were already colonized, with a diverse marine biota including cyanobacteria and underlying anoxygenic phototrophs (Schad et al. 2019b). Archean IF also exhibit a wide range of iron isotope ratios that cannot be explained by small isotopic effects resulting from direct seawater precipitation of iron silicates like greenalite (e.g. Planavsky et al. 2012a; Smith et al. 2017; Albut et al. 2019). Moreover, the transformation of greenalite into hematite requires either a carbonation reaction to siderite that then thermally decomposes to hematite (Rasmussen and Muhling 2018) or extensive sediment oxidation by secondary O_2-rich fluids (Rasmussen et al. 2014; Rasmussen and Muhling 2020). Recent hydrological modelling, however, suggests that such 'supergene' processes were not widespread throughout the IF record (Robbins et al. 2019b). In summary, there is compelling evidence indicating that Fe(II) silicate minerals were not the predominant water-column precipitates in the mass balance of IF, although they likely did precipitate in deeper, Fe(II)-rich seawater, e.g. seaward of the continental shelf.

The precipitation of Fe(III) occurred at the boundary between reduced upwelling waters rich in Fe(II) and the waters of the sunlit upper layer of the ocean (see Fig. 2). Three biological oxidation mechanisms have been proposed to explain this process: anoxygenic Fe(II)-based photoautotrophy, also

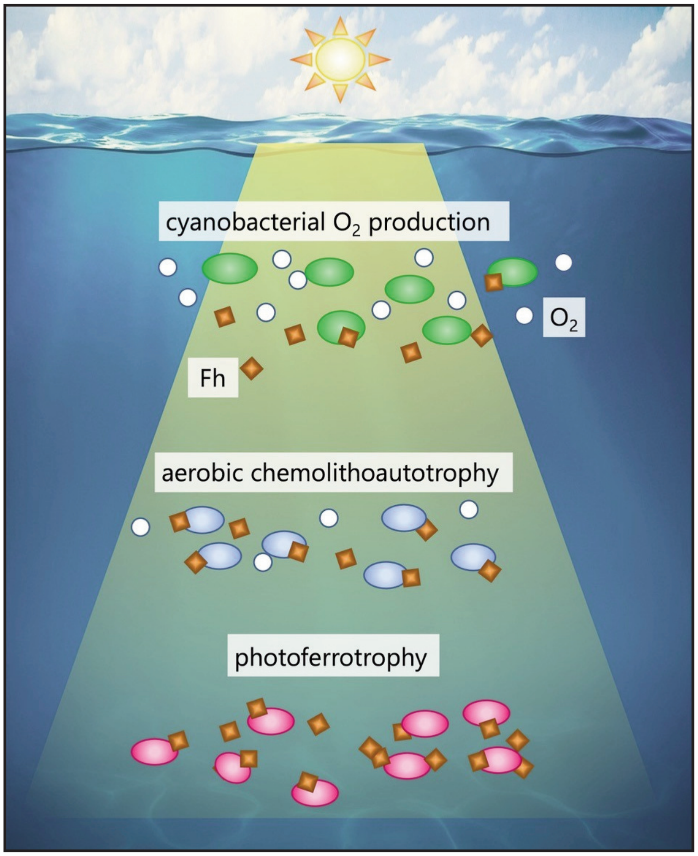

Figure 2. Three mechanisms of biological Fe(II) oxidation in the Precambrian oceans. (Top) reaction of cyanobacterially generated O_2 with dissolved Fe(II); (middle) oxidation via chemolithoautotrophic Fe(II) oxidizing bacteria that grow under low O_2 concentrations; and (bottom) direct oxidation via Fe(II)-based anoxygenic photosynthesis (photoferrotrophy) below the redoxcline where there is no free O_2. Fh = ferrihydrite.

known as photoferrotrophy (reaction 1); aerobic chemolithoautotrophy with O_2 produced by oxygenic photosynthesis (reactions 2a-b); and abiotic oxidation via O_2 from oxygenic photoautotrophy (reaction 3).

[1] $24Fe^{2+} + 6CO_2 + 66H_2O \rightarrow 24Fe(OH)_3 + C_6H_{12}O_6 + 48H^+$
[2a] $6H_2O + 6CO_2 \rightarrow C_6H_{12}O_6 + 6O_2$
[2b] $36Fe^{2+} + 3O_2 + 6CO_2 + 96H_2O \rightarrow C_6H_{12}O_6 + 36Fe(OH)_3 + 72H^+$
[3] $4Fe^{2+} + O_2 + 10H_2O \rightarrow 4Fe(OH)_3 + 8H^+$

Among the three biological mechanisms, photoferrotrophy is considered to be the most ancient (Hartman 1984; Widdel et al. 1993). Positive iron isotope fractionations, thought to represent a primary oxidative process operating under low O_2 availability, are observed in the approximately 3.78 Ga IF of the Isua Supracrustal Belt in Greenland and suggest the presence of photoferrotrophs in the Eoarchean seawater (Czaja et al. 2013). While it is generally agreed that cyanobacteria evolved before the onset of the GOE around 2.5 billion years ago, the exact timing of their emergence remains uncertain (e.g. Planavsky et al. 2021). Sustainable concentrations of O_2 in the ancient oceans are also not well established, with estimates ranging from very low levels in the Archean, on the order of a few nanomolar (nM) (Olson et al. 2013), to higher concentrations of up to 100 micromolar (mM) in the water column at a few hundred metres depth (Kendall et al. 2010). Under low O_2 conditions, aerobic chemolithoautotrophic species could have exploited the slow abiotic oxidation of Fe(II) (e.g. Søgaard et al. 2000) which were encountered just above the redoxcline in the ancient water column (Chan et al. 2016). As the oceans became more oxygenated, abiotic oxidation of Fe(II) (as described in reaction 3) likely became the primary mechanism for ferrihydrite precipitation, following the classic model proposed by Cloud (1965).

Several arguments favour a dominant role for photoferrotrophs before the GOE. First, they would have had a competitive advantage over early cyanobacteria, as they were better adapted to benefit from upwelling phosphorus-rich deep waters, thanks to their ability to grow under low-light conditions (Kappler et al. 2005). Cyanobacteria, on the other hand, have higher phosphorus requirements (Jones et al. 2015; Schad et al. 2019a). Second, the photoferrotrophs had first access to dissolved Fe(II) which is their electron donor, and even in modern ferruginous environments, such as Lake Matano in Indonesia, photoferrotroph activity controls dissolved Fe(II) concentrations in the water column (Crowe et al. 2008). Third, the ferruginous conditions associated with IF deposition may have been toxic to cyanobacteria (Swanner et al. 2015). In all likelihood, the relative roles of each metabolism varied in space and time, depending on nutrient availability and the influence of hydrothermal water inputs (Beukes and Gutzmer 2008). Determining the relative contributions of photoferrotrophs and cyanobacteria to IF deposition is an ongoing area of research (Konhauser et al. 2018).

The oxidation of dissolved Fe(II) would produce biomass that settled to the seafloor together with the Fe(III) minerals (e.g. Konhauser et al. 2002, 2005; Li et al. 2011; Posth et al. 2013a, b). If, as today, the organic carbon (C_{org}) was oxidized during burial by either diagenesis or metamorphism, the relevant question is which terminal electron acceptor was present at the seafloor during times of IF deposition, and at what concentrations? Despite the possibility of some oxic surface waters being generated by cyanobacterial activity as early as 3.0 Ga (e.g. Planavsky et al. 2014), deep waters, and by extension the seafloor, remained anoxic unlike today where sediment pore waters can have dissolved O_2 at depths of several millimetres, and locally even greater depths (Konhauser 2007). In the absence of O_2, the fermentation products in the bottom waters and/or shallow sediment would have been oxidized via some other anaerobic respiratory process. The paucity of O_2 would also have meant minimal nitrate (NO_3^-), manganese oxide (MnO_2) and sulphate (SO_4^{2-}) availability (Fig. 3A). By contrast, the ferric minerals in the primary IF sediment would have been favourable electron acceptors for the oxidation of organic matter (Walker 1984; Nealson and Myers 1990) through the process of dissimilatory iron reduction (DIR) by various bacteria (reaction 4). Significantly, coupling the reduction of some Fe(III) minerals to the oxidation of organic matter not only explains the low content of C_{org} in IF (< 0.5 wt.%; Gole and Klein 1981), but it also explains highly negative $\delta^{13}C$

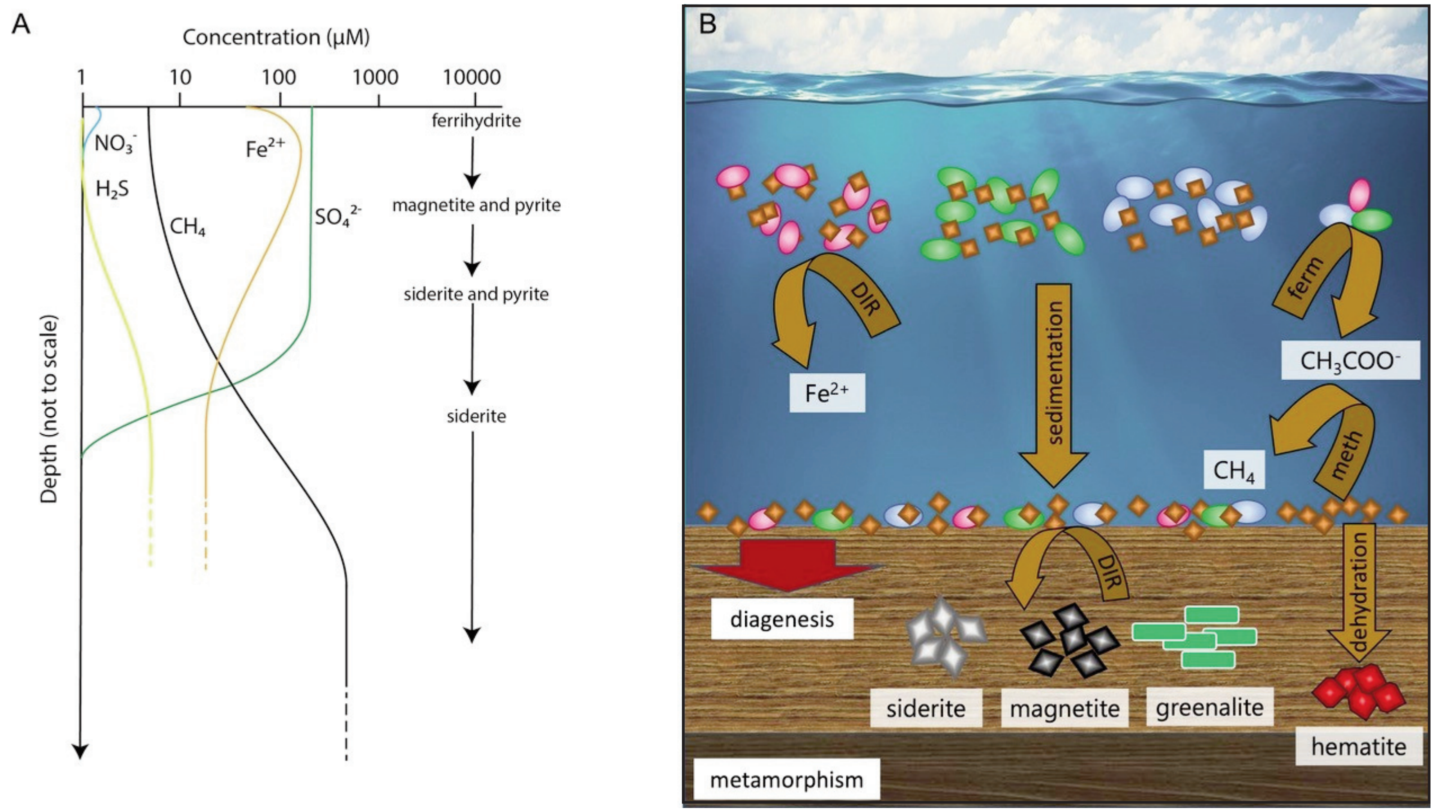

Figure 3. (A) Plausible Archean pore water profile during early diagenesis wherein minerals on right-hand side are dominant controls on pore water Fe speciation. (B) Schematic showing changes to the initial ferrihydrite and biomass associated with burial (diagenesis and metamorphism). After sedimentation, metabolically driven redox processes by fermenters and dissimilatory iron reducing microorganisms (DIRM) take place, possibly also involving methanogens. Pressure and temperature alter the source sediment and cause mineral overprinting. If biomass is present, DIR can lead to magnetite, siderite and greenalite precipitation, while in organic-lean sediments, ferrihydrite dehydrates to hematite. ferm = fermentation; meth = methanogenesis.

values of the early diagenetic Fe(II)–rich carbonate deposits (Baur et al. 1985; Craddock and Dauphas 2011), the highly negative δ^{56}Fe values in magnetite-rich IF (Johnson et al. 2008; Heimann et al. 2010), and the small-scale heterogeneity in δ^{56}Fe values between alternating IF bands (e.g. Steinhoefel et al. 2010). In sum, the negative δ^{13}C values indicate that organic matter was an important source of the C incorporated into the carbonate minerals, the negative δ^{56}Fe in magnetite indicates DIR, while the heterogeneity likely suggests variable degrees of partial Fe(II) oxidation in surface waters, precipitation of different mineral phases and/or post-depositional Fe redistribution but not wholescale overprinting by secondary fluids. Moreover, it explains the presence of Fe(II)-bearing minerals in IF (Fig. 3B): (1) magnetite or iron carbonate when the remineralization of buried organic matter was coupled to Fe(III) reduction (reactions 5 and 6), either during diagenesis or metamorphism (Köhler et al. 2013; Li et al. 2013; Halama et al. 2016); (2) hematite (reaction 7), through dewatering and silica release, when C_{org} was insufficient for complete Fe(III) reduction (Sun et al. 2015); and (3) iron silicate phases, such as greenalite (reaction 8), when silica sorbed onto ferric oxyhydroxides reacted with other cationic species during Fe(III) reduction within sediment pore waters (e.g. Morris 1993; Fischer and Knoll 2009).

[4] $8Fe(OH)_3 + CH_3COO^- \rightarrow 8Fe^{2+} + 2HCO_3^- + 15OH^- + 5H_2O$
[5] $2Fe(OH)_3 + Fe^{2+} \rightarrow Fe_3O_4$ (magnetite) $+ 2H_2O + 2H^+$
[6] $Fe^{2+} + HCO_3^- \rightarrow FeCO_3$ (siderite) $+ H^+$
[7] $2Fe(OH)_3 \rightarrow Fe_2O_3$ (hematite) $+ 3H_2O$
[8] $3Fe^{2+} + 2Si(OH)_4 + H_2O \rightarrow Fe_3Si_2O_5(OH)_4$ (greenalite) $+ 6H^+$

Recent experimental work also supports the possibility that the formation of ferrous silicate mineral phases may be the result of DIR (Nims and Johnson 2022). Finally, ferrous iron sorption to these particles may also have given rise to 'green rust'-type deposits that eventually transformed into magnetite or iron silicate minerals (Halevy et al. 2017; Li et al. 2017).

Although much of the discussion on DIR in IF has focused on processes within the sediment, it is also likely that Fe(III) reduction occurred in the water column. To test this possibility, Konhauser et al. (2005) modelled the ancient Fe cycle based simply on conservative experimental rates of photosynthetic Fe(II) oxidation in the photic zone. They showed that under ideal growth conditions, as much as 70% of the biologically produced Fe(III) could have been recycled back into the water column via fermentation and C_{org} oxidation coupled to DIR. By comparing the potential size of biomass generated phototrophically with the reducing equivalents required for Fe(III) reduction and magnetite formation, they also hypothesized that another anaerobic metabolic pathway might have been utilized in the surface sediment or water column to oxidize C_{org}, specifically a consortium of fermenters and methanogens (Konhauser et al. 2005). Interestingly, at Lake Matano, Crowe et al. (2011) demonstrated that more than 50% of organic matter formed in the water column is degraded through methanogenesis, despite high abundances of ferric oxyhydroxides in the lake sediment.

Even though biomass degradation underpins the conversion of primary IF sediment into the rocks we observe today, our understanding of the complex feedback loops between these microbial processes remains poorly resolved. A recent study by Schad et al. (2022) provided a first attempt to ascertain the interdependent effects of these microbial processes. Those authors co-cultivated photoferrotrophs and dissimilatory Fe(III)-reducing bacteria (DIRB) and observed that both metabolic processes can be coupled, where DIR reduced the cell-Fe(III) mineral aggregates formed by photoferrotrophs and the latter re-oxidized the Fe(II) formed by the DIRB. Crucially, however, their experiments required lactate to be added as C_{org} source and electron donor for the DIRB. This is not surprising given that many anaerobic heterotrophs cannot directly utilize complex organic compounds as their C_{org} source and electron donors but instead rely on fermentative bacteria to produce simple organic compounds such as hydrogen gas (H_2), lactate, or acetate (reaction 9; Rico et al. 2023; Mahmoudi et al. 2023). Consequently, what remains unknown is if the biomass formed by the photoferrotrophs during the initial primary production would in due course become available for DIRB or other downstream microbial processes such as methanogenesis (Konhauser et al. 2005).

[9] $C_6H_{12}O_6 + 2H_2O \rightarrow 2CH_3COO^-$ (acetate) $+ 2CO_2 + 4H_2 + 2H^+$

WHY IRON FORMATIONS ARE USEFUL AS ANCIENT SEAWATER PALEOPROXIES

It has often been argued that IF are deep water sediments due to the lack of current- and wave-generated structures. This is true, but one needs to consider that storm wave base is typically < 50 m (Immenhauser 2009), although waves reaching greater depths do occur (e.g. Peters and Loss 2012). Thus, most IF precipitation would have occurred on the continental shelf (Fig. 4), which today averages 130 m (Tyson and Pearson 1991). For comparison, sea level is believed to have shown an approximately 400 m range of variation over geological time (Trendall 2002). Moreover, the preservation of IF in the rock record argues against their deposition on a subducting deep seafloor. On the landward side, IF are often juxtaposed against either siliciclastic or carbonate sediments, and with minor amounts of volcanic rocks (Gross 1980). They typically formed in open-marine environments during high sea level (e.g. Simonson and Hassler 1996). The presence of siliciclastic sediment depended upon riverine input, and it is not uncommon to find IF interbedded with shale. Often that shale is also organic rich (i.e. black shale) which indicates the addition of planktonic biomass to the clastic sediment (Bekker et al. 2010). Interestingly, experimental studies using photoferrotrophs and cyanobacteria to precipitate ferrihydrite have shown that some cells aggregate with the ferrihydrite (e.g. Posth et al. 2010; Li et al. 2021), whereas other cells have the propensity to remain unmineralized, especially in the presence of dissolved silica (e.g. Gauger et al. 2016; Schad et al. 2019b). The latter could have led to the large-scale deposition of IF lean in organic matter, which in turn, facilitated the deposition in coastal sediments of organic-rich shale that fueled microbial methanogenesis (Thompson et al. 2019).

As authigenic chemical sediments, IF effectively captured the evolving elemental and isotopic signatures of marginal marine seawater, and in this regard, my research group and collaborators have pioneered their exploitation for better understanding Earth's transition to an oxygenated planet. The utility of IF is based on several assumptions and conditions. First, evidence supporting the idea that IF record authigenic marine signatures includes marine-like rare earth element and yttrium (REE+Y) patterns and small-scale chemical variations that argue for the preservation of environmental signals (e.g. Bau and Möller 1993; Bau and Dulski 1996; Bolhar et al. 2004; Alexander et al. 2008; Pecoits et al. 2009; Haugaard et al. 2013; Robbins et al. 2019a). A concern potentially compromising the IF record is the possibility of post-depositional mobilization of trace elements, which can overprint or even eradicate authigenic marine signatures. However, limited post-depositional mobilization or addition of trace elements in IF is indicated by systematic REE and Fe isotope variations, both within and between Fe-rich mesobands despite experiencing diagenetic and metamorphic conditions up to amphibolite facies (e.g. Frost et al. 2007; Whitehouse and Fedo 2007; Steinhoefel et al. 2010). In fact, trace element compilation efforts for IF have often limited their scope to samples falling at greenschist facies or less to provide the most robust estimates possible of trace element abundances. Second, ferrihydrite, the likely precursor phase for hematite and magnetite in IF, can faithfully preserve the elemental and isotopic compositions of seawater, as has been demonstrated through ferrihydrite adsorption and diagenesis experiments (e.g. Døssing et al. 2011; Robbins et al. 2015; but see also Halevy et al. 2017 for a different view). Third, this seawater signal is commonly uncontaminated by continentally derived detrital materials, given that BIF (versus GIF) generally contain very low levels of detrital tracer elements such as aluminum (Al) and titanium (Ti) (Holland 1978). Collectively, this means that IF geochemical data often provide a purely 'authigenic' record of marine chemistry.

The chemical signals archived in 'BIF' can be harnessed by leveraging the predictable behaviour of adsorption reactions that take place on the surface of authigenic ferrihydrite. These ferrihydrite minerals were initially formed from, and reached equilibrium with, the surrounding seawater during their precipitation. In natural environments, where trace elements are captured and stored by ferrihydrite through a combination of adsorption and co-precipitation reactions, simplified distribution coefficient models can be employed to establish an empirical relationship between the concentration of an element in the precipitate and the dissolved concentration at the time of precipitation. This predictive characteristic of ferrihydrite

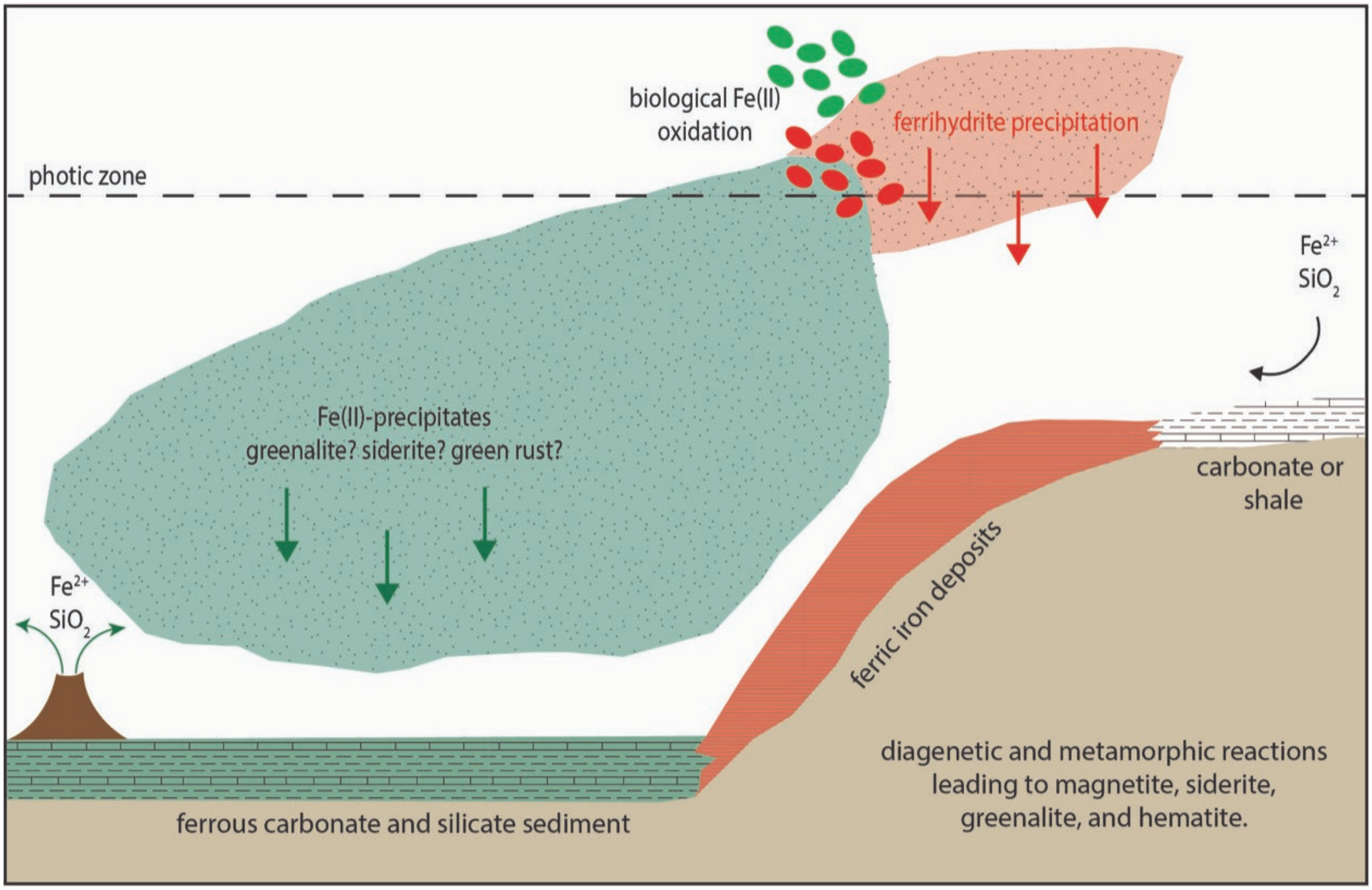

Figure 4. Cross-section of deep submarine source of dissolved Fe(II) that upwells onto the continental shelf where biological Fe(II) oxidation takes place. This leads to the precipitation of ferrihydrite as the precursor sediment for iron formations (IF). Some of ferrihydrite was later reduced through direct bacterial Fe(III) reduction by dissimilatory iron reduction utilizing organic carbon (biomass) as the electron donor. In the absence of a Fe(II) oxidant, the direct precipitation of greenalite or siderite may have taken place in the pelagic water column and continental slope. Along the coast either siliciclastic or carbonate sediments were deposited depending on the presence or absence of riverine input, respectively.

sorption reactions has been used to gain a deeper understanding of the IF record. Specifically, it provides insights into the limitations that Precambrian primary productivity may have faced, whether by the sequestration of bio-essential nutrients by the ferrihydrite itself, or its record of nutrient limitations driven by other factors such as different styles of volcanism, continental weathering, or even internal oceanic cycling (Robbins et al. 2016).

One alternative method for assessing ancient marine trace element concentrations in IF data, without relying on experimentally derived partition coefficients, involves analyzing the relationship between specific trace elements and iron within the IF record itself. Taking nickel (Ni) as an example, there is a clear correlation between the deposition of Fe and Ni. As Fe increases, Ni also increases, consistent with the expected behaviour of Ni sorption to ferrihydrite governed by partition coefficients. By plotting these variables on a graph, we can also overlay the scaling anticipated between a trace metal and Fe based on proposed partitioning scenarios (cf. Robbins et al. 2013; Konhauser et al. 2015). The advantage of this approach is that the hypothesized partitioning scenarios can be compared with the actual data from the IF record. If the proposed scenarios accurately represent the deposition of IF minerals, the lines representing these scenarios should encompass most of the IF data. In fact, when the K_D (distribution coefficient) values predicted by Konhauser et al. (2009) are superimposed on the graph (Fig. 5), nearly all the Ni/Fe values observed in the IF record fall within the predicted ranges. It is important to note that this agreement does not confirm the accuracy or validity of experimentally determined K_D values. The slope in the solid-phase Ni versus Fe space is calculated as $K_D*[Ni]_{sw}$ and is equally influenced by $[Ni]_{sw}$ (dissolved concentration of Ni in seawater). In the case of the partitioning scenarios proposed by Konhauser et al. (2009), $[Ni]_{sw}$ values were originally extrapolated from data in the rock record using experimentally determined K_D values. Therefore, the presented $K_D*[Ni]_{sw}$ scenarios (slopes in Ni versus Fe space) are tuned to this specific dataset, and the apparent correspondence may be considered circular. However, Figure 5 demonstrates two key points: (1) partitioning scenarios can be readily evaluated against rock record data to establish their plausibility, and (2) in future investigations, supposed free parameters (K_D, $[Ni]_{sw}$) could

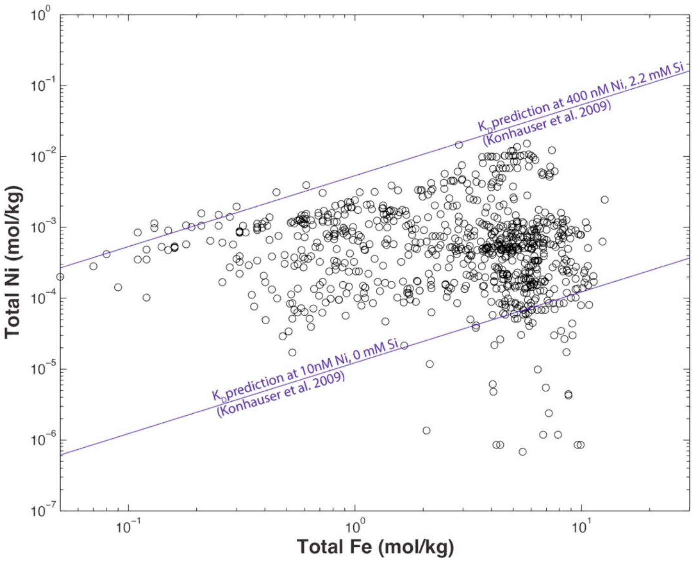

Figure 5. The scaling of Ni with Fe as recorded in the iron formations (IF) record. Superimposed on the IF data are the proposed partitioning scenarios of Konhauser et al. (2009). Note that almost all IF data are constrained by the lines representing the high silica, high Ni and low Si, low Ni partitioning scenarios. Cross plots such as these allow for proposed partitioning scenarios to be tested against IF data. Adapted from Konhauser et al. (2015).

potentially be adjusted based on rock record data to explore feasible scenarios in the K_D–$[Ni]_{sw}$ space. This approach was employed by Robbins et al. (2013) for zinc (Zn)/Fe when experimentally determined partition coefficients were not available.

It is important to note that while the K_D approach, when combined with rock record data, yields what may be considered quantitative constraints on ancient seawater composition, this approach is not without its limitations. Strictly speaking, K_D values are empirical relationships that describe the experimental system being considered. Their subsequent extrapolation to different conditions (pH, ionic strength, etc.) is therefore somewhat tenuous. However, they provide a relatively simple and effective method for generating first-order constraints on the composition of ancient seawater billions of years ago, and therein lies their true utility.

TRACE ELEMENT TEMPORAL TRENDS IN IRON FORMATIONS

In much of the modern Earth's oceans, microbial life has an abundance of C, nitrogen (N), and O_2. However, the scarcity of essential trace nutrients such as phosphorus (P), cobalt (Co), manganese (Mn), molybdenum (Mo), Ni, vanadium (V), and Zn limits primary production (e.g. Morel and Price 2003; Sunda 2012). This limitation has likely existed since the emergence of life over 3.8 Ga, when microbes began developing intricate strategies to scavenge metals and incorporate them from their aqueous surroundings. The availability of trace nutrients in seawater is influenced by long-term geological processes, including the gradual cooling of the upper mantle, changes in volcanic activity and continental composition, and the intermittent accumulation of atmospheric O_2, which facilitated oxidative weathering reactions. The notion that these events may have played a role in directing microbial evolution at the enzymatic level over billions of years is a relatively recent but profound concept (see Anbar and Knoll 2002). This is because microbial evolutionary innovations ultimately influenced the habitability of Earth for the more complex organisms that emerged later. In this context, we will explore how IF have been used to understand the composition of seawater for three trace elements in deep geological time. The primary objective is to gain a better understanding of the co-evolution of the Precambrian environment and biosphere and especially as it relates to atmospheric oxygenation.

Phosphorus

Throughout Earth's history, P has been the primary element limiting global marine primary production on geologic timescales (Tyrrell 1999; Kipp and Stüeken 2017; Reinhard et al. 2017; Laakso and Schrag 2018; Hao et al. 2020). Marine phytoplankton likely emerged during the Archean eon, making it crucial to understand the availability of dissolved phosphorus (P_d) to gain insights into the early evolution of the marine biosphere. In present day surface waters of the oceans, P_d is typically found as protonated inorganic phosphate species (e.g. HPO_4^{2-}), with an average global ocean concentration of approximately 2.3 μM (Levitus et al. 1993; Bruland et al. 2014). However, the range of P_d concentrations in the Neoarchean and early Paleoproterozoic (2.8–2.0 Ga) oceans, spanning the GOE, remains unresolved.

Several studies have been conducted to reconstruct paleomarine phosphorus concentrations by examining the ratios of phosphorus to iron (P/Fe) in IF (Bjerrum and Canfield 2002; Konhauser et al. 2007a; Planavsky et al. 2010; Jones et al. 2015). These studies were based on the understanding that the phosphorus content in modern marine hydrothermal plume ferric oxyhydroxide precipitates (such as ferrihydrite) can be used to establish an empirical relationship between seawater P_d and the ratio of solid-phase phosphorus to iron (P_s/Fe_s) in the ferric oxyhydroxide precipitates (Feely et al. 1998). This relationship exists because the precipitated ferric oxyhydroxides have a strong affinity for phosphorus. The relationship is quantified by a linear distribution coefficient where

$$K_D = \frac{P_s/Fe_s}{P_d}.$$

Building upon this relationship, Bjerrum and Canfield (2002) investigated the IF record to estimate ancient seawater P_d and found that during the Archean P_d averaged 0.15 μM (ranging from 0.03 to 0.29 μM), which corresponds to approximately 10–25% of present-day levels. The authors argued that IF served as a significant sink for P, resulting in a P crisis. This finding was noteworthy because it resolved a paradox that existed then. While a number of studies on the genomes of modern cyanobacteria (e.g. Sánchez-Baracaldo et al. 2022), geochemical indicators for free O_2 (e.g. Planavsky et al. 2014), and fossilized microbialites (Homann et al. 2015) all suggested the potential evolution of cyanobacteria before 3.0 Ga, based on the rock record it is widely accepted that permanent atmospheric oxygenation (i.e. the GOE) did not occur until after 2.5 Ga (e.g. Ostrander et al. 2021). Consequently, the question arose: why did it take so long for O_2 to accumulate in the atmosphere? The Bjerrum and Canfield study pointed towards nutrient limitation as a potential factor.

However, when using P_s/Fe_s ratios as a paleo-proxy, it is crucial to consider the evolution of the silicon (Si) cycle and dissolved silica concentrations (Si_d; H_4SiO_4) due to the inverse relationship between the K_D value for phosphate–ferrihydrite sorption and Si_d, caused by the competitive adsorption of aqueous silica species (Konhauser et al. 2007a). Modern seawater typically has Si_d concentrations below 0.1 mM (Tréguer et al. 1995), while Si_d concentrations during much of the Precambrian may have been saturated with respect to amorphous silica (2.2 mM) (Siever 1992). Such significant differences in Si_d can result in substantial changes to the K_D value for P adsorption onto ferric oxyhydroxide. Indeed, Konhauser et al. (2007a) demonstrated that ferrihydrite precipitation in the presence of high Si concentrations, which leads to Si-rich ferrihydrite (Reddy et al. 2016; Zheng et al. 2016), adsorbs less P compared to ferrihydrite formed under low Si concentrations. As a result, estimated P_d values for the Archean were calculated to be as high as 5.25 ± 2.63 μM. Subsequently, Planavsky et al. (2010) combined the partitioning coefficients derived by Konhauser et al. (2007a) with P/Fe ratios in the IF record and suggested that P levels in the Precambrian oceans were at least as high as modern seawater, and possibly even higher. Jones et al. (2015) subsequently conducted similar partitioning coefficient experiments but included Mg^{2+} and Ca^{2+} in the experimental solutions to better approximate seawater composition. This subtle difference in experimental conditions resulted in estimated Archean P_d concentrations ranging from 0.04–0.13 μM. These examples highlight the susceptibility of P_d estimates to variability in the proposed K_D values. This may be an area of future research that could benefit from the application of more robust, thermodynamically grounded surface complexation models that can be iteratively tested to identify the ways in which accessory cations or anions affect partitioning of biologically critical elements such as P.

Using a different approach, Rasmussen et al. (2021b) reported the ubiquitous presence of nanometre-sized apatite crystals in IF dating between 3.46 to 2.46 Ga. The apatite is uniformly distributed within greenalite-rich layers. The authors subsequently argued that abundant greenalite precipitation in the open ocean led to high phosphate concentrations in seawater, perhaps approaching 100 μM. They argued that dissolved Fe^{2+} would have been limited by greenalite precipitation, thus inhibiting the formation of vivianite ($Fe_3[PO_4]_2 \bullet H_2O$), a potential deep sea phosphorus trap (Derry 2015). This work has support from experiments and models that show that Fe^{2+} significantly increases the solubility of phosphate minerals in anoxic systems, with possible P_d ranging from 200–400 μM (Brady et al. 2022).

Nickel

Nickel plays a crucial role in numerous prokaryotic metalloenzymes. It is essential for carbon reduction in both acetogenic and methanogenic bacteria and is a component of important cofactors such as methyl-coenzyme M reductase and acetyl-CoA synthase that are necessary for methane (CH_4) production (e.g. Hausinger 1987). Additionally, Ni is used in hydrogenases and carbon monoxide dehydrogenase, contributing to the reduction of CO_2 to CO and the production of acetyl-CoA (e.g. Ragsdale and Kumar 1996). In non-methanogenic organisms, Ni may be involved in urease activity and is also found in a superoxide dismutase present in various marine organisms, including planktonic cyanobacteria that may have evolved during the Neoproterozoic (Boden et al. 2021).

Initial estimates of dissolved Ni concentrations (Ni_d) in the early ocean were obtained through geochemical modelling (Saito et al. 2003) and microbial genomics (Zerkle et al. 2005). These studies suggested that seawater Ni_d was relatively consistent from the Archean to the present day. This presumed uniformity was mainly attributed to Ni behaving conservatively under various redox conditions in water. However, a compilation of Ni contents in IF over time (Konhauser et al. 2009) revealed a consistent and rapid decline in Ni_d around 2.7 Ga (Fig. 6A). This trend remained evident even after a near doubling of available IF data (Konhauser et al. 2015), indicating the observed decline in Ni within IF was a robust, first-order trend. By utilizing experimentally derived Ni partitioning coefficients for Si-rich ferrihydrite (considering elevated Si_d during the Precambrian), it was estimated that paleomarine Ni_d decreased by over 50% between 2.7 and 2.5 Ga, dropping from approximately 400 nM to 200 nM (Konhauser et al. 2009). This decline was attributed to mantle cooling, which led to a decrease in the frequency of Ni-rich ultramafic eruptions and subsequently limited the availability of Ni-source rocks susceptible to weathering. This trend was subsequently shown to have been captured in the sedimentary to early diagenetic pyrite record (Large et al. 2014) and recently been verified in an analysis of more than 96,000 continental volcanic rocks (Liu et al. 2021).

The decline in Ni_d would have had significant implications for microorganisms that relied on Ni, particularly CH_4-producing bacteria known as methanogens. These bacteria have a unique requirement for Ni in their CH_4-producing enzymes and have been implicated in regulating O_2 levels on ancient Earth. The CH_4 they produced reacted with O_2, keeping atmospheric levels of the latter low (Zahnle et al. 2006), although it can also at the same time contribute positively to atmospheric oxidation by promoting H_2 escape (Kasting et al. 2013). It is possible that a scarcity of Ni eventually triggered a cascade of events, starting with reduced CH_4 production, followed by the expansion of cyanobacteria into shallow-water habitats. In the end, this would have led to increased oxygenic photosynthesis and C_{org} burial, tipping the atmospheric balance in favour of O_2 and culminating in the GOE.

A study by Eickhoff et al. (2014) conducted a re-evaluation of the partitioning behaviour of Ni between biogenic and abiogenic ferrihydrite in the presence of silica. While the estimates presented by Eickhoff et al. (2014) cannot be directly compared to those of Konhauser et al. (2009) due to differences in their experimental approaches, their findings indicate

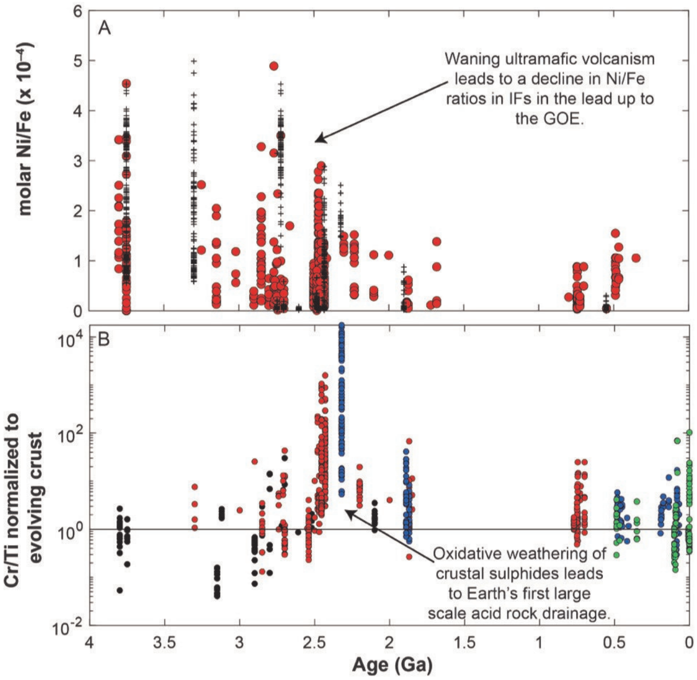

Figure 6. (A) Molar Ni/Fe ratios in iron formations (IF) adapted from Konhauser et al. (2015). Note red circles represent bulk analyses, with black + symbols representing laser ablation analyses; (B) molar Cr/Ti ratios in IF, normalized to evolving continental crust (Condie 1993). Symbols in (B) are black = Algoma-type IF; red = Superior-type IF; blue = granular iron formations and oolitic ironstones; green = Phanerozoic hydrothermal iron deposits. Adapted from Konhauser et al. (2011) and Hao et al. (2022). GOE = Great Oxidation Event.

that the presence of biomass leads to a decrease in Ni sorption onto ferrihydrite. Consequently, the estimates of paleomarine Ni_d based on IF may have been underestimated. This suggests that the decline in the paleomarine Ni reservoir, and the subsequent famine experienced by methanogenic bacteria, as described by Konhauser et al. (2009), might have occurred closer to the onset of the GOE.

Chromium

While chromium (Cr) has a limited biological role in most higher-level organisms, it is generally recognized as a toxin (Frausto da Silva and Williams 2001). Therefore, temporal patterns in seawater are unlikely to directly reflect evolutionary controls. Instead, studies in the sedimentary record have focused on analyzing Cr abundances and isotope compositions to track oxygenation in surface environments. The value of these investigations lies in the behaviour of reduced Cr, specifically Cr(III), which is immobile under neutral to alkaline pH conditions, but becomes mobile when either subjected to acidic conditions (Rai et al. 1989) or oxidized to Cr(VI) (Oze et al. 2007). Additionally, Cr stable isotopes are significantly fractionated during redox reactions (e.g. Ellis et al. 2002). Consequently, changes in Cr abundances and isotopic compositions are likely indicators of variations in the redox state of the oceans or atmosphere, as well as related shifts in Cr mobility mechanisms and sediment sources.

Based on the above understanding, Cr isotopes have been used to track the oxygenation of the atmosphere and oceans. In the case of 2.8–2.6 Ga IF, small variations in Cr isotope composition were initially proposed to represent short bursts of atmospheric O_2 that triggered the mobilization of Cr through oxidative weathering and its subsequent sequestration in IF prior to the GOE (Frei et al. 2009). The authors argued that the observed increases in δ^{53}Cr values ranging from +0.04 to +0.29‰ in IF at 2.7 Ga, and again at 1.8 Ga, resulted from the oxidation of Cr(III) to Cr(VI), with oxidation likely catalyzed by Mn(IV) oxides. Subsequently, Konhauser et al. (2011) examined the temporal trends in the degree of Cr enrichment in IF and found that the former was mostly immobile on land until approximately 2.48 Ga. However, within the subsequent 160 million years, during a period coinciding with independent evidence of oxygenation associated with the GOE, there were significant excursions in Cr abundances and Cr/Ti ratios, indicating an unprecedented scale of Cr solubilization (Fig. 6B) at a time when Cr isotope fractionation remained minimal, indicating that Cr was mobilized in Cr(III) rather than Cr(IV) form. The authors proposed that only the oxidation of a previously stable and abundant crustal pyrite reservoir by aerobic, chemolithoautotrophic Fe(II)-and S-oxidizing bacteria could have generated the necessary level of acidity to dissolve Cr(III) from ultramafic source rocks and residual soils. In other words, the emergence of novel microbial metabolisms coincided with atmospheric O_2 becoming available. During this period, muted δ^{53}Cr variations from –0.3 to +0.3‰ were interpreted as indicative of Cr cycling in its reduced form (Konhauser et al. 2011), in contrast to the highly variable values associated with ocean oxygenation during the Neoproterozoic (up to +4.9‰; Frei et al. 2009). This significant shift in weathering patterns, starting at 2.48 Ga, represents the earliest known example of acid rock drainage and persisted until the exposed crustal reservoir of pyrite was depleted, marking the end of an era characterized by intense chemical weathering on Earth.

To investigate earlier indications of photosynthetic O_2 production, researchers examined Cr isotope data from rocks in the Pongola Supergroup, South Africa. Crowe et al. (2013) discovered that the δ^{53}Cr isotope compositions of 2.96 Gyr old paleosols were fractionated compared to crustal values, suggesting the oxidative mobilization of Cr and the presence of low levels of atmospheric O_2 (~10^{-4} of present atmospheric levels, PAL). This O_2 level was necessary to oxidize Fe(II) to Fe(III) and thus prevent the ferrous iron from reducing Cr(VI) to Cr(III) during transport to the ocean. Interestingly, the analysis of roughly contemporaneous IF from the same region revealed δ^{53}Cr values up to 0.28‰. The authors proposed that the IF captured a mobile, δ^{53}Cr-enriched pool of Cr(VI) originating from oxidative weathering on the continents. This finding suggests the existence and activity of oxygenic photosynthesis approximately 500 million years prior to the GOE. The concept of early O_2 production is supported by the Mo isotope composition of the IF within the Pongola Supergroup, as the correlation between Mo isotope composition and Mn/Fe ratio indicates the presence of MnO_2 and its adsorption of isotopically light Mo during that period (Planavsky et al. 2014). However, it is also possible that the observed Cr isotope fractionation in the 2.96 Ga paleosols, as reported by Crowe et al. (2013), is a result of localized O_2 production by cyanobacteria within a microbial mat (Lalonde and Konhauser 2015) or an artifact of modern weathering (Albut et al. 2018). In either scenario, the IF record of Cr, particularly in terms of its abundance and isotopic composition, offers valuable insights into O_2 production through photosynthesis, either in the early oceans or on land, and the associated oxidative weathering on the early continents. The early production of O_2 is consistent with recent genomic evidence for the emergence of oxygen producing or using enzymes (Jabłońska and Tawfik 2021) and sedimentological evidence including the observed relationship between Mo isotopes and Mn (Planavsky et al. 2014; Albut et al. 2018), Mn(IV) oxide deposition (Ossa Ossa et al. 2016; Robbins et al. 2023), and spatially resolved Mn enrichments that suggest a gradient from more reducing to oxidizing conditions that parallels the transition from deeper to shallower waters (Smith and Beukes 2023).

Evidence for environmental oxygenation prior to the GOE, such as the Cr isotopes discussed above, have been interpreted as transient "oxygen oases", effectively temporary refugia where O_2 was being produced and aerobic metabolisms could have been established. In this sense, oxygen oases are often viewed as being relatively small or short-lived, akin to a 'whiff' of O_2 (e.g. Anbar et al. 2007). Earth systems models predict that while much of the open ocean in the Archean would have been devoid of O_2, in oxygen oases local O_2 concentrations could have been as high as 1–10 mM (Olson et al. 2013). Nevertheless, how long-lived and extensive such oases were remains to be answered. A recent study on the Pongola and Witwatersrand supergroups by Smith et al. (2023) found carbonate concretions with depleted $\delta^{13}C$ and Mn enrichments, suggesting that free O_2 in the environment was present over a much wider area and for longer than previously thought. The authors suggested that the free O_2 led to the deposition of MnO_2 and subsequent respiration by bacteria yielded the isotopically depleted Mn(II)-rich carbonate concretions. Constraining the extent and longevity of early oxygenation events highlights the need for continuing to study Archean to Paleoproterozoic IF.

IRON FORMATIONS AS PROXIES FOR EARTH'S OXYGENATION

According to the hypothesis presented by Zahnle et al. (2006), the accumulation of O_2 in the atmosphere was hindered by its high chemical reactivity with biogenic CH_4, so as long as CH_4 production remained high, O_2 could not accumulate into the atmosphere. Their model proposed that oxidative weathering of sulphide minerals on land increased the supply of dissolved sulphate to the oceans, leading to the ecological dominance of sulphate-reducing bacteria (SRB) over methanogens around 2.4 Ga as the former can exhaust the supply of labile C_{org} and H_2 that both types of bacteria use as electron donors in their metabolisms. Additionally, the anaerobic (microbial) oxidation of CH_4 by SO_4^{2-} would have suppressed the release of CH_4 from sediments due to increasing SO_4^{2-} concentrations during that period (Catling et al. 2007). However, evidence in the rock record for widespread oxidative weathering of terrestrial sulphide phases, a significant oceanic sulphate reservoir, and the onset of widespread ocean euxinia only appears after the GOE (Poulton et al. 2004; Reinhard et al. 2009). An alternative hypothesis proposed by Konhauser et al. (2009) suggested that the decline in large-scale methanogenesis occurred prior to, and not necessarily because of, increasing environmental oxygenation. Their model indicates a specific progression in Earth's system evolution, where a cooler mantle after 2.7 Ga initiated chemical changes in volcanism and trace element abundances in the oceans, leading to a decline in global methanogenesis. Ultimately, this facilitated the transition from anoxic to oxic atmospheric conditions at approximately 2.45 Ga.

The connection between the decline of methanogens and the rise of cyanobacteria may not be coincidental. In a competitive environment where microorganisms vie for resources, the success of one species can suppress others through competitive exclusion (Hibbing et al. 2010; Weber et al. 2014). A given bacterium can enhance its competitive advantage by producing antimicrobial compounds or evolving resistance to external chemicals. While no pathogenic species have been identified among methanogens, they possess toxin/antitoxin systems (Cavicchioli et al. 2003). Furthermore, a study on acidic peat bogs demonstrated that the addition of the antibiotic rifampicin inhibited the growth of acetogens without affecting the growth of methanogens (Bräuer et al. 2004). It is plausible that pre-2.7 Ga, methanogens were simply more competitive than cyanobacteria and thus widely distributed throughout the oceans, ranging from shallow waters to the sediment. In addition, based on predictions of evolving Fe:P ratios in Precambrian upwelling waters, Jones et al. (2015) suggested that photoferrotrophs would likely have fared better than the cyanobacteria while the oceans were highly ferruginous (with Fe:P > 424, as based on the Redfield ratio). But, as soon as the dissolved Fe:P ratio fell below 424, iron would be exhausted, leaving P to fuel other modes of photoautotrophy, such as oxygenic photosynthesis. Similarly, Swanner et al. (2015) demonstrated experimentally that highly ferruginous waters may have been toxic to cyanobacteria due to the accumulation of reactive oxygen species (ROS) within the cells, resulting in decreased photosynthetic efficiency and slower growth rates. Rampant methanogenesis, whether supported by higher H_2 fluxes or organic matter produced by anoxygenic phototrophy, would have contributed to the maintenance of the largely anoxic conditions. Consequently, this allowed for the dispersal of Fe(II), which would have hindered cyanobacterial proliferation if the Fe(II)-related limitations identified by Jones et al. (2015) and Swanner et al. (2015) were indeed crucial factors. Further, Mloszewska et al. (2018) experimentally demonstrated that unattenuated ultraviolet radiation (uv-C) induces high rates of mortality for planktonic cyanobacteria in the upper reaches of the water column, thus implying that cyanobacterial expansion of the ancient oceans would have been suppressed.

Around 2.7 Ga, a combination of factors coincided that would have promoted a decline in methanogens and the simul-

https://doi.org/10.12789/geocanj.2023.50.201

taneous rise of cyanobacteria, in addition to the decrease in seawater Ni concentrations. The emergence of new continents led to an increased supply of solutes and sediment through weathering processes (Lalonde and Konhauser 2015; Wu et al. 2023), which resulted in the development of stable continental platforms with nutrient-rich, shallow waters favourable for colonization by both benthic and planktonic cyanobacteria (although see Sánchez Baracaldo 2015 for an alternate opinion that planktonic cyanobacteria did not evolve until around 800 Ma). The timing correlates well with the diversification of marine stromatolites (McNamara and Awramik 1992). Indeed, genomic data for extant cyanobacteria have led to the suggestion that multicellularity in cyanobacteria evolved perhaps 200–300 Myr before the GOE (Schirrmeister et al. 2013). The transition to multicellularity represents an important change in organism complexity because filamentous growth can improve cell motility which would allow for movement over sediment, while cooperation of cells can increase metabolic fitness and diversification compared to single cells (e.g. Knoll 1984; Bonner 1998; Koschwanez et al. 2011). Collectively this could have led to new adaptive strategies such as the formation of microbial mats (Sánchez Baracaldo et al. 2022). Moreover, the increased consumption of CO_2 by cyanobacteria led to widespread deposition of calcium carbonate on the seafloor, forming thick beds that extended across vast areas spanning thousands of square kilometres (Grotzinger and Knoll 1999) to facilitate benthic cyanobacterial growth and their calcification throughout the shallow littoral zones. Overall, the combination of stable continental platforms, the evolution of motile and large filamentous cyanobacteria, and increased nutrient supply created an environment where cyanobacteria thrived and produced increasing amounts of O_2, further driving the decline of methanogens.

A decrease in methanogen populations may also have been caused by declining fluxes of H_2 due to diminishing serpentinization of the seafloor. This may have coincided with the reduction in olivine-rich oceanic crust production at the end of the 2.7 Ga mantle plume event and the stabilization of continental cratons (Barley et al. 2005). According to Kump and Barley (2007), the transition from predominantly submarine volcanism to more subaerial volcanism further contributed to the decrease in abiotic H_2 fluxes, as subaerial volcanism releases more oxidized gases such as H_2O, CO_2 and SO_2. Alternatively, Gaillard et al. (2011) proposed that a decrease in volcanic degassing pressure associated with the growth of continental crust led to higher emissions of H_2 which then escaped to space, thus resulting in a net gain of atmospheric O_2. In either case, the diminishing supply of H_2 would have played a role in the decline of biogenic CH_4 production (Kharecha et al. 2005), even if methanogens continued to grow directly on the seafloor crust, where both Ni and H_2 sources remained locally abundant (e.g. Brazelton et al. 2006; Amend et al. 2011).

A third factor which may have contributed to a decline of methanogens and simultaneous proliferation of cyanobacteria was changing seawater Fe^{2+} concentrations. Dissolved iron episodically declined in the shallow regions of continental shelves due to the cessation of plume-driven submarine volcanism and a lowering of sea level. This change created the conditions required for the development of oxygen oases on semi-restricted carbonate platforms, exemplified by extensive stromatolites in the 2.65–2.46 Ga Campbellrand Subgroup in South Africa (Sumner 1997). The existence of dissolved O_2 in seawater along the slope is inferred from various indicators. Shifts towards heavier N isotopes in shale organic carbon indicate the onset of an oxygenated N cycle (Godfrey and Falkowski 2009). Variations in abundances of rhenium (Re) and Mo in shale reflect cycling of these elements in deep oxygenated seawater (Kendall et al. 2010), while the rimmed margins of the platform, as described by Sumner and Beukes (2006), could have provided sheltered lagoons where cyanobacteria thrived, protected from the delivery of Fe(II)-rich water sourced from the deeper regions. This is supported by the deposition of Fe-rich shale along the slope and IF deeper in the basin (Klein and Beukes 1989). The geochemical indicators of O_2 then disappeared during transgressions when deep seawater flooded the platform with Fe(II)-rich waters thought to have been sourced from plume-driven submarine volcanism (Barley et al. 2005).

Evidence for a shift from a CH_4-dominated ocean to an ocean dominated by cyanobacteria is clearly observed in the 150-million-year section (2.72–2.57 Ga) of late Archean shallow- and deep-water sediments found in the Hamersley Basin in Western Australia. In a study by Eigenbrode and Freeman (2006), $\delta^{13}C_{org}$ values were reported for 175 kerogen samples, ranging from –57 to –28‰. The oldest samples contained the most depleted isotopic values, which can be best explained by biological CH_4 assimilation and oxidation by methanotrophic microorganisms. Methane oxidation requires electron acceptors such as O_2, NO_3^-, or SO_4^{2-}. The latter two indirectly depend on O_2 to form oxidized species, although there have been models (e.g. Konhauser et al. 2005) and experimental evidence (Beal et al. 2009) suggesting that Fe(III) can also function as electron acceptor for microorganisms to oxidize CH_4. Therefore, methanotrophy may not necessarily be linked to O_2.

Interestingly, a δ^{13}Corg shift of 29‰ in the kerogens occurred in shallow water carbonate sediment (changing from –57 to –28‰) over that time, while only a 5‰ shift (–45 to –40‰) was observed in the deep water sediment. These patterns indicate a gradual transition in shallow waters from a microbial habitat strongly influenced by CH_4 cycling at 2.72 Ga to one that was more influenced by oxygenic photosynthesis by 2.57 Ga (Eigenbrode and Freeman 2006): cyanobacteria tend to fractionate carbon between –20‰ to –30‰ (e.g. Garcia et al. 2021). In deeper settings, the kerogens remained highly ^{13}C-depleted, indicating that these environments continued to be dominated by communities involved in CH_4 production and consumption and were not yet affected by the significant changes in carbon cycling occurring in shallow waters. By comparing the data from the Hamersley Basin to other locations, Eigenbrode and Freeman (2006) further suggested that a global-scale expansion of oxygenated habitats coincided with the transition from anoxic ecosystems to microbial communities fueled by oxygenic photosynthesis, occurring before the oxygenation of the atmosphere 2.45 Ga.

Around 2.45 Ga, as the GOE began, aerobic chemolithoautotrophic weathering of pyrite on land caused a significant increase in acidity which led to an elevated flux of solutes, which were previously low due to their insolubility under an anoxic atmosphere at the Earth's crustal surface (Konhauser et al. 2011). One specific example relevant to the earlier discussion is SO_4^{2-}, which started to appear in significant concentrations in the marine environment around 2.5 Ga (Reinhard et al. 2009). The accumulation of SO_4^{2-} in the oceans continued until around 2.0 Ga (Planavsky et al. 2012b; Blättler et al. 2018), when it is believed that atmospheric O_2 levels started to decline (Partin et al. 2013; Scott et al. 2014), marking the beginning of what is commonly referred to as Earth's "boring billion" period. With the increased supply of SO_4^{2-} to the oceans, marine SRB would have begun to dominate the anoxic regions of the water column. This further marginalized the methanogens, relegating them to sulphate-poor sediment, like their current distribution. As a consequence of the progressive decline in methane production, which is a potent greenhouse gas, the climate started to cool, eventually leading to significant Paleoproterozoic glaciations (Zahnle et al. 2006).

Concomitant with increased acidity was also the supply of other insoluble elements to seawater. Konhauser et al. (2011) argued that the increased concentrations of Cr in IF between 2.45 to 2.32 Ga was due to the mobilization of Cr(III) from both ultramafic rocks and soils. Specifically, those authors suggested that dissolved Cr^{3+} or $Cr(OH)^{2+}$ was then transported to the oceans via acidic streams or groundwater, and upon mixing with seawater, would have rapidly precipitated out of solution as a $(Fe,Cr)(OH)_3$ phase that became incorporated in IF. However, streams and groundwater with low pH would be naturally buffered by more alkaline waters flowing through non-acid-generating rock types (i.e. silicate-weathering reactions that control the inorganic carbon system). Therefore, much of the Cr(III) mobilized by this pulse of low-pH oxidative weathering presumably never made it to the oceans, instead being lost from solution along catchment pathways. To address this apparent contradiction, Hao et al. (2022) sought an alternative mode of Cr transport, namely the erosion and subsequent transport of suspended sediment with anomalous Cr enrichments. In an experimental study designed to test the complexation of Cr(III) to common soil clay minerals, the authors demonstrated that Cr(III) was strongly bound to kaolinite in particular under acidic conditions and weakly desorbed under marine conditions. Extending those results to the interpretation of the Cr record in IF, Hao et al. (2022) suggested that under intense chemical weathering conditions, not only did acidity promote the solubilization of Cr(III) from primary Cr(III)-bearing minerals, but that parent rocks were more systematically weathered to an advanced state dominated by kaolinite – creating ideal conditions for Cr adsorption. Erosion of regolith that scavenged mobilized Cr(III) could then facilitate transport of Cr(III)-bearing kaolinite – the "kaolinite shuttle" – to coastal environments where it contributed to the high Cr abundances preserved in the Paleoproterozoic IF.

Konhauser et al. (2011) also concluded that acidity would have solubilized minerals that contained nutrients, e.g. apatite, releasing dissolved P, and thus leading to increased nutrient supply to the oceans and enhanced primary productivity. Bekker and Holland (2012) further argued that the largest positive carbon isotope excursion, the so-called the Lomagundi Event (LE), ca. 2.22 to 2.06 Ga, was caused by such an acidic P flux from land. It has been widely argued – though not universally agreed upon – that the LE marks a period of enhanced organic C_{org} burial (e.g. cyanobacteria), such that the isotopically light carbon was incorporated into the sediment pile while the isotopically heavy carbon was incorporated into marine carbonate minerals (see Schidlowski et al. 1976 but see also Mayika et al. 2020 and Prave et al. 2022 for alternative views). By this model, the extensive burial of cyanobacterial biomass led to the accumulation of O_2 in the atmosphere. In fact, it has been hypothesized that during the LE, Earth's surface environments experienced a release of O_2 to the extent of 12 to 22 times the present atmospheric O_2 inventory (Karhu and Holland 1996).

Nonetheless, the question remains: how did the dissolved phosphorus released during acid weathering find its way from land to the oceans? In the present day, most of the P delivered to the oceans is in the form of suspended sediment, with less than 10% of total P being transported as dissolved anions through rivers (Berner and Rao 1994). Similar to the Cr story, P is predominantly transported as a particulate phase, including P adsorbed onto iron(III)-aluminum(III)-oxyhydroxides or clay minerals, or complexed with organic matter (Gérard 2016). A significant portion of adsorbed P settles in estuaries and marginal marine environments through the flocculation of particulate phases, where it remains inaccessible to plankton until remobilization within the sediment pile (Conley et al. 1995). In the absence of plants, the only organic compounds transported to the oceans would have originated from degraded continental microbial mats (e.g. Lalonde and Konhauser 2015), which are unlikely to have had a significant impact on the P cycle. Moreover, during the LE, iron oxyhydroxides would have been solubilized in sulphide-rich soils, like observations in certain black shale weathering environments today (e.g. Joeckel et al. 2005). Expanding on this framework, Hao et al. (2021) demonstrated that the main mechanism by which P was delivered to the oceans during that time was likely through an active kaolinite shuttle. However, unlike Cr, P quickly desorbs from kaolinite when exposed to marine conditions. Importantly, the authors also conducted experiments showing that the released P was bioavailable to marine cyanobacteria. In one culture lacking P input, the cyanobacteria entered a death phase by day 14, while the culture 'seeded' with P-bearing kaolinite resulted in a population of cells that exponentially increased in density. In summary, the high adsorption capacity of kaolinite for P under acidic, freshwater conditions, coupled with its low capacity under alkaline, marine conditions, enhanced P bioavailability and promoted cyanobacterial productivity in nearshore environments after the GOE.

https://doi.org/10.12789/geocanj.2023.50.201

On a final note, it is worth noting that during the GOE, certain oxidized compounds were mobilized for the first time, posing a toxic threat to microbes that had evolved in O_2-deprived marine environments. One example is arsenate, the pentavalent oxidized form of arsenic (As), which exhibits toxicity to all three domains of life even at very low concentrations and shows a strong inverse correlation with marine primary production (e.g. Smedley and Kinniburgh 2002). It has been proposed that the widespread deposition of IF during the transition from the Archean to the Paleoproterozoic facilitated the preferential incorporation of P over As(V) into ferric oxyhydroxides like ferrihydrite. This resulted in a simultaneous increase in As(V) concentration and depletion of P in seawater, negatively impacting marine primary productivity (Chi Fru et al. 2016; Hemmingsson et al. 2018). A study conducted by Chi Fru et al. (2019), which analyzed sedimentary rocks spanning from 2.9 to 1.9 Ga, further demonstrated that the GOE coincided with a significant rise in arsenate levels in IF and the presence of arsenic sulphides in marine shale. This notable increase in O_2-sensitive tracers aligns with the proliferation of key arsenic oxidants, including O_2, NO_3^-, and MnO_2. The substantial surge in arsenic sulphides by at least tenfold after 2.45 billion years ago supports the hypothesis of a transition to sulphide-rich waters at mid-depth continental margins following the GOE. Additionally, the substantial elevation in arsenate content, accounting for approximately 60% of the total arsenic concentration in shale, suggests the establishment of an oxidative component in the arsenic cycle for the first time in Earth's history. These findings underscore the worldwide emergence of a new selective pressure on the survival of marine microbial communities during the GOE, characterized by the global presence of toxic, oxidized species such as arsenate in seawater.

CONCLUSION

In this contribution we aimed to integrate available geochemical data from IF into a coherent narrative explaining the mechanisms underpinning the rise of atmospheric O_2 and its subsequent regulation of Earth's surface systems. The sequence begins with a cooling Earth around 2.7 Ga, leading to the eruption of lavas with lower Ni content both on land and underwater. As these volcanic rocks contained less Ni, their chemical weathering resulted in a reduced flux of Ni to seawater. This had biological implications as marine microorganisms dependent on Ni, such as methanogens, started experiencing nutrient deprivation. Around 2.6 Ga, methanogens became marginalized in shallow shelf environments, making way for cyanobacterial expansion, which gave rise to new stromatolites. Before the GOE and the permanent oxygenation of Earth's atmosphere, the O_2 produced by these cyanobacteria created oxygen oases that facilitated the development of aerobic metabolisms. Constraining the extent of such oases with respect to both space and time presents an opportunity to continue to integrate detailed geochemical and sedimentological observations from IFs and correlative units.

By approximately 2.45 Ga, O_2 had becoming increasingly pervasive in Earth surface environments, oxygenating the

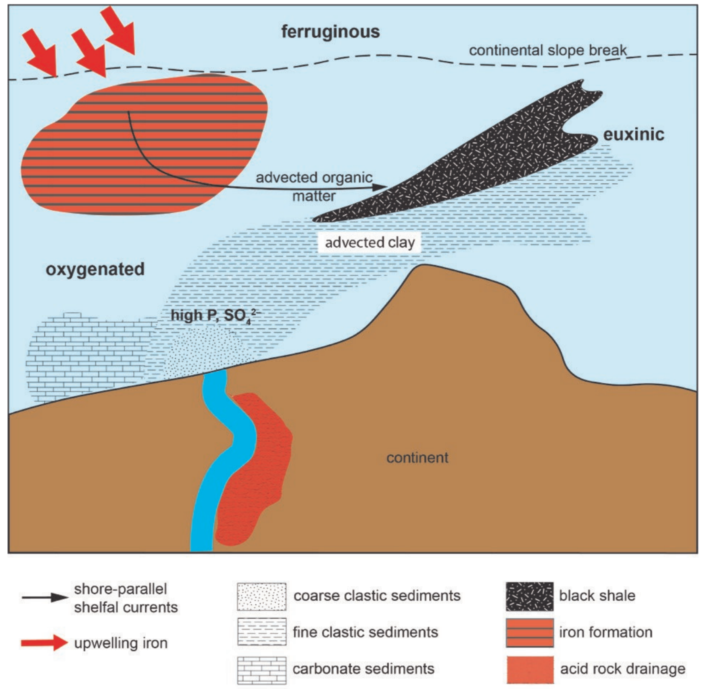

Figure 7. Schematic showing the spatial distribution of iron formations (IF), siliciclastic and carbonate sediments on the Archean continental shelf. The panel also emphasizes how plankton could be advected from the shelf where IF were precipitated to become incorporated into black shale. Prevailing redox conditions and nutrient supplies are indicated in bold text.

atmosphere and marking the GOE. This event resulted in massive oxidative weathering of the Earth's crust and the release of elements previously locked in reduced mineral phases, such as pyrite. Concurrently, aerobic metabolisms evolved on land, including chemolithoautotrophic bacteria that oxidized reduced Fe and S in minerals such as pyrite. Increased fluxes of dissolved SO_4^{2-} reached the oceans, leading to greater bacterial sulphate reduction in the water column. This resulted in higher levels of dissolved sulphide, the production of euxinic waters (low oxygen, sulphidic conditions), and the terminal displacement of methanogens from the water column to bottom sediments in most environments. Pyrite oxidation also led to elevated acidity in rivers and groundwater, promoting the chemical alteration of primary minerals into highly weathered phases like kaolinite (Fig. 7). Importantly, kaolinite served as an elemental shuttle, facilitating the increased availability of key nutrients such as P, which, in turn, stimulated higher primary productivity. Intriguingly, the ability of cyanobacteria to indirectly enhance their own nutrient supply through O_2-driven chemical weathering may represent an unrecognized positive biological feedback mechanism on primary productivity. This scenario is reminiscent of the Gaia hypothesis where the Earth functions as a self-regulating system with the geosphere, atmosphere, hydrosphere, and biosphere all interconnected and evolving as a whole (Lovelock 1972). The Lomagundi carbon isotope excursion around 2.22 Ga may be an expression of these feedbacks, ultimately resulting in increased marine phytoplankton productivity and organic matter burial. Simultaneously, toxic elements like As would have affected the existing marine biosphere, prompting some species to adapt while potentially leading to the extinction of others. In this regard, it is intriguing to speculate that the end of the Lomagundi event, which appears to have coincided with a significant drop in atmospheric O_2 levels, may be somehow linked to a microbial mass extinction, or at the very least, marginalization of those existing cyanobacteria due to some unresolved factor.

ACKNOWLEDGEMENTS

The lead author extends gratitude to the Geological Association of Canada for the honour of receiving the Logan Medal. The content presented in this work represents a concise overview of more than twenty years of research, a feat made possible through the dedicated contributions of numerous graduate students who gathered samples from various corners of the globe, conducted a wide array of geochemical and mineralogical analyses, amalgamated their findings, and, in the end, published our collective data. Additionally, I wish to express appreciation for the financial assistance provided by the Natural Sciences and Engineering Research Council of Canada.

REFERENCES

Albut, G., Babechuk, M.G., Kleinhanns, I.C., Benger, M., Beukes, N.J., Steinhilber, B., Smith, A.J.B., Kruger, S.J., and Schoenberg, R., 2018, Modern rather than Mesoarchaean oxidative weathering responsible for the heavy stable Cr isotopic signatures of the 2.95 Ga old Ijzermijn iron formation (South Africa): Geochimica et Cosmochimica Acta, v. 228, p. 157–189, https://doi.org/10.1016/j.gca.2018.02.034.

Albut, G., Kamber, B.S., Brüske, A., Beukes, N.J., Smith, A.J.B, and Schoenberg, R., 2019, Modern weathering in outcrop samples versus ancient paleoredox information in drill core samples from a Mesoarchaean marine oxygen oasis in Pongola Supergroup, South Africa: Geochimica et Cosmochimica Acta, v. 265, p. 330–353, https://doi.org/10.1016/j.gca.2019.09.001.

Alexander, B.W., Bau, M., Andersson, P., and Dulski, P., 2008, Continentally-derived solutes in shallow Archean seawater: Rare earth element and Nd isotope evidence in iron formation from the 2.9 Ga Pongola Supergroup, South Africa: Geochimica et Cosmochimica Acta, v. 72, p. 378–394, https://doi.org/10.1016/j.gca.2007.10.028.

Amend, J.P., McCollom, T.M., Hentscher, M., and Bach, W., 2011, Catabolic and anabolic energy for chemolithoautotrophs in deep-sea hydrothermal systems hosted in different rock types: Geochimica et Cosmochimica Acta, v. 75, p. 5736–5748, https://doi.org/10.1016/j.gca.2011.07.041.

Anbar, A.D., and Knoll, A.H., 2002, Proterozoic ocean chemistry and evolution: a bioinorganic bridge?: Science, v. 297, p. 1137–1142, https://doi.org/10.1016/j.gca.2011.07.041.

Anbar, A.D., Duan, Y., Lyons, T.W., Arnold, G.L., Kendall, B., Creaser, R.A., Kaufman, A.J., Gordon, G.W., Scott, C., Garvin, J., and Buick, R., 2007, A whiff of oxygen before the Great Oxidation Event?: Science, v. 317, p. 1903–1906, https://doi.org/10.1126/science.1140325.

Barley, M.E., Bekker, A., and Krapež, B., 2005, Late Archean to early Paleoproterozoic global tectonics, environmental change and the rise of atmospheric oxygen: Earth and Planetary Science Letters, v. 238, p. 156–171, https://doi.org/10.1016/j.epsl.2005.06.062.

Bau, M., and Dulski, P., 1996, Distribution of yttrium and rare-earth elements in the Penge and Kuruman iron-formations, Transvaal Supergroup, South Africa: Precambrian Research v. 79, p. 37–55, https://doi.org/10.1016/0301-9268(95)00087-9.

Bau, M., and Möller, P., 1993, Rare earth element systematics of the chemically precipitated component in early Precambrian iron formations and the evolution of the terrestrial atmosphere-hydrosphere-lithosphere system: Geochimica et Cosmochimica Acta: v. 57, p. 2239–2249, https://doi.org/10.1016/0016-7037(93)90566-F.

Baur, M.E., Hayes, J.M., Studley, S.A., and Walter, M.A., 1985, Millimeter-scale variations of stable isotope abundances in carbonates from banded iron-formations in the Hamersley Group of Western Australia: Economic Geology, v. 80, p. 270–282, https://doi.org/10.2113/gsecongeo.80.2.270.

Beal, E.J., House, C.H., and Orphan, V.J., 2009, Manganese- and iron-dependent marine methane oxidation: Science, v. 325, p. 184–187, https://doi.org/10.1126/science.1169984.

Bekker, A., and Holland, H.D., 2012, Oxygen overshoot and recovery during the early Paleoproterozoic: Earth and Planetary Science Letters, v. 317–318, p. 295–304, https://doi.org/10.1016/j.epsl.2011.12.012.

Bekker, A., Slack, J.F., Planavsky, N., Krapež, B., Hofmann, A., Konhauser, K.O., and Rouxel, O.J., 2010, Iron formation: The sedimentary product of a complex interplay among mantle, tectonic, oceanic, and biospheric processes: Economic Geology, v. 105, p. 467–508, https://doi.org/10.2113/gsecongeo.105.3.467.

Berner, R.A., and Rao, J.-L., 1994, Phosphorus in sediments of the Amazon River and estuary - Implications for the global flux of phosphorus to the sea: Geochimica et Cosmochimica Acta, v. 58, p. 2333–2339, https://doi.org/10.1016/0016-7037(94)90014-0.

Beukes, N.J., and Gutzmer, J., 2008, Origin and paleoenvironmental significance of major iron formations at the Archean-Paleoproterozoic boundary, *in* Hagemann, S., Rosière, C.A., Gutzmer, J., and Beukes, N.J., *eds.,* Banded Iron Formation-Related High-Grade Iron Ore: Reviews in Economic Geology, v. 15, p. 5–47, https://doi.org/10.5382/Rev.15.01.

Bjerrum, C.J., and Canfield, D.E., 2002, Ocean productivity before about 1.9 Gyr ago limited by phosphorus adsorption onto iron oxides: Nature, v. 417, p. 159–162, https://doi.org/10.1038/417159a.

Blättler, C.L., Claire, M.W., Prave, A.R., Kirsimäe, K., Higgins, J.A., Medvedev, P.V., Romashkin, A.E., Rychanchik, D.V., Zerkle, A.L., Paiste, K., Kreitsmann, T., Millar, I.L., Hayles, J.A., Bao, H., Turchyn, A.V., Warke, M.R., and Lepland, A., 2018, Two-billion-year-old evaporites capture Earth's great oxidation: Science, v. 360, p. 320–323, https://doi.org/10.1126/science.aar2687.

Boden, J.S., Konhauser, K.O., Robbins, L.J., and Sánchez-Baracaldo, P., 2021, Timing the evolution of antioxidant enzymes in cyanobacteria: Nature Communications, v. 12, 4742, https://doi.org/10.1038/s41467-021-24396-y.

Bolhar, R., Kamber, B.S., Moorbath, S., Fedo, C.M., and Whitehouse, M.J., 2004, Characterization of early Archaean chemical sediments by trace element signatures: Earth and Planetary Science Letters, v. 222, p. 43–60, https://doi.org/10.1016/j.epsl.2004.02.016.

Bonner, J.T., 1998, The origins of multicellularity: Integrative Biology, v. 1, p. 27–36, https://doi.org/10.1002/(SICI)1520-6602(1998)1:1<27::AID-INBI4>3.0.CO;2-6.

Brady, M.P., Tostevin, R., and Tosca, N.J., 2022, Marine phosphate availability and the chemical origins of life on Earth: Nature Communications, v. 13, 5162, https://doi.org/10.1038/s41467-022-32815-x.

Bräuer, S.L., Yavitt, J.B., and Zinder, S.H., 2004, Methanogenesis in McLean Bog, an acidic peat bog in upstate New York: stimulation by H_2/CO_2 in the presence of rifampicin, or by low concentrations of acetate: Geomicrobiology Journal, v. 21, p. 433–443, https://doi.org/10.1080/01490450490505400.

Brazelton, W.J., Schrenk, M.O., Kelley, D.S., and Baross, J.A., 2006, Methane- and sulfur-metabolizing microbial communities dominate the Lost City Hydrothermal Field ecosystem: Applied and Environmental Microbiology, v. 72, p. 6257–6270, https://doi.org/10.1128/AEM.00574-06.

Bruland, K.W., Middag, R., and Lohan, M.C., 2014, Controls of trace metals in seawater, *in* Holland, H.D., and Turekian, K.K., *eds.,* Treatise on Geochemistry (Second Edition). Elsevier, Oxford, p. 19–51, https://doi.org/10.1016/B978-0-08-095975-7.00602-1.

Canfield, D.E., 1998, A new model for Proterozoic ocean chemistry: Nature, v. 396, p. 450–453, https://doi.org/10.1038/24839.

Catling, D.C., Claire, M.W., and Zahnle, K.J., 2007, Anaerobic methanotrophy and the rise of atmospheric oxygen: Philosophical Transactions of the Royal Society A, v. 365, p. 1867–1888, https://doi.org/10.1098/rsta.2007.2047.

Cavicchioli, R., Curmi, P.M.G., Saunders, N., and Thomas, T., 2003, Pathogenic archaea: do they exist?: BioEssays, v. 25, p. 1119–1128, https://doi.org/10.1002/bies.10354.

Chan, C.S., Emerson, D., and Luther, G.W., 2016, The role of microaerophilic Fe-oxidizing micro-organisms in producing banded iron formations: Geobiology, v. 14, p. 509–528, https://doi.org/10.1111/gbi.12192.

Chi Fru, E., Rodríguez, N.P., Partin, C.A., Lalonde, S.V., Andersson, P.S., Weiss, D.J., El Albani, A., Rodushkin, I., and Konhauser, K.O., 2016, Cu isotopes in marine black shales record the Great Oxidation Event: Proceedings of the National Academy of Sciences, v. 113, p. 4941–4946, https://doi.org/10.1073/pnas.1523544113.

Chi Fru, E., Somogyi, A., El Albani, A., Medjoubi, K., Aubineau, J., Robbins, L.J., Lalonde, S.V., and Konhauser, K.O., 2019, The rise of oxygen-driven arsenic cycling at ca. 2.48 Ga: Geology, v. 47, p. 243–246, https://doi.org/10.1130/G45676.1.

Cloud, P.E., Jr., 1965, Significance of the Gunflint (Precambrian) microflora: Science, v. 148, p. 27–35, https://doi.org/10.1126/science.148.3666.27.

Condie, K.C., 1993, Chemical composition and evolution of the upper continental crust: contrasting results from surface samples and shales: Chemical Geology, v. 104, p. 1–37, https://doi.org/10.1016/0009-2541(93)90140-E.

Conley, D.J., Smith, W.M., Cornwell, J.C., and Fisher, T.R., 1995, Transformation of particle-bound phosphorus at the land-sea interface: Estuarian, Coastal and

Shelf Science, v. 40, p. 161–176, https://doi.org/10.1016/S0272-7714(05)80003-4.

Craddock, P.R., and Dauphas, N., 2011, Iron and carbon isotope evidence for microbial iron respiration throughout the Archean: Earth and Planetary Science Letters, v. 303, p. 121–132, https://doi.org/10.1016/j.epsl.2010.12.045.

Crowe, S.A., Jones, C., Katsev, S., Magen, C., O'Neill, A.H., Sturm, A., Canfield, D.E., Haffner, G.D., Mucci, A., Sundby, B., and Fowle, D.A., 2008, Photoferrotrophs thrive in an Archean ocean analogue: Proceedings of the National Academy of Sciences, v. 105, p. 15938–15943, https://doi.org/10.1073/pnas.0805313105.

Crowe, S.A. Katsev, S., Leslie, K., Sturm, A., Magen, C., Nomosatryo, S., Pack, M.A., Kessler, J.D., Reeburgh, W.S., Roberts, J.A., González, L., Haffner, G.D., Mucci, A., Sundby, B., and Fowle, D.A., 2011, The methane cycle in ferruginous Lake Matano: Geobiology, v. 9, p. 61–78, https://doi.org/10.1111/j.1472-4669.2010.00257.x.

Crowe, S.A., Døssing, L.N., Beukes, N.J., Bau, M., Kruger, S.J., Frei, R., and Canfield, D.E., 2013, Atmospheric oxygenation three billion years ago: Nature, v. 501, p. 535–538, https://doi.org/10.1038/nature12426.

Czaja, A.D., Johnson, C.M., Beard, B.L., Roden, E.E., Li, W., and Moorbath, S., 2013, Biological Fe oxidation controlled deposition of banded iron formation in the ca. 3370 Ma Isua Supracrustal Belt (West Greenland): Earth and Planetary Science Letters, v. 363, p. 192–203, https://doi.org/10.1016/j.epsl.2012.12.025.

Derry, L.A., 2015, Causes and consequences of mid Proterozoic anoxia: Geophysical Research Letters, v. 42, p. 8538–8546, https://doi.org/10.1002/2015GL065333.

Dorland, H.C., 1999, Paleoproterozoic Laterites, Red Beds and Ironstones of the Pretoria Group With Reference to the History of Atmospheric Oxygen: Unpublished MSc Thesis, Rand Afrikaans University, Johannesburg, South Africa, 147 p.

Døssing, L.N., Dideriksen, K., Stipp, S.L.S., and Frei, R., 2011, Reduction of hexavalent chromium by ferrous iron: A process of chromium isotope fractionation and its relevance to natural environments: Chemical Geology, v. 285, p. 157–166, https://doi.org/10.1016/j.chemgeo.2011.04.005.

Eickhoff, M., Obst, M., Schröder, C., Hitchcock, A.P., Tyliszczak, T., Martinez, R.E., Robbins, L.J., Konhauser, K.O., and Kappler, A., 2014, Nickel partitioning in biogenic and abiogenic ferrihydrite: The influence of silica and implications for ancient environments: Geochimica et Cosmochimica Acta, v. 140, p. 65–79, https://doi.org/10.1016/j.gca.2014.05.021.

Eigenbrode, J.L., and Freeman, K.H., 2006, Late Archean rise of aerobic microbial ecosystems: Proceedings of the National Academy of Sciences, v. 103, p. 15759–15764, https://doi.org/10.1073/pnas.0607540103.

Ellis, A.S., Johnson, T.M., and Bullen, T.D., 2002, Chromium isotopes and the fate of hexavalent chromium in the environment: Science, v. 295, p. 2060–2062, https://doi.org/10.1126/science.1068368.

Feely, R.A., Trefry, J.H., Lebon, G.T., and German, C.R., 1998, The relationship between P/Fe and V/Fe ratios in hydrothermal precipitates and dissolved phosphate in seawater: Geophysical Research Letters, v. 25, p. 2253–2256, https://doi.org/10.1029/98GL01546.

Fischer, W.W., and Knoll, A.H., 2009, An iron shuttle for deepwater silica in Late Archean and early Paleoproterozoic iron formation: Geological Society of America Bulletin, v. 121, p. 222–235, https://doi.org/10.1130/B26328.1.

Frausto da Silva, J.J.R., and Williams, R.J., 2001, The Biological Chemistry of the Elements: The Inorganic Chemistry of Life (2nd ed.): Oxford University Press, Oxford, UK, 600 p.

Frei, R., Gaucher, C., Poulton, S.W., and Canfield, D.E., 2009, Fluctuations in Precambrian atmospheric oxygenation recorded by chromium isotopes: Nature, v. 461, p. 250–253, https://doi.org/10.1038/nature08266.

Frost, C.D., von Blanckenburg, F., Schoenberg, R., Frost, B.R., and Swapp, S.M., 2007, Preservation of Fe isotope heterogeneities during diagenesis and metamorphism of banded iron formation: Contributions to Mineralogy and Petrology, v. 153, p. 211–235, https://doi.org/10.1007/s00410-006-0141-0.

Gaillard, F., Scaillet, B., and Arndt, N.T., 2011, Atmospheric oxygenation caused by a change in volcanic degassing pressure: Nature, v. 478, p. 229–232, https://doi.org/10.1038/nature10460.

Garcia, A.K., Cavanaugh, C.M., and Kacar, B., 2021, The curious consistency of carbon biosignatures over billions of years of Earth-life coevolution: The ISME Journal, v. 15, p. 2183–2194, https://doi.org/10.1038/s41396-021-00971-5.

Gauger, T., Byrne, J.M., Konhauser, K.O., Obst, M., Crowe, S., and Kappler, A., 2016, Influence of organics and silica on Fe(II) oxidation rates and cell–mineral aggregate formation by the green-sulfur Fe(II)-oxidizing bacterium *Chlorobium ferrooxidans* KoFox – Implications for Fe(II) oxidation in ancient oceans: Earth and Planetary Science Letters, v. 443, p. 81–89, https://doi.org/10.1016/j.epsl.2016.03.022.

Gérard, F., 2016, Clay minerals, iron/aluminum oxides, and their contribution to phosphate sorption in soils – A myth revisited: Geoderma, v. 262, p. 213–226, https://doi.org/10.1016/j.geoderma.2015.08.036.

Godfrey, L.V., and Falkowski, P.G., 2009, The cycling and redox state of nitrogen in the Archaean ocean: Nature Geoscience, v. 2, p. 725–729, https://doi.org/10.1038/ngeo633.

Gole, M.J., and Klein, C., 1981, Banded iron-formations through much of Precambrian time: The Journal of Geology, v. 89, p. 169–183, https://doi.org/10.1086/628578.

Gross, G.A., 1980, A classification of iron-formation based on depositional environments: Canadian Mineralogist, v. 18, p. 215–222.

Grotzinger, J.P., and Knoll, A.H., 1999, Stromatolites in Precambrian carbonates: evolutionary mileposts or environmental dipsticks?: Annual Reviews of Earth and Planetary Sciences, v. 27, p. 313–358, https://doi.org/10.1146/annurev.earth.27.1.313.

Hagemann, S.G., Angerer, T., Duuring, P., Rosière, C.A., Figueiredo e Silva, R.C., Lobato, L., Hensler, A.S., and Walde, D.H.G., 2016, BIF-hosted iron mineral system: A review: Ore Geology Reviews, v. 76, p. 317–359, https://doi.org/10.1016/j.oregeorev.2015.11.004.

Halama, M., Swanner, E.D., Konhauser, K.O., and Kappler, A., 2016, Evaluation of siderite and magnetite formation in BIFs by pressure-temperature experiments of Fe(III) minerals and microbial biomass: Earth and Planetary Science Letters, v. 450, p. 243–253, https://doi.org/10.1016/j.epsl.2016.06.032.

Halevy, I., Alesker, M., Schuster, E.M., Popovitz-Biro, R., and Feldman, Y., 2017, A key role for green rust in the Precambrian oceans and the genesis of iron formations: Nature Geoscience, v. 10, p. 135–139, https://doi.org/10.1038/ngeo2878.

Hao, J., Knoll, A.H., Huang, F., Hazen, R.M., and Daniel, I., 2020, Cycling phosphorus on the Archean Earth: Part I. Continental weathering and riverine transport of phosphorus: Geochimica et Cosmochimica Acta, v. 273, p. 70–84, https://doi.org/10.1016/j.gca.2020.01.027.

Hao, W., Mänd, K., Li, Y., Alessi, D.S., Somelar, P., Moussavou, M., Romashkin, A.E., Lepland, A., Kirsimäe, K., Planavsky, N.J., and Konhauser, K.O., 2021, The kaolinite shuttle links the Great Oxidation and Lomagundi events: Nature Communications, v. 12, 2944, https://doi.org/10.1038/s41467-021-23304-8.

Hao, W., Chen, N., Sun, W., Mänd, K., Kirsimäe, K., Teitler, Y., Somelar, P., Robbins, L.J., Babechuk, M.G., Planavsky, N.J., Alessi, D.S., and Konhauser, K.O., 2022, Binding and transport of Cr(III) by clay minerals during the Great Oxidation Event: Earth and Planetary Science Letters, v. 584, 117503, https://doi.org/10.1016/j.epsl.2022.117503.

Hartman, H., 1984, The evolution of photosynthesis and microbial mats: A speculation on the banded iron formations, *in* Cohen, Y., Castenholz, R.W., and Halvorson, H.O., *eds.,* Microbial Mats: Stromatolites: Alan R. Liss, Incorporated, New York, p. 449–453.

Haugaard, R., Frei, R., Stendal, H., and Konhauser, K.O., 2013, Petrology and geochemistry of the ~2.9 Ga Itilliarsuk banded iron formation and associated supracrustal rocks, West Greenland: Source characteristics and depositional environment: Precambrian Research, v. 229, p. 150–176, https://doi.org/10.1016/j.precamres.2012.04.013.

Hausinger, R.P., 1987, Nickel utilization by microorganisms: Microbiological Reviews, v. 51, p. 22–42, https://doi.org/10.1128/mr.51.1.22-42.1987.

Heimann, A., Johnson, C.M., Beard, B.L., Valley, J.W., Roden, E.E., Spicuzza, M.J., and Beukes, N.J., 2010, Fe, C, and O isotope compositions of banded iron formation carbonates demonstrate a major role for dissimilatory iron reduction in ~ 2.5 Ga marine environments: Earth and Planetary Science Letters, v. 294, p. 8–18, https://doi.org/10.1016/j.epsl.2010.02.015.

Hemmingsson, C., Pitcain, I.K., and Chi Fru, E., 2018, Evaluation of phosphate-uptake mechanisms by Fe(III)(oxyhydr)oxides in early Proterozoic oceanic conditions: Environmental Chemistry, v. 15, p. 18–28, https://doi.org/10.1071/EN17124.

Hibbing, M.E., Fuqua, C., Parsek, M.R., and Peterson, S.B., 2010, Bacterial competition: surviving and thriving in the microbial jungle: Nature Reviews Microbiology, v. 8, p. 15–25, https://doi.org/10.1038/nrmicro2259.

Hoffman, P.F., Kaufman, A.J., Halverson, G.P., and Schrag, D.P., 1998, A Neoproterozoic snowball Earth: Science, v. 281, p. 1342–1346, https://doi.org/10.1126/science.281.5381.1342.

Holland, H.D., 1973, The oceans; A possible source of iron in iron-formations: Economic Geology, v. 68, p. 1169–1172, https://doi.org/10.2113/ gsecongeo.68.7.1169.

Holland, H.D., 1978, The Chemistry of the Atmosphere and Oceans: Wiley, New York, 369 p.

Holland, H.D., 1984, The Chemical Evolution of the Atmosphere and Oceans: Princeton University Press, Princeton, NJ, 598 p., https://doi.org/10.1515/

9780691220239.
Homann, M., Sansjofre, P., Van Zuilen, M., Heubeck, C., Gong, J., Killingsworth, B., Foster, I.S., Airo, A., Van Kranendonk, M.J., Ader, M., and Lalonde, S.V., 2018, Microbial life and biogeochemical cycling on land 3,220 million years ago: Nature Geoscience, v. 11, p. 665–671, https://doi.org/10.1038/s41561-018-0190-9.
Immenhauser, A., 2009, Estimating palaeo-water depth from the physical rock record: Earth-Science Reviews, v. 96, p. 107–139, https://doi.org/10.1016/j.earscirev.2009.06.003.
Isley, A.E., 1995, Hydrothermal plumes and the delivery of iron to banded iron formation: The Journal of Geology, v. 103, p. 169–185, https://doi.org/10.1086/629734.
Isley, A.E., and Abbott, D.H., 1999, Plume-related mafic volcanism and the deposition of banded iron formation: Journal of Geophysical Research, v. 104, p. 15461–15477, https://doi.org/10.1029/1999JB900066.
Jabłońska, J., and Tawfik, D.S., 2021, The evolution of oxygen-utilizing enzymes suggests early biosphere oxygenation: Nature Ecology & Evolution, v. 5, p. 442–448, https://doi.org/10.1038/s41559-020-01386-9.
Jiang, C.Z., and Tosca, N.J., 2019, Fe(II)-carbonate precipitation kinetics and the chemistry of anoxic ferruginous seawater: Earth and Planetary Science Letters, v. 506, p. 231–242, https://doi.org/10.1016/j.epsl.2018.11.010.
Joeckel, R.M., Ang Clement, B.J., and VanFleet Bates, L.R., 2005, Sulfate-mineral crusts from pyrite weathering and acid rock drainage in the Dakota Formation and Graneros Shale, Jefferson County, Nebraska: Chemical Geology, v. 215, p. 433–452, https://doi.org/10.1016/j.chemgeo.2004.06.044.
Johnson, C.M., Beard, B.L., Klein, C., Beukes, N.J., and Roden, E.E., 2008, Iron isotopes constrain biologic and abiologic processes in banded iron formation genesis: Geochimica et Cosmochimica Acta, v. 72, p. 151–169, https://doi.org/10.1016/j.gca.2007.10.013.
Johnson, J.E., Muhling, J.R., Cosmidis, J., Rasmussen, B., and Templeton, A.S., 2018, Low Fe (III) greenalite was a primary mineral from Neoarchean oceans: Geophysical Research Letters, v. 45, p. 3182–3192, https://doi.org/10.1002/2017GL076311.
Jones, C., Nomosatryo, S., Crowe, S.A., Bjerrum, C.J., and Canfield, D.E., 2015, Iron oxides, divalent cations, silica, and the early earth phosphorus crisis: Geology, v. 43, p. 135–138, https://doi.org/10.1130/G36044.1.
Kappler, A., Pasquero, C., Konhauser, K.O., and Newman, D.K., 2005, Deposition of banded iron formations by anoxygenic phototrophic Fe(II)-oxidizing bacteria: Geology, v. 33, p. 865–868, https://doi.org/10.1130/G21658.1.
Karhu, J.A., and Holland, H.D., 1996, Carbon isotopes and the rise of atmospheric oxygen: Geology, v. 24, p. 867–870, https://doi.org/10.1130/0091-7613(1996)024<0867:CIATRO>2.3.CO;2.
Kasting, J.F., 2013, What caused the rise of atmospheric O_2?: Chemical Geology, v. 362, p. 13–25, https://doi.org/10.1016/j.chemgeo.2013.05.039.
Kendall, B., Reinhard, C.T., Lyons, T.W., Kaufman, A.J., Poulton, S.W., and Anbar, A.D., 2010, Pervasive oxygenation along late Archaean ocean margins: Nature Geoscience, v. 3, p. 647–652, https://doi.org/10.1038/ngeo942.
Kharecha, P.A., Kasting, J.F., and Siefert, J.L., 2005, A coupled atmosphere-ecosystem model of the early Archean Earth: Geobiology, v. 3, p. 53–76, https://doi.org/10.1111/j.1472-4669.2005.00049.x.
Kipp, M.A., and Stueken, E.E., 2017, Biomass recycling and Earth's early phosphorus cycle: Science Advances, v. 3, eaao4795, https://doi.org/10.1126/sciadv.aao4795.
Klein, C., 2005, Presidential Address to the Mineralogical Society of America, Boston, November 6, 2001: Some Precambrian banded iron-formations (BIFs) from around the world: Their age, geologic setting, mineralogy, metamorphism, geochemistry, and origin: American Mineralogist, v. 90, p. 1473–1499, https://doi.org/10.2138/am.2005.1871.
Klein, C., and Beukes, N.J., 1989, Geochemistry and sedimentology of a facies transition from limestone to iron-formation deposition in the early Proterozoic Transvaal Supergroup, South Africa: Economic Geology, v. 84, p. 1733–1774, https://doi.org/10.2113/gsecongeo.84.7.1733.
Klein, C., and Beukes, N.J., 1993, Sedimentology and geochemistry of the glaciogenic late Proterozoic Rapitan iron-formation in Canada: Economic Geology, v. 88, p. 542–565, https://doi.org/10.2113/gsecongeo.88.3.542.
Knoll, A.H., 1984, The Archean/Proterozoic transition: A sedimentary and paleobiologies perspective, *in* Holland, H.D., and Trendall, A.F., *eds*., Patterns of Change in Earth Evolution: Dahlem Workshop Reports Physical, Chemical, and Earth Sciences Research Reports, v. 5, Springer, Berlin, p. 221–242, https://doi.org/10.1007/978-3-642-69317-5_13.
Köhler, I., Konhauser, K.O., Papineau, D., Bekker, A., and Kappler, A., 2013, Biological carbon precursor to diagenetic siderite with spherical structures in iron formations: Nature Communications, v. 4, 1741, https://doi.org/10.1038/ncomms2770.
Konhauser, K.O., 2007, Introduction to Geomicrobiology: Blackwell, Oxford. 425 p.
Konhauser, K.O., Hamade, T., Raiswell, R., Morris, R.C., Ferris, F.G., Southam, G., and Canfield, D.E., 2002, Could bacteria have formed the Precambrian banded iron formations?: Geology, v. 30, p. 1079–1082, https://doi.org/10.1130/0091-7613(2002)030<1079:CBHFTP>2.0.CO;2.
Konhauser, K.O., Newman, D.K., and Kappler, A., 2005, The potential significance of microbial Fe(III) reduction during Precambrian banded iron formations: Geobiology, v. 3, p. 167–177, https://doi.org/10.1111/j.1472-4669.2005.00055.x.
Konhauser, K.O., Lalonde, S.V., Amskold, L., and Holland, H.D., 2007a, Was there really an Archean phosphate crisis?: Science, v. 315, 1234, https://doi.org/10.1126/science.1136328.
Konhauser, K.O., Amskold, L., Lalonde, S.V., Posth, N.R., Kappler, A., and Anbar, A., 2007b, Decoupling photochemical Fe(II) oxidation from shallow-water BIF deposition: Earth and Planetary Science Letters, v. 258, p. 87–100, https://doi.org/10.1016/j.epsl.2007.03.026.
Konhauser, K.O., Pecoits, E., Lalonde, S.V., Papineau, D., Nisbet, E.G., Barley, M.E., Arndt, N.T., Zahnle, K., and Kamber, B.S., 2009, Oceanic nickel depletion and a methanogen famine before the Great Oxidation Event: Nature, v. 458, p. 750–753, https://doi.org/10.1038/nature07858.
Konhauser, K.O., Lalonde, S.V., Planavsky, N.J., Pecoits, E., Lyons, T.W., Mojzsis, S.J., Rouxel, O.J., Barley, M.E., Rosière, C., Fralick, P.W., Kump, L.R., and Bekker, A., 2011, Aerobic bacterial pyrite oxidation and acid rock drainage during the Great Oxidation Event: Nature, v. 478, p. 369–373, https://doi.org/10.1038/nature10511.
Konhauser, K.O., Robbins, L.J., Pecoits, E., Peacock, C., Kappler, A., and Lalonde, S.V., 2015, The Archean nickel famine revisited: Astrobiology, v. 15, p. 804–815, https://doi.org/10.1089/ast.2015.1301.
Konhauser, K.O., Planavsky, N.J., Hardisty, D.S., Robbins, L.J., Warchola, T.J., Haugaard, R., Lalonde, S.V., Partin, C.A., Oonk, P.B.H., Tsikos, H., Lyons, T.W., Bekker, A., and Johnson, C.M., 2017, Iron formations: A global record of Neoarchaean to Palaeoproterozoic environmental history: Earth-Science Reviews, v. 172, p. 140–177, https://doi.org/10.1016/j.earscirev.2017.06.012.
Konhauser, K.O., Robbins, L.J., Alessi, D.S., Flynn, S.L., Gingras, M.K., Martinez, R.E., Kappler, A., Swanner, E.D., Li, Y-L., Crowe, S.A., Planavsky, N.J., Reinhard, C.T., and Lalonde, S.V., 2018, Phytoplankton contributions to the trace-element composition of Precambrian banded iron formations: Geological Society of America Bulletin, v. 130, p. 941–951, https://doi.org/10.1130/B31648.1.
Koschwanez, J.H., Foster, K.R., and Murray, A.W., 2011, Sucrose utilization in budding yeast as a model for the origin of undifferentiated multicellularity: PLoS Biology, v. 9, e1001122, https://doi.org/10.1371/journal.pbio.1001122.
Kump, L.R., and Barley, M.E., 2007, Increased subaerial volcanism and the rise of atmospheric oxygen 2.5 billion years ago: Nature, v. 448, p. 1033–1036, https://doi.org/10.1038/nature06058.
Laakso, T.A., and Schrag, D.P., 2018, Limitations on limitation: Global Biogeochemical Cycles, v. 32, p. 486–496, https://doi.org/10.1002/2017GB005832.
Lalonde, S.V., and Konhauser, K.O., 2015, Benthic perspective on Earth's oldest evidence for oxygenic photosynthesis: Proceedings of the National Academy of Sciences, v. 112, p. 995–1000, https://doi.org/10.1073/pnas.1415718112.
Large, R.R., Halpin, J.A., Danyushevsky, L.V., Maslennikov, V.V., Bull, S.W., Long, J.A., Gregory, D.D., Lounejeva, E., Lyons, T.W., Sack, P.J., McGoldrick, P.J., and Calver, C.R., 2014, Trace element content of sedimentary pyrite as a new proxy for deep-time ocean-atmosphere evolution: Earth and Planetary Science Letters, v. 389, p. 209–220, https://doi.org/10.1016/j.epsl.2013.12.020.
Lechte, M., and Wallace, M., 2016, Sub-ice shelf ironstone deposition during the Neoproterozoic Sturtian glaciation: Geology, v. 44, p. 891–894, https://doi.org/10.1130/G38495.1.
Levitus, S., Conkright, M.E., Reid, J.L., Najjar, R.G., and Mantyla, A., 1993, Distribution of nitrate, phosphate and silicate in the world oceans: Progress in Oceanography, v. 31, p. 245–273, https://doi.org/10.1016/0079-6611(93)90003-V.
Li, Y., Sutherland, B.R., Gingras, M.K., Owttrim, G.W., and Konhauser, K.O., 2021, A novel approach to investigate the deposition of (bio)chemical sediments: The sedimentation velocity of cyanobacteria-ferrihydrite aggregates: Journal of Sedimentary Research, v. 91, p. 390–398, https://doi.org/10.2110/jsr.2020.114.
Li, Y.-L., Konhauser, K.O., Cole, D.R., and Phelps, T.J., 2011, Mineral ecophysiological data provide growing evidence for microbial activity in banded-iron formation: Geology, v. 39, p. 707–710, https://doi.org/10.1130/G32003.1.
Li, Y.-L., Konhauser, K.O., Kappler, A., and Hao, X.-L., 2013, Experimental low-grade alteration of biogenic magnetite indicates microbial involvement in generation of banded iron formations: Earth and Planetary Science Letters, v. 361,

p. 229–237, https://doi.org/10.1016/j.epsl.2012.10.025.
Li, Y.-L., Konhauser, K.O., and Zhai, M., 2017, The formation of primary magnetite in the early Archean oceans: Earth and Planetary Science Letters, v. 466, p. 103–114, https://doi.org/10.1016/j.epsl.2017.03.013.
Li, Z.-Q., Zhang, L.-C., Xue, C.-J., Zheng, M.-T., Zhu, M.-T., Robbins, L.J., Slack, J.F., Planavsky, N.J., and Konhauser, K.O., 2018, Earth's youngest banded iron formation implies ferruginous conditions in the Early Cambrian ocean: Scientific Reports, v. 8, 9970, https://doi.org/10.1038/s41598-018-28187-2.
Liu, H., Konhauser, K.O., Robbins, L.J., and Sun, W.D., 2021, Global continental volcanism controlled the evolution of oceanic nickel concentrations: Earth and Planetary Science Letters, v. 572, 117116, https://doi.org/10.1016/j.epsl.2021.117116.
Lovelock, J.E., 1972, Gaia as seen through the atmosphere: Atmospheric Environment (1967), v. 6, p. 579–580, https://doi.org/10.1016/0004-6981(72)90076-5.
Lyons, T.W., Reinhard, C.T., and Planavsky, N.J., 2014, The rise of oxygen in Earth's early ocean and atmosphere: Nature, v. 506, p. 307–315, https://doi.org/10.1038/nature13068.
Mahmoudi, N., Steen, A.D., Halverson, G.P., and Konhauser, K.O., 2023, Biogeochemistry of Earth before exoenzymes: Nature Geosciences, v. 16, p. 845–850, https://doi.org/10.1038/s41561-023-01266-4.
Maliva, R.G., Knoll, A.H., and Simonson, B.M., 2005, Secular change in the Precambrian silica cycle: Insights from chert petrology: Geological Society of America Bulletin, v. 117, p. 835–845, https://doi.org/10.1130/B25555.1.
Mayika, K.B., Moussavou, M., Prave, A.R., Lepland, A., Mbina, M., and Kirsimäe, K., 2020, The Paleoproterozoic Francevillian succession of Gabon and the Lomagundi-Jatuli event: Geology, v. 48, p. 1099–1104, https://doi.org/10.1130/G47651.1.
McNamara, K.J., and Awramik, S.M., 1992, Stromatolites: a key to understanding the early evolution of life: Science Progress, v. 76, p. 345–364, https://www.jstor.org/stable/43421308.
Mloszewska, A.M., Pecoits, E., Cates, N.L., Mojzsis, S.J., O'Neil, J., Robbins, L.J., and Konhauser, K.O., 2012, The composition of Earth's oldest iron-formations: The Nuvvuagittuq supracrustal belt (Quebec, Canada): Earth and Planetary Science Letters, v. 317–318, p. 331–342, https://doi.org/10.1016/j.epsl.2011.11.020.
Mloszewska, A.M., Cole, D.M., Planavsky, N.J., Kappler, A., Whitford, D.S., Owttrim, G.W., and Konhauser, K.O., 2018, UV radiation limited the expansion of cyanobacteria in early marine photic environments: Nature Communications, v. 9, 3008, https://doi.org/10.1038/s41467-018-05520-x.
Morel, F.M.M., and Price, N.M., 2003, The biogeochemical cycles of trace metals in the oceans: Science, v. 300, p. 944–947, https://doi.org/10.1126/science.1083545.
Morris, R.C., 1993, Genetic modelling for banded iron-formations of the Hamersley Group, Pilbara Craton, Western Australia: Precambrian Research, v. 60, p. 243–286, https://doi.org/10.1016/0301-9268(93)90051-3.
Nealson, K.H., and Myers, C.R., 1990, Iron reduction by bacteria: A potential role in the genesis of banded iron formations: American Journal of Science, v. 290, p. 35–45.
Nims, C., and Johnson, J.E., 2022, Exploring the secondary mineral products generated by microbial iron respiration in Archean ocean simulations: Geobiology, v. 20, p. 743–763, https://doi.org/10.1111/gbi.12523.
Olson, S.L., Kump, L.R., and Kasting, J.F., 2013, Quantifying the areal extent and dissolved oxygen concentrations of Archean oxygen oases: Chemical Geology, v. 362, p. 35–43, https://doi.org/10.1016/j.chemgeo.2013.08.012.
Ossa Ossa, F., Hofmann, A., Vidal, O., Kramers, J.D., Belyanin, G., Cavalazzi, B., 2016, Unusual manganese enrichment in the Mesoarchean Mozaan Group, Pongola Supergroup, South Africa: Precambrian Research, v. 281, p. 414–433, https://doi.org/10.1016/j.precamres.2016.06.009.
Ostrander, C.M., Johnson, A.C., and Anbar, A.D., 2021, Earth's first redox revolution: Annual Review of Earth and Planetary Sciences, v. 49, p. 337–366, https://doi.org/10.1146/annurev-earth-072020-055249.
Oze, C., Bird, D.K., and Fendorf, S., 2007, Genesis of hexavalent chromium from natural sources in soil and groundwater: Proceedings of the National Academy of Sciences, v. 104, p. 6544–6549, https://doi.org/10.1073/pnas.0701085104.
Partin, C.A., Bekker, A., Planavsky, N.J., Scott, C.T., Gill, B.C., Li, C., Podkovyrov, V., Maslov, A., Konhauser, K.O., Lalonde, S.V., Love, G.D., Poulton, S.W., and Lyons, T.W., 2013, Large-scale fluctuations in Precambrian atmospheric and oceanic oxygen levels from the record of U in shales: Earth and Planetary Science Letters, v. 369–370, p. 284–293, https://doi.org/10.1016/j.epsl.2013.03.031.
Pecoits, E., Gingras, M.K., Barley, M.A., Kappler, A., Posth, N.R., and Konhauser, K.O., 2009, Petrography and trace element geochemistry of the Dales Gorge banded iron formation: Paragenetic sequence, source and implications for palaeo-ocean chemistry: Precambrian Research, v. 172, p. 163–187, https://doi.org/10.1016/j.precamres.2009.03.014.
Percak-Dennett, E.M., Beard, B.L., Xu, H., Konishi, H., Johnson, C.M., and Roden, E.E., 2011, Iron isotope fractionation during microbial dissimilatory iron oxide reduction in simulated Archaean seawater: Geobiology, v. 9, p. 205–220, https://doi.org/10.1111/j.1472-4669.2011.00277.x.
Peters, S.E., and Loss, D.P., 2012, Storm and fair-weather wave base: A relevant distinction?: Geology, v. 40, p. 511–514, https://doi.org/10.1130/G32791.1.
Planavsky, N.J., Rouxel, O.J., Bekker, A., Lalonde, S.V., Konhauser, K.O., Reinhard, C.T., and Lyons, T.W., 2010, The evolution of the marine phosphate reservoir: Nature, v. 467, p. 1088–1090, https://doi.org/10.1038/nature09485.
Planavsky, N.J., Rouxel, O.J., Bekker, A., Hofmann, A., Little, C.T.S., and Lyons, T.W., 2012a, Iron isotope composition of some Archean and Proterozoic iron formations: Geochimica et Cosmochimica Acta, v. 80, p. 158–169, https://doi.org/10.1016/j.gca.2011.12.001.
Planavsky, N.J., Bekker, A., Hofmann, A., Owens, J.D., and Lyons, T.W., 2012b, Sulfur record of rising and falling marine oxygen and sulfate levels during the Lomagundi event: Proceedings of the National Academy of Sciences, v. 109, p. 18300–18305, https://doi.org/10.1073/pnas.1120387109.
Planavsky, N.J., Asael, D., Hofmann, A., Reinhard, C.T., Lalonde, S.V., Knudsen, A., Wang, X., Ossa Ossa, F., Pecoits, E., Smith, A.J.B., Beukes, N.J., Bekker, A., Johnson, T.M., Konhauser, K.O., Lyons, T.W., and Rouxel, O.J., 2014, Evidence for oxygenic photosynthesis half a billion years before the Great Oxidation Event: Nature Geoscience, v. 7, p. 283–286, https://doi.org/10.1038/ngeo2122.
Planavsky, N., Crowe, S.A., Fakhraee, M., Beaty, B., Reinhard, C.T., Mills, B.J.W., Holstege, C., and Konhauser, K.O., 2021, Evolution of the structure and impact of Earth's biosphere: Nature Reviews Earth & Environment, v. 2, p. 123–139, https://doi.org/10.1038/s43017-020-00116-w.
Posth, N.R., Hegler, F., Konhauser, K.O., and Kappler, A., 2008, Alternating Si and Fe deposition caused by temperature fluctuations in Precambrian oceans: Nature Geoscience, v. 1, p. 703–708, https://doi.org/10.1038/ngeo306.
Posth, N.R., Huelin, S., Konhauser, K.O., and Kappler, A., 2010, Size, density and composition of cell–mineral aggregates formed during anoxygenic phototrophic Fe(II) oxidation: Impact on modern and ancient environments: Geochimica et Cosmochimica Acta, v. 74, p. 3476–3493, https://doi.org/10.1016/j.gca.2010.02.036.
Posth, N.R., Konhauser, K.O., and Kappler, A., 2013a, Microbiological processes in banded iron formation deposition: Sedimentology, v. 60, p. 1733–1754, https://doi.org/10.1111/sed.12051.
Posth, N.R., Köhler, I., Swanner, E.D., Schröder, C., Wellman, E., Binder, B., Konhauser, K.O., Neumann, U., Berthold, C., Nowak, M., and Kappler, A., 2013b, Simulating Precambrian banded iron formation diagenesis: Chemical Geology, v. 362, p. 66–73, https://doi.org/10.1016/j.chemgeo.2013.05.031.
Poulton, S.W., Fralick, P.W., and Canfield, D.E., 2004, The transition to a sulphidic ocean ~1.84 billion years ago: Nature, v. 431, p. 173–177, https://doi.org/10.1038/nature02912.
Prave, A.R., Kirsimäe, K., Lepland, A., Fallick, A.E., Kreitsmann, T., Deines, Yu.E., Romashkin, A.E., Rychanchik, D.V., Medvedev, P.V., Moussavou, M., Bakakas, K., and Hodgskiss, M.S.W., 2022, The grandest of them all: the Lomagundi-Jatuli Event and Earth's oxygenation: Journal of the Geological Society, v.179, p. 2021–2036, https://doi.org/10.1144/jgs2021-036.
Ragsdale, S.W., and Kumar, M., 1996, Nickel-containing carbon monoxide dehydrogenase/acetyl-CoA synthase: Chemical Reviews, v. 96, p. 2515–2540, https://doi.org/10.1021/cr950058+.
Rai, D., Eary, L.E., and Zachara, J.M., 1989, Environmental chemistry of chromium: Science of the Total Environment, v. 86, p. 15–23, https://doi.org/10.1016/0048-9697(89)90189-7.
Rasmussen, B., and Muhling, J.R., 2018, Making magnetite late again: Evidence for widespread magnetite growth by thermal decomposition of siderite in Hamersley banded iron formations: Precambrian Research, v. 306, p. 64–93, https://doi.org/10.1016/j.precamres.2017.12.017.
Rasmussen, B., and Muhling, J.R., 2020, Hematite replacement and oxidative overprinting recorded in the 1.88 Ga Gunflint iron formation, Ontario, Canada: Geology, v. 48, p. 688–692, https://doi.org/10.1130/G47410.1.
Rasmussen, B., Krapež, B., and Meier, D.B., 2014, Replacement origin for hematite in 2.5 Ga banded iron formation: Evidence of postdepositional oxidation of iron-bearing minerals: Geological Society of America Bulletin, v. 126, p. 438–446, https://doi.org/10.1130/B30944.1.
Rasmussen, B., Muhling, J.R., Suvorova, A., and Krapež, B., 2017, Greenalite precipitation linked to the deposition of banded iron formations downslope from a late Archean carbonate platform: Precambrian Research, v. 290, p. 49–62, https://doi.org/10.1016/j.precamres.2016.12.005.

Rasmussen, B., Muhling, J.R., and Krapež, B., 2021a, Greenalite and its role in the genesis of early Precambrian iron formations – A review: Earth-Science Reviews, v. 217, 103613, https://doi.org/10.1016/j.earscirev.2021.103613.
Rasmussen, B., Muhling, J.R., Suvorova, A., and Fischer, W.W., 2021b, Apatite nanoparticles in 3.46–2.46 Ga iron formations: Evidence for phosphorus-rich hydrothermal plumes on early Earth: Geology, v. 49, p. 647–651, https://doi.org/10.1130/G48374.1.
Reddy, T.R., Zheng, X.-Y., Roden, E.E., Beard, B.L., and Johnson, C.M., 2016, Silicon isotope fractionation during microbial reduction of Fe(III)-Si gels under Archean seawater conditions and implications for iron formation genesis: Geochimica et Cosmochimica Acta, v. 190, p. 85–99, https://doi.org/10.1016/j.gca.2016.06.035.
Reinhard, C.T., Raiswell, R., Scott, C., Anbar, A.D., and Lyons, T.W., 2009, A late Archean sulfidic sea stimulated by early oxidative weathering of the continents: Science, v. 326, p. 713–716, https://doi.org/10.1126/science.1176711.
Reinhard, C.T., Planavsky, N.J., Gill, B.C., Ozaki, K., Robbins, L.J., Lyons, T.W., Fischer, W.W., Wang, C., Cole, D.B., and Konhauser, K.O., 2017, Evolution of the global phosphorus cycle: Nature, v. 541, p. 386–389, https://doi.org/10.1038/nature20772.
Rico, K.I., Schad, M., Picard, A., Kappler, A., Konhauser, K.O., and Mahmoudi, N., 2023, Resolving the fate of trace metals during microbial remineralization of phytoplankton biomass in precursor banded iron formation sediments: Earth and Planetary Science Letters, v. 607, 118068, https://doi.org/10.1016/j.epsl.2023.118068.
Robbins, L.J., Lalonde, S.V., Saito, M.A., Planavsky, N.J., Mloszewska, A.M., Pecoits, E., Scott, C., Dupont, C.L., Kappler, A., and Konhauser, K.O., 2013, Authigenic iron oxide proxies for marine zinc over geological time and implications for eukaryotic metallome evolution: Geobiology, v. 11, p. 295–306, https://doi.org/10.1111/gbi.12036.
Robbins, L.J., Swanner, E.D., Lalonde, S.V., Eickhoff, M., Paranich, M.L., Reinhard, C.T., Peacock, C.L., Kappler, A., and Konhauser, K.O., 2015, Limited Zn and Ni mobility during simulated iron formation diagenesis: Chemical Geology, v. 402, p. 30–39, https://doi.org/10.1016/j.chemgeo.2015.02.037.
Robbins, L.J., Lalonde, S.V., Planavsky, N.J., Partin, C.A., Reinhard, C.T., Kendall, B., Scott, C., Hardisty, D.S., Gill, B.C., Alessi, D.S., Dupont, C.L., Saito, M.A., Crowe, S.A., Poulton, S.W., Bekker, A., Lyons, T.W., and Konhauser, K.O., 2016, Trace elements at the intersection of biological and geochemical evolution: Earth-Science Reviews, v. 163, p. 323–348, https://doi.org/10.1016/j.earscirev.2016.10.013.
Robbins, L.J., Konhauser, K.O., Warchola, T.J., Homann, M., Thoby, M., Foster, I., Mloszewska, A.M., Alessi, D.S., and Lalonde, S.V., 2019a, A comparison of bulk versus laser ablation trace element analyses in banded iron formations: Insights into the mechanisms leading to compositional variability: Chemical Geology, v. 506, p. 197–224, https://doi.org/10.1016/j.chemgeo.2018.12.036.
Robbins, L.J., Funk, S.P., Flynn, S.L., Warchola, T.J., Li, Z., Lalonde, S.V., Rostron, B.J., Smith, A.J.B., Beukes, N.J., de Kock, M.O., Heaman, L.M., Alessi, D.S., and Konhauser, K.O., 2019b, Hydrogeological constraints on the formation of Palaeoproterozoic banded iron formations: Nature Geoscience, v. 12, p. 558–563, https://doi.org/10.1038/s41561-019-0372-0.
Robbins, L.J., Fakhraee, M., Smith, A.J.B., Bishop, B.A., Swanner, E.D., Peacock, C.L., Wang, C.-L., Planavsky, N.J., Reinhard, C.T., Crowe, S.A., and Lyons, T.W., 2023, Manganese oxides, Earth surface oxygenation, and the rise of oxygenic photosynthesis: Earth-Science Reviews, v. 239, 104368, https://doi.org/10.1016/j.earscirev.2023.104368.
Rosing, M.T., and Frei, R., 2004, U-rich Archaean sea-floor sediments from Greenland – indications of >3700 Ma oxygenic photosynthesis: Earth and Planetary Science Letters, v. 217, p. 237–244, https://doi.org/10.1016/S0012-821X(03)00609-5.
Saito, M.A., Sigman, D.M., and Morel, F.M.M., 2003, The bioinorganic chemistry of the ancient ocean: the co-evolution of cyanobacterial metal requirements and biogeochemical cycles at the Archean–Proterozoic boundary?: Inorganica Chimica Acta, v. 356, p. 308–318, https://doi.org/10.1016/S0020-1693(03)00442-0.
Sánchez-Baracaldo, P., 2015, Origin of marine planktonic cyanobacteria: Scientific Reports, v. 5, 17418, https://doi.org/10.1038/srep17418.
Sánchez-Baracaldo, P., Bianchini, G., Wilson, J.D., and Knoll, A.H., 2022, Cyanobacteria and biogeochemical cycles through Earth history: Trends in Microbiology, v. 30, p. 143–157, https://doi.org/10.1016/j.tim.2021.05.008.
Schad, M., Halama, M., Bishop, B., Konhauser, K.O., and Kappler, A., 2019a, Temperature fluctuations in the Archean ocean as trigger for varve-like deposition of iron and silica minerals in banded iron formations: Geochimica et Cosmochimica Acta, v. 265, p. 386–412, https://doi.org/10.1016/j.gca.2019.08.031.
Schad, M., Konhauser, K.O., Sánchez-Baracaldo, P., Kappler, A., and Bryce, C., 2019b, How did the evolution of oxygenic photosynthesis influence the temporal and spatial development of the microbial iron cycle on ancient Earth?: Free Radical Biology and Medicine, v. 140, p. 154–166, https://doi.org/10.1016/j.freeradbiomed.2019.07.014.
Schad, M., Byrne, J.M., ThomasArrigo, L.K., Kretzschmar, R., Konhauser, K.O., and Kappler, A., 2022, Microbial Fe cycling in a simulated Precambrian ocean environment: Implications for secondary mineral (trans)formation and deposition during BIF genesis: Geochimica et Cosmochimica Acta, v. 331, p. 165–191, https://doi.org/10.1016/j.gca.2022.05.016.
Schidlowski, M., Eichmann, R., and Junge, C.E., 1976, Carbon isotope geochemistry of the Precambrian Lomagundi carbonate province, Rhodesia: Geochimica et Cosmochimica Acta, v. 40, p. 449–455, https://doi.org/10.1016/0016-7037(76)90010-7.
Schirrmeister, B.E., de Vos, J.M., Antonelli, A., and Bagheri, H.C., 2013, Evolution of multicellularity coincided with increased diversification of cyanobacteria and the Great Oxidation Event: Proceedings of the National Academy of Sciences, v. 110, p. 1791–1796, https://doi.org/10.1073/pnas.1209927110.
Scott, C., Wing, B.A., Bekker, A., Planavsky, N.J., Medvedev, P., Bates, S.M., Yun, M., and Lyons, T.W., 2014, Pyrite multiple-sulfur isotope evidence for rapid expansion and contraction of the early Paleoproterozoic seawater sulfate reservoir: Earth and Planetary Science Letters, v. 389, p. 95–104, https://doi.org/10.1016/j.epsl.2013.12.010.
Siever, R., 1992, The silica cycle in the Precambrian: Geochimica et Cosmochimica Acta, v. 56, p. 3265–3272, https://doi.org/10.1016/0016-7037(92)90303-Z.
Simonson, B.M., and Goode, A.D.T., 1989, First discovery of ferruginous chert arenites in the early Precambrian Hamersley Group of Western Australia: Geology, v. 17, p. 269–272, https://doi.org/10.1130/0091-7613(1989)017%3C0269:FDOFCA%3E2.3.CO;2.
Simonson, B.M., and Hassler, S.W., 1996, Was the deposition of large Precambrian iron formations linked to major marine transgressions?: The Journal of Geology, v. 104, p. 665–676, https://www.jstor.org/stable/30081160.
Smedley, P.L., and Kinniburgh, D.G., 2002, A review of the source, behaviour and distribution of arsenic in natural waters: Applied Geochemistry, v. 17, p. 517–568, https://doi.org/10.1016/S0883-2927(02)00018-5.
Smith, A.J.B., 2018, The iron formations of southern Africa, *in* Siegesmund, S., Basei, M.A.S., Oyhantçabal, P., and Oriolo, S., *eds*., Geology of Southwest Gondwana: Regional Geology Reviews, Springer, Cham, p. 469–491, https://doi.org/10.1007/978-3-319-68920-3_17.
Smith, A.J.B., and Beukes, N.J., 2023, The paleoenvironmental implications of pre-Great Oxidation Event manganese deposition in the Mesoarchean Ijzermijn Iron Formation Bed, Mozaan Group, Pongola Supergroup, South Africa: Precambrian Research, v. 384, 106922, https://doi.org/10.1016/j.precamres.2022.106922.
Smith, A.J.B., Beukes, N.J., and Gutzmer, J., 2013, The composition and depositional environments of Mesoarchean iron formations of the West Rand Group of the Witwatersrand Supergroup, South Africa: Economic Geology, v. 108, p. 111–134, https://doi.org/10.2113/econgeo.108.1.111.
Smith, A.J.B., Beukes, N.J., Gutzmer, J., Czaja, A.D., Johnson, C.M., and Nhleko, N., 2017, Oncoidal granular iron formation in the Mesoarchaean Pongola Supergroup, southern Africa: Textural and geochemical evidence for biological activity during iron deposition: Geobiology, v. 15, p. 731–749, https://doi.org/10.1111/gbi.12248.
Smith, A.J.B., Beukes, N.J., Cochrane, J.M., Gutzmer, J., 2023, Manganese carbonate-bearing mudstone of the Witwatersrand-Mozaan succession in southern Africa as evidence for bacterial manganese respiration and availability of free molecular oxygen in Mesoarchaean oceans: South African Journal of Geology, v. 126, p. 29–48, https://doi.org/10.25131/sajg.126.0005.
Søgaard, E.G., Medenwaldt, R., and Abraham-Peskir, J.V., 2000, Conditions and rates of biotic and abiotic iron precipitation in selected Danish freshwater plants and microscopic analysis of precipitate morphology: Water Research, v. 34, p. 2675–2682, https://doi.org/10.1016/S0043-1354(00)00002-6.
Steinhoefel, G., von Blackenburg, F., Horn, I., Konhauser, K.O., Beukes, N.J., and Gutzmer, J., 2010, Deciphering formation processes of banded iron formations from the Transvaal and the Hamersley successions by combined Si and Fe isotope analysis using UV femtosecond laser ablation: Geochimica et Cosmochimica Acta, v. 74, p. 2677–2696, https://doi.org/10.1016/j.gca.2010.01.028.
Sumner, D.Y., 1997, Carbonate precipitation and oxygen stratification in late Archean seawater as deduced from facies and stratigraphy of the Gamohaan and Frisco formations, Transvaal Supergroup, South Africa: American Journal of Science, v. 297, p. 455–487, https://doi.org/10.2475/ajs.297.5.455.
Sumner, D.Y., and Beukes, N.J., 2006, Sequence stratigraphic development of the Neoarchean Transvaal carbonate platform, Kaapvaal, Craton, South Africa:

South African Journal of Geology, v. 109, p. 11–22, https://doi.org/10.2113/gssajg.109.1-2.11.
Sun, S., Konhauser, K.O., Kappler, A., and Li, Y.-L., 2015, Primary hematite in Neoarchean to Paleoproterozoic oceans: Geological Society of America Bulletin, v. 127, p. 850–861, https://doi.org/10.1130/B31122.1.
Sunda, W.G., 2012, Feedback interactions between trace metal nutrients and phytoplankton in the ocean: Frontiers in Microbiology, v. 3, 204, https://doi.org/10.3389/fmicb.2012.00204.
Swanner, E.D., Mloszewska, A.M., Cirpka, O.A., Schoenberg, R., Konhauser, K.O., and Kappler, A., 2015, Modulation of oxygen production in Archaean oceans by episodes of Fe(II) toxicity: Nature Geoscience, v. 8, p. 126–130, https://doi.org/10.1038/ngeo2327.
Thompson, K.J., Kenward, P.A., Bauer, K.W., Warchola, T., Gauger, T., Martinez, R., Simister, R.L., Michiels, C.C., Llirós, M., Reinhard, C.T., Kappler, A., Konhauser, K.O., and Crowe, S.A., 2019, Photoferrotrophy, deposition of banded iron formations, and methane production in the Archean oceans: Science Advances, v. 5, eaav2869, https://doi.org/10.1126/sciadv.aav2869.
Tosca, N.J., and Tutolo, B.M., 2023, Hydrothermal vent fluid-seawater mixing and the origins of Archean iron formation: Geochimica et Cosmochimica Acta, v. 352, p. 51–68, https://doi.org/10.1016/j.gca.2023.05.002.
Tréguer, P., Nelson, D.M., Van Bennekom, A.J., DeMaster, D.J., Leynaert, A., and Quéguiner, B., 1995, The silica balance in the world ocean: A reestimate: Science, v. 268, p. 375–379, https://doi.org/10.1126/science.268.5209.375.
Trendall, A.F., 2002, The significance of iron-formation in the Precambrian stratigraphic record, *in* Altermann, W., and Corcoran, P.L., *eds.,* Precambrian Sedimentary Environments: A Modern Approach to Ancient Depositional Systems: International Association of Sedimentologists Special Publications, v. 33, p. 33–66, https://doi.org/10.1002/9781444304312.ch3.
Trendall, A., and Blockley, J., 1970, The Iron Formations of the Precambrian Hamersley Group, Western Australia with Special Reference to the Associated Crocidolite: Western Australia Geological Survey Bulletin, v. 119, 366 p.
Tyrrell, T., 1999, The relative influences of nitrogen and phosphorus on oceanic primary production: Nature, v. 400, p. 525–531, https://doi.org/10.1038/22941.
Tyson, R.V., and Pearson, T.H., 1991, Modern and ancient continental shelf anoxia: an overview: Geological Society, London, Special Publications, v. 58, p. 1–24, https://doi.org/10.1144/GSL.SP.1991.058.01.01.
Walker, J.C.G., 1984, Suboxic diagenesis in banded iron formations: Nature, v. 309, p. 340–342, https://doi.org/10.1038/309340a0.
Weber, M.F., Poxleitner, G., Hebisch, E., Frey, E., and Opitz, M., 2014, Chemical warfare and survival strategies in bacterial range expansions: Journal of the Royal Society Interface, v. 11, 20140172, https://doi.org/10.1098/rsif.2014.0172.
Whitehouse, M.J., and Fedo, C.M., 2007, Microscale heterogeneity of Fe isotopes in >3.71 Ga banded iron formation from the Isua Greenstone Belt, southwest Greenland: Geology, v. 35, p. 719–722, https://doi.org/10.1130/G23582A.1.
Widdel, F., Schnell, S., Heising, S., Ehrenreich, A., Assmus, B., and Schink, B., 1993, Ferrous iron oxidation by anoxygenic phototrophic bacteria: Nature, v. 362, p. 834–836, https://doi.org/10.1038/362834a0.
Wu, X., Zhu, J., He, H., Xian, H., Yang, Y., Ma, L., Liang, X., Lin, X., Li, S., Konhauser, K.O., and Li, Y., 2023, Geodynamic oxidation of the Archean terrestrial surfaces: Communications Earth & Environment, v. 4,132, https://doi.org/10.1038/s43247-023-00789-3.
Zahnle, K.J., Claire, M., and Catling, D., 2006, The loss of mass-independent fractionation in sulfur due to a Palaeoproterozoic collapse of atmospheric methane: Geobiology, v. 4, p. 271–283, https://doi.org/10.1111/j.1472-4669.2006.00085.x.
Zerkle, A.L., House, C.H., and Brantley, S.L., 2005, Biogeochemical signatures through time as inferred from whole microbial genomes: American Journal of Science, v. 305, p. 467–502, https://doi.org/10.2475/ajs.305.6-8.467.
Zheng, X.-Y., Beard, B.L., Reddy, T.R., Roden, E.E., and Johnson, C.M., 2016, Abiologic silicon isotope fractionation between aqueous Si and Fe(III)-Si gel in simulated Archean seawater: Implications for Si isotope records in Precambrian sedimentary rocks: Geochimica et Cosmochimica Acta, v. 187, p. 102–122, https://doi.org/10.1016/j.gca.2016.05.012.

Received August 2023
Accepted as revised October 2023

ARTICLE

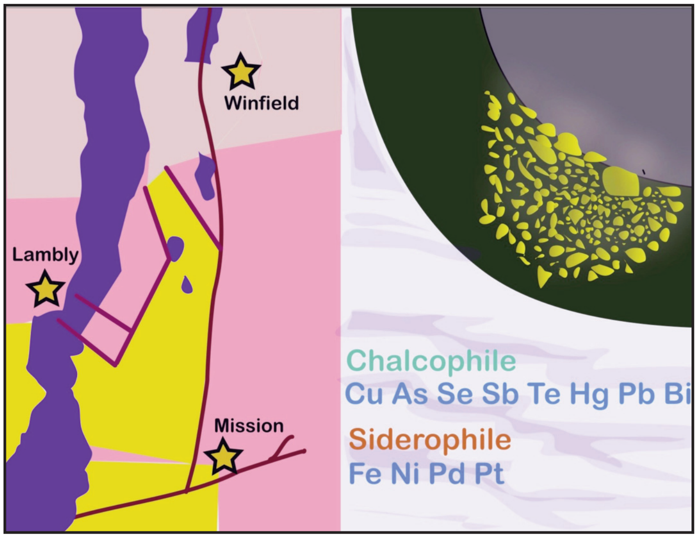

Trace Element Composition of Placer Gold Across the Okanagan Fault, Kelowna, British Columbia, Canada

John Greenough and Mikkel Tetland

Department of Earth, Environmental and Geographic Sciences
University of British Columbia, Okanagan
3333 University Way
Kelowna, British Columbia, Canada, V1V 1V7
E-mail: john.greenough@ubc.ca

SUMMARY

For 100 years, placer gold has been important to the settlement, economic development, and, recently, recreational geology of the Kelowna, British Columbia, area. It is best-known to occur in modern-day, Mission Creek and Lambly Creek sedimentary rocks, as well as a paleoplacer occurrence in Miocene sediments of the historical Winfield mine. The Mission Creek and Winfield localities are east of the west-dipping, low-angle, normal Okanagan Fault, which has been active since the Eocene. Lambly Creek is west of the fault. Late Paleozoic to Eocene igneous and metasedimentary rocks occur in the Lambly Creek catchment but Eocene gneiss units, unroofed by the fault, occur on the Okanagan Valley's east side. This study tests the hypothesis that native placer gold compositions vary across the Okanagan Fault reflecting different sources and histories for the gold. A modest number of Au and Ag analyses (23 analyses) in usefully representative placer gold samples were determined on a scanning electron microscope with an energy dispersive spectrometer (SEM-EDS). Spots analyzed for Au and Ag were also analyzed for 19 trace elements using laser ablation inductively coupled plasma mass spectrometry (LA-ICP-MS). Mercury was semi-quantitatively determined in 'unknown' gold grains by first estimating its concentration (~3.69 ppm) in the AuRM2 external standard. Proportions of Au:Ag:Cu in grain cores indicate all the gold came from mesothermal/hypogene or possibly Au porphyry bedrock deposits though primary signatures may have been obscured by metamorphism or weathering. Winfield and Mission Creek grains tend to have higher siderophile Fe, Ni, Pd and Pt and chalcophile elements As, Se, Te, Hg, Pb and Bi but lower Cu and Sb concentrations than Lambly Creek gold. Mercury is distinctly higher in Winfield and Mission Creek gold than in Lambly Creek gold from the west side of the valley; the element appears particularly useful for 'fingerprinting' gold. Lambly Creek gold compositions indicate derivation from two orogenic/hypogene sources from greenstone and plutonic/hydrothermal rocks present in the catchment area. Modern day Mission Creek and Miocene paleoplacer Winfield grains have a similar hypogene trace element signature but there are no known local bedrock gold sources. The Mission Creek and Winfield gold grain cores are surrounded by < 10 μm, Au-rich, Ag- and trace element-poor, rims. Lambly Creek grains lack such rims. The Au-rich rims on modern day Mission Creek and Miocene Winfield gold may reflect prolonged near-surface exposure with surficial electrochemical dissolution of hypogene trace elements or the biological precipitation of gold. Low Ag and red colouration on the surface of grains support the biological precipitation hypothesis. The shared trace element signature, together with the Au-rich rims indicate that modern day placer gold in Mission Creek was multiply reworked from Miocene paleoplacers similar to the Winfield occurrence as a result of uplift and erosion of rocks on the east side of Okanagan Fault.

RÉSUMÉ

Pendant 100 ans, l'or placérien a joué un rôle important dans le peuplement, le développement économique et, plus récemment, la géologie récréative de la région de Kelowna, en Colombie-Britannique. Il est surtout connu pour se trouver dans les roches sédimentaires modernes de Mission Creek et Lambly Creek, ainsi qu'en tant que gisement paléoplacérien

Geoscience Canada, v. 50, https://doi.org/10.12789/geocanj.2023.50.202 pages 259–276

dans les sédiments miocènes de l'ancienne mine de Winfield. Les localités Mission Creek et Winfield sont à l'est de la faille d'Okanagan, une faille normale à faible pendage vers l'ouest et active depuis l'Éocène. Lambly Creek se trouve à l'ouest de la faille. Des roches ignées et métasédimentaires du Paléozoïque supérieur à l'Éocène sont présentes dans le bassin versant de Lambly Creek, mais des unités de gneiss de l'Éocène, exposées par la faille, se trouvent du côté est de la vallée d'Okanagan. Cette étude teste l'hypothèse selon laquelle les compositions de l'or natif placérien varient le long de la faille d'Okanagan, reflétant différentes sources et histoires pour l'or. Un nombre restreint d'analyses d'Au et d'Ag (23 analyses) dans des échantillons représentatifs d'or placérien ont été effectuées au microscope électronique à balayage avec un spectromètre à dispersion d'énergie (MEB-EDS). Les zones analysées pour l'Au et l'Ag ont également été analysées pour 19 éléments traces à l'aide d'un spectromètre de masse à plasma induit par couplage inductif par ablation au laser (LA-ICP-MS). Le mercure a été déterminé de manière semi-quantitative dans des grains d'or « inconnus » en estimant d'abord sa concentration (~3,69 ppm) dans l'étalon externe AuRM2. Les proportions d'Au, d'Ag et de Cu dans les noyaux des grains indiquent que tout l'or provient de gîtes mésothermaux/hypogènes ou éventuellement de gisements rocheux porphyriques aurifères, bien que les signatures primaires aient pu être masquées par du métamorphisme ou de l'altération. Les grains de Winfield et Mission Creek ont tendance à avoir des concentrations plus élevées en éléments sidérophiles Fe, Ni, Pd et Pt et en éléments chalcophiles As, Se, Te, Hg, Pb et Bi, mais des concentrations plus faibles en Cu et Sb que l'or de Lambly Creek. Le mercure est nettement plus élevé dans l'or de Winfield et Mission Creek que dans l'or de Lambly Creek du côté ouest de la vallée; l'élément semble particulièrement utile pour le traçage de l'or. Les compositions aurifères de Lambly Creek indiquent une origine de deux sources orogéniques/hypogènes provenant des roches vertes et des roches plutoniques/hydrothermales présentes dans le bassin versant. Les grains modernes de Mission Creek et des grains paléoplacériens du Miocène de Winfield ont une signature d'éléments traces hypogènes similaire, mais il n'existe aucune source d'or connue dans la roche-mère locale. Les noyaux des grains d'or de Mission Creek et de Winfield sont entourés de bordures de moins de 10 μm de large, riches en Au et pauvres en Ag et en éléments traces. Les grains de Lambly Creek ne présentent pas de telles bordures. Les bordures riches en Au sur l'or moderne de Mission Creek et l'or miocène de Winfield peuvent refléter une exposition prolongée près de la surface avec une dissolution électrochimique superficielle des éléments traces hypogènes ou la précipitation biologique de l'or. La faible teneur en Ag et la coloration rouge à la surface des grains soutiennent l'hypothèse d'une précipitation biologique. La signature commune en éléments traces, ainsi que les bordures riches en Au, indiquent que l'or placérien moderne de Mission Creek a été remanié à plusieurs reprises à partir de paléoplacers du Miocène similaires à ceux de Winfield, résultant du soulèvement et de l'érosion des roches du côté est de la faille d'Okanagan.

Traduit par la Traductrice

INTRODUCTION

The golden glitter of panned placer gold has captured imaginations for millennia but, curiously, the origins, means of natural concentration and composition of this gold remain poorly understood despite gold's economic importance. At only ~ 4 parts per billion in Earth's crust, gold is rarely visible as the native element in rocks, but it is retrievable in small quantities by panning in many stream and beach sediments (Boyle 1979). Numerous major lode and placer gold deposits have been discovered by following minor placer gold occurrences upstream to their source (McClenaghan and Cabri 2011) and the composition of placer gold can help identify bedrock sources (Garnett and Bassett 2005; McInnes et al. 2008; Banks et al. 2018). However, some placer gold occurrences and economic deposits have elusive sources (McInnes et al. 2008) or are associated with low grade to uneconomic bedrock gold mineralization (Boyle 1979). Gold particles in placers range from dust-sized to nuggets that far exceed the size of grains in the bedrock source (Garnett and Bassett 2005). The paradox of gold in clastic sediments being coarser than in the bedrock source has been ascribed to physical amalgamation, chemical precipitation, biochemical precipitation, and precipitation from organic complexes in tropical swamps, soils, and lateritic regoliths (Hough et al. 2009; Reith et al. 2010; 2013; Large et al. 2013). Importantly, this supergene gold appears relatively pure (Groen et al. 1990; McCready et al. 2003).

The lure of placer gold encouraged early European settlement in Kelowna (Roed 2004) and it is not difficult to find 'colour' (i.e. yellow native gold) in streams on both sides of the Okanagan Valley. The geology across the valley is very different (Fig. 1). On the east side, there are amphibolite-facies, mid-crustal gneiss units (metamorphic grade indicates 15+ km depth), last metamorphosed during the Eocene. Thus, they have been unearthed by perhaps 15 km of vertical uplift and tens of kilometres of sub-horizontal normal movement on the continental scale (hundreds of kilometres long) low-angle Okanagan Fault (Tempelman-Kluit and Parkinson 1986). Just 10 km to the west, and across the valley, are Pennsylvanian to Triassic rocks added to North America in the Mesozoic, Mesozoic plutonic rocks, and Cenozoic (Eocene) volcanic rocks that erupted when the east-side gneiss units were being metamorphosed (Tempelman-Kluit and Parkinson 1986; Tempelman-Kluit 1989; Greenough and Roed 2014).

This study tests the hypothesis that the chemical compositions of placer gold grains from either side of the Okanagan valley reflect different bedrock geology and sources of placer gold that are the result of prolonged fault movement and uplift of rocks on the east side of the valley. To achieve this, we report 22 chemical analyses of the trace element content of 12 representative gold grains suitably large enough for analysis and/or multiple analysis by laser ablation inductively coupled plasma mass spectrometry (LA-ICP-MS). These data are supplemented by morphology and mineral inclusion descriptions of the chemically analyzed grains. Fryer et al. (1995) predicted that LA-ICP-MS has immense potential for analyzing native gold. Pioneering studies such as Watling et al. (1994, 1995), McCandless et al. (1997), Outridge et al. (1998), Watling

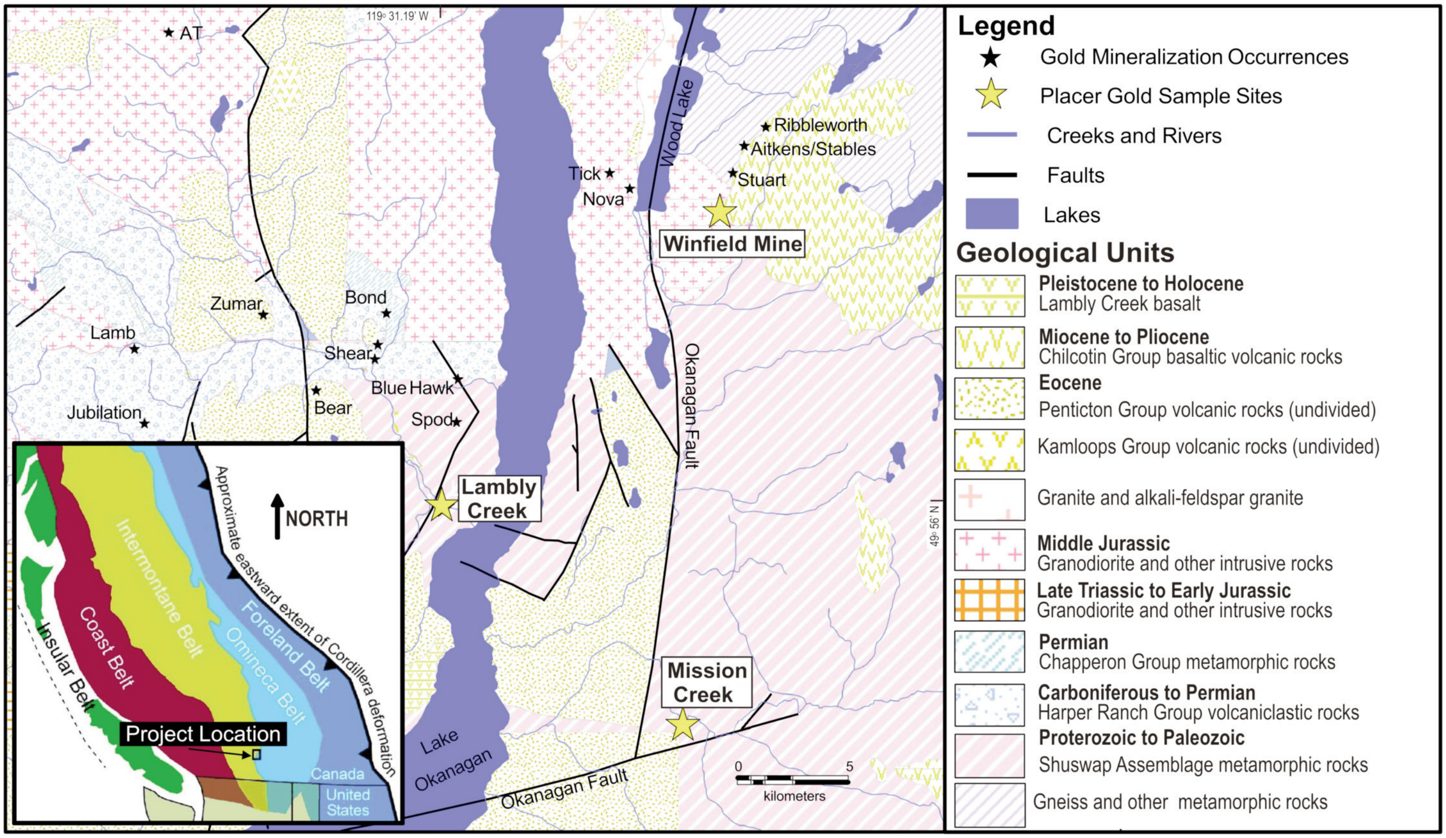

Figure 1. Bedrock geology map of the central Okanagan area (modified from Massey et al. 2005). Yellow stars indicate sampled field sites which occur within 7 m of 49°55'58.1" N, 119°31'11.5" W (latitude and longitude; Lambly Creek), 49°50'57.4" N, 119°22'31.2" W (Mission Creek), and 10 m of 50°03'14.8" N, 119°21'27.4" W (Winfield Mine). Small black stars are MinFile gold mineralization occurrences in the project area that may represent sources of placer gold. Inset shows physiographic belts of the Canadian Cordillera and location of the study area. Gold location references follow: 1) Lambly Creek area: AT (Dun/Esperon), Scott and Osatenko 1980; Lamb, Pautler 1988; Jubilation, Morrison 1989; Zumar, Murray 1991; Bear, Lenard 1996; Bond, Lenard 1987a; Shear, Lenard 1987b; Spod, Gourlay 1989; Blue Hawk, Mark 1988; Lambly, is the Lambly Creek placer gold sampling site. 2) Winfield area: west of Wood Lake, Tick and Nova, White 1968; Osatenko 1980; east of Wood Lake, Ribbleworth, Aitkens/Stables and Stuart, Mathews 1987; Winfield (Mine), Murray 1991. 3) Mission Creek area: BC Ministry of Energy and Mines 1996; Roed 2004.

(1999), Penney (2001), Rasmussen et al. (2006) and Brostoff et al. (2008) showed that gold from different sources tends to have distinct trace element signatures but inter-study concentration comparisons were difficult due to accuracy issues. There has been progress quantifying the trace element composition of native gold (e.g. McInnes et al. 2008; Tetland et al. 2017; Hastie et al. 2020, 2023; Melo-Gómez et al. 2022; Liu and Beaudoin 2021; Liu et al. 2021) and in the use of minor elements and the composition of inclusions in gold for fingerprinting and identifying gold bedrock sources (Chapman et al. 2022, 2023a,b). Our LA-ICP-MS trace element analyses utilize a calibration reference material (AuRM2) where microanalytical heterogeneity is small relative to natural variation in native gold between individual gold deposits (Tetland et al. 2017). The quantitative analyses can be compared with future gold trace element data. We also estimate Hg concentrations in AuRM2, use them to calculate Hg (semi-quantitatively) in our Okanagan samples, and argue that Hg is probably important for fingerprinting gold. Finally, we make the case that gold from either side of the Okanagan Valley appears different in composition and possibly morphology. This apparently reflects different bedrock sources, the history of uplift on Okanagan Fault and the extent of prolonged gold recycling in fluvial systems.

GEOLOGICAL SETTING

The study area is located along the boundary between the Intermontane and Omineca belts of the Canadian Cordillera (Monger and Price 1979) (Fig. 1 and inset). To the east, the Omineca belt contains Proterozoic and Paleozoic rocks that were intensively metamorphosed during the Mesozoic and Cenozoic. To the west are Paleozoic to early Mesozoic arc-related rocks of the Intermontane belt containing the accreted Slide Mountain and Quesnel exotic terranes (Nesbitt and Muehlenbachs 1995). The Omineca belt formed due to sub-parallel subduction of the Intermontane belt oceanic plates, subsequent closure of the Slide Mountain ocean, and accretion of an allochthonous volcanic island arc (e.g. Monger and Price 1979). Numerous post-accretion, mid-Jurassic, and Eocene age felsic plutons intrude the two belts (Armstrong 1988; Gabrielse and Yorath 1991).

Structurally, the project area underwent compression and easterly directed thrusting, obduction of oceanic crust, plutonism, and associated metamorphism during the Early to Mid

https://doi.org/10.12789/geocanj.2023.50.202

Jurassic. Strike-slip faulting and a second major metamorphic and plutonic event occurred during the mid-Cretaceous to Paleogene (Nesbitt and Muehlenbachs 1995). An east–west extensional tectonic regime followed during the Paleocene–Eocene and produced the ductile to brittle, low-angle, west-dipping, extensional, Okanagan Fault (Tempelman-Kluit and Parkinson 1986; Tempelman-Kluit 1989). This extension unearthed large areas of amphibolite-facies orthogneiss and paragneiss on the east side of the Okanagan Valley (Madsen et al. 2006). An episode of recent uplift ≤ 1000 m apparently started at ~ 2 Ma (Boyle 1982).

The east side of Okanagan Lake is dominated by the Proterozoic to Phanerozoic, predominantly amphibolite facies metamorphic units of the Omineca belt (Fig. 1). On the west side, dominantly in the Lambly Creek (Bear Creek) catchment (centre-left of the map), Paleozoic volcanic arc-related rocks of the Intermontane belt are present including fine grained siliciclastic rocks, volcaniclastic rocks, and a small greenstone belt (Bond Au-Ag quartz vein showing). Extensive post-accretion plutons (including the Okanagan Batholith) intruded the area during the Mid Jurassic. They are mostly exposed in the northwest of the map area. Eocene alkali feldspar granite intrusions are also exposed along with consanguineous volcanic and sedimentary assemblages forming extensive cover rocks on both sides of Okanagan Lake. Remnants of the extensive Miocene to Pliocene Chilcotin Group basalt also act as cover rocks. The youngest rocks in the project area are the Pleistocene Lambly Creek basalt (Roed et al. 2014). These young volcanic rocks show that the region is by no means geodynamically stable. The Okanagan Fault may be offset by the late, northeast–southwest-trending oblique (normal/right-lateral strike-slip/transcurrent) Mission Creek Fault that underlies our Mission Creek sampling site (Greenough and Roed 1995). Alternatively, the lateral offset of Okanagan Lake at Kelowna may simply reflect the physiographic expression of a small change in dip on the low angle Okanagan Fault (Okulitch 2013; Roed 2014a).

The study area probably experienced multiple glacial–interglacial events over the past 1.8 Ma but the oldest Pleistocene sediments (glacial till and eolian dune deposits) in all Western Canada occur beneath ~ 1 Ma Lambly Creek basalt (Roed et al. 2014) at West Kelowna. Surficial deposits blanketing the Kelowna study area include widespread thin (< 1 m) glacial till, varved glacial lake sediments (up to 40 m thick) that rim the valley bottom, and numerous glacial outwash sand and gravel deposits topped with eolian sand (Fulton and Smith 1978). Placer gold is not associated with these glacial/late glacial deposits.

SAMPLING LOCATIONS

The three placer/paleoplacer gold occurrences sampled appear as yellow stars in Figure 1, with latitude and longitude given in the caption. The Mission Creek sediments and Winfield Mine occurrences to the east are on Omineca belt rocks whereas the Lambly Creek placer is located on Intermontane belt units. Both Mission Creek and the Winfield Mine were economically exploited whereas Lambly Creek was not.

Winfield Mine

The Winfield paleoplacer camp consists of the 1930s Winfield mine east of Wood Lake, which we sampled, and similar occurrences to the northeast including the Stuart, Aitkens/Stables and Ribbleworth paleoplacer deposits (Mathews 1987, Murray 1991; Fig. 1). All are hosted in Miocene unconsolidated river gravel or conglomerate overlying basement rocks predominantly made up of orthogneiss and overlain by Miocene to Pliocene Chilcotin Group basalt (Mathews 1987).

The paleoplacer host rocks represent sediment deposited in extensive, structurally controlled, Miocene paleo-river valleys (Boyle 1982). The sinuous channels, up to a kilometre wide, are intermittently preserved from the Winfield Mine in the north down to Hydraulic Lake (southeast of Mission Creek and just off Fig. 1). Paleoflow indicators show drainage from the northwest to southeast. Sediment preservation was enhanced by the capping Chilcotin Group basalt which prevented erosion during Pleistocene glaciations. Paleoclimate studies indicate the region experienced temperate conditions with moderate, uniformly distributed precipitation during sediment deposition (Boyle 1982).

These Miocene sedimentary units serve as host rocks to significant basal-type uranium mineralization (Boyle 1982) including the Tyee deposit near Hydraulic Lake just southeast of Figure 1. They were explored by Union Oil Company for uranium from 1976 to 1979 and U mineralization is interpreted to be post-depositional, specifically post-Chilcotin Group basalt, and resulted from leaching of U from intrusive basement rocks by meteoric water which infiltrated the Miocene sediments through structures that controlled the paleochannels. These oxidized U-bearing fluids encountered reduced organic matter in the sediments depositing mainly urano-phosphate complexes (Boyle 1982).

The Winfield Mine paleoplacer deposit was discovered in 1936 and two exploration drifts of 52 and 107 m were dug. Small-scale mining continued until 1945 yielding a total reported 2.33 kg of gold (Mathews 1987; BC Ministry of Energy and Mines 1993).

Mission Creek

The Mission Creek placer was the most productive gold deposit in the central Okanagan (Roed 2004). It is hosted in active fluvial sediments and recent bench deposits of Mission Creek. The highest gold abundances occur 12 km east of the mouth of Mission Creek and just downstream from a conglomerate postulated to be the source of the placer gold (Roed 2004, 2014b) due to juxtaposition. There are no reports of gold from the poorly exposed conglomerate. The conglomerate is underlain by sandstone, siltstone and dacite of the Eocene Penticton Group and overlain by Pleistocene till deposits. In the upper reaches of Mission Creek, it is conformably overlain by a dark volcanic unit resembling the Pleistocene Lambly Creek basalt. South of the Mission Creek Fault (Fig. 1), the conglomerate is juxtaposed against Shuswap, Proterozoic to Paleozoic high-grade metamorphic rocks. The conglomerate is apparently an interglacial alluvial deposit (Roed 1995, 2014b), though the only age constraints are that it is

Eocene to pre-Holocene in age. Clasts in the conglomerate are closely packed and mostly well rounded and include granitic, dioritic and argillaceous lithologies. It is mostly lithified with some friability and extensive limonitic alteration yielding a rusty appearance. A cross-section from water well data indicates the conglomerate represents the recharge area of a major aquifer, the Rutland Aquifer, which underlies the east side of Kelowna.

Placer mining in the central Okanagan started with the discovery of gold at Mission Creek in 1861 (Roed 2004). Records of placer gold mining at Mission Creek began in 1876 and mining continued until the 1930s (Roed 2004; BC Ministry of Energy and Mines 1996). Mining methods included both open pit and, apparently, underground operations. During the peak of mining activity (1876–1895) the recorded production, which likely represents a minimum value due to underreporting, is listed at 20.56 kg of gold (BC Ministry of Energy and Mines 1996). Eight overburden drill-holes tested Mission Creek in 1975 and results were considered very promising, yet inconsistent, and no further work was conducted (BC Ministry of Energy and Mines 1996). Today, the area is within the Scenic Canyon Regional Park.

Lambly Creek

Lambly Creek contains placer gold in its modern sediments, but it has not been economically significant. Rocks in the catchment include Paleozoic volcaniclastic and fine-grained siliciclastic rocks with minor volcanic arc-related greenstone (Fig. 1). The area is intruded by granodiorites of Late Triassic, Early Jurassic and Mid Jurassic ages. Overlying these are Eocene Penticton Group volcanic rocks and the Pleistocene Lambly Creek basalt. Various types of bedrock mineralization, and potential Lambly Creek gold sources, occur in the drainage basin (Fig. 1). The Bond Au–Ag quartz vein showing is hosted in greenstone with pyrite weathering to limonite. It is epithermal (Lenard 1987a) and vein 'grab' samples assayed up to 12 g/t gold and 7 g/t silver. The Shear occurrence consists of polymetallic stockwork veins containing Ag-Pb-Zn ± Au (Lenard 1987b). Assays up to 18.5 g/t Au are recorded and associated minerals include galena, pyrite and quartz. The Zumar showing is another, sheared, polymetallic stockwork-type vein, but it also contains Cu and shows hematite and sericite alteration (Murray 1991). The Lamb occurrence (Pautler 1988) is possibly a skarn-related Ag-Cu ± Au showing; bulk assays indicate ≤ 2.4 g/t Ag and 0.19% Cu. Northeast of Lambly Creek is the Spod low sulphidation gold mineralization (Gourlay 1989) showing multiple stages of andesite-hosted quartz veins and zones of propylitic alteration. One drill core intercepted 3 m of 0.785 g/t Au. In the north to northwest of the study area is Cu-Mo alkaline-porphyry-related mineralization including the AT (Dun/Esperon) occurrence (Scott and Osatenko 1980). It is possible that gold in Lambly Creek was derived from gravel deposits beneath a flow regarded as Lambly Creek basalt in the upper reaches of the creek (Roed, personal communication 2015). However, these rocks have not been dated and there are no river gravels in the sediment section underlying the Lambly Creek basalt at West Kelowna (Roed et al. 2014).

METHODS

Sampling, Mounting and Petrographic Analysis

Placer gold was hand panned from Mission Creek, Lambly Creek, and the Winfield Mine and the largest grains from each locality (n = 7, 10 and 7, respectively) examined in detail and geochemically analyzed. Gold from Mission and Lambly creeks came from recent fluvial sediments within 50 cm of the sediment surface; some directly overlying bedrock. Grains from the Winfield mine were panned at the entrance to a 30 m drift into loosely consolidated gravel overlying metamorphosed basement rocks. Sediments were panned down to a heavy mineral concentrate and care taken to ensure recovery of even small (< 50 μm) gold particles. Gold grains were removed from the gold pan concentrate using adhesive tape and the pan thoroughly cleaned by repeated rinsing with water, wiping between rinses, and inspecting the pan to ensure no sediment remained.

Gold grain samples were catalogued, photographed, and roundness, particle size, grain morphology, surface texture and colour recorded. They were oriented with their long axis horizontal, set in resin on glass discs, and polished with diamond paste at the Western University. Multiple large grains were put on some discs, but small grains required individual mounting to avoid loss during polishing. The polished grains were examined under reflected light with a Nikon Eclipse 50 iPOL petrographic microscope and the following parameters described: 1) mineral inclusions were subjectively classified as hypogene (internal) or detrital sediment picked up during transport (rounded and near the outside edge); 2) variations in the colour of gold (light yellow to yellow orange) within and between grains; 3) modal abundances of inclusions-by-type and gold-by-colour quantified; 4) grain shape, morphology and cross-sectional area estimated; and 5) features such as folded edges, rough surfaces and embayments noted.

SEM-EDS Analysis

Sample discs were carbon-coated to 20 nm thickness at CF Mineral Research, Kelowna. The SEM-EDS analyses were performed at the Fipke Laboratory for Trace Element Research (FiLTER), UBC Okanagan, Kelowna, using a Tescan Mira3 XMU Scanning Electron Microscope (SEM) equipped with an Oxford Aztec™ X-max energy dispersive spectrometer (EDS) containing an 80 mm^2 silicon drift detector. Data processing utilized Oxford Aztec© software. Instrument operating parameters (Table 1) were optimized daily using a metallic copper strip, with Ag and Au precision and accuracy estimated from replicate analyses of the reference material MAC 80Au – 20Ag with a composition 80 wt.% Au and 20 wt.% Ag. It approximates the average Au and Ag concentrations in our Okanagan placer gold samples.

The SEM-EDS provided Au and Ag concentrations in native gold samples as well as mineral-identifying element con-

https://doi.org/10.12789/geocanj.2023.50.202

Table 1. Instrument operating parameters.

SEM-EDS		**LA-ICP-MS Laser**	
Livetime:	14.0 s	Wavelength	193 nm
Process Time:	4 s	Energy	5.5 J/cm^2
Accelerating Voltage:	20.00 kV	Laser repetition rate	10 Hz
Magnification:	375 x	Sample cell He gas	0.7 L/min.
Working Distance:	14.0 mm	Spot size	108.5 μm/64.1 μm[1]
Specimen Tilt (degrees):	0°	Laser-off background	1 min.
Elevation (degrees):	30.4°	Laser-on analysis	1 min.
Azimuth (degrees):	0°	Washout time	1 min.
Number of Channels:	2048	**ICP-MS**	
Energy Range (keV):	20 keV	Plasma power	1200 W
Energy per Channel (eV):	10.0 eV	Cool gas	16 L/min.
Detector Type:	X-Max	Auxiliary gas	1.3 L/min.
Window Type:	SATW	Sample gas	1.13 L/min.
Pulse Pile Up Correction:	Succeeded	Sample cone	Ni
		Guard electrode	On

[1] Laser spot size reduced to 64.1 μm for small Winfield and Lambly Creek gold grains.

centration data for inclusions within the gold grains. The detection limit for most elements was ~ 0.1 wt.%. For Ag and Au in native gold, a minimum of two spot analyses were made per gold grain with at least one core and one rim measurement. Line scans were performed where there was a supergene grain rim, or grain heterogeneity was suspected. Select gold grains were mapped to show elemental zonation of grains. The EDS analyses supplied Ag concentrations used as an internal standard for the LA-ICP-MS trace element analyses.

LA-ICP-MS Analysis

Trace element analysis used a Photon Machines Analyte 193 EXCIMER laser coupled with a Thermo Fisher Element XR ICP-MS at FiLTER operated in triple detector mode. Gold and Ag were measured by SEM/EDX. Instrument operating parameters appear in Table 1. Isotopes used to determine the concentrations of 19 trace element concentrations and to use Ag as an internal standard, were measured in low resolution mode and appear in Table 2. Samples and standards went through a one-hour ultrasonic bath in de-ionized water to remove surface contamination. Spot analyses were performed due to the small size of many grains and to avoid inclusions (Table 1). Background was measured for one minute before turning the laser on for a minute. The laser-on time yielded ablation pits with a depth to diameter ratio ≤ 0.5 to avoid elemental fractionation effects (Potts et al. 1995; Mank and Mason 1999). Each sample analysis was followed by a minute of washout time and washout was periodically monitored to ensure elements, particularly Hg from samples, did not raise background in subsequent analyses.

GLITTER software (van Achterbergh et al. 2004) was used for data reduction. The laser-on signals for elements were inspected and trace element concentrations calculated from non-anomalous portions of the signal. Silver concentrations from the SEM-EDS analyses on spots of the same size and location as the LA-ICP-MS analyses acted as the internal standard. The London Bullion Market Association (LBMA) AuRM2 gold reference material bearing 22 trace elements (Murray 2009) was used as an external standard. Although AuRM2 appears slightly heterogeneous at a micron-scale (Milidragovich et al. 2016), we used a large laser spot (108.5 μm) and analyzed the standard twice at both the start and end of sample 'runs' to mitigate any effect of microanalytical heterogeneity on calibration. Tetland et al. (2017) showed, using reference material data collected at the same time as our Kelowna area samples were analyzed, that under these analytical conditions AuRM2 is suitably homogeneous for use in LA-ICP-MS 'fingerprinting' given the large natural variations in the composition of native gold. Accuracy estimates used replicate estimates of trace element concentrations in AuRM2 with the Royal Canadian Mint FAU 7 (gold with 14 trace elements added) as an external standard (see results for details).

Four elements, P, V, Hg, and U, not intentionally added during the manufacture of the AuRM2 reference material, were detected by LA-ICP-MS. The contents of P, V, and U in samples are not reported because their concentrations and homogeneity in AuRM2 are unknown. In the case of Hg, Tetland (2015) reported replicate SEM/EDS analyses of two non-Okanagan native gold grains (AUS9 from the Prophet placer gold deposit, Australia and BC1 from an unknown placer occurrence in northern BC) with between 3.1 and 3.5 wt.% Hg. This allowed a semi-quantitative determination of Hg in AuRM2 which was used to estimate concentrations in our Kelowna-area unknowns. We iteratively inserted Hg concentrations into the AuRM2 external reference material file and repeatedly ran GLITTER until the predicted LA-ICP-MS concentrations in the high Hg, non-Okanagan samples matched the concentrations from the SEM/EDS analysis. The match indicates AuRM2 has 3.69 ppm Hg. The estimated Hg concentrations in Okanagan samples are based on this semi-quantitative assessment of the average Hg concentration in AuRM2. An assessment of Hg heterogeneity in the reference material following ISO guidelines described in Jochum et al. (2011) and Tetland et al. (2017) indicates 30% heterogeneity. This is slight-

Table 2. Element concentrations (ppm) in Kelowna, British Columbia, placer gold, with precision and accuracy estimates and average detection limits.

Sample/ Isotope[1, 2]	^{24}Mg	^{27}Al	^{48}Ti	^{55}Mn	^{57}Fe	^{60}Ni	^{65}Cu	^{68}Zn	^{75}As	^{77}Se	^{103}Rh	^{105}Pd	^{107}Ag[3]	^{118}Sn	^{121}Sb	^{130}Te	^{195}Pt	Au[3]	^{202}Hg[4]	^{208}Pb	^{209}Bi	Ag/Au	Cu/ (Au+Ag)
LAM2	0.098	0.28			1.30		1.75	0.41		2.01		0.016	19270		1.34	0.21	0.10	980700	0.51		0.0050	0.020	0.0000018
LAM2B	0.52	3.95	1.12	3.07	7.99		13.0		11.7	8.93	0.083		143500	0.29	13.7	1.00	0.79	856500	4.41			0.168	0.0000130
LAM2C	1.23	8.81	0.45		6.24		15.7	1.07		6.23	0.0056	0.14	143500		19.2	0.93	0.35	856500	2.30	0.068	0.017	0.168	0.0000157
LAM6	0.95	11.8	0.48	2.11	7.88		19.2			8.80		0.65	74100	0.51	0.12	1.31	0.37	925900	36.4	0.062	0.045	0.080	0.0000192
LAM7				3.16	10.8		376		13.0	11.5	0.065	0.27	114200		28.7	2.35	1.24	885800	7.61		0.045	0.129	0.0003765
LAM7B		0.95		2.29	10.7		256		12.1	10.2	0.053	0.22	113800		19.2	0.76	0.93	886200	5.60	0.045	0.021	0.128	0.0002563
LAM8	3.19	21.6	0.71		7.28	0.23	2.71		8.57	11.3	0.0095	0.16	245000		0.24	0.69	0.45	755000	11.9	0.22	0.024	0.325	0.0000027
MIS1					33.8		39.8		2.80	17.2	0.017	1.70	112000	0.20	0.76		2.07	888000	781	0.0179	1.13	0.126	0.0000398
MIS1B	0.32	0.41	0.76		27.1		82.3			13.8	0.0075	2.15	112000	0.091	2.39	0.97	1.86	888000	803	1.24	0.085	0.126	0.0000823
MIS1C	0.68		2.08		39.8	1.62	63.4		3.80	31.7	0.029	1.84	112000		1.30	0.98	1.65	888000	859	0.023	0.078	0.126	0.0000634
MIS2	52.6	5.21	56.6		76.1	3.54	49.4	62.6	9.87	41.6	0.045	0.33	177600	0.16	22.7		1.56	822400	42.1		0.17	0.216	0.0000494
MIS2B					39.4		54.0			29.8	0.012		178300		32.9	1.15	1.27	821700	47.9		0.12	0.217	0.0000540
MIS4	1.26	1.77	2.10	8.97	62.5	0.62	8.23		43.9	44.2	0.19	0.28	244400	1.32	4.71		3.15	755600	365		0.035	0.323	0.0000082
MIS4B					50.0		5.67			51.0		0.19	251400	0.23	5.45	2.34	1.91	748600	190		0.081	0.336	0.0000057
WIN1				2.57	13.0	0.89	61.2		10.0	10.8	0.037	0.24	179600	0.18	17.9	0.78	1.38	820400	86.9	0.064	0.039	0.219	0.0000612
WIN1B					12.8		64.2			11.9	0.017	0.31	179600		26.7	1.55	1.59	820400	76.6		0.039	0.219	0.0000642
WIN1C	0.59				14.1		61.6			11.7	0.015	0.35	180800		21.5	1.62	1.44	819200	78.3	0.046	0.066	0.221	0.0000616
WIN2				26.6	42.8		94.7		75.9	27.9	0.40	0.33	69820	1.38	1.56	5.59	1.68	930200	329		0.13	0.075	0.0000947
WIN3		10.1		6.32	24.4		41.5		27.7	17.5		0.44	209500		0.71	2.21	1.51	790500	982	0.151	0.14	0.265	0.0000415
WIN5					11.4		119			10.2		0.14	120200			1.77	2.00	879800	5.46	0.079	0.035	0.137	0.0001192
WIN5B	5.25	61.0	21.1		7.36	0.35	79.9			5.84	0.012	0.13	120200		0.31	1.16	1.43	879800	4.37	0.25	0.093	0.137	0.0000799
WIN5C	1.71	10.5	8.07	4.58	7.93		21.1	1.71	9.57	5.52	0.036	0.096	120000		0.076	2.48	0.72	880000	4.13	0.166	0.047	0.136	0.0000211
WIN6	0.67				9.77		74.6		3.13	9.15		14.3	212000	0.24	2.92	5.93	1.76	788000	36.1	0.23	0.38	0.269	0.0000746
Average LAM	1.20	7.90	0.69	2.66	7.46	0.23	97.9	0.74	11.4	8.42	0.043	0.24	121900	0.40	11.8	1.04	0.60	878100	9.82	0.099	0.026	0.139	0.0000979
Standard Dev. LAM	1.19	8.06	0.31	0.53	3.21		153	0.47	1.93	3.34	0.034	0.22	69560	0.16	11.4	0.67	0.40	69550	12.3	0.081	0.016	0.095	0.0001534
Average MIS	13.7	2.46	15.4	8.97	46.9	1.93	43.3	62.6	15.1	32.7	0.050	1.08	169700	0.40	10.0	1.36	1.92	830300	441	0.427	0.24	0.204	0.0000433
Standard Dev. MIS	25.9	2.47	27.5		17.2	1.48	28.1		19.5	13.9	0.070	0.91	61070	0.52	12.6	0.66	0.60	61070	366	0.704	0.39	0.091	0.0000281
Average WIN	2.06	27.2	14.6	10.0	15.9	0.62	68.7	1.71	25.3	12.3	0.086	1.81	154600	0.60	8.96	2.57	1.50	845400	178	0.141	0.11	0.183	0.0000687
Standard Dev. WIN	2.19	29.3	9.22	11.2	11.3	0.38	28.5		29.7	6.84	0.154	4.67	48730	0.68	11.1	1.88	0.35	48730	318	0.081	0.11	0.067	0.0000285
AuRM2 Conc.[5]	9.9	28.3	31.6	28.2	30.1	29.2	31.6	31.4	47.1	37.4	39.6	29.2	99.6	29.4	11.3	12	30.2	999300	3.69	28.9	9.7		
Precision (% RSD)[6]	6.42	6.74	8.63	18.7	11.0	5.99	6.95	8.72	15.0	11.0	10.9	13.1	1.74	8.99	11.2	19.0	10.9	0.44	33.8	11.4	13.4		
Accuracy %[7]	1.0		9.7	7.4	45.3	2.2	3.3	5.9	22.4			11.6	0.72	3.7			0.30	0.18		3.4	12.9		
Detection Limit[8]	0.14	0.42	0.29	0.90	2.06	0.19	0.23	0.80	1.37	1.89	0.0063	0.024	0.33	0.071	0.048	0.28	0.014		0.34	0.012	0.0041		

Notes

[1] In the column giving samples, LAM = Lambly Creek; MIS = Mission Creek; WIN = Winfield paleo-placer mine.
[2] All concentrations in ppm. Blank cells represent "below detection limit" (BDL) as determined by GLITTER for an individual analysis except in Precision and Accuracy where blank = not determined/determinable.
[3] Ag and Au concentrations are by SEM/EDS analysis. Ag was used as the internal standard during LA-ICP-MS analysis and 107Ag was the isotope measured.
[4] Hg concentrations are semiquantitative. The element was not added to, and concentration not reported for, the external standard AuRM2. Hg concentrations in AuRM2 are also semi-quantitative. See text.
[5] AuRM2 Conc. = ppm element concentrations in AuRM2 from Murray (2009). Hg estimated using two high Hg gold samples. See text for details.
[6] Precision is based on 24 replicate analyses of AuRM2 and for Ag and Au, 5 replicate analyses of the MAC 80Au–20Ag reference material.
[6] Precision = % RSD = (mean AuRM2/standard deviation on mean)*100.
[7] Accuracy = (|Mean measured – Accepted|/ Accepted) * 100%. Accuracy for Ag and Au is based on the mean of 5 replicate analyses of MAC 80Au–20Ag
[7] Accuracy for trace elements was calculated using means (n = 24) of replicate analyses of AuRM2 with FAU7 (Penny 2001) as an extermnal standard (assumed homogeneous).
[7] Blank cells = element not present in FAU7.
[8] Average detection limit in ppm from all sample analyses; detection limit is 3 standard deviations above background.

ly to somewhat higher than for the 'added' elements in AuRM2 which are generally ≤ 20% (Tetland et al. 2017). Variability in the reference material will add to analytical uncertainty and be reflected in precision estimates. However, our estimates (results section) indicate that Hg precision is ± 34%. Precision of 100% reflects variation by a factor of ± 2, but concentrations vary by a factor of 1900 within the Okanagan data set; far outside what can be ascribed to precision issues. Duplicate analyses of the AuRM2 external reference material at both the start and end of 'runs' helped to average out the impact of any reference material heterogeneity.

The concentrations of 19 trace elements in 23 LA-ICP-MS analyses of Okanagan placer native gold, together with major elements Au and Ag by SEM-EDS, appear in Table 2. Some of the 22 elements (Si, Ca, Cr) added to the AuRM2 reference material were not detected in most of our Okanagan gold analyses and are not reported in Table 2. Silver is a trace element in AuRM2 but a major element in the Okanagan gold analyses. Determination of the semi-quantitative concentrations of Hg in our Okanagan samples (Table 2) was discussed above.

Grains selected for LA-ICP-MS analysis had to be large enough to accommodate a minimum 64.1 μm laser spot diameter and at the same time avoid inclusions. Where present, gold-rich (identified in SEM/EDX scans), yellow-orange 'supergene' rims were avoided because all were significantly thinner than the width of the laser beam and any analyses would be composite.

Exploratory Statistical Methods

The exploratory statistical technique known as multi-dimensional scaling (MDS) was used to uncover patterns in sample associations and groupings based on all trace element data for each sample. Greenough et al. (2007) discussed the application of MDS to geochemical data sets. Multi-dimensional scaling has the ability to summarize variance in a data set in a small number of dimensions and thus plots here have 2 dimensions. Dimensions 1 and 2 are unitless and simply represent overall chemical differences based on the elements used to compare samples. Relationships between samples on a MDS diagram are determined from a matrix of sample-versus-sample Pearson correlation coefficients. Two samples plotting close together on the diagram would yield a sample-versus-sample, X–Y plot where all elements form a line yielding a high correlation coefficient. Two samples on opposite sides of the MDS plot would generate a comparatively scattered X–Y plot or a plot with a negative correlation. Because axes on MDS plots are unitless, it is not possible to plot new analyses on the diagram in the future without reprocessing all our data together with the new analyses. Said another way, it is not a classic 'discrimination diagram'.

The MDS diagrams were prepared by: 1) Z-scoring (= standardizing) to put all elements on the same scale so that concentration units do not impact comparisons of samples:

$$Z = (\text{mean } x - x)/\sigma$$

Where:

mean x is the average trace element concentration
x = the sample's concentration
σ = the standard deviation.

2) Data were correlated using Pearson's correlation coefficient = *r*. 3) Matrices of sample-versus-sample *r* values were used to compare samples in Systat™ statistical software (Wilkinson et al. 1992). 4) All calculations used a Kruskal loss function and ≤ 50 iterations to converge input *r* values (measured object distances) with output MDS plot distances (Wilkinson et al. 1992).

Petrography and Gold Grain Morphology

Gold grain characteristics are summarized below with details in Tetland (2015) Appendix A. Lambly Creek has the smallest average gold grain size (0.18 mm long dimension) with a range of 0.04 to 2 mm. Generally, grains are abraded with moderately smooth to well rounded edges. Many exhibit embayments and folded edges; most have fine grained detrital inclusions embedded in the surface. They are light yellow but range to slightly yellow-orange near the rim (Fig. 2a, 2b). The core of one grain contains < 10 μm, grey-pink anhedral sulphide inclusions (pyrrhotite; Fig. 2c, 2d). Several large primary or detrital quartz inclusions were observed.

Gold grains from Mission Creek were comparatively large, averaged 0.62 mm long, and several multi-millimetre flakes were collected. Grains are extremely flattened compared to Lambly Creek, with most being smooth and well-rounded. Detrital inclusions are limited and primary inclusions were not observed. Colour is mostly light yellow with some deeply coloured, Au-rich rims ≤ 20 μmthick (Fig. 2e, 2f).

The Winfield gold grains averaged 0.49 mm long but ranged from fine flour (< 200 μm) to flakes > 1 mm. Edges are subrounded to smooth with evidence of folding and incorporation of detrital grains. Gold colour is light yellow with thin yellow-orange to rare red-orange rims (Fig. 2g, 2h). No definitive primary inclusions were found but one gold grain has a subhedral magnetite grain near the core. The gold pan heavy mineral concentrates contained little or no magnetite, but garnet was abundant.

RESULTS

Precision and Accuracy

Table 2 gives sample element contents, isotopes used for LA-ICP-MS analysis (top row), precision (relative standard deviation, RSD; equation in Table 2 notes) and accuracy estimates. Silver and Au were determined by SEM-EDS analysis (~ 0.1 wt.% detection limit) and can be considered 'major elements'. Accuracy and precision for Au and Ag were calculated from replicate SEM-EDS analyses of the MAC 80Au–20Ag reference material and are 0.18% and 0.44% for Au and 0.72% and 1.74% for Ag (Table 2).

For trace elements, precision comes from 24 replicate analyses of AuRM2 made in association with the 'unknown' analyses. Silicon, Ca and Cr were added to AuRM2 but we do

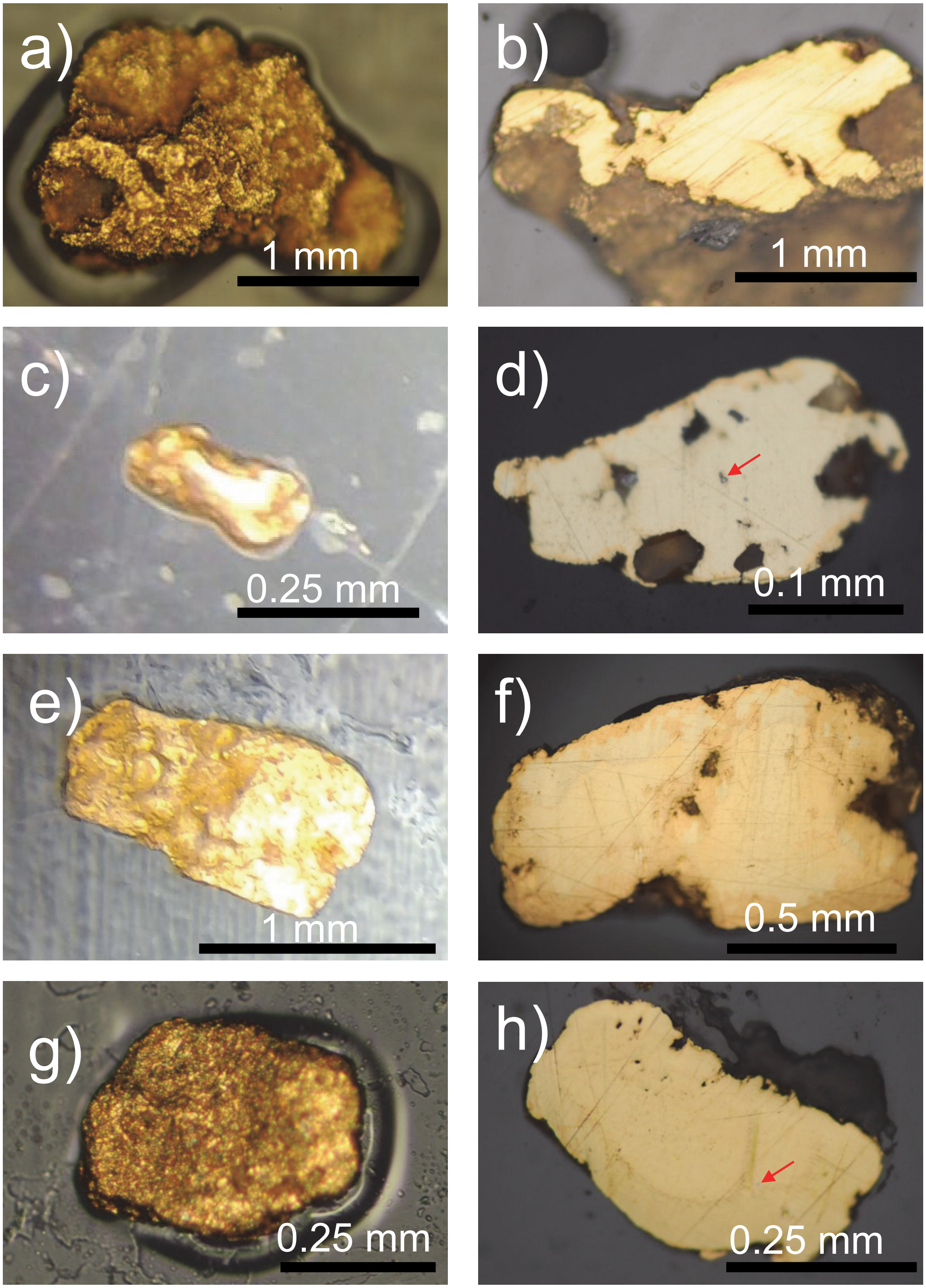

Figure 2. Photomicrographs of gold grains from the study area; a), c), e), g) unpolished grains, and b), d), f), h) same grains (respectively) under reflected light after mounting and polishing. a) LAM2 gold grain from Lambly Creek showing in b) a faint Au enriched rim (darker yellow) under reflected light. c) LAM8 gold grain from Lambly Creek. d) Red arrow on polished LAM8 points to a primary sulphide inclusion of pyrrhotite. Note the thin, darker yellow Au-enriched rim. e) MIS2 gold grain from Mission Creek. f) MIS2 shows a deeply coloured Au-rich rim up to 80 µm thick, and the rim has an irregular 'coral-like' contact with the core of the grain. g) Unpolished WIN5 gold grain; note local red-orange tinge on grain surface. h) Polishing reveals a thin Au enriched rim on WIN5; arrow points to small (~ 0.01 mm), interior magnetite grain possibly of primary origin.

not report concentrations for them because low abundance isotopes had to be used during analysis to avoid mass interferences and this resulted in poor precision. Semi-quantitative Hg has an elevated RSD value (34%). Moderately elevated (15–30%) elements include Mn, As, and Te. All other elements have precision better than 15% RSD (Table 2). Silver acted as an internal standard. Accuracy for elements other than Au and Ag is expressed as the percentage difference between the average (n = 24) predicted concentration of an element in AuRM2, using FAU 7 as an external standard (FAU 7 concentrations from Penney 2001) and the accepted concentrations in AuRM2 from Murray (2009; accuracy equation in Table 2). Low percentages reflect predicted concentrations close to the accepted concentrations. FAU 7 only contains 16 elements with known concentrations and for the accuracy calculations we assume element homogeneity in FAU 7. Sixty percent of elements (Mg, Ni, Cu, Sn, Pt, Pb, Ti, Mn, Zn) have accuracy between 1 and 10%; higher values were derived for Pb and Bi (10–15%), As (22%) and Fe (> 40%) (Table 2).

SEM-EDS Major Element Results

Only Au and Ag were quantitatively detected by SEM-EDS (~0.1 wt.% detection limit). Silver concentrations in grain cores vary from 5 to 26 wt.% yielding a fineness range of 950 to 740 (fineness = Au/(Au + Ag + Cu + Hg + trace elements) * 1000); pure gold fineness = 1000). Gold-rich rims occur at each locality resulting in variations in major alloying element concentrations; see the line-scans (Fig. 3), and element maps (Fig. 4). Gold grain cores volumetrically dominate and tend to be homogeneous. Detrital inclusions of magnetite, quartz and possibly feldspars were observed and SEM-EDS analyses show that there are also primary (non-detrital) sulphide inclusions in Lambly Creek grains (Fig. 4b).

Mission Creek samples have an average grain core concentration of 83.4 wt.% Au. Three of five grains have rims with higher Au and lower Ag concentrations with some exhibiting thick (20 μm) Au-rich rims (Fig. 3a). These Au-rich rims follow cracks, crevices and embayments in and along gold grains. MIS2 shows two separate grain core compositions that may reflect the depth that the gold grain was sectioned (Fig. 4a).

Lambly Creek gold has an average core Au concentration of 84.8 wt.%. Rims with higher Au concentrations (up to 100 wt.%) are present in three out of six grains. Internally, the cores of individual grains have homogeneous major element compositions. Grains exhibiting Au-rich rims show relatively sharp core–rim compositional changes. However, not all grains had compositional changes at the rim (Fig. 3b) and are internally homogeneous. The SEM-EDS elemental map for LAM8, a composite grain, shows a very thin, 5 μm-wide Au-rich and Ag-poor rim together with detrital inclusions of quartz and feldspar(?) and a primary sulphide crystal (pyrrhotite; Fig. 4b).

Gold grains from the Winfield mine have an average core Au concentration of 84.0 wt.%. Three out of five grains have a Au-rich, Ag-poor rim with a maximum Au concentration of 98 wt.% and internally the gold grains are homogeneous (Fig. 3c).

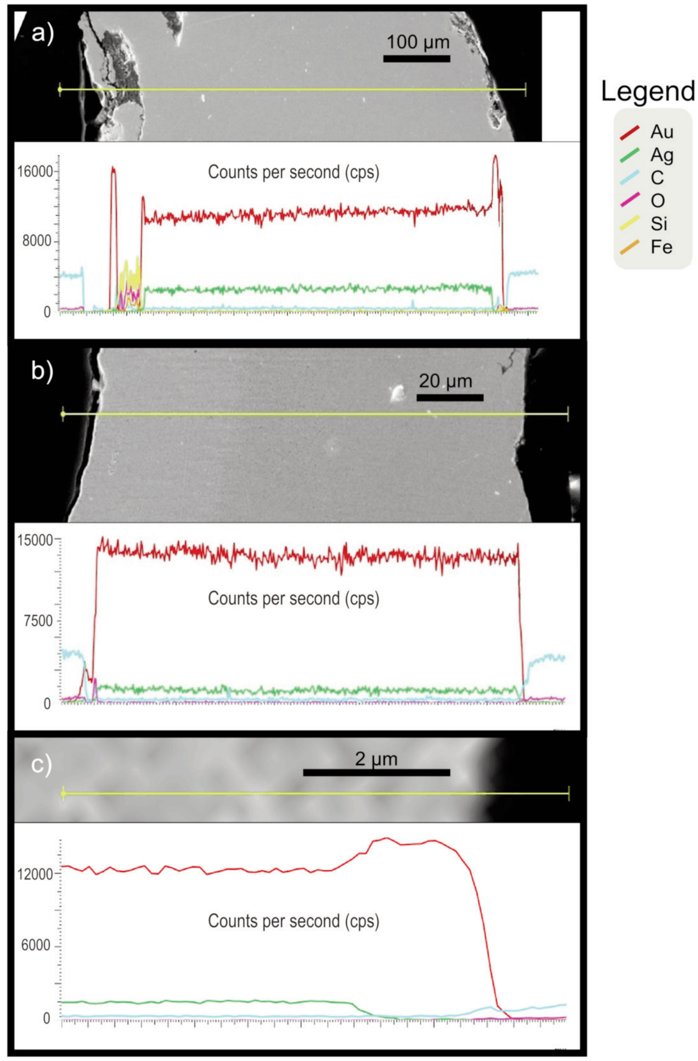

Figure 3. SEM-EDS line-scans across representative Okanagan gold grains with backscatter images above the scans showing line location, grain boundaries and some internal features. Line-scans were created by measuring relative intensity of element-diagnostic K, L and M series X-ray signal peaks for detectable elements along the line. Grains tend to show Au-rich rims and Ag concentrations drop at grain edges. a) Gold grain MIS4 has Au-rich rims and an embayment with detrital material fill on the left side. In b) grain LAM7 shows internal homogeneity and no Au-rich rims. c) In WIN5 the Ag signal (green) dies off on the outer two microns of the grain. Note that the X-axis distance scale is very different on each graph.

LA-ICP-MS Trace Elements

Data and averages for each placer occurrence (Table 2) show that the most abundant trace elements (defined here as < 0.1% = < 1000 ppm) are Hg and Cu; they are over 10 times higher than all other trace elements except Fe. Mercury is particularly high with some analyses approaching 1000 ppm. The least abundant element, Rh, is consistently ~50 ppb. All other elements fall between 0.1 and 10 ppm.

Mean Cu, As, Rh, Pd, Sn, Sb, and Te do not show large differences between localities though samples from Lambly Creek have lower average abundances for most trace elements, aside from Cu and Sb, which are higher in these samples (Table 2). Mission Creek samples are enriched in the lithophile ele-

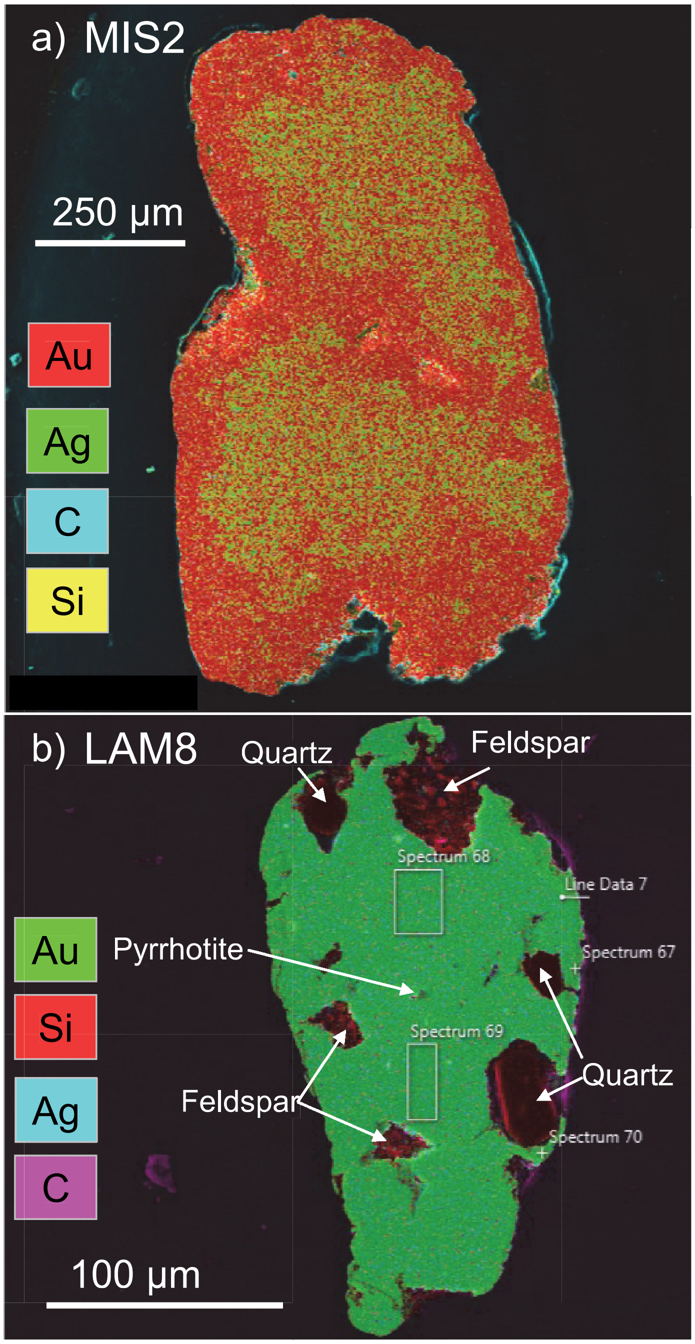

Figure 4. SEM-EDS composite image element maps showing major element analyses for areas in a single gold grain. Colours represent proportional intensity of signal in cps for individual elements detected. a) Coloured map showing variations in major element concentrations in MIS2. Note very distinctive Au-rich and Ag-poor rim surrounding the grain's core. b) Coloured map of LAM8 gold grain which shows a less distinctive Au-rich rim and various mineral inclusions within the gold grain. Rectangles (e.g. Spectrum 68), lines and points provide an example of the spatial distribution of places in grains analyzed to determine major element variation and composition of grains.

ments Mg and Ti, as well as siderophile and chalcophile Fe, Ni, Zn, Se, Pt, Bi, and Hg, but have low Pb. Winfield gold grains have abundant Al, Mn, Pd and high Hg.

Probability plots (Fig. 5) illustrate differences in element concentrations between localities, and the distribution of concentrations between samples at one locality. Trends for Fe, Se, and Hg data are sub-parallel for all localities but Mission Creek is distinguished by higher concentration ranges. All Winfield analyses show very similar Cu values but Mission and Lambly creeks have variable Cu concentrations. In addition, Te concentrations are higher in Winfield samples. Rhodium and Pd values show similar trends for all three locations. Overall, Lambly Creek samples are perhaps most distinct with somewhat lower concentrations for a number of elements, particularly Bi, Hg and Pt, and Pt is also highly variable.

A MDS plot (Fig. 6), calculated using the quantitative trace element data, places samples/analyses with similar trace element signatures close together. The major elements Au and Ag were not used in preparing the graph, nor was semi-quantitative Hg, but inclusion of Hg in the calculations does not significantly change the relative positions of samples/analyses. Thus, the plot summarizes the relationships between the analyses of samples, based on 18 element chemical space, in only two dimensions. Mission Creek and Winfield analyses plot together although with some scatter. Lambly Creek analyses plot in two discrete fields with the smaller field containing two analyses from the same gold grain (LAM7).

DISCUSSION

Precision, Accuracy and Homogeneity

Precision and accuracy, and homogeneity of AuRM2 are assessed in Tetland et al. (2017) based on data collected while analyzing our Kelowna-area samples. Reproducibility of AuRM2 analyses (Table 2) reveals that, of the 18 LA-ICP-MS trace elements with certified homogeneity at a macroscopic scale, seven (39%) have precision (% RSD) better than 10% (Mg, Al, Ti, Ni, Cu, Zn, and Sn), nine (50%) are between 10 and 15% (Fe, As, Se, Rh, Pd, Sb, Pt, Pb, and Bi) and two (11%) fall between 15 and 20% (Mn and Te). Silver was added to AuRM2, but LA-ICP-MS precision cannot be estimated because it was used as the internal standard. Precision and accuracy for Ag and Au in Table 2 were calculated from replicate SEM-EDS analyses of the MAC 80Au–20Ag reference material and are excellent. Mercury is present in AuRM2 at detectable levels, but not intentionally added during manufacture, and therefore not certified for homogeneity at any scale. Precision on Hg is 34%. The precision estimates for half the elements (10 to 15%) reflect modest signal (background-corrected counts per second = cps) as a result of low concentrations in AuRM2 (Table 2; Tetland et al. 2017). The moderately elevated RSD values of Mn and Te are primarily due to low signal intensity, but are acceptable for the purposes of this study. The reproducibility of AuRM2 element concentrations provides a metric for expected reproducibility of duplicate sample analyses of natural gold. Most elements exhibit variation due to analytical precision that is negligible compared to natural geochemical variation in placer gold systems (Table 2).

Accuracy (Table 2; Tetland et al. 2017) was estimated by treating AuRM2 as an unknown, using the matrix-matched gold reference material FAU 7 as an external standard and comparing the mean (n = 24) calculated concentrations in

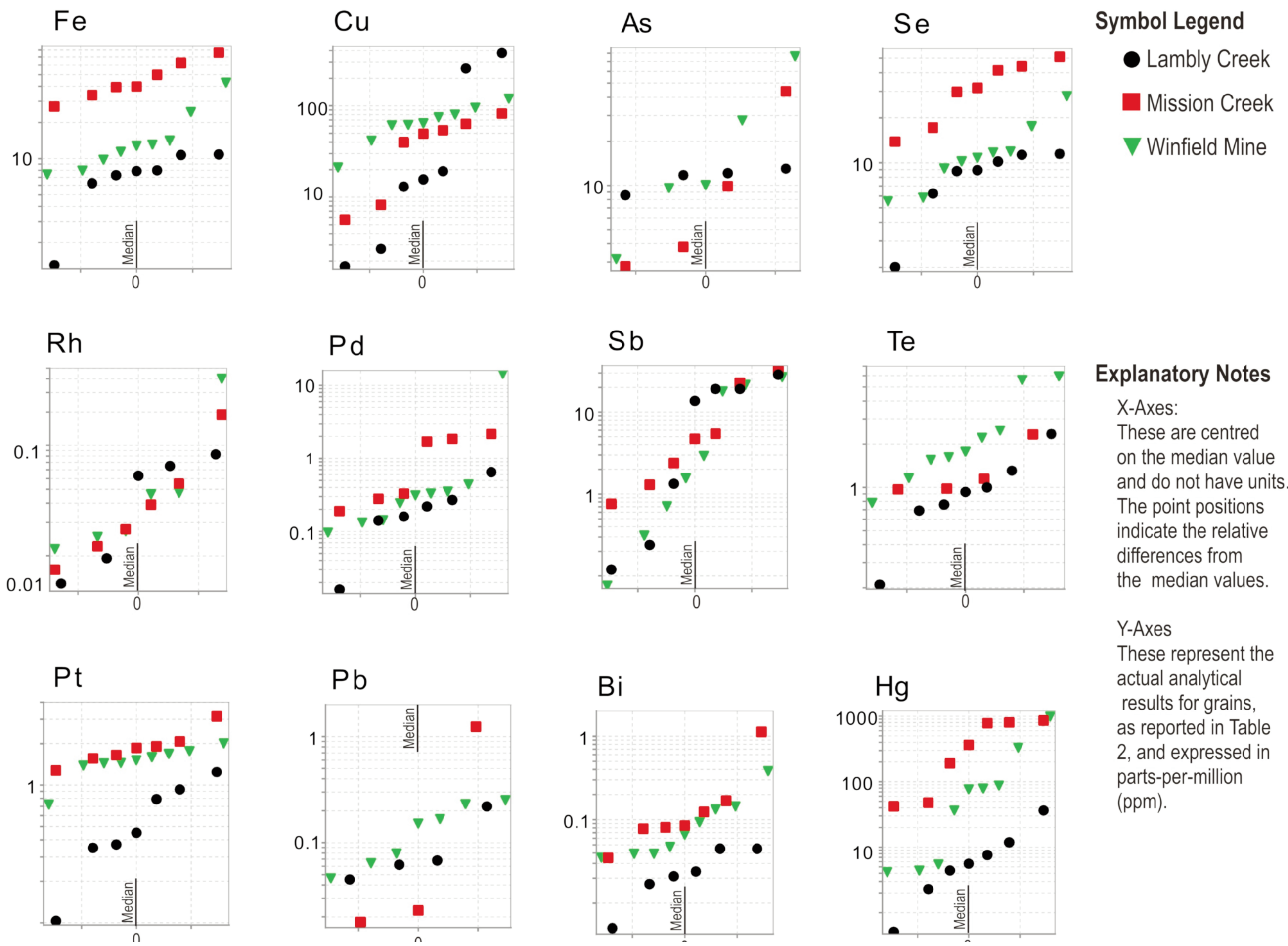

Figure 5. Probability plots of select trace elements (ppm) from Kelowna area samples. These plots order individual analyses from each locality from lowest to highest concentration for each element. A normal score of 0 (X-axis) represents the median value for an element from each locality, and element concentrations on the Y axis are in ppm.

AuRM2 with those determined by bulk solution ICP-MS (Murray 2009). The calculations assume FAU 7 is homogeneous and since it shows some heterogeneity the accuracy estimates represent minimum values (Tetland et al. 2017). For the 15 trace elements added to FAU 7 (excluding Ag, the internal standard), reasonable accuracy was confirmed with most elements showing less difference (< 10%) from given values than variation associated with precision (generally better than 15%; Table 2). Iron shows the poorest accuracy.

Tetland et al. (2017) assessed homogeneity in AuRM2 and concluded that all added elements are suitably homogeneous for use in LA-ICP-MS fingerprinting studies of native gold. For Hg, which was not intentionally added to AuRM2, some component of the variability reflected in precision estimates (Table 2) is probably due to heterogeneity in the reference material.

Comments on Inferring Potential Sources of Gold

Sections below review potential bedrock sources of our native gold samples. The composition of gold from these sources is unknown but their geologic environment, and gold environmental discrimination diagrams from the literature can potentially narrow sources for the samples. A possible complication is that the major and trace element composition of bedrock gold may be modified by metamorphism and gold remobilization in low-melting point chalcophile element rich melts (Hg, Te, Sb, Bi) resulting in higher purity gold with lower silver, and elevated Hg (Hastie et al. 2020; Hastie et al. 2023; Melo-Gómez et al. 2021, 2022). The elemental signature of gold in a primary deposit may be lost or obscured and placer gold will reflect the impact of these secondary processes. Similarly, diffusion of trace elements in a weathering or near-surface environment might theoretically modify the composition of gold. There are gold-rich rims on some of our Winfield and Mission Creek grains, but replicate analyses of the interior of grains (e.g. MIS1, 1B, 1C; Table 2; Fig. 6) indicate homogeneous compositions and there are no gold-rich zones in the interior of grains that support amalgamation of grains with different sources and histories. Finally, mercury has been used to collect gold at surficial temperatures from ore during mining and so placer gold might scavenge Hg in the weathering environment. However, there is no evidence for detectable Hg in the SEM line scans across gold-rich rims of our Winfield and Mission Creek gold (Fig. 3).

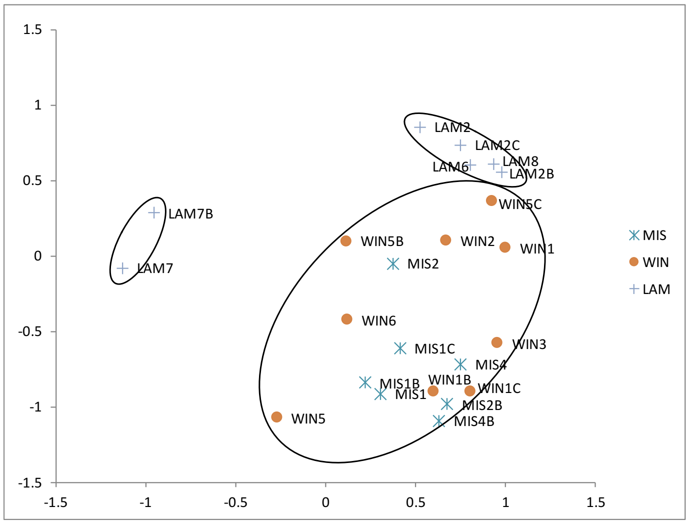

Figure 6. MDS plot comparing the overall composition of Kelowna area samples based on all trace elements in Table 2 except semi-quantitative Hg and excluding major elements Au and Ag. Samples plotting close together tend to have similar geochemical compositions. Fields illustrate that Lambly Creek (LAM) analyses plot in two separate fields apart from Mission Creek (MIS) and Winfield (WIN) analyses. For more explanation of the MDS methods, see the earlier section on Exploratory Statistical Methods.

Winfield and Mission Creek Gold

The cores of all placer gold grains from the three gold localities Winfield, Mission Creek and Lambly Creek show high Ag/Au and low Cu/(Au + Ag) ratios (> 0.08 and < 0.0004, respectively) indicating they came from mesothermal/hypogene or Au porphyry bedrock sources (e.g. Townley et al. 2003). However, the Mission Creek and Winfield placer gold grains show cores with somewhat similar hypogene gold compositions which are mantled by Au-rich rims formed in a supergene environment. In contrast, the Lambly Creek gold grains largely lack supergene Au-rich rims and form two geochemical populations of gold, both distinct from Mission Creek and Winfield placer gold. Due to the modest number of samples, subjective descriptive grain morphology alone would be inadequate for distinguishing gold bedrock sources. However, when also examining quantitative geochemical analyses of grain compositions, discussed below, Lambly Creek gold appears distinct from Mission Creek and Winfield gold. We compare Mission Creek and Winfield placer gold and explore potential bedrock sources and travel history and then contrast them with Lambly Creek gold.

Major and trace element data support a similar bedrock environment of formation, and similarities in the transport history for Mission Creek and Winfield gold. Descriptive morphology and inclusion information supports these interpretations though the small number of grains would make conclusions based solely on this information unreliable. In addition to both Mission Creek and Winfield gold exhibiting Au-rich supergene rims, grains have a similar size distribution, from flour gold (< 200 μm) gold to millimetre-size flakes, and most show a flattened and rounded morphology. These properties indicate an extended transport distance (Grant et al. 1991) and prolonged exposure in weathering environments (see supergene text below). Individual Mission Creek and Winfield grains have variable compositions but exploratory statistical methods (MDS plot; Fig. 6), which simultaneously use all element data to portray relationships, indicate that overall the Mission Creek and Winfield gold grains have significantly overlapping compositions which are distinct from Lambly Creek gold. In addition, simple averages (Table 2) and ranked probability plots (Fig. 5) confirm that, for most elements, the gold grains from the two localities are similar. However, Fe, Se and possibly Hg appear higher in Mission Creek, compared to Winfield gold, but this may be misleading. It is not obvious that there is information available for Proterozoic or Phanerozoic Au deposits but Fe in Archean Abitibi mesothermal gold deposits (Greenough et al. 2021; Se and Hg data unavailable) is highly variable. The standard deviation on the mean divided by the mean *100 is 116%, 256% and 109% for the Hollinger, McIntyre and Aunor deposits (respectively), whereas for all Mission Creek and Winfield analyses together it is only 66%. This indicates Mission Creek and Winfield gold was derived from distal, similar types of deposits, or possibly different portions of the same deposit. An assessment of whether element variability in the Okanagan gold samples reflects micro-inclusions, which would confound fingerprinting, is given in the section Trace Element "Fingerprinting" of Native Gold.

Various limitations can be placed on the potential original hypogene source or sources for Mission Creek and Winfield gold. In the case of Mission Creek gold, the extent of the current fluvial system does not appear to account for the extensive transport indicated by morphology. There are two Mo-Cu porphyry occurrences, Tick and Nova (White 1968; Osatenko 1980), close to the Winfield paleoplacer occurrence (Fig. 1) but they are unlikely sources because they are not Au or Au-Cu porphyry showings. Gold from Au-rich porphyries tends to exhibit a higher Cu content than that from orogenic settings (Morrison et al. 1991; Townley et al. 2003) though we note that metamorphic gold remobilization may result in higher purity gold with higher Cu and lower Ag (Hastie et al. 2020, 2023; Melo-Gómez et al. 2021, 2022). All our analyses have low Cu (Table 2). The proximity does not explain the morphological indications of significant transport distance. There are no known gold sources for either the Mission Creek or Winfield placer gold in the local Omineca belt plutonic and metamorphic rocks on the east side of the Okanagan Fault. The metamorphic rocks experienced amphibolite-facies conditions and contain < 5 cm-wide quartz veins and pods (Nesbitt and Muehlenbachs 1995) that are unlikely gold sources.

Boyle (1982) made paleohydrologic reconstructions, apparently based on present-day altitude of bedrock below stream channels and not on sedimentary structures, for Miocene to early Pliocene coarse-grained clastic sediments underlying plateau basalt east of Kelowna. The results suggest northwest to southeast water flow in Miocene to early Pliocene rivers that yielded the gravel deposits and placer gold at the Winfield Mine. The modern-day, geochemically and morphologically similar Mission Creek placer gold may have had a similar geographic origin to the Winfield Mine gold. Potential bedrock sources for the Mission Creek and Winfield placer gold are extensive, uneconomic, quartz-carbonate vein gold occurrences predominantly in greenschist-facies rocks of the Omineca belt (Nesbitt and Muehlenbachs 1995). However, elsewhere in the Omineca belt there is significant orogenic gold mineralization (Zhang et al. 1989); vein fluid inclusions indicate H_2O-CO_2 fluids with minor CH_4 at 300–380°C (Nesbitt and Muehlenbachs 1995). This is the most likely source in the region for the hypogene portion of Mission Creek and Winfield placer gold, but we cannot eliminate the possibility that the actual source deposits have been completely or partially eroded away, or that the gold came from widespread, but small and/or low grade, uneconomic occurrences.

A supergene gold rim can be seen on Mission Creek and Winfield placer gold grains (Figs. 3 and 4). Major element analyses show significant Au-rich rims on grains indicating extended exposure to surficial or weathering environments. Variability in Mission Creek and Winfield gold trace element signatures is reflected in the Figure 6 MDS plot and may be related to grains containing a hypogene core and supergene rim. Although we attempted to avoid rims during LA-ICP-MS analysis any overlap of core and rim regions in the laser ablation pits could have led to intermediate trace element signatures.

Modes of supergene gold formation are not well established. Hypotheses include electro-refining (Groen et al. 1990; McCready et al. 2003), coupled dissolution and reprecipitation (Putnis 2009) and bacterial precipitation (Reith et al. 2010). The formation of supergene gold rims on these samples due to dissolution of Ag is unlikely, because as an incipient Au-rich rim forms it would shield the dissolution of additional Ag deeper within the grain. Diffusion rates of Ag in gold grains are extraordinarily low at low temperatures (Groen et al. 1990) and cannot account for the thickness of Au-rich supergene rims. This leaves the possibility that organic (bacterial) precipitation, inorganic precipitation, or electro-refining formed the supergene rim.

Microbially precipitated gold documented at the Prophet gold mine (Reith et al. 2010, 2013) is typified by the presence of biofilms containing nanoparticulate, biologically precipitated gold that aggregates to the placer gold grain and shows a reddish surface tinge. A similar reddish tinge occurs on some Winfield samples (Fig. 2g). Although reddish Fe-oxides could occur on gold grains in various sedimentary environments, the high gold content of Winfield rims is another feature resembling the biologically precipitated Prophet gold (Reith et al. 2010, 2013). Gold grains mobilized in an active fluvial placer system may have these surface films removed because they are not commonly observed on Mission Creek grains. It is likely that such films would be favoured on gold grains that are in an immobile position for a long period of time, or precipitation may occur after the placer system becomes dormant (e.g. Winfield). This is supported by a study at Rich Hill, Arizona, where films only occur on immobile gold grains (Kamenov et al. 2013). The Winfield and Mission Creek samples of this study support microbial precipitation even though they were not collected to best preserve films (cf. methods in Reith et al. 2010).

The U mineralization associated with sediments hosting the Winfield paleoplacer gold is significant as the redox-controlled U mineralization is epigenetic and related to circulation of post-depositional fluids (Boyle 1982). Fluid circulation for an extended period of time after deposition of the placer gold would provide an opportunity for precipitation of supergene gold. Unlike Mission Creek, and especially Lambly Creek, the heavy mineral concentrate at the Winfield site did not contain magnetite which is typically abundant in placer settings (Boyle 1979). It is possible magnetite was destroyed by oxidation to hematite from significant volumes of oxidized fluids. Oxidized settings may promote Au mobilization as a soluble urano-organo-gold complex. This mode of transportation has been proposed to explain formation of secondary gold in the world class Witwatersrand gold deposits in South Africa (Large et al. 2013) and coprecipitation of Au and U has been noted in some Australian deposits (Wilde et al. 1989; Mernagh et al. 1994) although in these cases high gold mobility was ascribed to high Eh and chloride complexing.

In summary, Winfield and Mission Creek placer gold appears to have similar hypogene bedrock sources for the cores of grains. Mission Creek gold is modern (Holocene) and apparently derived from interglacial (Pleistocene?) sediments eroded from conglomerate at the base of the Rutland aquifer. Both sediments are younger than the coarse-grained Miocene river sediments that contain the Winfield gold. Both Mission Creek and Winfield gold grains show low-Ag supergene rims indicative of prolonged exposure to a weathering environment and the morphology of grains indicates extensive transport. These features suggest significant reworking and recycling of placer gold on the east side of Okanagan Lake. The Miocene age paleoplacer gold deposits (Winfield type) have been eroded and reworked in at least one, and possibly more, cycles of erosion into contemporary creeks such as Mission Creek.

Lambly Creek Gold

Lambly Creek placer gold displays marked differences in composition compared to gold from the east side of the Okanagan Fault. Morphologically the grains are rougher, less flattened, smaller in size, and carry abundant primary mineral inclusions. The irregular shape and presence or preservation of primary mineral inclusions in small grains implies a proximal gold source. There is little variation in the major element chemistry of grain cores compared to other Kelowna samples, and Au-rich rims are poorly developed to absent on Lambly Creek gold. This suggests very limited supergene precipitation and less time under surficial conditions.

The Lambly Creek gold carries two trace element signatures, both distinct from Mission Creek/Winfield fingerprints (Fig. 6). Two analyses had hundreds of ppm Cu, an order of magnitude more than the other Lambly Creek analyses (Table 2). A possible source is the porphyry Cu-Mo Brenda deposit 25 km southwest of Lambly Creek, but it is not known to contain native gold (Weeks et al. 1995). The Elk deposit, 55 km west of Okanagan Lake, contains free gold in intrusive-hosted quartz veins and represents another possible source containing up to 301,000 oz of Au (Pooley et al. 2011) but Cu is not a significant metal in the deposit (Northcote 2022). The high Cu Lambly Creek analyses, and associated Ag concentrations, resemble some greenstone-hosted orogenic gold from the McIntyre and Aunor mines in the Abitibi Greenstone Belt, Timmins, Ontario, Canada (Greenough et al. 2021). Geologic mapping (Lenard 1987a) shows a small greenstone belt within the catchment basin which contains a vein hosted Au-Ag occurrence, the Bond showing (labelled 8 on Fig. 1), assaying up to 12 g/t Au. Based on available information, this is perhaps the most likely source of the high-Cu gold grains.

The origin of the other type of Au is even less certain because there are several primary gold mineralization sources in the Lambly Creek catchment (see Geological Setting section). The Au mineralization could be related to emplacement of the Okanagan Batholith and possible sources include the stockwork Au-Ag-Pb-Zn veins of the Shear (Lenard 1987b) or Zumar occurrences (Murray 1991), skarn-related mineralization of the Lamb occurrence (Pautler 1988), or the low sulphidation Spod occurrence (Gourlay 1989). The Brenda Cu-Mo porphyry deposit (with Au-Ag as a by-product; Greenough et al. 2004) represents another possible source but as noted above it is not known for native gold (Weeks et al. 1995). In addition, the Elk deposit described above contains free gold and is a possible source (Pooley et al. 2011; Northcote 2022).

The dramatic differences in gold across the continent-scale Okanagan Fault appear to be related to tectonism and fault movement. Gold in Miocene to Recent placer gold deposits on the east side of the Okanagan Fault (Winfield and Mission Creek gold) has similar hypogene bedrock sources, supergene rims indicating prolonged exposure to weathering environments and external morphology consistent with extensive transportation. This indicates that continual movement on the upthrown side of Okanagan Fault over tens of millions of years led to continual recycling of placer gold, development of supergene rims, and gold morphology indicative of extensive transport as a result of recycling. In contrast, placer gold on the west side of the fault has not been recycled and shows hypogene gold compositions consistent with derivation from presently exposed bedrock sources. Compared to the west side of the Okanagan Fault the recycling of placer gold on the east side led to larger and higher grade placer ‘deposits’, compared to the west side over time (Garnett and Bassett 2005). Thus, these geological processes apparently had a major impact on the settlement and economic development of the BC interior and Kelowna area.

Trace Element “Fingerprinting” of Native Gold

To use trace or minor elements to fingerprint native gold and determine if concentrations are representative of a deposit, it is important to know if an element is dissolved in gold or largely present in randomly distributed micro-inclusions. Selection of spots for analysis in individual BC gold grains avoided visible inclusions but sub-micron mineral inclusions might not be obvious in the one-minute signal used to calculate element concentrations. Exploratory statistical analysis (e.g. principal component analysis or multidimensional scaling) has been used to compare element behaviour in multiple analyses of samples from one ore deposit and uncover element associations suggesting the presence of sub-micron mineral grains. The deposit origin of our BC gold samples is not known and so this approach cannot be used to assess the presence of micro-inclusions, but we review what was learned from previous studies. McInnes et al. (2008) studied Mesozoic mesothermal gold from a showing in central British Columbia and found that of the detected elements (V, Fe, Cu, As, Pd, Ag, Sb, Pt, Au and Bi) only Fe and As correlate indicating they may be controlled by arsenopyrite inclusions in the native gold. Greenough et al. (2021) evaluated element associations in three Archean, Abitibi greenstone belt deposits, Hollinger, McIntyre and Aunor. They noted chalcophile (Cu, Pb, Zn, Te, Sb, As, Bi, Sn) and siderophile (Ag, Pt, Pd, Rh, Fe?, Ni, Cr) trace or minor elements tend to fingerprint deposits and appear to be dissolved in Au. Lithophile elements (Si, Ti, Al, Mn, Mg, Ca) proved minimally useful for distinguishing deposits and some element concentrations may be controlled by micro-inclusions such as tourmaline. Liu et al. (2021) found that Fe, As, S and Hg can form lattice impurities or micro-inclusions in native gold but Liu and Beaudoin (2021) argued that Pd, Ag, Sb, Pb, Cu, Hg, and Te contents have a high potential to discriminate gold from different deposit types. The above information is supported by earlier experiments (Watling et al. 1994; McCandless et al. 1997; Miller et al. 2001; Penney 2001). As a generalization, the chalcophile and siderophile elements tend to be dissolved in gold, or occur as lattice impurities, and are useful for fingerprinting, but there are deposit-specific deviations from the norm where concentrations may largely reflect randomly distributed micro-inclusions.

Mean concentrations of elements by locality in Table 2 imply that Si, Ca and Cr should be important for fingerprinting native gold, but these elements have low precision and accuracy and we cannot eliminate the possibility that mean differences are related to the interception of silicate/oxide micro-inclusions by the laser. However, we saw no evidence of these in the time-resolved signal received by the ICP-MS. If present, the micro-inclusions were so small that mixing during sample cell wash-out prevented seeing anomalies in the signal. If these elements are impacted by micro-inclusions, the order-of-magnitude differences in Mg, Al and Ti could reflect intersection of silicate and/or oxide phases. Other elements with 2 to 45 times concentrations differences between mean Winfield, Mission and Lambly creeks analyses include Fe, Ni, Cu, As, Se, Rh, Pd, Te, Pt, Hg, Pb, and Bi (Table 2) with Hg concentration differences the largest. Of these, the probability plots show that Mission Creek samples have high Fe, Ni, Se and Hg but low As. Bismuth is similar in Mission Creek and Winfield samples and higher than in Lambly Creek. Winfield samples have the highest Te and Pb. Lambly Creek samples have the lowest Fe and Cu (except two have the highest Cu observed) and the lowest Pt, Bi and Hg. Overall, Winfield samples tend to have intermediate compositions that are closest to Mission Creek.

Over forty elements have been detected in native gold using various analytical techniques (e.g. Antweiler and Campbell 1977, 1982; Watling et al. 1994, 1995, 2014; McCandless et

https://doi.org/10.12789/geocanj.2023.50.202

al. 1997; Outridge et al. 1998; Watling 1999; Penney 2001; Rasmussen et al. 2006; Brostoff et al. 2008); McInnes et al. 2008; Banks et al. 2018) but various analytical issues have compromised the determination of actual trace element concentrations. Confirmation of homogeneity in AuRM2 (Tetland et al. 2017) opened the door to the use of LA-ICP-MS to study the trace element composition of gold. Based on the results here (e.g. Figs. 5 and 6) the chalcophile trace elements Cu, As, Se, Sb, Te, Hg, Pb and Bi, and siderophile Fe, Ni, Pd and Pt are particularly useful for distinguishing Kelowna area gold samples. Of all these elements, Hg shows the largest range in concentrations indicating it could be particularly useful for fingerprinting. Our results corroborate studies of the composition of gold in numerous deposits across Ontario, Canada (Melo-Gómez et al. 2021, 2022) where Hg, Sb, Pd, and Cd concentrations are independent of gold content and apparently reflect geological factors. Copper concentrations tend to negatively correlate with Au due to closure; as Au goes up, other elements go down, but like us, these studies found that Cu fingerprints deposits. Future work should accurately determine Hg in AuRM2 using solution analytical methods and ascertain the degree of homogeneity in the reference material at the micro-analytical scale.

CONCLUSIONS

1. Gold from Lambly Creek on the west side of Okanagan Fault has smaller grain sizes than from Mission Creek or the Winfield mine (east side). Lambly Creek grains show embayments, folded edges, are abraded and moderately smooth to rounded and contain primary and detrital inclusions. In contrast Mission Creek and Winfield grains are flatter, smooth and rounded, lack inclusions, and have deeply coloured, yellow-orange to rare reddish orange, < 20 μm Au-rich rims; characteristics suggesting distant transport and prolonged exposure to surface and supergene conditions
2. Placer gold in Mission Creek appears recycled from Miocene paleoplacer deposits such as at the Winfield Mine as a result of continual isostatic uplift of unearthed rocks on the east side of Okanagan Fault. There is no obvious local hypogene gold source for Mission Creek and Winfield gold. Future mineral exploration should focus on Miocene fluvial deposits.
3. Extended time (Miocene–present) under surficial conditions with post-depositional circulation of oxidized fluids (also related to U-mineralization) led to supergene gold precipitation on Kelowna area paleoplacer gold. Gold may have been carried as urano–organo–gold complexes, chloride complexes, or precipitated microbially as nanoparticles.
4. Two distinct trace element signatures were found for Lambly Creek gold supporting ≥ 2 hypogene sources for placer gold in the catchment. One group of grains has elevated Cu and could carry an orogenic gold signature sourced from the greenstone-hosted Bond occurrence. The low Cu group appears to have an intrusion-hosted gold signature.
5. Many trace elements show average concentration differences among the three sampling sites from 2 to over 45 times. The chalcophile elements Cu, As, Se, Sb, Te, Hg, Pb and Bi, and siderophile elements Fe, Ni, Pd and Pt are particularly useful for distinguishing Kelowna area gold samples. Of all these elements, Hg shows the largest range in concentrations indicating the element will be particularly useful for future fingerprinting studies.
6. Future work should confirm the concentration of Hg in AuRM2 using solution analytical methods and ascertain the degree of homogeneity in the reference material at the microanalytical scale.

ACKNOWLEDGEMENTS

Research was supported by funding from NSERC with graduate student support for MT from UBC Okanagan. The late Dr. Robert Kerrich supported early stages of the work and Dr. Yuan Chen and Dr. Kyle Larson sat on the thesis supervisory committee. Assistance in collecting samples was provided by Alejandro Velasquez, Mackenzie Plovie, James Baker, and Jim Moody. Polishing and mounting of gold grains was performed by Stephen Wood at Western University. Dr. Mike Hinds (Royal Canadian Mint) provided access to the gold reference material FAU 7. Dave Arkinstall at the UBC Okanagan FiLTER lab helped with SEM and LA-ICP-MS analysis. CF Mineral Research, Kelowna provided carbon-coating services and aided in polishing gold reference materials. Funding for the FiLTER lab was provided by a generous donation from Dr. Charles Fipke. Reviews for Geoscience Canada (three anonymous plus E. Hastie and H. Liu) led to major improvements. C. Murphy encouraged us and handled the manuscript. A. Kerr and R. Raeside made improvements during copy-editing.

REFERENCES

Antweiler, J.C., and Campbell, W.L., 1977, Application of gold compositional analyses to mineral exploration in the United States: Journal of Geochemical Exploration, v. 8, p. 17–29, https://doi.org/10.1016/0375-6742(77)90041-3.

Antweiler, J.C., and Campbell, W.L., 1982, Gold in exploration geochemistry, *in* Levinson, A.L., *ed.,* Precious Metals in the Northern Cordillera: Association of Exploration Geochemistry, Calgary, AB, p. 33–44.

Armstrong, R., 1988, Mesozoic and early Cenozoic magmatic evolution of the Canadian Cordillera, *in* Clark, S.P., Jr., and Burchfiel, B.C., *eds.,* Processes in Continental Lithospheric Deformation: Geological Society of America Special Papers, v. 218, p. 55–91, https://doi.org/10.1130/SPE218-p55.

Banks, D.A., Chapman, R.J., and Spence-Jones, C., 2018, Detrital gold as a deposit-specific indicator mineral by LA-IPS-MS analysis: Geoscience Report 2018–21, 49 p. Available at: https://cdn.geosciencebc.com/project_data/GBC Report2018-21.pdf.

BC Ministry of Energy and Mines, 1993, MINFILE detail report for Winfield (Eley/Hall) occurrence: British Columbia Geologic Survey, MINFILE Report: 082LSW093.

BC Ministry of Energy and Mines, 1996, MINFILE detail report for Mission Creek occurrence: British Columbia Geologic Survey MINFILE Report: 082ENW105.

Boyle, D.R., 1982, The formation of basal-type uranium deposits in south central British Columbia: Economic Geology, v. 77, p. 1176–1209, https://doi.org/10.2113/gsecongeo.77.5.1176.

Boyle, R.W., 1979, The geochemistry of gold and its deposits (together with a chapter on geochemical prospecting for the element): Energy, Mines and Resources Canada, Geological Survey 280, 584 p. Available at: https://publications.gc.ca/site/eng/9.817728/publication.html.

Brostoff, L.B., González, J.J., Jett, P., and Russo, R.E., 2008, Trace element fingerprinting of ancient Chinese gold with femtosecond laser ablation-inductively coupled mass spectrometry: Journal of Archaeological Science, v. 36, p. 461–466, https://doi.org/10.1016/j.jas.2008.09.037.

Chapman, R., Mortensen, J.K., and Murphy, R., 2023a, Compositional signatures of gold from different deposit types in British Columbia, Canada: Minerals, v. 13, 1072, https://doi.org/10.3390/min13081072.

Chapman, R., Torvela, T., and Savastano, L., 2023b, Insights into regional metallogeny from detailed compositional studies of alluvial gold: An example from the Loch Tay area, central Scotland: Minerals, v. 13, 140, https://doi.org/10.3390/min13020140.

Chapman, R.J., Mortensen, J.K., Allan, M.M., Walshaw, R.D., Bond, J., and MacWilliam, K., 2022, A new approach to characterizing deposit type using mineral inclusion assemblages in gold particles: Economic Geology, v. 117, p. 361–381, https://doi.org/10.5382/econgeo.4863.

Fryer, B.J., Jackson, S.E., and Longerich, H.P., 1995, The design, operation and role of the laser-ablation microprobe coupled with an inductively coupled plasma–mass spectrometer (LAM-ICP-MS) in the Earth sciences: Canadian Mineralogist, v. 33, p. 303–312.

Fulton, R.J., and Smith, G.W., 1978, Late Pleistocene stratigraphy of south-central British Columbia: Canadian Journal of Earth Sciences, v. 15, p. 971–980, https://doi.org/10.1139/e78-105.

Gabrielse, H., and Yorath, C.J., 1991, Tectonic synthesis, *in* Gabrielse, H., and Yorath, C.J., *eds*., Geology of the Cordilleran Orogen in Canada: Geological Survey of Canada, Series no. 4, p. 679–705, https://doi.org/10.4095/134123.

Garnett, R.H.T., and Bassett, N.C., 2005, Placer deposits, *in* Hedenquist, J.W., Thompson, J.F.H., Goldfarb, R.J., and Richards, J.P., *eds.,* One Hundredth Anniversary Volume: Economic Geology, p. 813–843, https://doi.org/10.5382/AV100.25.

Gourlay, A., 1989, Assessment report for the QPX Minerals Inc. spod claim: British Columbia Geologic Survey, Assessment Report: 18499.

Grant, A.H., Lavin, O.P., and Nichol, I., 1991, The morphology and chemistry of transported gold grains as an exploration tool: Journal of Geochemical Exploration, v. 40, p. 73–94, https://doi.org/10.1016/0375-6742(91)90032-P.

Greenough, J.D., and Roed, M.A., 1995, History of bedrock in the Kelowna area, *in* Roed, M.A., and Dobson, D.A., *eds.,* Geology of the Kelowna Area and Origin of the Okanagan Valley, British Columbia: Kelowna Geology Committee, p. 27–39.

Greenough, J.D., and Roed, M.A., 2014, Geological history of bedrock in the Kelowna area, *in* Greenough, J.D., and Roed, M.A., *eds.,* Okanagan Geology, British Columbia, 3rd Edition: Kelowna Geology Committee, p. 27–39.

Greenough, J.D., Hughes, B., Capstick, D., and Roed, M.A., 2004, Mineral resources, *in* Roed, M.A., and Greenough, J.D., *eds.,* Okanagan Geology, British Columbia: Kelowna Geology Committee, p. 131–146.

Greenough, J.D., Dostal, J., and Mallory-Greenough, L.M., 2007, Incompatible element ratios in French Polynesia basalts: describing mantle component fingerprints: Australian Journal of Earth Sciences, v. 54, p. 947–958, https://doi.org/10.1080/08120090701488271.

Greenough, J.D., Velasquez, A., Shaheen, M.E., Gagnon, J., Fryer, B.J., Tetland, M., Chen, Y., and Mossman, D., 2021, Laser ablation ICP-MS trace element composition of native gold from the Abitibi Greenstone belt, Timmins, Ontario: Canadian Journal of Earth Sciences, v. 58, p. 593–609, https://doi.org/10.1139/cjes-2019-0134.

Groen, J.C., Craig, J.R., and Rimstidt, J.D., 1990, Gold-rich rim formation on electrum grains in placers: Canadian Mineralogist, v. 28, p. 207–228.

Hastie, E.C.G., Kontak, D.J., and Lafrance, B., 2020, Gold remobilization: Insights from gold deposits in the Archean Swayze greenstone belt, Abitibi Subprovince, Canada: Economic Geology, v. 115, p. 241–277, https://doi.org/10.5382/econgeo.4709.

Hastie, E.C.G., Kontak, D.J., Lafrance, B., Petrus, J.A., Sharpe, R., and Fayek, M., 2023, Evaluating geochemical discriminants in Archean gold deposits: A Superior Province perspective with an emphasis on the Abitibi greenstone belt: Economic Geology, v. 118, p. 123–155, https://doi.org/10.5382/econgeo.4979.

Hough, R.M., Butt, C.R.M., and Fischer-Bühner, J., 2009, The crystallography, metallography and composition of gold: Elements, v. 5, p. 297–302, https://doi.org/10.2113/gselements.5.5.297.

Jochum K.P., Weis U., Stoll B., Kuzmin D., Yang Q., Raczek I., Jacob D.E., Stracke A., Birbaum K., Frick D.A., Günther, D., and Enzweiler, J., 2011, Determination of reference values for NIST SRM 610–617 glasses following ISO guidelines: Geostandards and Geoanalytical Research, v. 35, p. 397–429, https://doi.org/10.1111/j.1751-908X.2011.00120.x.

Kamenov, G.D., Melchiorre, E.B., Ricker, F.N., and DeWitt, E., 2013, Insights from Pb isotopes for native gold formation during hypogene and supergene processes at Rich Hill, Arizona: Economic Geology, v. 108, p. 1577–1589, https://doi.org/10.2113/econgeo.108.7.1577.

Large, R.R., Meffre, S., Burnett, R., Guy, B., Bull, S., Gilbert, S., Goemann, K., and Danyushevsky, L., 2013, Evidence for an intrabasinal source and multiple concentration processes in the formation of the Carbon Leader Reef, Witwatersrand Supergroup, South Africa: Economic Geology, v. 108, p. 1215–1241, https://doi.org/10.2113/econgeo.108.6.1215.

Lenard, N., 1987a, Assessment report for the Lenard, N Bond 1 claim: British Columbia Geologic Survey, Assessment Report: 16027.

Lenard, N., 1987b, Assessment report for the Lenard, N Shear 1-7 claims: British Columbia Geologic Survey, Assessment Report: 16094.

Lenard, N., 1996, Assessment report for the Lenard, N Host claim: British Columbia Geologic Survey, Assessment Report: 24594.

Liu, H., and Beaudoin, G., 2021, Geochemical signatures in native gold derived from Au-bearing ore deposits: Ore Geology Reviews, v. 132, 104066, https://doi.org/10.1016/j.oregeorev.2021.104066.

Liu, H., Beaudoin, G., Makvandi, S., Jackson, S.E., and Huang, X., 2021, Multivariate statistical analysis of trace element compositions of native gold from orogenic gold deposits: Implication for mineral exploration: Ore Geology Reviews, v. 131, 104061, https://doi.org/10.1016/j.oregeorev.2021.104061.

Madsen, J.K., Thorkelson, D.J., Friedman, R.M., and Marshall, D.D., 2006, Cenozoic to Recent plate configurations in the Pacific Basin: Ridge subduction and slab window magmatism in western North America: Geosphere, v. 2, p. 11–34, https://doi.org/10.1130/GES00020.1.

Mank, A.J.G., and Mason, P.R.D., 1999, A critical assessment of laser ablation ICP-MS as an analytical tool for depth analysis in silica-based glass samples: Journal of Analytical Atomic Spectrometry, v. 14, p. 1143–1153, https://doi.org/10.1039/a903304a.

Mark, D., 1988, Assessment report for the Parkwood Resources Bluehawk 1 claim: British Columbia Geologic Survey Assessment Report Report: 17501.

Massey, N.W.D, MacIntyre, D.G., Desjardins, P.J., and Cooney, R.T., 2005, Digital geology map of British Columbia: British Columbia Ministry of Energy and Mines, GeoFile 2005-1.

Mathews, W.M., 1988, Neogene geology of the Okanagan Highland, British Columbia: Canadian Journal of Earth Science, v. 25, p. 725–731, https://doi.org/10.1139/e88-068.

McCandless, T.E., Baker, M.E., and Ruiz, J., 1997, Trace element analysis of natural gold by laser ablation ICP-MS: A combined external/internal standardisation approach: Geostandards Newsletter, v. 21, p. 271–278, https://doi.org/10.1111/j.1751-908X.1997.tb00675.x.

McClenaghan, M.B., and Cabri, L.J., 2011, Review of gold and platinum group element (PGE) indicator minerals methods for surficial sediment sampling: Geochemistry: Exploration, Environment, Analysis, v. 11, p. 251–263, https://doi.org/10.1144/1467-7873/10-im-026.

McCready, A.J., Parnell, J., and Castro, L., 2003, Crystalline placer gold from the Rio Neuquen, Argentina: Implications for the gold budget in placer gold formation: Economic Geology, v. 98, p. 623–633, https://doi.org/10.2113/gsecongeo.98.3.623.

McInnes, M., Greenough, J.D., Fryer, B.J., and Wells, R., 2008, Trace elements in native gold by solution ICP-MS and their use in mineral exploration: A British Columbia example: Applied Geochemistry, v. 23, p. 1076–1085, https://doi.org/10.1016/j.apgeochem.2007.12.027.

Melo-Gómez, J.D., Hastie, E.C.G., Gibson, H.L., Tait, K.T., and Petrus, J.A., 2021, Gold fineness across Ontario: An update on the Gold Fingerprinting Project, *in* Summary of Field Work and Other Activities, 2021: Ontario Geological Survey, Open File Report 6380, p. 13-1 to 13-9.

Melo-Gómez, J.D., Hastie, E.C.G., Gibson, H.L., Tait, K.T., and Petrus, J.A., 2022, Trace element content of gold across Ontario: An update on the Gold Fingerprinting Project, *in* Summary of Field Work and Other Activities, 2022: Ontario Geological Survey, Open File Report 6390, p. 15-1 to 15-11.

Mernagh, T.P., Heinrich, C.A., Leckie, J.F., Carville, D.P., Gilbert, D.J., Valenta, R.K., and Wyborn, L.A.I., 1994, Chemistry of low temperature hydrothermal gold, platinum, and palladium (+ or – uranium) mineralization at Coronation Hill, Northern Territory, Australia: Economic Geology, v. 89, p. 1053–1073, https://doi.org/10.2113/gsecongeo.89.5.1053.

Milidragovic, D., Beaudoin, G., and Jackson, S.E., 2016, In-situ trace element characterization of three gold reference materials using EPMA and LA-ICP-MS: Geological Survey of Canada, Open File 8096, 26 p., https://doi.org/10.4095/299097.

Miller, D., Desai, N., Grigorova, D., and Smith, W., 2001, Trace-element study of gold from southern African archaeological sites: South Africa Journal of Science, v. 97, p. 297–300, https://hdl.handle.net/10520/EJC97347.

Monger, J.W.H., and Price, R.A., 1979, Geodynamic evolution of the Canadian Cordillera – progress and problems: Canadian Journal of Earth Sciences, v. 16, p. 770–791, https://doi.org/10.1139/e79-069.

Morrison, G.W., Rose, W.J., and Jaireth, S., 1991, Geological and geochemical controls on the silver content (fineness) of gold in gold-silver deposits: Ore Geology Reviews, v. 6, p. 333–364, https://doi.org/10.1016/0169-1368(91)90009-V.

Morrison, M., 1989, Assessment report for the Jubilation 1-2 claims: British Columbia Geologic Survey Assessment Report: 19110.

Murray, J., 1991, Assessment report for the Amarado Res. Zumar 2-4 claims: British Columbia Geologic Survey Assessment Report: 21600.

Murray, S., 2009, LBMA certified reference materials: Gold project final update: Alchemist, v. 55, p. 11–12.

Nesbitt, B.E., and Muehlenbachs, K., 1995, Geochemical studies of the origins and effects of synorogenic crustal fluids in the southern Omineca Belt of British

Columbia, Canada: Geological Society of America Bulletin, v. 107, p. 1033–1050, https://doi.org/10.1130/0016-7606(1995)107<1033:GSOTOA>2.3.CO;2.

Northcote, B., 2022, Exploration and mining in the south central region, British Columbia, *in* Provincial Overview of Exploration and Mining in British Columbia, 2021: Ministry of Energy, Mines and Low Carbon Innovation, British Columbia Geological Survey, Information Circular 2022-01, p. 85–104.

Okulitch, A.V., (*compiler*), 2013, Geology, Okanagan Watershed, British Columbia: Geological Survey of Canada, Open File 6839, scale 1:100,000, https://doi.org/10.4095/292220.

Osatenko, M., 1980, Assessment report for the Cominco Ltd. Woodsdale claim: British Columbia Geologic Survey Assessment Report: 08922.

Outridge, P.M., Doherty, W., and Gregoire, D.C., 1998, Determination of trace elemental signatures in placer gold by laser ablation-inductively coupled plasma-mass spectrometry as a potential aid for gold exploration: Journal of Geochemical Exploration, v. 60, p. 229–240, https://doi.org/10.1016/S0375-6742(97)00049-6.

Pautler, J., 1988, Assessment report for the Kerr Addison Mines Lamb 1-8 claims: British Columbia Geologic Survey Assessment: 17854.

Penney, G., 2001, Fingerprinting gold using laser ablation microprobe-inductively coupled plasma-mass spectrometry (LAM-ICP-MS): An exploration tool: Unpublished Honours Thesis, Memorial University of Newfoundland, NL, 65 p.

Pooley, R., Lomas, S., Hawthorn, G., and Alexander, R., 2011, NI 43-101 technical report for a preliminary economic assessment on the Elk Gold Project, Merritt, British Columbia, Canada: Almaden Minerals, Vancouver, BC, Project Code: ALM003.

Potts, P.J., Bowles, J.F.W., Reed, S.J.B., and Cave, M.R., (*editors),* 1995, Microprobe Techniques in the Earth Sciences (1st edition): Springer New York, NY, 419 p., https://doi.org/10.1007/978-1-4615-2053-5.

Putnis, A., 2009, Mineral replacement reactions: Reviews in Mineralogy and Geochemistry, v. 70, p. 87–124, https://doi.org/10.2138/rmg.2009.70.3.

Rasmussen, K.L., Mortensen, J.K., and Falck, H., 2006, Morphological and compositional analysis of placer gold in the South Nahanni River drainage, Northwest Territories, *in* Emond, D.S., Lewis, L.L., and Weston, L.H., *eds.,* Yukon Exploration and Geology 2006: Yukon Geological Survey, p. 237–250.

Reith, F., Fairbrother, L., Nolze, G., Wilhelmi, O., Clode, P.L., Gregg, A., Parsons, J.E., Wakelin, S.A., Pring, A., Hough, R., Southam, G., and Brugger, J., 2010, Nanoparticle factories: Biofilms hold the key to gold dispersion and nugget formation: Geology, v. 38, p. 843–846, https://doi.org/10.1130/G31052.1.

Reith, F., Brugger, J., Zammit, C.M., Nies, D.H., and Southam, G., 2013, Geobiological cycling of gold: From fundamental process understanding to exploration solutions: Minerals, v. 3, p. 367–394, https://doi.org/10.3390/min3040367.

Roed, M.A., 1995, Groundwater resources, *in* Roed, M.A., and Dobson, D.A., *eds.,* Geology of the Kelowna Area and Origin of the Okanagan Valley, British Columbia: Kelowna Geology Committee, p. 131–134.

Roed, M.A., 2004, Gold mining, Gallagher's Canyon, *in* Roed, M.A., and Greenough, J.D., *eds.,* Okanagan Geology, British Columbia: Kelowna Geology Committee, p. 131–132.

Roed, M.A., 2014a, Addendum, new geologic discoveries and projects in the Okanagan, *in* Greenough, J.D., and Roed, M.A., *eds.,* Okanagan Geology, British Columbia, 3rd Edition: Kelowna Geology Committee, p. 205–226.

Roed, M.A., 2014b, Groundwater resources, *in* Greenough, J.D., and Roed, M.A., *eds.,* Okanagan Geology, British Columbia, 3rd Edition: Kelowna Geology Committee, p. 145–148.

Roed, MA., Barendregt, R.W., Benowitz, J.A., Smith, C.A.S., Sanborn, P.T., Greenough, J.D., Huscroft, C., Layer, P.W., Mathewes, R.W., and Tessler, D., 2014, Evidence for an Early Pleistocene glaciation in the Okanagan Valley, southern British Columbia: Canadian Journal of Earth Sciences, v. 51, p. 125–141, https://doi.org/10.1139/cjes-2013-0106.

Scott, A., and Osatenko, M., 1980, Assessment report for the Cominco Ltd. Esperon claim: British Columbia Geologic Survey Assessment Report: 08664.

Tempelman-Kluit, D., and Parkinson, D., 1986, Extension across the Eocene Okanagan crystal[sic] shear in southern British Columbia: Geology, v. 14, p. 318–321, https://doi.org/10.1130/0091-7613(1986)14<318:EATEOC>2.0.CO;2.

Tempelman-Kluit, D.J., 1989, Geology, Penticton, west of sixth meridian, British Columbia: Geological Survey of Canada, "A" Series Map 1736A, https://doi.org/10.4095/127379.

Tetland, M., 2015, Trace element analysis of placer gold: Unpublished MSc Thesis, University of British Columbia, Okanagan, BC, 206 p.

Tetland, M., Greenough, J., Fryer, B., Hinds, M., and Shaheen, M.E., 2017, Suitability of AuRM2 as a reference material for trace element micro-analysis of native gold: Geostandards and Geoanalytical Research, v. 41, p. 689–700, https://doi.org/10.1111/ggr.12171.

Townley, B.K., Hérail, G., Maksaev, V., Palacios, C., de Parseval, P., Sepulveda, F., Orellana, R., Rivas, P., and Ulloa, C., 2003, Gold grain morphology and composition as an exploration tool: application to gold exploration in covered areas: Geochemistry: Exploration, Environment, Analysis, v. 3, p. 29–38, https://doi.org/10.1144/1467-787302-042.

van Achterbergh, E., Ryan, C.G., and Griffin, W.L., 2004, GLITTER user's manual on-line interactive data reduction for the LA-ICP-MS microprobe: GEMOC National Key Centre, Macquarie University, p. 1–72.

Watling, R.J., 1999, Novel application of laser ablation inductively coupled plasma mass spectrometry in forensic science and forensic archaeology: Spectroscopy, v. 14, p. 16–34.

Watling, R.J., Herbert, H.K., Delev, D., and Abell, I.D., 1994, Gold fingerprinting by laser ablation inductively coupled plasma mass spectrometry: Spectrochimica Acta, Part B: Atomic Spectroscopy, v. 49, p. 205–219, https://doi.org/10.1016/0584-8547(94)80019-7.

Watling, R.J., Herbert, H.K., and Abell, I.D., 1995, The application of laser ablation-inductively coupled plasma-mass spectrometry (LA-ICP-MS) to the analysis of selected sulphide minerals: Chemical Geology, v. 124, p. 67–81, https://doi.org/10.1016/0009-2541(95)00025-H.

Watling, R.J., Scadding, C.J., and May, C.D., 2014, Chemical fingerprinting of gold using laser ablation-inductively coupled plasma-mass spectrometry (LA-ICP-MS): Journal of the Royal Society of Western Australia, v. 97, p. 87–96.

Weeks, R.M., Bradburn, R.G., Flintoff, B.C., Harris, G.R., and Malcolm, G., 1995, The Brenda Mine: the life of a low-cost porphyry copper-molybdenum producer (1970–1990), southern British Columbia: Porphyry Copper Deposits of the Canadian Cordillera, Canadian Institute of Mining Special, v. 46, p. 192–200.

White, G., 1968, Assessment report for the Agricola Mines Deer and Tick claims: British Columbia Geologic Survey Assessment Report: 01694.

Wilde, A.R., Bloom, M.S., and Wall, V.J., 1989, Transport and deposition of gold, uranium, and platinum-group elements in unconformity-related uranium deposits, *in* Keays, R.R., Ramsay, W.R.H., and Groves, D.I., *eds.,* The Geology of Gold Deposits: The Perspective in 1988: Economic Geology Monograph, 6, p. 637–660, https://doi.org/10.5382/Mono.06.49.

Wilkinson, L., Hill, M., and Vang, E., 1992, SYSTAT: statistics, Version 5.2 edition: Systat, Evanston, Illinois, USA.

Zhang, X., Nesbitt, B.E., and Muehlenbachs, K., 1989, Gold mineralization in the Okanagan Valley, southern British Columbia; fluid inclusion and stable isotope studies: Economic Geology, v. 84, p. 410–424, https://doi.org/10.5382/Mono.06.49.

Received August 2023
Accepted as revised November 2023

ARTICLE

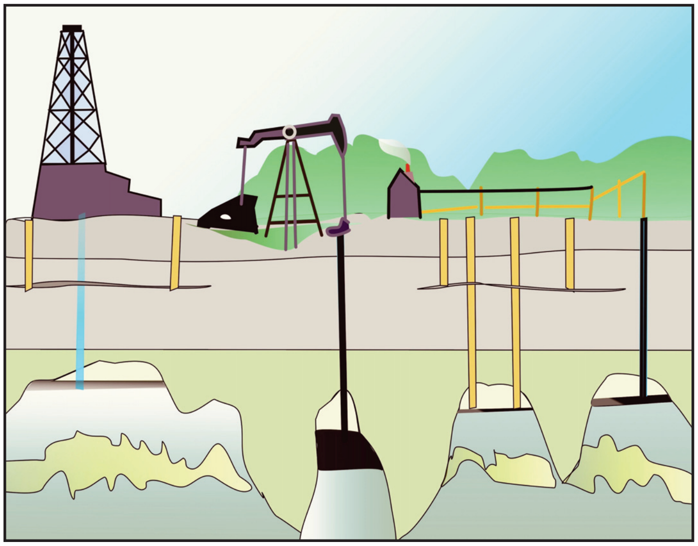

The Implications of Ontario's Historical Oil and Gas Drilling and Abandonment Practices for Abandoning Orphan and Legacy Wells

Dru J. Heagle[1] and Robert Sealey[2]

[1]*CanmetENERGY-Ottawa*
1 Haanel Drive, Ottawa, Ontario, K1A 1M1, Canada
E-mail: dru.heagle@NRCan-RNCan.gc.ca

[2]*Retired Ontario Oil and Gas Drilling and Production Inspector*

SUMMARY
Oil and gas exploration in Ontario began in the mid-1800s, leading to the first oil well drilled in 1858 and the first commercial gas well drilled in 1889. These early discoveries kicked off a boom of exploration and development drilling activity, but well records were not mandatory until 1919 after the introduction of the Natural Gas Act R.S.O.1918, c. 12. The Ontario Bureau of Mines estimated 10,000 operating oil wells in the province at the turn of the 20th century, but there are only records for approximately 1,500 wells. By 1970 there were an estimated 50,000 wells drilled in the province though there are only records for 27,000 wells, indicating there may be tens of thousands of unrecorded or lost wells in southwestern Ontario.

Wells that are not properly plugged are a conduit for fluid movement, including brine, natural gas, oil, and hydrogen sulphide, to move from the subsurface to the surface. Historical well abandoning regulations required wells to be plugged with inferior materials including wood, clay, and rubble. Cement was not the standard plugging material until 1964. There are orphaned and legacy wells leaking natural gas and sulphur water (groundwater containing dissolved sulphate and hydrogen sulphide) creating a risk to public safety. Orphaned and legacy wells are also a risk for subsurface energy projects including geological storage of carbon dioxide, hydrogen, and compressed air energy, because the wells may provide a pathway for injected fluids to return to the surface. This study reviews well construction, legislation, and abandonment practices in Ontario beginning in 1858 and identifies five factors impacting the plugging and abandonment of orphaned and legacy wells.

Further work is required to locate unreported or lost wells and to develop new techniques to permanently plug wells to limit gas leakage, reduce greenhouse gas emissions, and improve public and environmental safety.

RÉSUMÉ
La prospection pétrolière et gazière en Ontario a commencé au milieu des années 1800, conduisant au premier puits de pétrole foré en 1858 et au premier puits de gaz commercial foré en 1889. Ces premières découvertes ont donné le coup d'envoi à un essor des activités de forage d'exploration et d'exploitation, mais l'enregistrement des puits n'est devenu obligatoire qu'en 1919, après l'adoption de la Loi sur le gaz naturel, R.S.O.1918, c. 12. Le Bureau des mines de l'Ontario estime à 10 000 le nombre de puits de pétrole en exploitation dans la province au début du XXe siècle, mais il n'existe des registres que pour environ 1 500 puits. En 1970, on estimait à 50 000 le nombre de puits forés dans la province, mais il n'existe des registres que pour 27 000 puits, ce qui indique qu'il pourrait y avoir des dizaines de milliers de puits non répertoriés ou perdus dans le sud-ouest de l'Ontario.

Les puits qui ne sont pas correctement obturés constituent un conduit pour le mouvement des fluides, y compris la saumure, le gaz naturel, le pétrole et le sulfure d'hydrogène, qui se déplacent du sous-sol vers la surface. Les anciennes réglementations relatives à l'abandon des puits exigeaient que les puits soient obturés avec des matériaux de qualité inférieure, notam-

Geoscience Canada, v. 50, https://doi.org/10.12789/geocanj.2023.50.203 pages 277–294

ment du bois, de l'argile et des gravats. Ce n'est qu'en 1964 que le ciment est devenu le matériau d'obturation normalisé. Il existe des puits orphelins et anciens qui laissent échapper du gaz naturel et de l'eau sulfureuse (eau souterraine contenant du sulfate et du sulfure d'hydrogène dissous), ce qui constitue un risque pour la sécurité publique. Les puits orphelins et les puits anciens constituent aussi un risque pour les projets énergétiques souterrains, notamment le stockage géologique du dioxyde de carbone, le stockage de l'hydrogène et le stockage de l'énergie par air comprimé, car les puits peuvent permettre aux fluides injectés de remonter à la surface. Cette étude révise les pratiques de construction, de législation et d'abandon des puits en Ontario depuis 1858 et identifie cinq facteurs ayant un impact sur les activités d'obturation et d'abandon des puits orphelins et des anciens puits.

D'autres travaux sont nécessaires pour localiser les puits non déclarés ou perdus et pour mettre au point de nouvelles techniques d'obturation permanente des puits afin de limiter les fuites de gaz, de réduire les émissions de gaz à effet de serre et d'améliorer la sécurité du public et de l'environnement.

INTRODUCTION

There have been previous studies that examine the impact of oil and gas development in Ontario. Armstrong (2019) discussed the environmental impacts of early oil and gas development, particularly in the Oil Springs and Petrolia areas of southwestern Ontario (Fig. 1). May (1998) examined early oil and gas development in Ontario, focusing on the economics, innovation, and people that played significant roles. Gray (2008) also described early oil and gas development in Ontario as well as prominent events across Canada. Skuce et al. (2015) developed a geochemical tool for identifying leaking intervals in wells in southwestern Ontario by fingerprinting water geochemistry in each bedrock formation. However, there has not been a published study of the construction and condition of early oil and gas wells drilled in Ontario, particularly from the viewpoint of abandoning leaking wells. This study reviews well construction, legislation, and abandonment practices in Ontario beginning in 1858, to identify five factors impacting abandonment of orphaned and legacy wells.

The process of permanently taking a well out of service by plugging the well according to regulations has been described as plug and abandon, plugging, legal abandonment, or wellbore abandonment (Energy Safety Canada 2023). Regulations in many jurisdictions use the term "abandon", which is the term used in this study. An abandoned well is permanently shut down, plugged, with the wellhead removed and the site cleaned up and considered safe and secure by regulators. A well that is not plugged, not producing, and does not have a responsible operator is referred to as an orphaned well. The term "legacy well" is used in this study to describe a well that was properly abandoned to the standards of the time, and for which there is no current operator. Although these are the definitions for abandoned, orphaned, and legacy wells used in this study, it is important to note that the historical use of the term abandon was inconsistent, and did not always include plugging a well, but was also used to describe an orphaned well.

Oil and gas exploration in Ontario began in the mid-1800s (Logan 1852), and the first oil well was drilled in 1858 (Ontario Bureau of Mines 1892). At the beginning of the 20th century there were more than 10,000 production wells (Ontario Bureau of Mines 1901), and an estimated 50,000 oil and gas wells were drilled by 1970 in southwestern Ontario (Hutt 1970). However, there are only records for 27,000 oil and gas wells in Ontario (Carter et al. 2021a). Few well records were kept before 1919, when record keeping became mandatory under the Ontario Natural Gas Act, and many drilled wells before 1919 were never reported or the records were lost (Caley 1946). Some well operators orphaned their wells, resulting in the knowledge of the wells' existence, location, or depth being lost (Harkness 1937, 1949, 1952). Wildcat drilling is a term referring to drilling exploratory wells outside of known oil and gas plays. Wildcat wells were more commonly unproductive, or dry, and were left without properly abandoning them (Clapp 1914).

Wells that were abandoned before 1907 were plugged with wood and rubble (Act to Prevent the Wasting of Natural Gas, S.O. 7 Edward VII c. 47). Cement, wood plugs, and lead were used to plug wells from 1907 until the 1960s, when long cement plugs, consistent with todays standards, were adopted under O. Reg. 420/68. Early well repair and plugging operations were also challenged by poor equipment (Harkness 1937) as well as limited drilling and plugging experience (Harkness 1946). However, cementing operations completed to today's standards with modern equipment may also fail due to improper cementing operations and cement degradation over time (Dusseault et al. 2000; Dusseault and Jackson 2014; Natural Resources Canada 2019). There are wells that were abandoned according to the standards of their time more than 100 years ago and the plugs have degraded due to exposure to brine and "sulphur water" (groundwater containing dissolved sulphate and hydrogen sulphide).

There are several examples of orphaned and legacy wells in Ontario that leak brine and gases at surface. Leaking wells in Elgin County were abandoned around 2010 (Carter et al. 2014). Leaking abandoned wells in Norfolk County resulted in resident evacuations (Sonnenberg 2019) and other leaking wells in Norfolk County have been studied to determine the source of methane and hydrogen sulphide emissions (Jackson et al. 2020). A leaking abandoned well supplied the fuel that produced an explosion in Wheatly Ontario in 2021, causing injuries and destroying two buildings (Ensing 2021).

Hydrogen sulphide and natural gas are greenhouse gases, therefore leaks of these gases from orphaned or legacy wells are a source of greenhouse gas emissions. Unplugged or poorly plugged wells provide a pathway between the subsurface and atmosphere for fluid transport. This pathway may also be a risk for subsurface energy projects in Ontario that involve gas injection, including geological storage of carbon dioxide (Dessanti 2023), compressed air energy storage (Colthorpe 2021), and underground hydrogen storage (Lemieux et al. 2019).

There are industry best practices for properly abandoning wells but plugging older wells is often complicated because

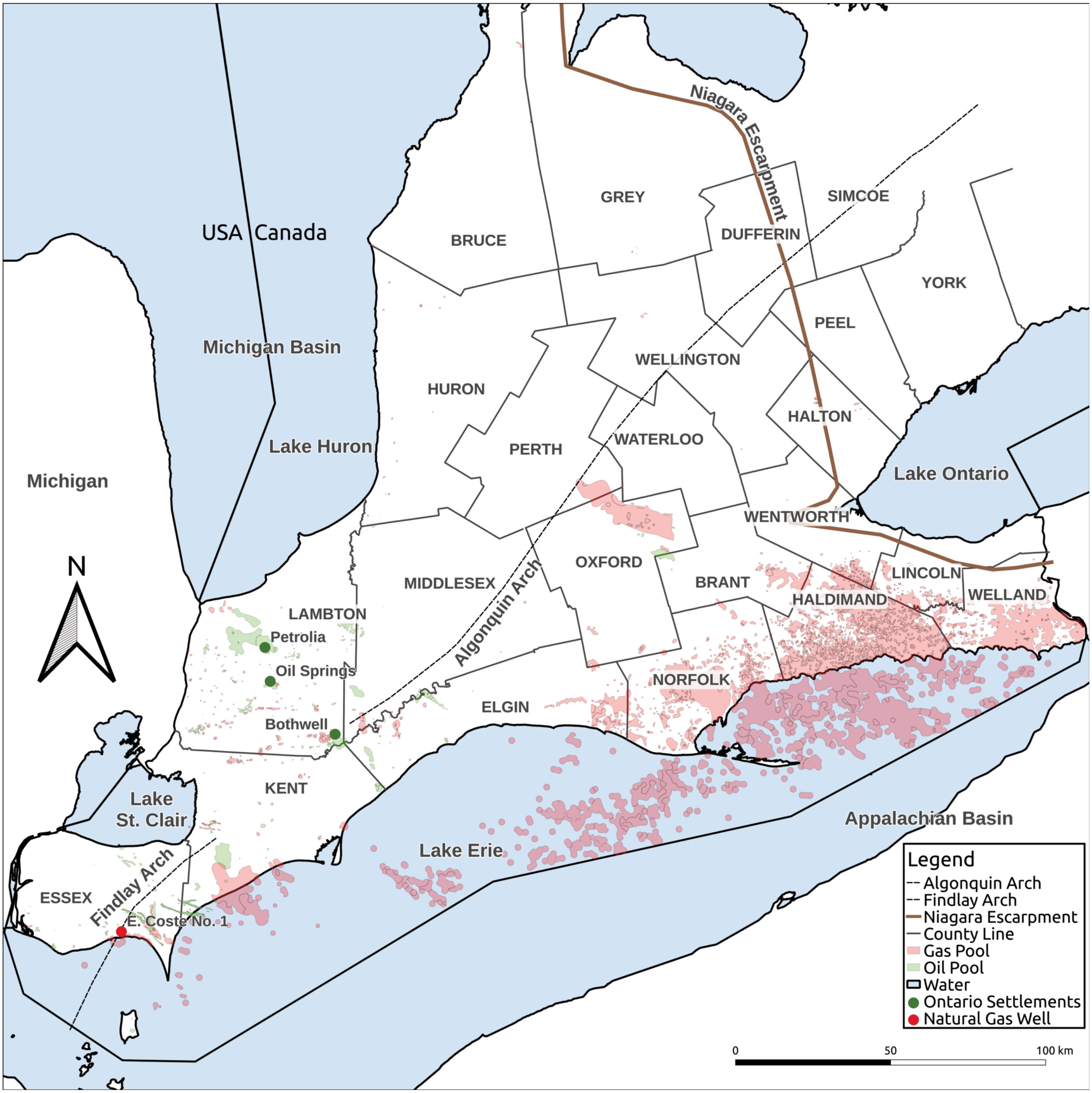

Figure 1. Study area including the first three oil field discoveries and the first commercial natural gas well.

rock can breakout from the wall of the well, or casing may be broken off in the well (Energy Safety Canada 2023). Ontario has had a program to abandon wells since 1960, originally named the Abandoned Works Fund, which was created through the Energy Act R.S.O. 1960 c. 122. The current Abandoned Works Program was refined in 2005 to abandon oil and gas wells to protect public health and drinking water resources. The challenges for the program are locating and plugging orphaned and legacy wells that have a wide range of construction methods and have plugs that have deteriorated over time.

STUDY AREA

This study focuses on southwestern Ontario, the primary oil and gas region of the province, which is bounded to the south by Lake Erie, to the west by Lake Huron and the state of Michigan, USA, and to the east by the Niagara Escarpment

(Fig. 1). The area is relatively flat with numerous lakes and rivers overlying glacial drift. The geology of the area is described in detail by Armstrong and Carter (2010) but is summarized here. The basement rocks are Precambrian crystalline metamorphic, igneous, and metasedimentary rocks referred to as the Canadian Shield. The Precambrian rocks have a southwest-plunging structural high known as the Algonquin Arch that separates the Michigan structural basin to the northwest and the Appalachian foreland basin to the southeast. In the most southwestern part of Ontario is the Findlay Arch, which is the southwestern extension of the Algonquin Arch (Carter et al. 2021b).

Sedimentation in southwestern Ontario began in the Cambrian and continued until the Devonian and potentially the Mississippian, with periods of uplift and erosion, marked by regional unconformities (Armstrong and Carter 2010). Paleozoic sedimentary strata consist of an interlayered succession of carbonates, shales, siltstones, evaporites, and sandstones. The bedrock formations dip to the southwest at 3 to 6 m/km along the Algonquin Arch into a structural low, the Chatham Sag, which is located between the Algonquin Arch and the Findlay Arch (Armstrong and Carter 2010). The bedrock dips at 3 to 12 m/km down the flanks of the arches westward into the Michigan structural basin and southward into the Appalachian foreland basin (Armstrong and Carter 2010; Carter et al. 2021b). Paleozoic strata are much thicker to the west of the Niagara Escarpment, ranging from 540 m to nearly 1400 m in the Chatham Sag, and 1600 m at the international border beneath Lake Huron (Carter et al. 2021b).

Figure 2 shows the terminology from Armstrong and Carter (2010) for the Paleozoic strata in Brant, Haldimand, Lincoln, Norfolk, Oxford, Welland, and Wentworth counties as well as eastern and central Lake Erie, which is referred to as the Eastern Counties in Figure 2. Also shown in Figure 2 are the terms used by Sir William Logan, the founding director of the Geological Survey of Canada (GSC), in the mid to late 1800's and the terms used by geologists and drillers circa 1925 (Harkness 1925). Figure 2 is intended to relate the geological terms for each unit, group or formation and not intended to illustrate unit thicknesses or duration of sedimentation. There are other rock formations for other counties listed by Harkness (1925) and Armstrong and Carter (2010) that are not shown in Figure 2 and the drillers terminology did not cover all of the labelled units in 1925 but did identify the pertinent formations.

Groundwater in Ontario becomes increasingly saline, Na-Ca-Cl-(SO_4), with distance down-dip (Carter et al. 2021b). A zone of brackish to saline water with elevated levels of sulphate and hydrogen sulphide (H_2S) is commonly found in southwestern Ontario and is referred to as sulphur water in the Ontario oil and gas community (Bailey Geological Services and Cochrane 1985; Skuce et al. 2015). Carter et al. (2021b) created a regional hydrostratigraphic framework including the sulphur water zone, which occurs from a few tens of metres to a maximum of 350 m below ground level (Carter and Sutherland 2020). The sulphur water zone occurs in all formations but is particularly prominent in the Lucas, Dundee, Bass Islands, and Guelph formations (Carter et al. 2015), and can be found beneath 22,000 km^2 of southern Ontario (Carter et al. 2021b). Below the sulphur water zone, there are several permeable units from the Silurian down to the Cambrian sandstone that contain brine with total dissolved solids concentrations between 200 and 400 g/L and are believed to be modified remnants of highly evaporated Paleozoic seawater (Dollar et al. 1991; Hobbs et al. 2011; Skuce 2014).

OVERVIEW OF EARLY DRILLING TECHNIQUES

Percussion drilling, including the spring-pole and cable tool methods, was the primary drilling method for the first six decades of the oil and gas industry (Gray 2008), but the methods were not effective for drilling through glacial drift. To get through the glacial drift, wells were dug by hand and reinforced with wood cribbing or augured with 0.1 to 0.3 m diameter auger bits (Gray 2008). Many of the wells drilled after 1863 augured a 0.25 m diameter well to 3.7 or 4.6 m below ground surface then inserted a heavy stove pipe before reducing the well diameter as they worked down lengths of progressively smaller diameter until the rock was reached, producing a well approximately 0.14 m in diameter at the top of bedrock (Harkness n.d.).

Spring-pole rigs were used to drill wells in Oil Springs beginning around 1859 (Gray 2008). These rudimentary percussion drills used a 6 m cantilevered pole anchored to the ground at the butt end and levered about one-third of its length on a fulcrum. The drill bit and other downhole tools hung from the thin end of the pole, attached by rods, rope, and/or cables. Drillers jumped or rocked back and forth on the cantilevered spring pole to raise and lower the end of the spring pole. A cast-iron drill bit was attached by a line to the end of the spring pole and the percussion of the drill bit on the underlying rock chipped the rock apart. Spring-pole-drilled wells were not more than 0.1 m in diameter and were typically shallow (tens of metres), though some wells reported by the United States Geological Survey reached 90 m depth (Bowman 1911).

Edwin Drake drilled the first oil well in the United States in Titusville, Pennsylvania, in 1861 using a cable tool rig (Gray 2008). The cable tool system used an engine and a series of wheels and pulleys to raise and drop a heavy chisel on to the rock from an oil derrick erected over the well (Bowman 1911; Clapp 1914). The rock fragments created from the chisel were cleaned from the well using a bailer. Cable tool rigs could be erected in three to four days by a skilled crew (Bowman 1911) and were standard equipment in the United States by 1884 (Gray 2008).

Improvements in cable tool drilling led to the development of the Canadian Drilling System in the 1880s (Gray 2008). The Canadian System modified the derrick to incorporate sled-like runners to make it easier to move the derrick across land (Bowman 1911) and used steam engines to turn a flywheel, which moved a belt that moved the drill wheel (International Oil Drillers 2023). A camshaft mounted to the drill wheel converted the circular motion of the drill wheel into vertical motion, allowing a walking beam to pound a drill bit (Interna-

Time Scale	Logan's Terms (1850)	Niagara Area Terms (ca.1925)			Drillers' Terms (ca.1925)	Eastern Counties Terms (Armstrong and Carter 2010)	
DEVONIAN	Portage and Chemung	Port Lambton			Black shale	Port Lambton (western counties)	
		Huron				Kettle Point	
	Hamilton	Hamilton		Ipperwash	Top rock	Hamilton	Hungry Hollow
				Petrolia	Upper soap		Arkona
				Widder beds	Middle lime		
				Olentangy	Lower soap		Marcellus
	Corniferous	Delaware			Big lime	Dundee	
		Onondoga				Detroit River	Amherstburg - Onondoga
	Oriskany	Springvale				Bois Blanc/Springvale	
		Oriskany			White sand	Oriskany	
SILURIAN	Lower Helderburg Group (Onondaga)	Cayaugan	Akron		White lime	Bass Islands/Bertie	
			Bertie				
		Salina - Camillus - shale, salt and gypsum			Salt and gypsum or lime and shale	Salina Units	
	Guelph	Niagaran	Guelph		Guelph and Niagara lime	Guelph	
	Niagara		Lockport	Barton Beds			
				Gasport		Lockport	Goat Island
							Gasport
				De Cew		Clinton	Decew
				Rochester	Niagara Shale		Rochester
		Clinton	Irondequoit		Clinton dolomite		Irondequoit
	Clinton		Reynolds				Reynales
			Furnaceville		Clinton shale		Thorold
	Medina	Medina	Thorold		(not named)		
			Grimsby		Red Medina	Cataract	Grimsby
		Cataract	Cabot Head				Cabot Head
			Manitoulin		Blue shale		Manitoulin
			Whirlpool		White Medina		Whirlpool
ORDOVICIAN		Richmond	Queenston		Red shale	Queenston	
	Hudson River		Meadowvale, Streetsville, Erindale		Hudson River Shale	Georgian Bay - Blue Mountain	
		Dundas	Credit, Humber, Danforth, Rosedale				
	Utica	Utica			Utica shale		
		Collingwood				Trenton	Coburg
	Trenton	Trenton			Trenton		Sherman Fall
							Kirkfield
	Black River	Black River				Black River	Coboconk
							Gull River
							Shadow Lake
CAM-BRIAN	Potsdam	Arkose			Potsdam	Little Falls	
						Theresa	
						Potsdam	

Figure 2. Stratigraphic correlation chart for the Paleozoic strata of southwestern Ontario that also includes the common drilling terms used circa 1925.

tional Oil Drillers 2023). The system used an early version of drill rods made of wood 0.05 to 0.1 m in diameter and 5.5 m in length, spliced together and reinforced at the joint by irons (Bowman 1911). Rods could be added to the string to advance the drill bit deeper. Sometimes the buckling and breaking of the rods prevented the rods from being removed from the well and the well was abandoned (Bowman 1911), presumably with rods and casing remaining downhole. The last recorded well drilled using the Canadian Drilling System was near Acton in Halton Township in 1959. The rig was decommissioned after the well was drilled, but the rig was rebuilt for display purposes in 1996 as shown in Figure 3.

Rotary drilling was introduced to the oil and gas industry in Texas around 1900 (Bowman 1911) and the technology continued to improve in the 20th century. Rotary rigs began operating in Ontario in 1955 with seven wells rotary-drilled that year, compared to 383 wells by cable tool rigs (Ontario Fuel Board 1955). By 1988 there were 135 wells drilled by rotary rigs and 64 wells drilled by cable tool rigs (Carter 1992). Rotary drilling uses a rotating drill bit at the bottom end of a string of steel drill pipe to bore into the rock. Water flushed through the string of drill rods cleans the drill cuttings from the well, which is more efficient than cable tool rigs that bailed cuttings from the well. The top of the rotary drill pipe string is connected to the swivel, which is attached to the derrick and allows the drill pipe to be raised and lowered in the well, and allows the drill pipe to be rotated. There are other advantages with rotary drilling that are outside the scope of this study. Bowman (1911) has a detailed discussion of early rotary drilling techniques.

Early practices drilled wells with a range of well diameters that were not standardized. From 1920 to 1922 North American oilfield equipment manufacturers and oil and gas producers worked together to standardize materials used in the industry to reduce the overhead cost of manufacturing equipment (Harkness 1923). The list of standardized equipment included: well casing, tubing, rig irons, threads, line pipe, weights of valves, flanges, and gas connections (Harkness 1923). Wells drilled before standard sizes were adopted may have diameters that are not consistent with current well drilling techniques, which is important to consider when plugging a well.

Cable tool and rotary drill rigs use steel casing to stabilize the well and keep glacial drift and rock fragments from entering the well. The casing also holds water out of the well and prevents drilling and production fluids from the well from entering aquifers. Modern practices use a 'surface casing' installed to depths below drinking water zones and cemented in place to limit the connection between the well and drinking water aquifers. Although the cement is relied on to prevent fluids from moving up the well in the annular space between the casing and the rock or glacial drift, poor cementing practices may allow leakage to occur (Dusseault and Jackson 2014). Once the surface casing is in place, drilling continues until the desired depth is reached. Wells are completed to prepare the well for production; this includes lowering piping or production tubing into the well, installing pumps, and configuring the top of the well (or well head) to control the fluids produced from the well and to prevent fluids from entering the well. Despite the engineering required to complete a well, a well is a pathway for fluid movement. Fluids can enter or leave the well at permeable horizons unless the horizons are isolated with cemented casing or plugged with cement or other types of plugs.

Figure 3. Canadian Drilling System rig rebuilt in 1996.

FIRST OIL AND GAS DISCOVERIES IN ONTARIO

Oil

The settlers in Enniskillen Township, Lambton County, knew of "gum oil" in the local swamps in 1830 (Clapp 1914). Sir William Logan reported "asphalt or mineral pitch" in Enniskillen Township and springs of petroleum along the Thames River in Mosa Township to the Legislative Assembly of Canada, where the discoveries were made public record (Logan 1852). James Williams from Hamilton, Ontario, went to Enniskillen in 1858 to investigate if the petroleum from the gum oil could be refined to lamp fuel and lubricating oil. Williams dug a well in the gum oil and liquid petroleum entered the well, creating North America's first oil well. Prospectors arrived the following year, 1859, creating the community of Oil Springs. Williams used the spring-pole rig to drill a productive oil well 44 m deep sometime between 1859 and 1861 (Gray 2008). Significant milestones in Ontario oil and gas exploration and development as well as key legislation regarding well abandonment are shown in Figure 4A.

There was little development in the Oil Springs field until January 1862, when John Shaw dug through 14 m of glacial

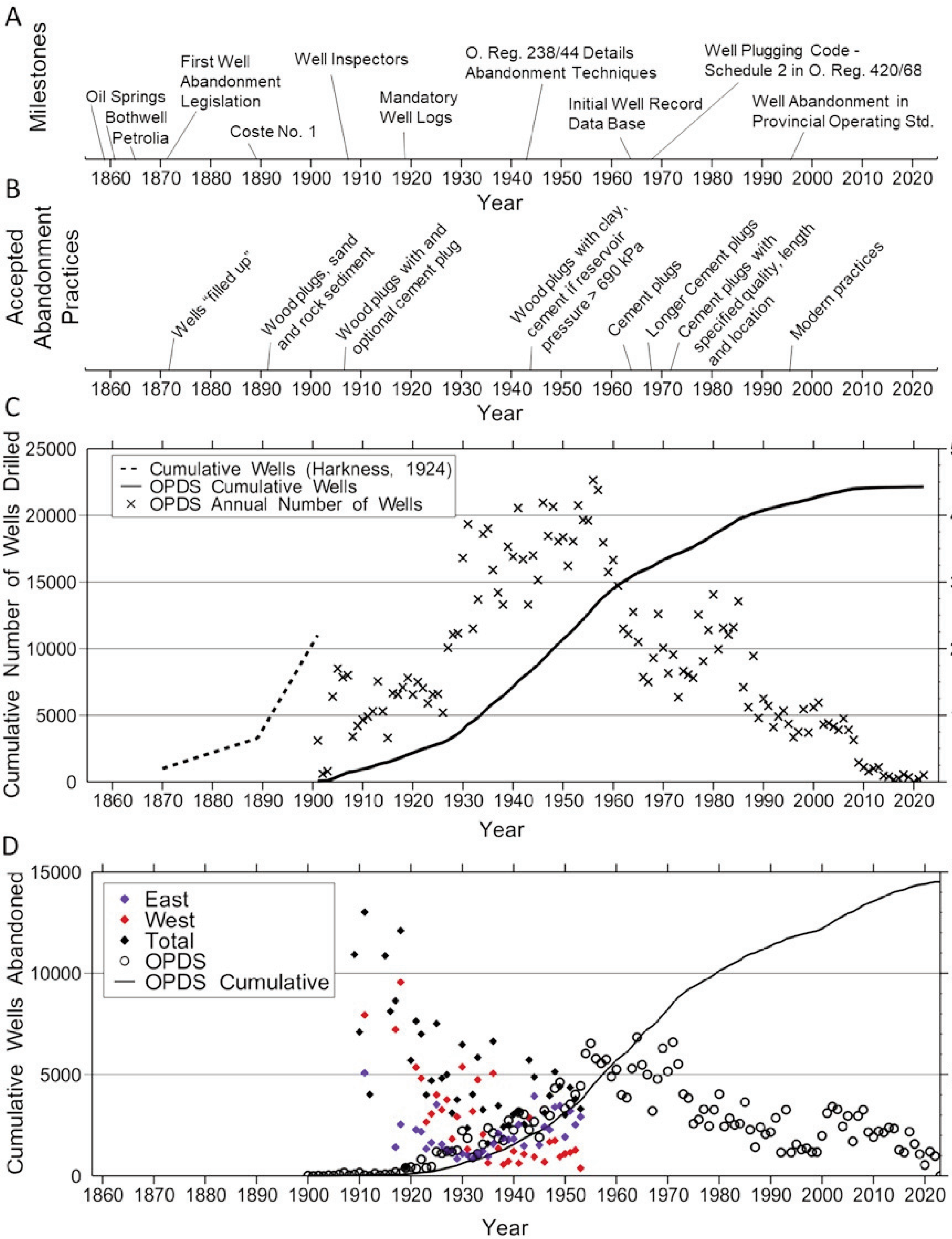

Figure 4. Timelines showing A) milestones for oil and gas development and well abandonment; B) the progression of accepted abandonment practices; C) the cumulative and annual number of wells drilled reported in the Annual Reports including Harkness (1924) and recorded in the Ontario Petroleum Data System (OPDS); D) the cumulative and annual number of abandoned wells reported in the Annual Reports and the recorded well abandonments in the OPDS.

drift then used a spring pole rig to drill through 41 m through rock to create Canada's first gushing oil well, which produced an oil exploration boom. Brumell (1892) listed 33 flowing wells in Enniskillen Township in Lambton County and by 1860 hundreds of derricks had been erected (Clapp 1914), but the location of each well was not recorded (Ontario Bureau of Mines 1892).

The next oil discovery was near Bothwell, Kent County, near the western border of Mosa Township in 1861 (Clapp 1914). Natural petroleum seeps in the Thames River led to numerous exploration wells being drilled along both sides of the river, but there were few records or descriptions of where these wells were (Harkness n.d.). John Lick began drilling the first productive well in the Bothwell field in September 1862 (Gray 2008). Other wells followed, but the lack of drilling experience and understanding of Ontario's oil and gas system led to wells drilled below the oil reservoir into an underlying aquifer, allowing saline water to enter the reservoir. The influx of saline water inhibited the production of oil (and gas) diminishing the use of the field. At the end of 1865 the 31 remaining wells in the field were pumping large volumes of water and an additional 172 wells were not in operation (Harkness n.d.; Gray 2008). By 1867 production in the field ended and remained idle until 1895 when drilling extended the field west and the oil field was revived (Ontario Bureau of Mines 1896).

Oil was discovered in Petrolea in 1865. The town name Petrolea was changed to Petrolia due to a clerical error around 1914. Exploration began in the Petrolia area because of the discovery of gum oil similar to in the Oil Springs area. Drilling techniques were similar to those used in Oil Springs and the first flowing well was drilled in Petrolia in 1865 (Caley 1946). Petrolia was the primary centre of oil development in Canada in 1867 (Armstrong 2019). Although 2500 wells were drilled in the area by 1890 (Clapp 1915), there are no reliable records for these wells (Caley 1946).

Following the discovery of oil at Oil Springs, Bothwell and Petrolia, oil exploration occurred throughout Ontario. Exploration was underway in eastern Ontario near Whitby, Bainsville, Pembroke, Caledonia Springs, North Gower, and in other townships, but there were few records for many of these wells regarding location, drilling methods, or depths (Brumell 1892). Wildcat exploration also occurred within towns, including in Toronto on Parliament St. and in Ottawa near Patterson Creek (Brumell 1892). New fields were developed in Thamesville, Dutton, Raleigh, Wheatley, Leamington, Essex, Romney, Onondoga, Belle River, Dover, and Mosa (Harkness 1924).

Natural Gas

Natural gas seeps were known throughout Canada before 1800, including Caledonia Springs in Prescott County and the Burning Spring at Niagara Falls, but the gas was not widely exploited (Selwyn 1891; Ontario Bureau of Mines 1892). A few private residential gas wells were drilled into the glacial drift in Kent County in the 1860s and used the gas for heating fuel and lighting, but none of these wells produced gas at a commercial scale (Ontario Bureau of Mines 1892). Private wells were also drilled in Welland County in 1866 (Ontario Bureau of Mines 1892) and Port Colborne in 1885 (Selwyn 1891). There were also indications of other low production gas wells (less than 1400 m^3 of gas per day) drilled in southern Ontario before 1887 but there were no records for the wells (Selwyn 1891).

Eugene Coste, a former oil and gas engineer with the GSC, used an anticline theory developed by Dr. Sterry Hunt (Hunt 1861) to explore for gas in South Gosfield Township, Essex County (Malcolm 1915). Drilling began in 1888 on the Coste No. 1 well near the Findlay Arch (Figure 1), and on January 23, 1889 (Fig. 4A), from a depth of 314 m, natural gas flowed from the well at a rate of 280,000 m^3 per day, becoming Canada's first commercial gas well (Gray 2008). A second well was drilled in the same area as the Coste No. 1 well and was used to supply the municipalities of Kingsville and Ruthven in 1890 (Ontario Bureau of Mines 1892).

Similar to the expansion of exploration after the Oil Springs and Petrolia gushers, natural gas exploration occurred in numerous townships in southern Ontario, but exploration was more concentrated in the counties surrounding the gas wells in Essex (Ontario Bureau of Mines 1892). By 1891 there were three established gas fields including Essex County, glacial drift deposits in Kent County, and the field spanning Welland and Haldimand counties. Although the natural gas supply was abundant, there was little consumption of natural gas domestically, and gas was sold via pipeline to Detroit and Buffalo in 1894 (Ontario Bureau of Mines 1895).

MILESTONES IN THE ONTARIO OIL AND GAS INDUSTRY AND WELL PLUGGING REGULATIONS

Early oil and gas discoveries encountered significant volumes of hydrocarbons and the flow of oil and gas from the wells was often difficult to control (Armstrong 2019; Ontario Bureau of Mines 1892). The lack of drilling experience and necessary equipment to control the flows resulted in significant waste of oil and gas, which was scrutinized by the public (Armstrong 2019). Some wells that were drilled through aquifers had groundwater invading oil horizons, limiting the oil production in the Bothwell field, as described above. These circumstances led to the creation of the first legislation in Ontario to plug oil wells in 1872 called an Act "to provide for the filling up of or otherwise shutting off the water flowing in to abandoned Oil Wells" S.O. 1872 c. XXXIX (Table 1). The intent of the Act was to seal off the water horizons from abandoned wells to protect the producing wells. The methods for plugging the well were not specific in the 1872 Act, indicating that "the abandoned well should be filled up, or the water flowing therein shut off in some other and what manner".

The concern for wasting oil and gas resources was a common theme in many early reports and appears to have been the primary motivation behind the legislation and practices until 1996. Significant changes to abandonment practices under the Ontario Acts and Regulations from 1872 to 2023 are listed in Table 1 and the progression of accepted abandonment practices is shown in Figure 4B. There were amendments to many of the Acts that are not listed in Table 1 because the changes

Table 1. List of Ontario Acts with significant changes to plugging and abandonment practices.

Year	Act or Regulation	Notes
1872	Act to provide for the filling up of or otherwise shutting off the water flowing into abandoned Oil Wells S.O. 1872 c. XXXIX	The intent of the Act was to preserve oil reservoirs by limiting water inflow. Abandoned wells were to be filled but the methods or materials were not indicated.
1892	Act to Prevent the wasting of natural gas and to provide for the plugging of abandoned oil wells S.O. 1892, c. 56	The intent of the Act was to preserve gas reservoirs and limit the loss of leaking gas by limiting water inflow. Wells were plugged with a 1 m long wooden plug and filled with sand or rock sediment.
1907	Act to prevent the wasting of natural gas and to provide for plugging of all abandoned wells S.O. 1907 c. 47	Wells to be plugged with wooden plugs with an option to use an overlying cement plug. Wood plugs were 1 m or longer and installed across a water bearing horizon. Two appointed Inspectors oversaw plugging operations.
1918	Natural Gas Act, R.S.O. 1918, c. 12	Introduced the Natural Gas Commissioner. Act required license to drill well, well records, report plugging and abandonment methods.
1924	Well Drillers Act R.S.O. 1924, c. 75	Plugging methods are the same as the 1907 Act. Inspectors review well abandonments, and the Act requires reporting of plugging methods.
1944	Well Drillers Act O. Reg. 238/44 – Natural Gas and Oil Wells.	The Regulation required improved plugging methods as described in the text.
1954	Ontario Fuel Board Act R.S.O. 1954, c. 63	O. Reg 199/54 required the proposed plugging approach and actual methods and results to be filed with the Fuel Board. Plugging methods were consistent with O. Reg 238/44.
1960	Energy Act R.S.O. 1960, c. 122	This Act is concurrent with the Ontario Fuel Board Act governing oil and gas; requiring dry or abandoned wells to be plugged.
1960	Ontario Energy Board Act R.S.O. 1960, c. 271	Continued to use the approach under O. Reg. 199/54.
1964	Energy Act R.S.O. 1964 O. Reg 326/64 Exploration / Drilling and Production	Cement was made the standard for abandonment plugs and the proposed abandonment method must be approved by an inspector.
1968	Energy Act R.S.O. 1964 O. Reg. 420/68 Exploration / Drilling and Production	The length of plugs is increased and there are specific plugs required in abandoned wells.
1971	Petroleum Resources Act R.S.O. 1971 c. 94	The Petroleum Resources Act applies concurrently with the Energy Act 1960 and covers drilling, plugging and abandonment as well as other up-stream activities.
1972	Petroleum Resources Act R.S.O. 1971 O. Reg 45/72 Exploration, Drilling and Production	Schedule 2 – Well Plugging Code no significant changes from 420/68.
1990	Petroleum Resources Act O. Reg 915 Exploration, Drilling and Production	Schedule 2 – Well Plugging Code no significant changes from 420/68.
1996	Oil, Gas and Salt Resources Act R.S.O. 1990 c. 30 P.2	Replaced Petroleum Resources Act. Introduces Provincial Operating Standards for plugging and abandoning wells.
1997	Oil, Gas and Salt Resources Act R.S.O. 1990 O. Reg. 245/97 Exploration, Drilling and Production	Current 2023 regulation outlining requirements for upstream oil and gas activities, including plugging and abandonment.

https://doi.org/10.12789/geocanj.2023.50.203

were administrative or did not impact how a well was abandoned.

The amount of natural gas wasted in 1891 was reported to be enormous (Ontario Bureau of Mines 1892). One example was a creek-side well that was cased with a wooden pipe to 30 m depth. Gas erupted from the well projecting water, rock and stones up to 15 m in the air (Ontario Bureau of Mines 1892). Gas was allowed to escape from the well for six or seven years before the flow stopped (Ontario Bureau of Mines 1892). The first legislation to address natural gas waste was "An Act to Prevent the Wasting of Natural Gas and to Provide for the Plugging of all Abandoned Wells" S.O. 1892, c. 56 (Table 1, Fig. 4A). The intent of the Act was to plug wells within two months after production ceased, to prevent gas wasting and to preserve the reservoir. The Act required abandoned wells to be filled with sand or rock sediment from the bottom of the well to 7.6 m above the gas horizon. The well was plugged with a seasoned wood plug at least 1 m long and the same diameter as the well and installed 1.5 m below the bottom of the casing. Once the casing was removed, a second plug was installed above the first plug and the well was backfilled with 7.6 m of sand or rock sediment.

There was an estimated total of 10,000 oil wells being pumped in Ontario at the turn of the 20th century (Ontario Bureau of Mines 1901) and 11,000 wells in operation in 1901 (Harkness 1924; Fig. 4C). Oil production was primarily from the Oil Springs, Petrolia, Bothwell, Dutton (Kent County) and Thamesville (Essex County) fields. Ontario oil fields gained a reputation for having numerous wells in a field, with limited production coming from each well. Initially, the only developed oil reservoir was known as the Corniferous limestone (Ontario Bureau of Mines 1901), now referred to as the Dundee Formation (Armstrong and Carter 2010; Fig. 2). In 1902 the "Gurd Gusher" was drilled in the Raleigh field, Kent County, in the "Middle Lime" (Ontario Bureau of Mines 1902) or Hamilton Group (Fig. 2). Gas production at the turn of the century was dominantly from the Essex and Welland fields; a new discovery in Hepworth (Ontario Bureau of Mines 1901) produced gas from the Clinton and Cataract (formerly Medina) groups (Ontario Bureau of Mines 1905).

By 1901 the Ontario oil and gas fields were being depleted (Ontario Bureau of Mines 1902). Three quarters of the wells in the Essex gas field were flooded with saline groundwater, inhibiting gas production. The low production combined with natural gas exports to Detroit caused concerns that the Essex field would not be able to meet domestic demand and prompted the Ontario government to prohibit the export of natural gas from the Essex field to Detroit in 1901. By 1903 the Essex field was practically abandoned due to the limited gas production (Ontario Bureau of Mines 1904).

The failure of the Essex gas field combined with numerous reports of wasting natural gas from open wells and poorly maintained pipelines led to the 1907 Act to Prevent the Wasting of Natural Gas and to Provide for the Plugging of all Abandoned Wells S.O. 1907 c. 47 (Table 1). The Act had two primary objectives; the first was to maintain the quality of oil and gas reservoirs by preventing water from flooding oil or gas-bearing horizons. The second objective was to limit wasting gas that was leaking from wells, pipelines and other equipment. The Act required wells to be completed in a manner to prevent gas leaks two weeks after drilling. Dry wells were to be abandoned by pulling the casing and plugging the well to prevent fresh or salt water from entering the reservoir. Plugging was conducted with a wood plug or optionally a wood plug with an overlying layer of cement. Well inspections were now conducted by Provincial Inspectors who could also add specific provisions for each abandonment.

Two Inspectors were appointed to enforce proper well abandonment. One inspector was responsible for the western counties (Lambton, Kent and Essex) and the other the eastern counties (Elgin, Welland and Haldimand-Norfolk; Ontario Bureau of Mines 1909). The first inspection reports indicated many of the wells in the Enniskillen area required work to improve the condition of the well, in some cases it was difficult to identify well operators, and the number of lost or orphaned wells was unclear. Wells in other counties were in better condition likely because they were not as old as the Enniskillen wells (Ontario Bureau of Mines 1909). Oil and gas production improved by 1915 and was credited to decreased groundwater invasion of the reservoirs as a result of the well plugging and abandonment work (Ontario Bureau of Mines 1915), though there were continued reports of gas wasting. At the time of the federal election in the fall of 1908 the Tilbury East landscape was illuminated by towering torches of natural gas leading the provincial government to impose a tax on wasted gas (Lauriston 1961). The tax on natural gas wasting was two cents per thousand cubic feet in 1917, with the Inspectors responsible for enforcement (Ontario Bureau of Mines 1918).

The Tilbury gas field was discovered in 1911 and was the primary gas producer in Ontario in 1916 (Ontario Bureau of Mines 1917). Production from the field in 1917 was not able to keep up with winter demand, which led to a home fuel shortage (Ontario Bureau of Mines 1918). Gas production was diminished by water flooding the wells, inhibiting gas flow to the wells and limiting gas production. Public complaints applied pressure to the government that resulted in the Natural Gas Act R.S.O. 1918 c. 12 (Table 1, Fig. 4A), which limited the sale of natural gas to industry, focusing consumption on residences (Ontario Bureau of Mines 1918).

The Natural Gas Act was revised in 1919 to require drillers to obtain a license to drill a well and to provide proper well records and drill cutting samples (Estlin 1921). The GSC collected voluntary submissions of drill cuttings and drill core samples from wells being drilled to explore for and develop oil, gas, and salt resources in Canada, beginning in the 1800s. The samples were stored in Ottawa (Carter 2017). The first well records under the Natural Gas Act included information location, depths to the tops of rock formations, total well depth, and the estimated production. The following year the records included the name of the well logger, measured reservoir pressure, the depths of water, gas or oil encountered, and the date of completion (Harkness 1922). Reporting the method of plugging and abandoning wells was mandatory beginning in 1922 (Harkness 1923). The well operator was added to the reports in 1925 (Harkness 1926), but the drilling method (e.g. the Canadian Drilling System or rotary drilling) was not listed. Many wells prior to the Natural Gas Act R.S.O. 1918, c. 12, do not have well records, particularly dry wells and abandoned wells where the casing was pulled (Caley 1946).

The number of wells abandoned was reported annually in the Department of Mines annual reports (described below as Annual Reports) beginning in 1909 and ended in 1953, although the number of reported wells abandoned in the eastern territory was intermittent before 1919 (Fig. 4D). The total number of wells abandoned each year was calculated as the sum of the reported abandoned wells in the Annual Reports from both territories for each year from 1909 to 1953. There were 12,735 reported wells abandoned between 1909 and 1953. The relatively higher number of wells abandoned in the western counties was likely due to earlier and more drilling activity relative to the eastern counties.

The Well Drillers Act R.S.O. 1924, c. 75 (Table 1), which worked concurrently with the Natural Gas Act, set out the rules for well licensing, drilling, and inspection, as well as plugging and abandonment. Inspectors noted improved conditions in the oil and gas fields in 1927 due to the abandonment of old wells and better care of the existing wells (Harkness 1928). The Annual Reports in the following years noted successful periods of plugging and abandonment that led to improved production (e.g. Harkness 1928, 1930), but there were reports of faulty casing and ineffective well plugging that led to neglected and flooded wells (Harkness 1925, 1927).

Impacts of the World Wars and the Depression on Well Abandonment

The Fletcher oil field was discovered in 1905 and covered approximately 5,600 acres in Kent County. The field produced oil from 276 wells in the Guelph formation and Salina units with a "heavy flow" of saltwater flowing up from below the oil (Koepke and Sanford 1966). The casings were pulled from the wells in 1919 because of the high price offered for old casing during the First World War. Without the casings in the wells saline groundwater flowed up the well to surface (Williams 1920). There were several examples of properties producing as many as 200 barrels of oil per month that had casings pulled and sold (Williams 1920). The methods of well abandonment for the Fletcher field after the casings were removed were not reported.

The economic downturn of the Great Depression from 1929 through the mid 1930s had significant impacts on oil and gas wells. Abandoned wells were stripped of casing and pipe to be used in other wells, but the metal was corroded and weak (Harkness 1929). The corroded casings allowed natural gas and oil leaks to occur. This was particularly difficult to address in the spring when the fields were flooded, preventing access to the wells but allowing surface water to flood the wells (Harkness 1929). Limited capital investment through the Depression caused wells to deteriorate and well operators to orphan wells.

The war efforts during the Second World War limited capital investment into oil and gas infrastructure, necessitating equipment to be salvaged from waterlogged oil and gas fields and repurposed in operating fields (Harkness 1946, 1948a). Oil-field equipment was expensive and not readily available, which also promoted the reuse of casing and pipe even if it was corroded (Harkness 1946, 1948b). The hydrogen sulphide in the oil and groundwater water corroded equipment, gradually deteriorating the infrastructure (Harkness 1948a). Skilled labour, particularly for drilling and abandonment, was limited because nearly all experienced workers were on active war service (Harkness 1948a). The lack of skilled labour diminished the quality of well records (including accurate well locations) and well inspectors were not able to oversee many of the well plugging and abandonment operations (Harkness 1947).

The next significant regulatory change was Ontario Regulation (O. Reg.) 238/44 Natural Gas and Oil Wells (Table 1, Fig. 4A). Wooden plugs remained the primary seal but when a plug was driven to the bottom of a casing, the plug was required to seal both the open well and the casing. Wells with a pressure gradient greater than 6.9 kPa over a three-metre depth were to be backfilled with clay at least three metres above the gas producing formation, and a wooden plug placed above the clay. For wells with pressures greater than 690 kPa, two wooden plugs separated by three metres of tamped clay were required. In addition, six metres of cement was to be emplaced on top of the upper plug, then a third wooden plug installed on top of the cement. Finally, clay was tamped into the well to fill the well up to the bottom of the casing. Lead plugs could be used instead of cement plugs.

The "mud fluid method" of plugging was also acceptable under O. Reg. 238/44. The mud-fluid method was first used with cable tool rigs in California in 1909 and used a clay-water mix to create a mud with a greater density than water with the clay particles clogging the pores in rocks in the well (Collom 1922). The mud was used to inhibit the movement of gas into a well to seal off "gas sand" horizons. The drawback of the mud fluid method was that any larger grained materials in the mud, such as sand or rock fragments from the well, would not seal off the gas horizons, and allowed gas to enter the well and escape if another plug was not used (Collom 1922).

At the end of the Second World War there were 975 reported abandoned wells due to the inclusion of "idle wells" with abandoned wells (Harkness 1948a). The 975 idle wells were not operational for fifteen or twenty years, but it is not known if they were abandoned or orphaned (Harkness 1948a) and they are not shown in Figure 4D. There were no subsequent reports of these wells in the Annual Reports, making it difficult to determine if they were properly abandoned. There were also reports of thousands of wells that were abandoned with clay plugs, which was permitted under O. Reg. 238/44. There was concern about the stability of the clay if the reservoirs re-pressurized (Harkness 1948b), but there were no subsequent discussions of these wells. Significant oil and gas exploration resumed in 1949 but some companies were bankrupt, leaving operating wells in poor condition or orphaned (Harkness 1951).

Landowner complaints regarding the impact of newly drilled gas wells were notable in Welland and Haldimand counties in 1947. Sulphur water and natural gas were contaminating

https://doi.org/10.12789/geocanj.2023.50.203

domestic water wells and, in some cases, natural gas was being pumped into residences (Harkness 1949). Provincial Inspectors investigated the complaints and confirmed there were improperly cased wells allowing sulphur water to enter freshwater aquifers. However, in most cases the problem was that water wells were drilled too deep and penetrated the sulphur water aquifer (Harkness 1949), allowing natural gas and hydrogen sulphide to move up the water well into overlying aquifers. These historical water wells may continue to be a factor for hydrogen sulphide leaking from wells today.

Modernization of Plugging Practices

The Ontario Fuel Board Act R.S.O. 1954, c.63, revised and consolidated the oil and gas legislation and introduced the Fuel Board (Ontario Fuel Board 1955). The function of the Fuel Board was to control and regulate all phases of the natural gas industry. Land leases, drilling permits, and reporting requirements were modernized in a manner consistent with current practices. The detail included in the Fuel Board annual reports after 1954 was significantly less than the detailed reporting by the Department of Mines (from 1892 to 1953). Abandoned wells were not included in the Fuel Board reports but were contained in the well records and well license information. Well plugging methods in the 1950s remained consistent with O. Reg. 238/44.

The Department of Energy Resources was established by legislation in 1960, assuming oversight, regulation, and reporting responsibility for oil and gas in Ontario (Ontario Department of Energy Resources 1961). The Energy Act R.S.O. 1960, c. 122, addressed well abandonment practices, created the Abandoned Works Fund for the completion or removal of works, and prescribed the procedure for payment of money into and out of the fund. The Ontario Fuel Board was dissolved in 1960, with the administrative functions assumed by the Department of Energy Resources, and the judicial functions were taken over by the Ontario Energy Board under the Ontario Energy Board Act R.S.O. 1960, c. 271 and the Energy Act R.S.O. 1960, c. 122. The Ontario Energy Board has remained Ontario's energy sector regulator since 1960, although there have been several new Acts and amendments regarding oil and gas in the province. The introduction of O. Reg. 326/64 (Table 1) disallowed the use of clay for well plugging, prescribing cement plugs as the standard for abandonment. O. Reg. 326/64 also required an application for a permit to bore, drill or deepen a well (Form 103) as well as a scaled plan showing the well co-ordinates, certified by an Ontario Land Surveyor or Professional Engineer. Previous descriptions and maps of well locations were relative to cultural or natural landmarks such as buildings, intersections and water bodies, but the scaled plan significantly improved the accuracy of well locations.

Standard well abandonment methods improved with the introduction of O. Reg. 420/68, that listed Schedule 2, the Well Plugging Code. Additives to cement were permitted for faster curing, or viscosity reduction etc., but the cement had to have a minimum weight of 1737 kg/m^3. Bridge plugs could be made of wood, stone, gravel, or lead, but could not include a non-drillable material. The intervals between plugs were to be filled with water or drilling mud, adding another barrier to fluid flow. Cement plugs were to be set above and below each water interval as well as across each oil and gas horizon and were now longer, with a minimum length of 7.6 m above and 7.6 m below fluid zones. In addition to plugging the porous oil and gas horizons in a well, 7.6 m plugs were to be set in the top of the Cambrian, Trenton, Queenston, Clinton-Cataract, Guelph, Salina, Dundee, and bedrock formations to prevent fluid flow into or out of these oil and gas-bearing formations. Separate rules were also introduced regarding well casings in the abandonment process. If surface casing was left in a well, the well had to either have a cap welded to the casing or be plugged with 3 m of cement prior to cutting the casing off one m below surface. When the surface casing was removed from the well, the well was filled to surface with clay or sand or cuttings as the surface casing was withdrawn and a final cement plug was set between one and two metres from surface.

The Petroleum Resources Act R.S.O. 1971, c. 94 (Fig. 4A) took responsibility for oil and gas exploration, drilling and production. The enabling regulation (O. Reg. 45/72) contained Schedule 2, the Well Plugging Code that identified all of the essential elements from O. Reg. 420/68. The Petroleum Resources Act was amended and renamed the Oil, Gas and Salt Resources Act R.S.O. 1990, c. 30 P.2. The enabling regulation was written in 1997 O. Reg. 245/97 and created five different classes of examiners, including the Class I examiner who was responsible for examining wells with respect to used casing, cement quality, isolation of porous zones, cement tops, well control equipment, and well abandonment. Abandonment requirements were no longer listed in the regulation; they were moved to a Provincial Operating Standard that could be updated without legislative approval, streamlining the process to update abandonment practices.

Ontario Petroleum Data System

The 'Ontario Well Data System' was developed in 1964 through a partnership between the University of Western Ontario and the Ontario Department of Energy and Resources Management (Hutt 1970). The information from all the available petroleum well records was transcribed into the new system, producing a database of 10,000 well records in southern Ontario (Hutt 1970).

The Ontario government established the Petroleum Resources Laboratory in London, Ontario, in 1971, under the Petroleum Resources Act (Table 1). The existing Ontario rock sample collection was shipped from the GSC in Ottawa to the Petroleum Resources Laboratory, and Ontario began to consolidate the geological information derived from oil and gas exploration and development (Oil, Gas, and Salt Resources Library 2023).

The Petroleum Resources Laboratory was renamed the Oil, Gas and Salt Resources Library (OGSRL) in 1997 (Carter 2017) with the enactment of the Oil, Gas and Salt Resources Act R.S.O. 1990, c. 30 P.2. The library is operated by the Oil, Gas and Salt Resources Corporation under the terms of a Trust Agreement with the Ontario government. The Corporation is a subsidiary of the Ontario Petroleum Institute (OPI), which is a non-profit industry association that represents explorationists, producers, contractors, geologists, petroleum engineers and other professionals, individuals, or companies directly related to the oil and gas, hydrocarbon storage, and solution-mining industries of Ontario. The library collection includes well drilling and completion records, rock chip samples from 13,000 wells, rock core samples from 1000 unique wells, and over 20,000 geophysical logs (Clark et al. 2020).

The Ontario Well Data System was updated to an Oracle platform database that is maintained by the Ontario Ministry Natural Resources and Forestry and the Ontario Oil Salt and Gas Resources Library and was renamed the Ontario Petroleum Data System, or OPDS (Carter and Castillo 2006). The database has records for approximately 27,000 wells with location co-ordinates and a well location accuracy code indicating the accuracy of the geographic co-ordinates for the wells, with the accuracies ranging from 1 metre to over 1000 metres (Clark et al. 2020). Over 95% of the wells have coordinates with accuracies within 200 metres (Clark et al. 2020). There have been several quality assurance reviews of the petroleum well records, with a focus on well locations and geological formation tops, most recently during the completion of 3-D models of the bedrock geology of southern Ontario by the Geological Survey of Canada (Carter et al. 2021a).

There is a discrepancy between the 10,000 wells reported by the Ontario Bureau of Mines (1901) and the 1518 well records in the OPDS drilled before 1900 (Fig. 4C). The discrepancy highlights how many wells do not have records and how many wells have been lost. The cumulative number of wells in Ontario provided by Harkness (1924) is shown separately from the number of well records in the OPDS shown in Figure 4C because there were no well records. If the values are combined, the total number of wells in southwestern Ontario would exceed 32,000 wells. The wells in the OPDS were mapped as the number of wells per km^2 and show multiple areas that have more than 125 recorded wells per km^2 (Fig. 5A). The high oil well densities around Petrolia, Oil Springs, and Bothwell stand out in Figure 5A, as well as the high density in Middlesex County that is currently named the Glencoe oil field but was historically known as the Mosa field. The other high-density oil well area is the Tilbury pool in Kent County. The high-density of gas wells is associated with the gas pool in Norfolk, Haldimand, and Welland counties. For comparison, the areas of lower well density, such as in Perth County, are as low as one well per km^2, although there may be localized areas with higher well densities.

The OPDS has records for abandoned wells that include the plugging date and some information regarding the plugging contractor, number of depth intervals plugged, length of each interval, amount of cement used in each interval, the type of cement used as well as a section of plugging notes for more complicated plugging operations. The total number of wells abandoned listed in the OPDS (Fig. 4D) is fewer than the number of abandoned wells reported in the Annual Reports until 1937. This is likely due to limited record keeping although well plugging and abandonment records were required under the Natural Gas Act R.S.O. 1918 (Table 1). After 1937, the number of abandoned wells in the Annual Reports and in the OPDS are similar except for during the Second World War, when the lack of reporting and drilling expertise was noted (Harkness 1947, 1948a). There are a total of 14,500 abandoned wells in the OPDS for southwestern Ontario and the distribution of abandoned wells is similar to the distribution of drilled wells, only there are fewer recorded abandoned wells (Fig. 5). There are records for approximately 7,000 wells abandoned before 1964 (Fig. 4D) that would have been abandoned with rock sediment, wood plugs, clay, and potentially a cement plug depending on the year the well was plugged and the reservoir pressure (Fig. 4B). Cement plugs became the standard method for plugging wells in 1964 (O. Reg. 326/64, Table 1, Fig. 4B). There may be thousands of wells in Ontario that were not abandoned using cement plugs.

The wells shown in Figure 5 represent the known well locations. Clapp (1914) identified wildcat drillers as potential sources of unplugged wells because wildcat drillers worked rapidly, abandoning dry wells without casing off the water or properly abandoning the wells. The locations of some wildcat wells are unknown and are unlikely to have been abandoned and would not be captured in Figure 4 or Figure 5.

OTHER FACTORS AFFECTING THE CONDITION OF WELLS FOR ABANDONMENT

Well Maintenance and Enhanced Oil Recovery

Well maintenance and early Enhanced Oil Recovery techniques also had an impact on the condition of wells. The Roberts Torpedo was an iron container with dynamite or nitroglycerine that was lowered down a well then exploded, which was referred to as 'shooting a well' (May 1998). Shooting a well was the earliest reported technique for enhancing oil and gas recovery in Ontario (Selwyn 1891) but wells were also shot to clean out accumulated sediment, paraffin, salt, and other matter (Harkness 1933). The first reported well that was shot was in 1872 in Lambton County and the technique was used without regulation for 19 years (May 1998). Wells in other fields were also shot, including in Welland (Selwyn 1891), Dawn (Ontario Bureau of Mines 1892), Tilbury (Hume 1932; Harkness 1923), and Dover West (Hume 1932). There were limited notes and reports of wells being shot, though according to May (1998) it was a regular practice. The last reported well shooting was Pinetree et al. Dover 8-10-V in December 1979, which was shot with 230 kg of nitroglycerine.

Chemical treatments by the Dowell Company of Michigan improved recovery in ten wells in the Petrolia field and four wells in the Oil Springs field, but the results were not economical and there were limited details on their use (Harkness 1933). Acid treatments were introduced in Ontario in 1932 (Harkness 1933), but the challenge with the Ontario wells was the "home made" casing packers that were designed with one packer that could isolate an interval between the packer and the bottom of the well. The problem was the rock was permeable and the acid moved from the well into the formation (Harkness 1937). The packer system was not able to isolate low permeability

https://doi.org/10.12789/geocanj.2023.50.203

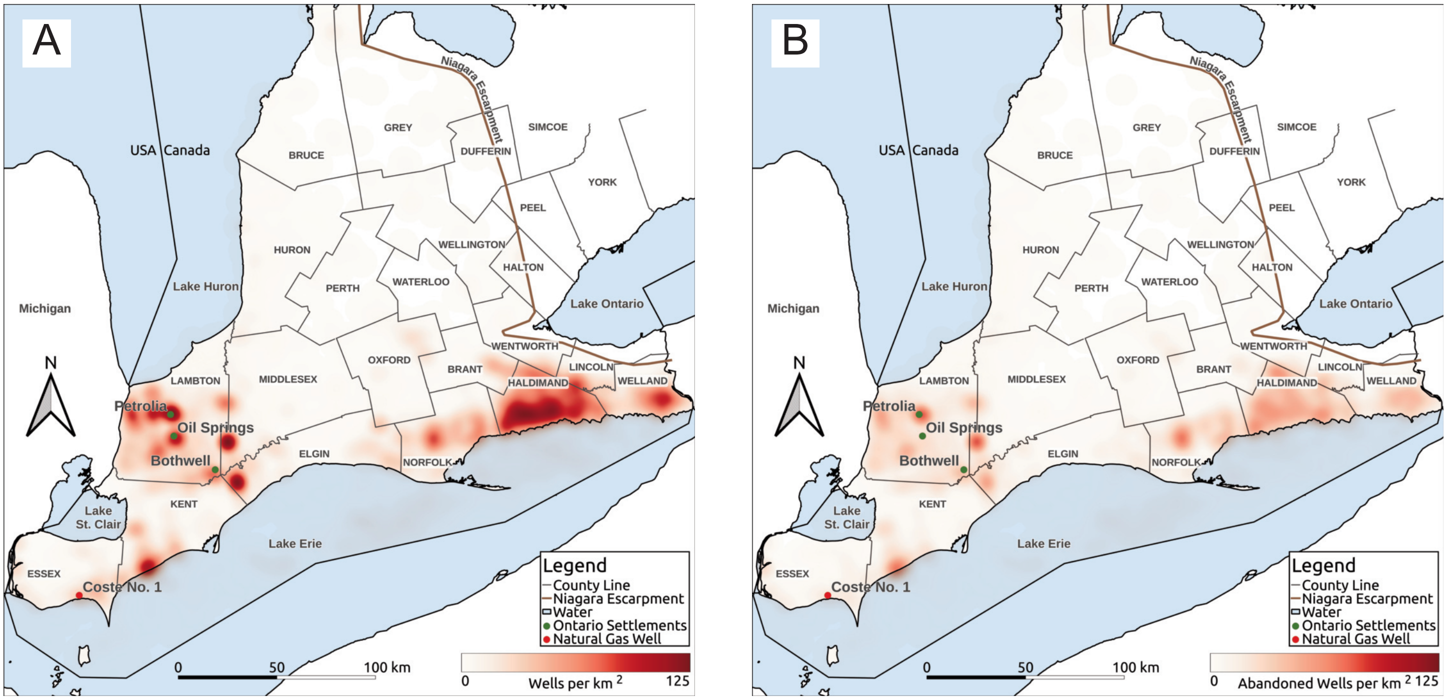

Figure 5. Well density maps for A) drilled wells in the Ontario Petroleum Data System (OPDS) (n = 22,156); and B) abandoned wells in the OPDS (n = 14,507).

zones in a well where the acid treatment could increase the permeability. Although the acid treatments did not have the desired effect, there were small production increases in wells due to the thorough cleaning of the limestone walls of the well, removing the accumulated paraffin, scale, and other sediment (Harkness 1937).

Gas injection used in the Oil Springs area in 1951 improved short-term oil recovery (Harkness 1953). Gas and water injection was also proposed for the Rodney field (Harkness 1954), and was promoted as a technique to improve recovery for several years (Oakley 1963). Finally, water floods were carried out in the Petrolia and Oil Springs fields, but few details were reported (Ontario Fuel Board 1955; Oakley 1963).

The use of well maintenance and enhanced oil recovery (EOR) techniques may have significant implications for subsequent well abandonment. Shot wells will likely have debris and casing in the well and the rock walls may be fractured to an unknown distance into the rock. The explosions will have impacted the condition of the wells, and the wells may be difficult to plug due to debris in the well, the larger diameter of the well, or additional pathways created in the fractured rock for fluids to travel through. Similarly, wells treated with acid may have additional pathways created for fluid flow and the well diameter may be larger at the treated horizon.

Impacts of Hydrogen Sulphide

The issues of poor well construction and poor abandonment practices are compounded by the presence of hydrogen sulphide in the oil, gas, and groundwater. Some Ontario crude oils, principally from the Devonian oil pools, have a high hydrogen sulphide content that readily corrodes equipment, requiring frequent replacement of equipment including pumps, sucker rods, tubing, cables, jerker rods, and pump jacks (Harkness 1948a). There are notes regarding sulphur gas and sulphur water dating back to a gas well drilled in Humberstone Township, Welland County in 1866 (Ontario Bureau of Mines 1892). Gas fields along the shore of Lake Erie also contain hydrogen sulphide, including the Eden gas field south of Tillsonburg which produced natural gas with 0.7 % volume hydrogen sulphide (Harkness 1936), the Tilbury field (up to 0.6 % volume; Harkness 1923), and the Declute field (0.7 % by volume; Caley 1946). The corrosive effects of the hydrogen sulphide on steel well casings, production piping, and tubing is known in the Ontario petroleum industry. For example, Figure 6 shows the corrosion of on a section of ten-year-old 7.3 cm diameter tubing from the Morpeth gas field.

The impact of sulphur water on groundwater resources was discussed above and identified by landowner complaints in 1947 (Harkness 1949). Inspectors identified the problem as water wells and gas wells that were drilled into the sulphur water zone that created a pathway for the sulphur water to move into overlying aquifers. Artesian flow of sulphur water from oil and gas wells occurs in topographic lows near the Lake Erie shoreline, such as Big Otter Creek (Elgin County) and Big Creek (Norfolk County), where it constitutes a drilling hazard (Carter et al. 2021b). Static water level maps for the Lucas-Dundee Aquifer from a 3-D hydrostratigraphic model, which is readily accessible using free viewer software (Carter et al. 2022), can be used to predict where artesian flow of sulphur water may occur in Ontario.

IMPLICATIONS FOR WELL ABANDONMENT

A review of the history of oil and gas exploration and development in Ontario identified five factors to consider when abandoning wells.

Figure 6. Production tubing (7.3 cm diameter) from the Morpeth gas field showing corrosion due to hydrogen sulphide.

1. Well Location. The first challenge to properly abandon an orphaned or legacy well is to locate it. There were an estimated 50,000 wells drilled by 1970 (Hutt 1970) but there are only 27,000 wells in the database (Clark et al. 2020), suggesting there are numerous wells that are not accounted for. Few well records were kept before the implementation of the Natural Gas Act R.S.O. 1918, and many drilled wells were not reported or were lost (Caley 1946). There were also periods when record keeping was poor or wells were lost, such as during the Great Depression (Harkness 1929). Much of the skilled drilling and oilfield experience was lost during the Second World War, lowering the accuracy of well locations and quality of well plugging operations (Harkness 1947). The accuracy of reported well locations improved under the Energy Act in 1964. Though not discussed in the text above, changes to the landscape have also made it more challenging to locate wells. Wells drilled near the shoreline of Lake Erie or at the edge of a ravine may no longer be evident or easily accessible due to erosion changing the landscape. Land development has also encroached on areas of oil and gas development, impacting the ability to locate and access orphaned or legacy wells.
2. Well Construction. Drilling techniques and the equipment available to drillers changed remarkably from 1858 to the modern era, which had significant implications for well construction. Early casings were made of wood or steel in a range of diameters. Some wells were cased without cement, allowing for the casing to be removed once drilling was completed. The majority of wells in Ontario were drilled using a cable tool method. The standardization of equipment in 1922 resulted in cost reductions and efficiencies for operating drill rigs. This also produced wells with predictable diameters, which is important for plugging operations. Methods for plugging legacy wells must be adaptable for a range of well sizes and for cased or uncased wells.
3. Well Condition. Wells abandoned more than a century ago have corroded cement and casing that may make it challenging to access the rest of the well beneath. Shooting a well was designed to fracture the rock but may have also damaged the casing and cement. Acid treatments were also designed to increase the permeability of the rock surrounding the well but may have also degraded casing and cement. Shot and acid-treated wells may also be irregularly shaped with pockets of exploded or acidized rock, and plugging operations must be able to adapt to a range of well diameters within the same well.
4. Legacy Wells. Previous well plugging efforts may have pulled or partially pulled the casing, resulting in a poor well condition that will need to be addressed prior to plugging. Wells abandoned before 1964 were plugged with sediment, wood, rubble, clay, and some cement, and have a higher probability of leaking because of the deterioration of these poor plugging materials. It was not until 1964 that cement was used as the primary material for plugging wells, followed by long cement plugs in 1968. Even with modern techniques and equipment, poor cement operations make it possible for any well plug, new or old, to fail and leak. Well plugging operations should account for wood, steel, clay, drilling mud, wax, and other related hydrocarbons in the well that could inhibit plugging operations, in addition to other debris in the well that may impede access to the well. In addition, the steel surface casing may have been recovered in plugged wells, making it impossible to use magnetic methods to help locate the well.
5. Hydrogen sulphide. Hydrogen sulphide in oil, natural gas, and groundwater is known to corrode equipment, casings, and cement, impacting well conditions, and is a consideration for plugging a well. Hydrogen sulphide dissolved in groundwater continues to leak from legacy wells in Ontario and must be considered when planning abandonment operations. In particular, the potential impact to casing and cement corrosion, and the risk to workers, should be addressed before plugging operations begin. Water wells and oil and gas wells drilled into aquifers that contain sulphur water may also be a conduit for natural gas and hydrogen sulphide to move into overlying aquifers. Geological formations known to contain sulphur water are documented by Carter et al. (2021b) and the geographic and stratigraphic distribution is modelled and mapped in a 3D hydrostratigraphic model.

Further work is required to locate unreported or lost wells and to develop new techniques to find these wells. Current plugging operations rely on cement to plug the wells, but cement shrinkage, channeling, and fracturing create pathways through cement, impacting the long-term performance of cement plugs (Dusseault et al. 2000). New plugging techniques are required to permanently plug wells. Permanently plugging these wells will limit hydrocarbon and brine leakage from these wells, improving public safety and reducing greenhouse gas emissions. It should be noted that plugging standards for water wells in Ontario, O.Reg.903 Ontario Water Resources Act R.R.O 1990 permit the use of clay (bentonite) for plugging (Ontario Government 2023).

The detailed reporting in the Department of Mines annual reports was essential to understanding activities, successes, and failures in the Ontario oil and gas industry and provided context for understanding abandonment activities from 1891 to 1953. The annual reports from the Fuel Board and subsequent regulatory agencies did not have the same detail, limiting our understanding of activities from 1954 until now. It is important, particularly for well drilling and well plugging, to have detailed notes so the methods and results can be reviewed to improve future drilling and plugging performance.

ACKNOWLEDGEMENTS

This research was funded by the Program for Energy Research and Development from Natural Resources Canada, Government of Canada. The authors thank Terry Carter, Cath Ryan, and an anonymous reviewer for their thorough review and recommendations that greatly improved the manuscript. The authors also thank the Oil, Gas and Salt Resources Library for their GIS expertise creating the maps. Finally, thank you to the journal editors Andrew Kerr and Cindy Murphy for their input and Janice Allen for thorough copy editing.

REFERENCES

Armstrong, D.K., and Carter, T.R., 2010, The subsurface Paleozoic stratigraphy of southern Ontario: Ontario Geological Survey, Special Volume 7, 301 p.

Armstrong, R., 2019, An environmental history of oil development in southwestern Ontario, 1858–1885: Unpublished MA thesis, University of Western Ontario, Electronic Thesis and Dissertation Repository, 6717, https://ir.lib.uwo.ca/etd/6717.

Bailey Geological Services Ltd., and Cochrane, R.O., 1985, Evaluation of the conventional and potential oil and gas reserves of the Devonian of Ontario (Volume 1): Ontario Geological Survey, Open File Report 5555, 178 p.

Bowman, I., 1911, Well drilling methods: Department of the Interior, United States Geological Survey, Water Supply Paper 257, Washington, DC, 139 p.

Brumell, H.P.H, 1892, Report on natural gas and petroleum in Ontario prior to 1891: Geological Survey of Canada Annual Report, v. 5 (1890–91), 94 p., https://doi.org/10.4095/297058.

Caley, J.F., 1946, Palaeozoic geology of the Windsor-Sarnia area, Ontario: Geological Survey of Canada, Memoir 240, 227 p., https://doi.org/10.4095/101618.

Carter, T.R., 1992, Oil and gas exploration, drilling and production summary, 1988: Ontario Ministry of Natural Resources Oil and Gas Paper 11, 174 p.

Carter, T.R., 2017, Ontario oil, gas, and salt resources library: a model for groundwater data sharing in Ontario?: Geological Survey of Canada, Open File 8213, 25 p, https://doi.org/10.4095/305611.

Carter, T.R., and Castillo, A.C., 2006, Three-dimensional mapping of Paleozoic bedrock formations in the subsurface of southwestern Ontario: A GIS application of the Ontario Petroleum Well Database, *in* Harris, J.R., *ed.,* GIS for the Earth Sciences: Geological Association of Canada, Special Paper 44, p. 439–454.

Carter, T.R., and Sutherland, L., 2020, Interface mapping of hydrochemical groundwater regimes in the Paleozoic bedrock of southwestern Ontario, *in* Russell, H.A., and Kjarsgaard, B.A., *eds.,* Southern Ontario groundwater project 2014–2019: summary report: Geological Survey of Canada, Open File 8536, p. 37–48, https://doi.org/10.4095/321083.

Carter, T.R., Fortner, L., Skuce, M.E., and Longstaffe, F.J., 2014, Aquifer systems in southern Ontario: Hydrogeological considerations for well drilling and plugging (Presentation): Canadian Society of Petroleum Geologists, Calgary, AB, May13 2014. Available at: http://www.ogsrlibrary.com/downloads/Aquifers22-CSPG-2014-Carter-May13.pdf.

Carter, T.R., Wang, D., Castillo, A.C., and Fortner, L., 2015, Water type maps of deep groundwater from petroleum well records, southern Ontario: Ontario Oil, Gas and Salt Resources Library, Open File Data Release 2015-1, 10 p. 89 maps.

Carter, T.R., Logan, C.E., Clark, J.K., Russell, H.A.J., Brunton, F.R., Cachunjua, A., D'Arienzo, M., Freckelton, C., Rzyszczak, H., Sun, S., and Yeung, K.H., 2021a, A three-dimensional geological model of the Paleozoic bedrock of southern Ontario—version 2: Geological Survey of Canada, Open File 8795, https://doi.org/10.4095/328297.

Carter, T.R., Fortner, L.D., Russell, H.A.J., Skuce, M.E., Longstaffe, F.J., and Sun, S., 2021b, A hydrostratigraphic framework for the Paleozoic bedrock of southern Ontario: Geoscience Canada, v. 48, p. 23–58, https://doi.org/10.12789/geocanj.2021.48.172.

Carter, T.R., Logan, C.E., Clark, J.K., Russell, H.A.J, Priebe, E.H., and Sun, S., 2022, A three-dimensional hydrostratigraphic model of southern Ontario: Geological Survey of Canada, Open File 8927, 58 p., https://doi.org/10.4095/331098.

Clapp, F.G., 1914, Petroleum and natural gas resources of Canada, vol. I, technology and exploitation: Canada Mines Branch, Publication 291, 1914, 378 p., https://doi.org/10.4095/20747.

Clapp, F.G., 1915, Petroleum and natural gas resources of Canada, vol. II, description of occurrences: Canada Mines Branch, Publication 291, 1915, 404 p., https://doi.org/10.4095/305389.

Clark, J.K., Carter, T.R., Brunton, F.R., Logan, C.E., Somers, M., Sutherland L., and Yeung, K.H., 2020, Improving the 3-D geological data infrastructure of southern Ontario: Data capture, compilation, enhancement and QA/QC, *in* Russell, H.A.J., and Kjarsgaard, B.A., *eds.*, Southern Ontario Groundwater Project 2014–2019: Summary Report: Geological Survey of Canada, Open File 8536, p. 23–36, https://doi.org/10.4095/321081.

Collom, R.E., 1922, Prospecting and testing for oil and gas: United States Department of the Interior, Bulletin 201, 170 p.

Colthorpe, A., 2021, Advanced compressed air energy storage project gets funding help from Canadian government: Energy Storage, News article. Accessed June 2, 2023, https://www.energy-storage.news/advanced-compressed-air-energy-storage-project-gets-funding-help-from-canadian-government/.

Dessanti, C., 2023, RE: Proposed amendments to the Oil, Gas and Salt Resources Act to remove the prohibition on carbon sequestration (ERO: 019-6296): Ontario Chamber of Commerce, 2 p. Accessed June 14, 2023, https://policycommons.net/artifacts/3364348/re/4163003/.

Dollar, P.S., Frape, S.K., and McNutt, R.H., 1991, Geochemistry of formation waters, southwestern Ontario, Canada and southern Michigan, U.S.A.: Implications for origin and evolution: Ontario Geoscience Research Grant Program, Grant No. 249, Ontario Geological Survey, Open File Report 5743, 72 p.

Dusseault, M., and Jackson R., 2014, Seepage pathway assessment for natural gas to shallow groundwater during well stimulation, in production, and after abandonment: Environmental Geosciences, v. 21, p. 107–126, https://doi.org/10.1306/eg.04231414004.

Dusseault, M.B., Gray, M.N., and Nawrocki, P.A., 2000, Why oilwells leak: Cement behavior and long-term consequences (Presentation): International Oil and Gas Conference and Exhibition in China, Beijing, China, November 2000, Paper Number SPE-64733-MS, https://doi.org/10.2118/64733-MS.

Energy Safety Canada, 2023, IRP 27: Wellbore decommissioning: An industry recommended practice (IRP) for the Canadian oil and gas industry: Drilling and Completion Committee, v. 27, 126 p. Accessed July 10, 2023, https://www.energysafetycanada.com/resource/dacc-irp-volumes/dacc-irp-volume-27-wellbore-decommissioning.

Ensing, C., 2021, Wheatley explosion could be 'tip of the iceberg' in Ontario given number of abandoned wells: expert: Canadian Broadcasting Corporation, News article. Accessed June 1, 2023, https://www.cbc.ca/news/canada/windsor/wheatley-explosion-gas-wells-1.6161023.

Estlin, E.S., 1921, Part V: I-Natural gas in 1920, II-Oil field operations, 1920, *in* Thirtieth Annual Report of the Ontario Department of Mines: Ontario Department of Mines Annual Report 1920, Part V, p. 1–50, p. 51–56. Available at: https://www.geologyontario.mndm.gov.on.ca/mndmfiles/pub/data/imaging/ARV30//ARV30.pdf.

Gray, E., 2008, Ontario's petroleum legacy: The birth, evolution and challenges of a global industry: Heritage Community Foundation, 100 p. Available at: https://earlegray.com/wp-content/uploads/2018/07/Ontarios-petroleum-legacy.-Birth-of-an-industry.pdf.

Harkness, R.B., (*compiler*), n.d., The Harkness Reports: Ontario Petroleum Institute, Oil, Gas and Salt Resources Library. Accessed May 22, 2023, https://www.ogsrlibrary.com/harkness-reports.

Harkness, R.B., 1922, Part V: I-Natural Gas in 1921, II-Petroleum in 1921, *in* Thirty-First Annual Report of the Ontario Department of Mines: Ontario Department of Mines. Available at: https://www.geologyontario.mndm.gov.on.ca/mndmfiles/pub/data/imaging/ARV31/ARV31.pdf.

Harkness, R.B., 1923, Part V: 1-Natural Gas in 1922, II- Petroleum in 1922, *in* Thirty-Second Annual Report of the Ontario Department of Mines: Ontario Department of Mines. Available at: https://www.geologyontario.mndm.gov.on.ca/mndmfiles/pub/data/imaging/ARV32/ARV32.pdf.

Harkness, R.B., 1924, Part V: I-Natural Gas in 1923, II-Petroleum in 1923, *in* Thirty-Third Annual Report of the Ontario Department of Mines: Ontario Department of Mines. Available at: https://www.geologyontario.mndm.gov.on.ca/mndmfiles/pub/data/imaging/ARV33/ARV33.pdf.

Harkness, R.B., 1925, Part V: I-Natural Gas in 1924, II-Petroleum in 1924, *in* Thirty-Fourth Annual Report of the Ontario Department of Mines: Ontario Department of Mines. Available at: https://www.geologyontario.mndm.gov.on.ca/mndmfiles/pub/data/imaging/ARV34/ARV34.pdf.

Harkness, R.B., 1926, Part V: I-Natural Gas in 1925, II-Petroleum in 1925, *in* Thirty-Fifth Annual Report of the Ontario Department of Mines: Ontario Department of Mines. Available at: https://www.geologyontario.mndm.gov.on.ca/mndmfiles/pub/data/imaging/ARV35/ARV35.pdf.

Harkness, R.B., 1927, Part IV: I-Natural Gas in 1926, II-Petroleum in 1926, *in* Thirty-Sixth Annual Report of the Ontario Department of Mines: Ontario Department of Mines. Available at: https://www.geologyontario.mndm.gov.on.ca/mndmfiles/pub/data/imaging/ARV36/ARV36.pdf.

Harkness, R.B., 1928, Part V: I-Natural Gas in 1927, II-Petroleum in 1927, *in* Thirty-Seventh Annual Report of the Ontario Department of Mines: Ontario Department of Mines. Available at: https://www.geologyontario.mndm.gov.on.ca/mndmfiles/pub/data/imaging/ARV37/ARV37.pdf.

Harkness, R.B., 1929, Part V: I-Natural Gas in 1928, II-Petroleum in 1928, *in* Thirty-Eighth Annual Report of the Ontario Department of Mines: Ontario Department of Mines. Available at: https://www.geologyontario.mndm.gov.on.ca/mndmfiles/pub/data/imaging/ARV38/ARV38.pdf.

Harkness, R.B., 1930, Part V: I-Natural Gas in 1929, II-Petroleum in 1929, *in* Thirty-Ninth Annual Report of the Ontario Department of Mines: Ontario Department of Mines. Available at: https://www.geologyontario.mndm.gov.on.ca/mndmfiles/pub/data/imaging/ARV39/ARV39.pdf.

Harkness, R.B., 1933, Part V: I-Natural Gas in 1932, II-Petroleum in 1932, *in* Forty-Second Annual Report of the Ontario Department of Mines: Ontario Department of Mines. Available at: https://www.geologyontario.mndm.gov.on.ca/mndmfiles/pub/data/imaging/ARV42/ARV42.pdf.

Harkness, R.B., 1936, Part V: I-Natural Gas in 1934, II-Petroleum in 1934, *in* Forty-Fourth Annual Report of the Ontario Department of Mines: Ontario Department of Mines. Available at: https://www.geologyontario.mndm.gov.on.ca/mndmfiles/pub/data/imaging/ARV44/ARV44.pdf.

Harkness, R.B., 1937, Part V: I-Natural Gas in 1935, II-Petroleum in 1935, *in* Forty-Fifth Annual Report of the Ontario Department of Mines: Ontario Department of Mines. Available at: https://www.geologyontario.mndm.gov.on.ca/mndmfiles/pub/data/imaging/ARV45/ARV45.pdf.

Harkness, R.B., 1946, Part V: I-Natural Gas in 1943, II-Petroleum in 1943, *in* Fifty-Third Annual Report of the Ontario Department of Mines: Ontario Department of Mines. Available at: https://www.geologyontario.mndm.gov.on.ca/mndmfiles/pub/data/imaging/ARV53/ARV53.pdf.

Harkness, R.B., 1947, Part III: I-Natural Gas in 1944, II-Petroleum in 1944, *in* Fifty-Fourth Annual Report of the Ontario Department of Mines: Ontario Department of Mines. Available at: https://www.geologyontario.mndm.gov.on.ca/mndmfiles/pub/data/imaging/ARV54/ARV54.pdf.

Harkness, R.B., 1948a, Part III: I-Natural Gas in 1945, II-Petroleum in 1945, *in* Fifty-Fifth Annual Report of the Ontario Department of Mines: Ontario Department of Mines. Available at: https://www.geologyontario.mndm.gov.on.ca/mndmfiles/pub/data/imaging/ARV55/ARV55.pdf.:

Harkness, R.B., 1948b, Part III: I-Natural Gas in 1946, II-Petroleum in 1946, *in* Fifty-Sixth Annual Report of the Ontario Department of Mines: Ontario Department of Mines. Available at: https://www.geologyontario.mndm.gov.on.ca/mndmfiles/pub/data/imaging/ARV56/ARV56.pdf.

Harkness, R.B., 1949, Part III: I-Natural Gas in 1947, II-Petroleum in 1947, *in* Fifty-Seventh Annual Report of the Ontario Department of Mines: Ontario Department of Mines. Available at: https://www.geologyontario.mndm.gov.on.ca/mndmfiles/pub/data/imaging/ARV57/ARV57.pdf.

Harkness, R.B., 1951, Part III: I-Natural Gas in 1949, II-Petroleum in 1949, *in* Fifty-Ninth Annual Report of the Ontario Department of Mines: Ontario Department of Mines. Available at: https://www.geologyontario.mndm.gov.on.ca/mndmfiles/pub/data/imaging/ARV59/ARV59.pdf.

Harkness, R.B., 1952, Part III: I-Natural Gas in 1950, II-Petroleum in 1950, in Sixtieth Annual Report of the Ontario Department of Mines: Ontario Department of Mines. Available at: https://www.geologyontario.mndm.gov.on.ca/mndmfiles/pub/data/imaging/ARV60/ARV60.pdf.

Harkness, R.B., 1953, Part 3: I-Natural Gas in 1951, II-Petroleum in 1951, *in* Sixty-First Annual Report of the Ontario Department of Mines: Ontario Department of Mines. Available at: https://www.geologyontario.mndm.gov.on.ca/mndmfiles/pub/data/imaging/ARV61/ARV61.pdf.

Harkness, R.B., 1954, Part 3: I-Natural Gas in 1953, II-Petroleum in 1953, *in* Sixty-Third Annual Report of the Ontario Department of Mines: Ontario Department of Mines. Available at: https://www.geologyontario.mndm.gov.on.ca/mndmfiles/pub/data/imaging/ARV63/ARV63.pdf.

Hobbs, M.Y., Frape, S.K., Shouakar-Stash, O., and Kennell, L.R., 2011, Regional hydrogeochemistry − southern Ontario: Nuclear Waste Management Organization, Report NWMO DGR-TR-2011-12, Toronto, ON. Accessed June 17, 2021, https://archive.opg.com/pdf_archive/Deep%20Geologic%20Repository%20Documents/Geoscience%20Reports/D002_4.1.2_Regional-Hydrogeochemistry—-Southern-Ontario.pdf.

Hume, G.S., 1932, Oil and gas in eastern Canada: Geological Survey of Canada, Economic Geology Series No. 9, 197 p., https://doi.org/10.4095/102443.

Hunt, T.S., 1861, Notes on the history of petroleum or rock oil: Geological Survey of Canada. Accessed June 3, 2023, https://babel.hathitrust.org/cgi/pt?id=aeu.ark:/13960/t9x078r2f&view=1up&seq=4.

Hutt, R.B., 1970, The development and use of the Ontario well data system: Journal of Canadian Petroleum Technology, v. 9, p. 52–59, https://doi.org/10.2118/70-01-07.

International Oil Drillers, 2023, Drilling techniques (Website): Oil Museum of Canada Foundation. Accessed July 4th, 2023, https://internationaloildrillers.ca/collections/drilling-techniques.

Jackson, R.E., Dusseault, M.B., Frape, S., Illman, W., Phan ,T., and Steelman, C., 2020, Investigating the origin of elevated H_2S in groundwater discharge from abandoned gas wells, Norfolk County, Ontario (Presentation): GeoConvention 2020, Calgary, AB, 21–23 September 2020.

Koepke, W.E., and Sanford, B.V., 1966, Silurian oil and gas fields of southwestern Ontario: Geological Survey of Canada, Paper 65-30, 138 p., https://doi.org/10.4095/100975.

Lauriston, V., 1961, Blue flame of service: a history of Union Gas Company and the natural gas industry in southwestern Ontario: Union Gas Company of Canada, Chatham, ON, 126 p.

Lemieux, A., Shkarupin, A., and Sharp, K., 2019, Geologic feasibility of underground hydrogen storage in Canada: International Journal of Hydrogen Energy, v. 45, p. 32243–32259, https://doi.org/10.1016/j.ijhydene.2020.08.244.

Logan, W.E., 1852, Report of progress for the year 1850–1851: Geological Survey of Canada, 54 p., https://doi.org/10.4095/123558.

Malcolm, W., 1915, The oil and gas fields of Ontario and Quebec: Geological Survey of Canada, Memoir No. 81, 248 p., https://doi.org/10.4095/101579.

May, G., 1998, Hard Oiler!: The Story of Early Canadians' Quest for Oil at Home and Abroad: Dundurn Press, Toronto, ON, 270 p.

Natural Resources Canada, 2019, Technology roadmap to improve wellbore integrity: Summary report. Downloaded on June 1, 2023, from https://natural-resources.canada.ca/science-data/research-centres-labs/canmetenergy-research-centres/technology-roadmap-improve-wellbore-integrity/21964.

Oakley, K.A., 1963, Developments in oil and natural gas production southwestern Ontario: Journal of Canadian Petroleum Technology, v. 2, p.151–159, https://doi.org/10.2118/63-04-01.

Oil, Gas, and Salt Resources Library, 2023, Webpage. Accessed June 2nd, 2023, https://www.ogsrlibrary.com/library_ontario_oil_gas_salt.

Ontario Bureau of Mines, 1892, First report of the Ontario Bureau of Mines, 1891: Ontario Bureau of Mines, Annual Report, 1891, 253 p.

Ontario Bureau of Mines, 1895, Fourth report of the Ontario Bureau of Mines, 1894: Ontario Bureau of Mines, Annual Report, 261 p.

Ontario Bureau of Mines, 1896, Fifth report of the Ontario Bureau of Mines: Ontario Bureau of Mines, Annual Report, 1895, v. 5, 297 p.

Ontario Bureau of Mines, 1901, Tenth report of the Ontario Bureau of Mines: Ontario Bureau of Mines, Annual Report, 236 p.

Ontario Bureau of Mines, 1902, Eleventh report of the Ontario Bureau of Mines: Ontario Bureau of Mines, Annual Report, 309 p.

Ontario Bureau of Mines, 1904, Thirteenth report of the Ontario Bureau of Mines: Ontario Bureau of Mines, Annual Report, 684 p.

Ontario Bureau of Mines, 1905, Fourteenth report of the Ontario Bureau of Mines: Ontario Bureau of Mines, Annual Report, 894 p.

Ontario Bureau of Mines, 1909, Eighteenth report of the Ontario Bureau of Mines: Ontario Bureau of Mines, Annual Report, 484 p.

Ontario Bureau of Mines, 1915, Twenty-fourth annual report of the Ontario Bureau of Mines: Ontario Bureau of Mines, Annual Report, 531 p.
Ontario Bureau of Mines, 1917, Twenty-sixth annual report of the Ontario Bureau of Mines: Ontario Bureau of Mines, Annual Report, 363 p.
Ontario Bureau of Mines, 1918, Twenty-seventh annual report of the Ontario Bureau of Mines: Ontario Bureau of Mines, Annual Report, 656 p.
Ontario Department of Energy Resources, 1961, Report of the Department of Energy Resources for the year ended December 31st, 1960: Department of Energy Resources, Toronto, ON.
Ontario Fuel Board, 1955, First annual report of the Ontario Fuel Board: Ontario Fuel Board, Toronto, ON, 146 p.
Ontario Government, 2023, Water Supply Wells: Requirements and Best Practices: Ministry of the Environment and Climate Change's, Downloaded on July 15, 2023, https://www.ontario.ca/document/water-supply-wells-requirements-and-best-practices.
Selwyn, A.R.C., 1891, Geological and Natural History Survey of Canada: Geological Survey of Canada, Annual Report, v. 4, (1888–1889), 1120 p., https://doi.org/10.4095/225892.
Skuce, M.E., 2014, Isotopic fingerprinting of shallow and deep groundwaters in southwestern Ontario and its applications to abandoned well remediation: Unpublished MSc thesis, Western University, Electronic thesis and dissertation repository 1926, 267 p., https://ir.lib.uwo.ca/etd/1926/.
Skuce, M., Longstaffe, F.J., Carter, T.R., and Potter, J., 2015, Isotopic fingerprinting of groundwaters in southwestern Ontario: Applications to abandoned well remediation: Applied Geochemistry, v. 58, p. 1–13, https://doi.org/10.1016/j.apgeochem.2015.02.016.
Sonnenberg, M., 2019, Residents express concern over toxic gas levels: Simcoe Reformer, News article. Accessed June 1, 2023, https://www.simcoereformer.ca/news/local-news/residents-express-concern-over-toxic-gas-levels.
Williams, M.Y., 1920, Oil fields of Elgin, Essex and the southern part of Kent counties, *in* Summary Report 1919 E, Geological Survey of Canada, p. 7E–15E, https://doi.org/10.4095/292315.

Received August 2023
Accepted as revised November 2023

REPORT

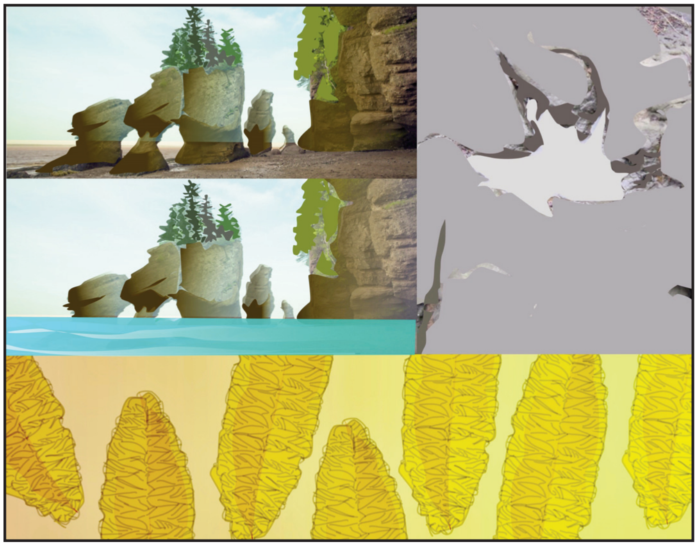

Canadian Geoscience Diplomacy in Collaboration with IUGS, UNESCO IGCP Geoparks, and World Heritage Geosites: Past, Present, and Future

Nikole Bingham-Koslowski[1], Katherine J.E. Boggs[2], Özlem Adiyaman Lopes[3], Daniel Lebel[1], Stephen Johnston[4] and Guy Narbonne[5]

[1]*Natural Resources Canada, Geological Survey of Canada*
601 Booth Street, Ottawa, Ontario, K1A 0E8, Canada
Email: nikole.bingham-koslowski@nrcan-rncan.gc.ca

[2]*Department of Earth and Environmental Sciences*
Mount Royal University
4825 Mount Royal Gate SW, Calgary, Alberta, T3E 6K6, Canada

[3]*UNESCO, 7 Place de Fontenoy, Paris, 75007, France*

[4]*Department of Earth and Atmospheric Sciences*
University of Alberta, Edmonton, Alberta, T6G 2E3, Canada

[5]*Department of Geological Sciences and Geological Engineering*
Queens University, 36 Union Street
Kingston, Ontario, K7L 3N6, Canada

SUMMARY
To commemorate the 60th anniversary of IUGS and the 50th anniversary of IGCP, the 2022 symposium entitled "IUGS, Geoparks, and IGCP – Retrospection, today and the future" was coordinated at the GAC-MAC-IAH-CNC-CSPG 2022 Conference in Halifax (16–18 May) with the companion Cliffs of Fundy UNESCO Geopark field trip (19–21 May). Canadian leadership within IUGS and IGCP includes J.M. Harrison as the first president of IUGS in 1961, Antony Berger's work publishing "*Episodes*", which is the IUGS' quarterly international scientific journal, and Canadian leadership on multiple IGCP projects summarized here. Two panel discussions examined the future of geosciences, UNESCO Geoparks and World Geoheritage Sites in Canada. The need for improved communications with politicians, policymakers, and the general public through education and outreach was emphasized in these panel discussions. UNESCO Geoparks (such as the Cliffs of Fundy), UNESCO World Heritage Geosites and significant museum displays represent vehicles for improving communications with the general public about geosciences and potentially inspiring future geoscientists. This report provides a summary of the symposium and explores some of the many themes that it addressed.

RÉSUMÉ
Pour commémorer le 60e anniversaire de l'UISG et le 50e anniversaire du PICG, le symposium de 2022 intitulé « UISG, Géoparcs et PICG – Rétrospection, aujourd'hui et l'avenir » a été coordonné lors de la conférence AGC-AMC-SNC-AIH-SCGP 2022 à Halifax (16–18 mai), avec une excursion au géoparc UNESCO des falaises de Fundy (19–21 mai). Le leadership canadien au sein de l'UISG et du PICG inclut J.M. Harrison en tant que premier président de l'UISG en 1961, le travail d'Antony Berger dans la publication d'« Épisodes », la revue scientifique internationale trimestrielle de l'UISG, et le leadership canadien sur plusieurs projets du PICG résumés ici. Deux tables rondes ont examiné l'avenir des géosciences, des géoparcs UNESCO et des sites du patrimoine géologique mondial au Canada. La nécessité d'améliorer les communications avec les politiciens, les décideurs politiques et le grand public par le biais de l'éducation et la sensibilisation a été soulignée lors de ces tables rondes. Les géoparcs de l'UNESCO (comme les falaises de Fundy), les sites géologiques du patrimoine mondial de l'UNESCO et les importantes expositions dans les musées représentent des moyens d'améliorer les communications avec le grand public

sur les géosciences et d'éventuellement inspirer de futurs géoscientifiques. Ce rapport offre un résumé du symposium et explore certains des nombreux thèmes qui ont été abordés.

Traduit par la Traductrice

INTRODUCTION

"Science diplomacy: the building and use of international scientific collaborations to identify and address issues facing humanity in the 21st century" (Fedoroff 2009).

To commemorate the 60th anniversary of the International Union of Geological Sciences (IUGS) and the 50th anniversary of the International Geoscience Programme (IGCP), a group led by K. Boggs organized a Canadian-focused symposium entitled "IUGS, Geoparks, and IGCP – Retrospection, Today and the Future" which was held during the GAC-MAC-IAH-CNC-CSPG 2022 conference (May 15–18) in Halifax, Nova Scotia, Canada (Table 1; Fig. 1). The symposium highlighted the contributions of Canadian geoscience diplomacy towards achieving positive global outcomes, with a specific focus on contributions associated with the United Nations Sustainable Development Goals, as listed in Table 2 (see also UN SDG; sdgs.un.org/goals). The symposium also raised the profile and awareness of IUGS, IGCP and Geoparks within the Canadian geoscience community, and in doing so, aimed to sustain and augment Canadian participation in those organizations. This is a key goal of the Canadian National Committee for IUGS which is co-chaired by K. Boggs and D. Lebel until 2026.

The Halifax 2022 conference was the annual joint meeting of the Geological Association of Canada (GAC) and Mineralogical Association of Canada (MAC). It was organized in partnership with the International Association of Hydrogeologists (Canadian National Chapter; IAH-CNC) and the Canadian Society of Petroleum Geologists (CSPG), now known as the Canadian Energy Geoscience Association. The conference was a huge success, despite the ongoing global COVID-19 pandemic, with more than 800 registrants of whom over 80% participated in person.

The first full day of the symposium (May 16) involved talks related to IUGS and IGCP including general presentations as well as summaries of specific IGCP projects (Table 1). Daniel Lebel, director of the Geological Survey of Canada, opened the session with a presentation highlighting key multi-generational contributions of Canadian geoscientists that advanced global geoscience with new concepts and initiatives over the last 180 years (Lebel and Bobrowsky 2022). These include the Canada-US geology map of America completed by William Logan with American James Hall, Tuzo Wilson and plate tectonic theory, Paul Hoffman and the 'United Plates of America' paper, and other important contributions. Some Canadian geoscientists, such as James Harrison and Digby McLaren, were key founders of the International Geological Congress (IGC) and IGCP, while several others contributed to geoscience education and outreach at the regional, national, and international scales. The day concluded with a keynote presentation by current IUGS president John Ludden regarding the direction that the field of geosciences is headed over the next decade, followed by a panel discussion entitled "The future of geosciences in Canada, IGCP and IUGS". The panel consisted of some of the speakers from that day and involved discussions based on their presentations as well as conversations related to current challenges in geosciences and the future of the field. The following half-day session (May 17) focused on United Nations Educational, Scientific and Cultural Organization (UNESCO) World Heritage Sites and Global Geoparks and concluded with a discussion panel on the "Future of Geoparks and World Geoheritage sites in Canada".

The companion Cliffs of Fundy Geopark field trip, "Telling the story of the Cliffs of Fundy UNESCO Global Geopark, Nova Scotia: linking geoheritage, indigenous heritage and culture", ran from 19–21 May 2022. The field trip was coordinated and led by Caleb Grant (Fig. 2F), the Resident Geoscientist with the geopark, whose personal aim is to "help make the geological wonders in Nova Scotia a little more accessible"; a foundational principle of the UNESCO Geoparks program. The role of the resident geoscientist, and the motivation behind the creation of such geoparks, is to increase connections between the academic community and the public, specifically when it comes to the geosciences. To achieve this goal, we rely on people, such as Caleb, who have a passion for geoscience, education, and communication.

The Cliffs of Fundy Geopark is located in Mi'kma'ki, the ancestral home of the Mi'kmaw nation and strives to honour the oral traditions of their cultural geoheritage. Two scientific highlights of the geopark include the world's highest tides in the Bay of Fundy and the evidence for both the formation and break up of Pangea. Notable field trip participants included John Calder (Fig. 2B), the executive director of the Cliffs of Fundy Geopark and a past chair of the Canadian Geoparks Network, and Godfrey Nowlan (Fig. 2E), the original chair of the Canadian Geoparks Network, who was instrumental in establishing the first Canadian Geoparks (Tumbler Ridge in British Columbia and Stonehammer in New Brunswick; Fig. 3).

This report presents a synopsis of this symposium, and the field trip, as well as background information on the organizations. It is hoped that these efforts will facilitate important discussions regarding the current and future state of geosciences, both in Canada and globally, and will help to create strategies to maintain and increase the relevancy of the field to society in support of the wider goals of the United Nations.

INTERNATIONAL UNION OF GEOLOGICAL SCIENCES (IUGS)

The IUGS is a non-political, non-governmental, non-profit organization that facilitates international cooperation and participation in the field of Earth sciences. IUGS is a member of the International Science Council, which consists of 121 national members representing over one million geoscientists with countries represented through adhering organizations (academies, geological surveys or geological societies; IUGS 2019). Canada has made significant contributions to the IUGS since its inception, including the leadership of J.M. Harrison as

Table 1. Presentations from the "IUGS, Geoparks, and IGCP – Retrospection, today and the future" symposium held at GAC-MAC-IAH-CNC-CSPG Halifax 2022 conference in May 2022 with presenting author emboldened. Talks are listed in order of presentation. The abstracts for each presentation are published in *Geoscience Canada*, volume 49, issue 2.

Day 1 – Monday 16 May

Lebel, D., and Bobrowsky, P., 2022. Canadian contributions to global geosciences: A few key highlights and future outlook.

Berger, A., 2022. Episodes and AGID – Two ventures with Canadian roots.

Henderson, C., 2022. The Permian System: A collaborative effort directed by the International Union of Geological Sciences (IUGS), the International Commission on Stratigraphy (ICS) and the Subcommission on Permian Stratigraphy (SPS).

Laflamme, M., and Schiffbauer, J., 2022. Subdividing the Ediacaran.

Pilarczyk, J., Brain, M., Green, A., Hein, C., Lau, A., and Ramos, N., 2022. From cores to code: IGCP 725's plan to bridge the gaps between geology, process, and numerical modelling to improve forecasts of coastal change.

Adiyaman Lopes, Ö., 2022. IGCP's outreach for 50 years: Evolution from east-west male researcher collaboration to global outreach with gender equality and a perspective for a sustainable future for our planet.

Narbonne, G., 2022. IGCP sedimentary and paleontological projects: 50 years of evolution from "stratigraphic correlation" to "deep-time global change", with a perspective for the future.

Kuiper, Y., Barr, S.M., Haissen, F., Montero, P.G., and Belkacim, S., 2022. The International Geoscience Programme (IGCP): An example and a fiftieth anniversary perspective.

Lesher, C.M., and Barnes, S-J., 2022. IGCP projects 161-336-427-479: Genesis and localization of magmatic Ni-Cu-PGE deposits.

Raymond, J., Blessent, D., Alcaraz, M., Malo, M., Daniele, L., and Somma, R., 2022. Geothermal resources for energy transition: past, present and future of IGCP Group 636.

Chi, G., Fayek, M., Delaney, G., Potter, E., Xue, C., Nie, F., Xu, D., Li, Z., Li., Z., Yi, L., Jin, R., Chen, Y., Song, H., and Xu, Z., 2022. Canada – China collaborative research on uranium deposits: A retrospection and vision for the future.

Bergquist, B., Fernandez, L., Vega, C., Szponar, N., Gerson, J., Nason, K., and Bernhardt, E., 2022. A new program aimed at understanding impacts of artisanal and small-scale gold mining in the Amazon (IGCP project 696).

Ludden, J., 2022. Geoscience for the next decade.

Day 2 – Tuesday 17 May

Calder, J., and Nowlan, G., 2022. UNESCO Global Geoparks in Canada: Their growth, potential, and challenges.

Brink, J., 2022. Head-Smashed-In Buffalo Jump: A UNESCO World Heritage Site in the Porcupine Hills of southwestern Alberta, Canada.

Caron, J-B., 2022. The Willner Madge Gallery Dawn of Life: Exposing the last four billion years of life on Earth at the Royal Ontario Museum.

Kerr, A., and Wylezol, P., 2022. The Cabox aspiring geopark on the scenic west coast of Newfoundland: Where the earth sciences revolution first resolved the tectonic revolutions of the distant past.

Boggs, K., O'Connor, K., Pavelka, J., and Nowlan, G., 2022. The Mackenzie Delta; A potential UNESCO Global Geopark for the future.

McKeever, P., and Narbonne, G., 2022. Geological World Heritage - A revised global framework for the application of criterion (viii) of the World Heritage Convention and a comparison with UNESCO Global Geoparks.

https://doi.org/10.12789/geocanj.2023.50.204

Figure 1. Presenters from the symposium. (A) Bridget Bergquist describing artisanal gold mining in the Amazon. (B) Daniel Lebel, Director General of the Geological Survey of Canada, characterizing Canadian contributions to global geosciences (photograph by D. Leary). (C) Yvette Kuiper presenting a fiftieth anniversary perspective of IGCP. (D) John Ludden, President of IUGS, announcing the first 100 IUGS geological Geoheritage sites with six Canadian sites mentioned in Figure 4 (courtesy of M. Burgess). (E) Antony Berger providing the history for Episodes and the Association of Geoscientists for International Development (AGID). (F) Özlem Adiyaman Lopes, UNESCO Programme Specialist (courtesy of Yongje Kim). (G) Guy Narbonne presenting "IGCP sedimentary and paleontological projects".

Table 2. The United Nations Sustainable Development Goals (sdgs.un.org/goals).

Goal	Description
1	No poverty
2	Zero hunger
3	Good health and well-being
4	Quality education
5	Gender equality
6	Clean water and sanitation
7	Affordable and clean energy
8	Decent work and economic growth
9	Industry, innovation, and infrastructure
10	Reduced inequality
11	Sustainable cities and communities
12	Responsible consumption and production
13	Climate action
14	Life below water
15	Life on land
16	Peace, justice, and strong institutions
17	Partnerships for the goals

the first President of IUGS in 1961 (Harrison 1978; Histon et al. 2022). Over the last 60 years, Canadian geoscientists served in many other elected positions and provided input on various geoscientific commissions, initiatives, and task groups (e.g. Lebel and Bobrowsky 2022; Narbonne 2022; Henderson 2022). Once every four years, the International Geological Congress (IGC), an international meeting sponsored by IUGS, is organized to promote "*the advancement of fundamental and applied research in the earth sciences*" (www.iugs.org/igc). The next IGC is scheduled for August 25–31 2024 in Busan, the Republic of Korea (www.igc2024korea.org/), where Canada will be delivering a bid to host IGC 2028 in Calgary (www.igc2028canada.org/).

The IUGS aims to facilitate and encourage international cooperation and participation in the field of Earth sciences. The objectives of the organization as defined by IUGS (2019) are:

1. Expanding awareness of the importance of the Earth sciences.
2. Producing authoritative geological standards.
3. Improving the exchange of and access to geoscience information.
4. Expanding geoscience professionalism.
5. Supporting education in the Earth sciences.
6. Addressing human and societal needs.
7. Capacity building.

The IUGS strives to meet its objectives by supporting broad-based scientific activities and programs as well as through the establishment and use of committees, commissions, task groups, initiatives, and joint programs run in tandem with other organizations. Topics supported by the organization include fundamental Earth science research, and economic and industrial applications, as well as social, educational, and environmental geoheritage (IUGS 2019). The IUGS is responsible for sponsoring symposia (such as the one in Halifax), and arranging field visits, as well as addressing issues of standardization as they apply to the field of Earth sciences. IUGS produces a quarterly international science journal called "*Episodes*" which is publicly available and contains original scientific research and review papers, as well as IUGS reports (Berger 2022; www.episodes.org/main.html).

The IUGS also oversees the International Commission on Stratigraphy (ICS) which is the largest and oldest scientific body in the IUGS. The ICS defines and updates global units (systems, series, and stages) for the International Chronostratigraphic Chart that defines the units (periods, epochs, and ages) of the International Geological Time Scale. The commission consists of seventeen subcommissions, each of which is responsible for a specific interval of geological time. Canada hosts thick and aerially extensive deposits of Neoproterozoic sedimentary rocks (the Windermere Supergroup in western Canada and the Conception Group in Newfoundland) and was a major player in a ground-breaking IUGS-ICS initiative to formally subdivide Precambrian strata into geologic periods. These studies resulted in the designation and ratification of the Ediacaran Period (635–539 Ma), the first geologic period ever recognized in the Proterozoic and the first new geologic period of any age named in more than a century (Knoll et al. 2004, 2006). The Ediacaran Subcommission is currently working on attempting to divide the Ediacaran Period into meaningful series and stages by reviewing possible biological, geological, and chemical markers (Laflamme and Schiffbauer 2022). Research on the soft-bodied remains of Ediacaran fauna from Canadian locations resulted in the designation of both the Discovery Geopark and the Mistaken Point UNESCO World Heritage Site in Newfoundland (Figs. 3 and 4, respectively).

The ICS is also responsible for maintaining the international Global Boundary Stratotype Sections and Points (GSSP) registry. Two of the 12 system-level GSSPs worldwide are in Canada: the GSSP for the base of the Cambrian is in the Fortune Head Ecological Reserve in Newfoundland and the GSSP for the Cambrian–Ordovician boundary is at Green Point, Newfoundland, in Gros Morne National Park, a UNESCO World Heritage Site (Fig. 4). Additionally, Crawford Lake in Ontario was chosen in July 2023 as the GSSP for the proposed Anthropocene epoch by the Anthropocene Working Group. Henderson (2022) presented an overview during the symposium of the evolution of the Permian system including summarizing the establishment of the GSSPs for the period.

INTERNATIONAL GEOSCIENCE PROGRAMME (IGCP)

The IGCP (formerly known as the International Geological Correlation Program) is a UNESCO program established and delivered in collaboration with IUGS (Kuiper et al. 2022) whose mission includes "*promoting sustainable use of natural resources, and advancing new initiatives related to geo-diversity, geo-heritage, and geohazards risk mitigation*" (www.iugs.org/igcp; en.unesco.org/international-geoscience-programme). The IGCP was established following the 1972 IGC in Montreal

Figure 2. Photographs from the Cliffs of Fundy UNESCO Global Geopark field trip. (A) Dark grey Triassic North Mountain Basalt overlying red Blomidon Formation playa mudstones, deformed by Cretaceous faulting. (B) John Calder, Interim Executive Director of Cliffs of Fundy Geopark, Past President of Canadian Geoparks Network on Little Dyke. (C) David Piper (Emeritus Scientist, Geological Survey of Canada - Atlantic) with historical fishing weir in distance, standing on the tombolo to Partridge Island (Wa'so'q in Mi'kmaq). (D) Welcome sign to Cliffs of Fundy UNESCO Geopark with the iconic painting of the Three Sisters by Gerald Gloade, a Mi'kmaw artist and current Program Development Officer for the Mi'kmawey Debert Project in Truro. (E) Godfrey Nowlan, Founding Chair of the Canadian National Committee for Geoparks. (F) Caleb Grant, Resident Geologist at the Cliffs of Fundy Geopark standing on Little Dyke Beach (G) Georgia Pe-Piper (Emerita Professor, Saint Mary's University) walking on the beach north of The Old Wife. (H) Vein of the zeolites stilbite (whitish) and chabazite (pink) in North Mountain basalt on the beach north of The Old Wife.

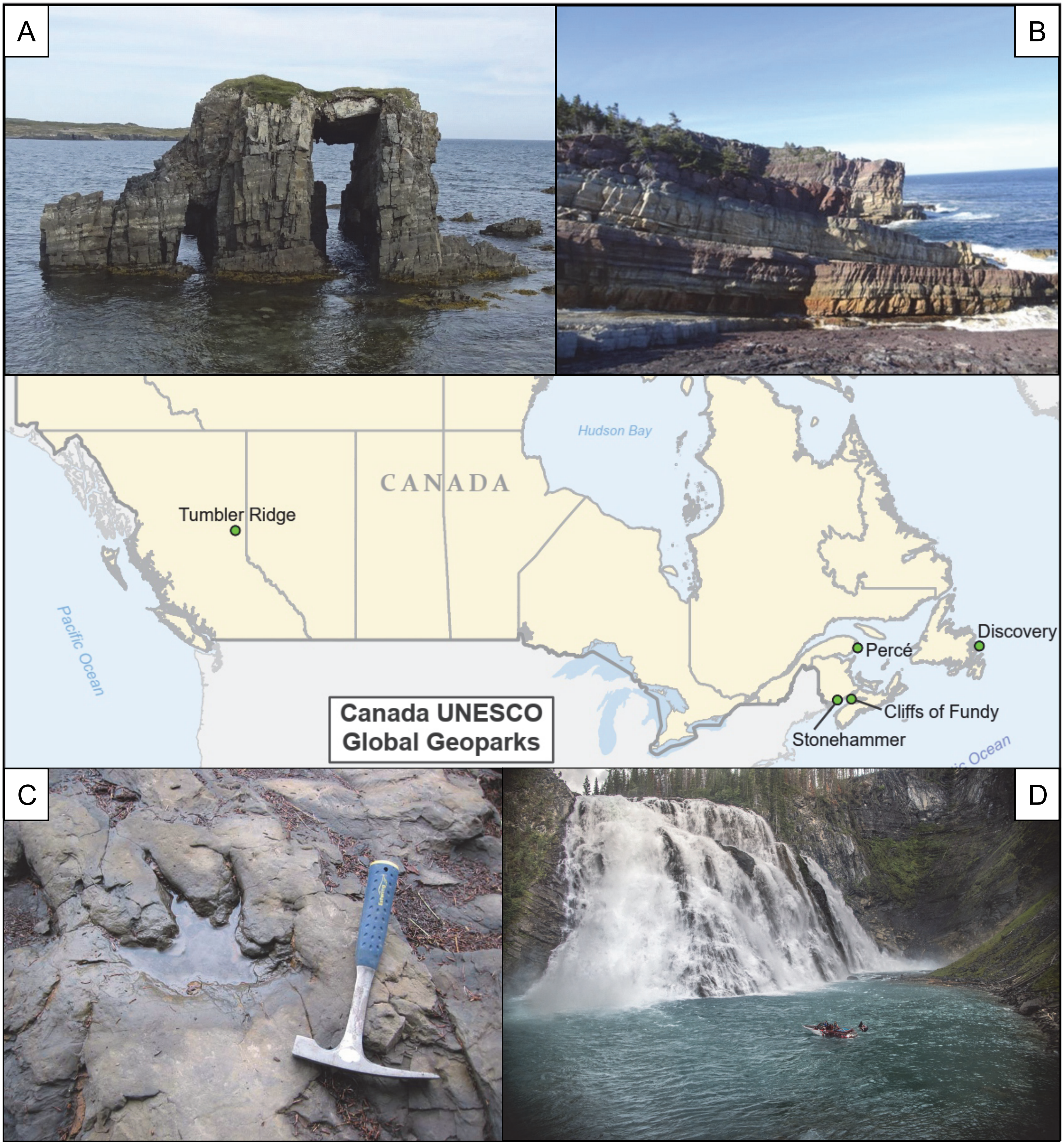

Figure 3. Map showing the location of the five Canadian UNESCO geoparks. (A) Arch Rock at Little Catalina, a triple sea arch that contains Ediacaran fossils, on the Bonavista Peninsula in Discovery UNESCO Geopark. (B) Brook Point in Discovery UNESCO Geopark, near King's Cove on the Bonavista Peninsula (Discovery UNESCO Geopark photographs courtesy of A. Hinchey). (C) Dinosaur footprint from Tumbler Ridge UNESCO Geopark (photograph courtesy of Tumbler Ridge Museum Foundation). (D) Kinuseo Falls, Tumbler Ridge UNESCO Geopark (photograph courtesy of Tumbler Ridge Museum Foundation).

Figure 4. Map showing the location of Canadian UNESCO World Heritage geology sites. (A-B) Ediacaran fossils from Mistaken Point showing cast of a rock surface showing multiple *Fractofusus* specimens (A) and tactile rock surface cast and 3-D bronze models of common species (B). (C) Cambrian fossils from the Burgess Shale; *Oesia* fossils and 3-D model of the worm living in its tube. (D) UNESCO introductory panels (courtesy of J.-B. Caron). Note that Anticosti Island was inscribed onto the UNESCO World Heritage site list in September 2023 (after submission of this article), making it Canada's newest World Heritage site.

(the last time that Canada hosted the IGC) with the aim of facilitating international cooperation in the geosciences (en.unesco.org/international-geoscience-programme; Narbonne 2022). The IGCP continues to push for maximum international participation and gender equality in accordance with the United Nations' goals. In the early years of the program, projects were typically led by male geologists from the northern hemisphere with co-leaders from less than five countries (Adiyaman Lopes 2022). Participation from developing countries has been historically hampered by language barriers, visa requirements, and a lack of financial support from national governments (Kuiper et al. 2022). Starting in 2012, IGCP began extensive outreach initiatives to increase global representation and gender equality with a focus on developing and under-represented countries. As of 2022, 42% of active project leads and 46% of participants identified as female geoscientists, with 42% of IGCP participants being early career scientists, and 47% from developing nations (Adiyaman Lopes 2022).

IGCP projects are typically funded for five years (Kuiper et al. 2022) and fall within one of five themes: earth resources, global change, geohazards, hydrogeology, and geodynamics (en.unesco.org/international-geoscience-programme; see also Derbyshire 2012; IGCP 2020). IGCP projects that were presented during the symposium are given below as examples for their associated categories, but no projects related to the hydrogeology or geodynamics themes were presented.

Earth Resources – Sustaining our Society

Lesher and Barnes (2022) discussed IGCP #161 (Magmatic sulphide deposits in mafic and ultramafic rocks), IGCP #336 (Petrology and metallogeny of intraplate mafic and ultramafic magmatism), IGCP #427 (Ore forming processes in dynamic magmatic systems), and IGCP #479 (Sustainable use of platinum group elements in the 21st century: Risks and opportunities). These four projects refined exploration models for magmatic sulphide deposits and continue to fuel current research. Chi et al. (2022) summarized IGCP #675 (Sandstone-type uranium deposits) which aims to increase global knowledge of sandstone-type uranium deposits, assess the application of novel techniques in the mining of these deposits, assist with developing guidance for their exploration, and help to facilitate the utilization of uranium in the energy transition (en.unesco.org/international-geoscience-programme/projects/675). Bergquist et al. (2022) summarized IGCP #696 (Impacts from artisanal and small-scale gold mining in the Amazon) which is an ongoing, Canada-led project that studies the release of mercury during such artisanal mining activity and potential health and environmental impacts (en.unesco.org/international-geoscience-programme/projects/696). Raymond et al. (2022) summarized IGCP #636 (Geothermal resources for energy transition), which strives to increase the understanding of geothermal reservoirs while advancing methodologies for characterizing and modelling these reservoirs to ensure the sustainable development of this resource (en.unesco.org/international-geoscience-programme/projects/636).

Global Change and the Evolution of Life

Narbonne (2022) summarized IGCP #588 (Preparing for coastal change), IGCP #639 (Sea-level change from minutes to millennia), IGCP #655 (Toarcian oceanic anoxic event), IGCP #630 (Permian–Triassic climatic and environmental extremes and biotic responses), IGCP #632 (Continental crises of the Jurassic), and IGCP #732 (Language of the Anthropocene). This suite of projects contributed to our understanding of deep time, providing new insights into the magnitude and timeframe of past, present, and future global change.

Geohazards – Risk and Mitigation Assessment for Sustainable Development

Pilarczyk et al. (2022) summarized IGCP #725 (Forecasting coastal change). The primary goal of this project is to enhance the ability to forecast system response to coastal change on a spatial and temporal scale (en.unesco.org/international-geoscience-programme/projects/725).

Other Topics

Additionally, "Special Topics" are defined annually by the IGCP Council and released under particular themes which are considered relevant for society. These include those related to geoheritage, geoparks, geodiversity, the Anthropocene, artificial intelligence applications in geoscience, and the enhancement of societal acceptance for the sustainable development of Earth resources (Adiyaman Lopes 2022). Seed funds from IGCP support projects that benefit society, increase capacity in the geosciences, and promote the advancement and sharing of knowledge between scientists (Adiyaman Lopes 2022; Kuiper et al. 2022). In November 2022 there were 58 active IGCP projects run by 376 ICGP project leaders from 92 countries. Over the past 50 years Canadians have been involved in numerous IGCP projects (see Table 3 for a list of past IGCP projects co-led by Canadians).

Cooperative Projects among Geological Surveys

The Geological Survey of Canada (GSC) is a founding member of the World Community of Geological Surveys (WCOGS), a community of best practices established in 2020 focused on linking these organizations, supporting global sustainable development, and helping develop responses to global issues. The mission and principles of WCOGS overlap with those of IUGS (Lebel and Hill 2020) and capitalized on the success of a special session on the "Changing Role of Geological Surveys" at the 2018 "Resources for Future Generations" conference held in Vancouver, Canada. This eventually led to the publication of a Geological Society of London special volume (Hill et al. 2020). This community of geological surveys will continue to support IUGS, IGCP and other international initiatives through individual or joint contributions. At this point, the WCOGS is focused principally on engaging leaders and staff from member organizations but is ensuring that most of the events are publicly available online. The first few events were initiated at the onset of the COVID-19 pandemic and have increased in frequency and diversity (see www.worldgeosurveys.org for more details and recorded presentations).

Table 3. Past IGCP projects with Canadian geoscientist co-leaders. Geoscientists not affiliated with a Canadian institution are identified. This list excludes those projects that were presented during the Halifax 2022 symposium. Information from Derbyshire (2012).

IGCP Project Number	IGCP Project Leads	IGCP Project Title	Years
92	A.M. Goodwin	Archean Geochemistry	1974–1983
160	J. Veizer	Precambrian Exogenic Processes	1977–1986
161	A.J. Naldrett	Sulphide Deposits in Mafic and Ultramafic Rocks	1977–1987
171	G.E.G. Westermann	Circum-Pacific Jurassic	1981–1985; 1986–1987
233	J.D. Keppie, R.D. Dallmeyer (USA)	Terranes in the Circum-Atlantic Palaeozoic Orogens	1985–1990; 1991
257	H.C. Halls	Precambrian Dyke Swarms	1987–1991
259/360	A.G. Darnley, J.A. Plant (UK)	International Geochemical Mapping; Global Geochemical Baselines	1988–1992; 1993–1997
290	M. Higgins, J.-C. Duchesne (Belgium)	Anorthosites and Related Rocks	1990–1994
293/386	H.H.J. Geldsetzer, Xu Dao-Yi (China)	Geochemical Event Markers in the Phanerozoic	1990–1993
314	L. Kogarko (Russian Federation), J. Keller (Germany), K. Bell	Alkaline and Carbonatitic Magmatism	1991–1995
315	I. Haapala (Finland), R.F. Emslie	Rapikivi Granites and Related Rocks	1991–1995; 1996
342	M. Zentilli, C. Dtassinari (Brazil), F. Munizaga (Chile)	Age and Isotopes of South American Ores	1992–1996; 1997
353	J.V. Matthews Jr., A. de Vernal	The Last Interglacial Period in the Circum-Arctic	1993–1997
354	P. Rongfu (China), P. Laznicka, J. Kunina (USA), D.V. Rundquist (Russian Federation), I. Plimer (Australia), T. Nakajima (Japan)	Economic Super Accumulations of Metals in Lithosphere	1995–1999; 2000
367	D.P. Scott	Late Quaternary Coastal Records of Rapid Change	1994–1998
371	R.P. Gorbatschev (Sweden), C.F. Gower	North Atlantic Precambrian (COPENA)	1994–1998; 1999
406	M.V.H. Wilson, T. Marss (Estonia), P. Mannik (Estonia)	Circum-Arctic Palaeozoic Vertebrates	1996–2000; 2001
415	J.T. Teller, R. Valkmae (Estonia)	Glaciation and Reorganization of Asia's Drainage	1997–2001
419	M. Wendorfi (Botswana), P.L. Binda	Foreland Basins of the Neoproterozoic Belts in Central-to-Southern Africa and South America	1998–2002
447	X. Meng (China), D.G.F. Long, R. Bourrouilli (France)	Proterozoic Molar-tooth Carbonates	2001–2005
450	S.S. Iyer, A.F. Kamona (Namibia), A. Misi (Brazil), J. Cailteux (DR Congo)	Proterozoic Sediment-hosted Base Metal Deposits of Western Gondwana	2000–2004
453	J.B. Murphy, J. Keppie (Mexico)	Modern and Ancient Orogens	2000–2004
454	O. Selinus (Sweden), P. Bobrowsky, E. Derbyshire (UK)	Medical Geology	2000–2004
463	C. Wang (China), M. Sarti (Italy), R.W. Scott (USA), L.F. Jansa	Upper Cretaceous Oceanic Red Beds	2002–2006
467	M.J. Orchard, I. Krystyn (Austria), J. Tong (China), S. Lucas (USA), H. Campbell (New Zealand), F. Hirsch (Japan), K. Ishida (Japan), Y. Zacharov (Russian Federation)	Triassic Time and Trans-Panthalassan Correlations	2002–2006; 2007
469	C.J. Cleal (UK), B.A. Thomas (UK), S. Oplustil (Czech Republic), Y. Tenchov (Bulgaria), E. Zodrow	Late Variscan Terrestrial Biotas and Paleoenvironments	2003–2007
474	B.R. Coleby (Australia), L.D. Brown (USA), F.A. Cook, G.S. Fuis (USA), R.W. Hubbs (UK), D.M. Finlayson (Australia), S. Li (China), O. Oncken (Germany)	Images of the Earth's Crust	2003–2007
479	J.E. Mungall, M. Ijina (Finland), C. Ferreiro-Filbo (Brazil)	Sustainable Uses of Platinum Group Elements	2003–2007
501	F.J.A.S. Barria (Portugal), W.S. Fyfe, O. Leonardos (Brazil), S. Li (China)	Soil Regeneration with Erosion Products and Other Wastes	2004–2005
502	R. Allen (Sweden), F. Torres (Spain), J. Peter, N. Cagatay (Turkey)	Global Comparison of Volcanic-hosted Massive Sulphide Districts	2004–2008
511	Jacques Locat, J. Mienert (Spain), R. Urgeles (Spain)	Submarine Mass Movements and Their Consequences	2005–2009
514	N. Patyk-Kara (Russian Federation), A.Duk-Rodkin, B. Hou (Australia), L. Ziyang (China), V. Doigopolov (Kazakhstan)	Fluvial Palaeosystems: Evolution and Mineral Deposits	2005–2009
521	V. Yanko-Homback, Irena Motnenko	Caspian-Black Sea-Mediterranean Corridor during the Last 30 ka: Sea level Change and Human Adaptive Strategies	2005–2009
526	F.I. Chiocci (Italy), L. Collins (Australia), M.M. de Mahiques (Brazil), R. Hetherington	Risks Resources and Record of the Past on the Continental Shelf	2007–2011
574	S. Johnston, G. Gutierrez-Alonso (Spain), A. Well (USA)	Bending and Bent Orogens and Continental Ribbons	2009–2013
587	P. Vickers-Rich (Australia), M. Fedonkin (Russian Federation), J. Gehling (Australia), G. Narbonne	Entity, Facies and Time – The Ediacaran (Vendian) Puzzle	2010–2014
600	A. Hou (China), D. Leach (USA), J. Richards, R. Goldfarb (USA)	Metallogenesis of Collisional Orogens	2011–2014

The priorities for the WCOGS Activity Committee for the next few years are nurturing the next generation of talent, geoscience education, linking women geoscientist leaders, collaborating with IGCP, and advancing technical sessions on global earthquake risk reduction, and landslides. The Secretariat organization rotates on a two-year period between member organizations with the GSC hosting the first two years. As of January 2023, the EuroGeoSurveys, a non-profit organization that represents the Geological Surveys of Europe, is the current WCOGS Secretariat and will serve until the end of 2024.

UNESCO GLOBAL GEOPARKS AND WORLD HERITAGE SITES

UNESCO Global Geoparks and geoscience-themed World Heritage Sites are important venues for promoting geoscience while engaging the individuals and families that visit these sites. These venues owe their origin to a 2005 report by the International Union for Conservation of Nature (IUCN) entitled "Geological World Heritage: A Global Framework" (Dingwall et al. 2005) that aimed to assist the World Heritage Convention in recognizing and protecting regions of geological and geomorphological heritage and inscribing such regions onto the World Heritage List (McKeever and Narbonne 2021). World Heritage Sites have "Outstanding Universal Value" which is evaluated using a series of criteria and conditions that cover cultural and natural properties, defined by the UNESCO World Heritage Centre (2019). The key properties that relate to geological features are encapsulated in criterion 8 of 10, which reads:

> *"Be outstanding examples representing major stages of earth's history, including the record of life, significant on-going geological processes in the development of landforms, or significant geomorphic or physiographic features"*

The UNESCO World Heritage Committee requested in 2013 and 2014 that IUCN revise the initial Dingwall et al. (2005) report to "*refine the proposed 13 themes, articulate the threshold of 'Outstanding Universal Value', and clarify the difference between the criterion of World Heritage and Geoparks*". At that time, geoparks were not designated by UNESCO but this changed in 2015 when UNESCO adopted the new designation of UNESCO Global Geopark and all pre-existing global geoparks became UNESCO Global Geoparks (McKeever and Narbonne 2021, 2022). McKeever and Narbonne (2021) published the "Geological World Heritage: A revised global framework for the application of criterion (viii) of the World Heritage Convention". This revised report identifies 11 themes (reduced from 13 in the 2005 report) for the evaluation of World Heritage sites that involve key geological properties. These 11 themes are as follows:

1. History of planet Earth and the evolution of life.
2. Tectonic systems.
3. Erosional systems.
4. Volcanic systems.
5. River, lake and delta systems.
6. Cave and karst systems.
7. Coastal systems.
8. Marine systems.
9. Glacial and periglacial systems.
10. Desert and semi-desert systems.
11. Meteorite impacts.

McKeever and Narbonne (2021, 2022) provide guidance and a framework for determining which designation, World Heritage or UNESCO Global Geopark, is appropriate when considering new geological and geomorphological attributes for international recognition and preservation.

Global geoparks are not parks in the traditional North American way of thinking but are instead places to reflect on and celebrate the connections between the land and the people that inhabit it (Calder and Nowlan 2022). UNESCO Global Geoparks are designated, defined geographical regions that have international geological significance, and are managed in the spirit of sustainable development with protection and education programs (en.unesco.org/global-geoparks). They connect the geology of a region with the natural and cultural heritage, to increase awareness of important societal issues such as climate change, resource sustainability, and natural-hazard risk (Calder and Nowlan 2022). Global geoparks combine conservation with sustainable development and are intended to be led by the local community (a 'bottom-up' approach) with the aim of increasing geotourism. As global geoparks focus on both land and people, aspiring geoparks should include Indigenous ways of knowing and culture, with Indigenous storylines presented parallel to the science (Calder and Nowlan 2022). In the Canadian context, geoparks provide opportunities for reconciliation with Indigenous peoples, offering a way to recognize and honour Indigenous culture and connections with the land.

As of November 2022, there are 177 UNESCO Global Geoparks spread over 46 countries (en.unesco.org/global-geoparks), with five in Canada; Tumbler Ridge (British Columbia), Percé (Quebec), Stonehammer (New Brunswick), Cliffs of Fundy (Nova Scotia), and Discovery (Newfoundland and Labrador). These locations are shown in Figure 3, with information at www.canadiangeoparks.ca. It is estimated that the number of geoparks in Canada will double by the end of the decade as several aspiring geoparks are currently working on their applications (www.canadiangeoparks.ca). An example of one such aspiring Canadian geopark is Cabox on the west coast of Newfoundland where the Precambrian to Late Ordovician Bay of Islands Igneous Complex, one of the first ophiolite sequences recognized, enables visitors to walk from ancient intertidal zones, onto the mantle, across the Moho (Kerr and Wylezol 2022). Assessments are underway to identify potential new global geopark candidates in Canada by focusing on regions that are under-represented. This is especially relevant for Canada's North as there are no current geoparks anywhere in the world that are located in permafrost regions. A geopark in the North would offer a unique perspective into the impacts of climate change, specifically with respect to changing permafrost conditions. Furthermore, a geopark in

Canada's North would ideally be Indigenous-led and directed, ensuring the inclusion and proper representation of Indigenous culture, with the aim of increasing geotourism to the region to benefit the communities. Katherine Boggs spoke on initiatives related to a possible future global geopark in the Mackenzie Delta region, where initial communication with local communities had just started prior to the onset of the COVID-19 pandemic and is soon set to resume (Boggs et al. 2022).

UNESCO is also responsible for the identification and designation of World Heritage sites which are locations that demonstrate "Outstanding Universal Value". There are over 1100 UNESCO World Heritage sites (both natural and cultural) worldwide, with 22 in Canada. Of these 22, nine sites were designated based on geoheritage criteria and represent a cross-section through the geodiversity of the Canadian landscape. The locations of these sites are indicated in Figure 4; more details are available at whc.unesco.org/en/list. Five of these sites (Canadian Rocky Mountain Parks, Dinosaur Provincial Park, the Joggins Fossil Cliffs, Gros Morne National Park, and Mistaken Point) were included in the world's "First 100 Geological Heritage Sites" recently compiled by IUGS (2022).

An overview of the Head-Smashed-In Buffalo Jump UNESCO World Heritage site in southwestern Alberta was presented by Brink (2022) during the symposium. Additionally, Caron (2022) described the Willner Madge Gallery 'Dawn of Life' exhibit at the Royal Ontario Museum (Toronto, Ontario, Canada), which contains fossil specimens from every Canadian province and territory. The gallery includes fossils from five UNESCO World Heritage Sites: Mistaken Point (Ediacaran) in Newfoundland, the Burgess Shale (Cambrian) in the Canadian Rocky Mountain Parks (British Columbia), the Joggins Fossil Cliffs (Carboniferous) in Nova Scotia, Miguasha (Devonian) and Anticosti Island (Ordovician–Silurian) in Quebec. The adjoining ROM James and Louise Temerty galleries of the Age of Dinosaurs contain dinosaur fossils from Dinosaur Provincial Park, also a UNESCO World Heritage Site (Fig. 4).

GEOSCIENCES FOR THE NEXT DECADE

The final presentation on Day 1 of the symposium was 'Geosciences for the next decade' by current IUGS president, John Ludden. His presentation provided context as to why the field of geoscience remains relevant in today's world and offered food for thought as to how this role will develop in the near future (Ludden 2022). Ludden stated that the study of Earth science is critical for furthering our understanding of our planet, for creating and maintaining a safe and healthy Earth, for sustainable development and growth, and for helping to reduce global economic inequalities. Ludden also showed that there are opportunities for geoscience to respond to, and be driven by, current major global societal factors. Examples include energy supply and decarbonization, a need to reduce global emissions, studying the geological risks along with the hazards, population change on a global scale, data science, environmental regulations, and public opinion on such matters. He noted that typical academic geoscience research has the tendency to focus on incremental science (i.e. small research questions with limited visibility) that do not by themselves address global issues. Ludden suggested that geoscientists should be trying to shift to big geoscience initiatives that tackle larger, more pressing problems with better visibility. This trend has gained momentum with geological survey organizations, as exemplified by the GSC, the United States Geological Survey, the Bureau de Recherches Géologiques in France, and other collaborative initiatives by EuroGeoSurveys.

Ludden acknowledged that the field of geoscience faces many challenges in its current state and in moving forward. For instance, progress is hampered by lack of connections between discovery science, applied science, and the translation of science. He observed that geoscientists have become proficient in identifying issues but tend to leave the problem resolution to engineers. Geoscientists must become more adept at communicating with other disciplines and at developing better working relationships, especially with engineering and socioeconomic fields, in order to facilitate and guide future initiatives. The geoscience community needs to develop meaningful strategies to increase enrolment in post-secondary Earth science programs to avert the possible skill shortages that this may eventually trigger. The number of university geoscience departments that are now closing due to diminishing enrollment is alarming (see Nature Reviews Earth and Environment editorial 2021). Furthermore, Ludden stated that there is a tendency for national geoscience policies to look inwards, specifically in regard to mineral resource exploration, leading to global inequities.

An over-arching challenge faced by geoscientists, as described by Ludden (2022), is the climate crisis, which also plays a major role in shaping the future. He reported on the UK-based Hutton Series on Climate Change (2020–2021) that brought together experts, business leaders, scientists, and concerned citizens who identified and defined ten key priorities, innovations, and actions needed to mitigate the climate crisis (www.panmurehouse.org/programmes/hutton-series). The Hutton Series identified several needs that are cross-disciplinary (science, engineering, finance, and citizens) which apply to various levels of government, from the people, to the researchers, to the policy-makers. Ludden (2022) stated that there needs to be a change to the global engineering ethos that prioritizes caring for the planet by developing and testing novel technological solutions. Governments need to provide leadership and policies that focus on long-term sustainability. This will also help to improve investor confidence and encourage citizens to support policies aimed at climate-change mitigation. Ludden further stressed that geoscientists, and geoscience industries, should lead by example for net-zero initiatives, with the aim that these strategies be implemented globally. The technology required to achieve an energy transition largely exists but requires optimization and a significant injection of capital. Furthermore, Ludden emphasized that the finance sector needs to modify its current way of thinking so that it can decouple economic growth from carbon emissions.

DISCUSSION PANELS

IUGS and IGCP Discussion Panel

The first day of the symposium concluded with a panel discussion, following John Ludden's talk, with most of the earlier IUGS and IGCP presenters serving as panelists. Several topics were inspired by the issues raised by John Ludden and are discussed in this section. The main points from each of the panel themes are summarized below, based on the opinions and experiences of panel experts and audience members. These provide some insights into potential issues facing the geoscience community with the aim of initiating further discussions. Various governments, universities, and organizations have already started to develop programs to address some of these issues, but novel ideas and initiatives are needed to ensure long-term, meaningful change.

Communication with Politicians, Policy- and Decision-Makers

There are numerous challenges when it comes to communicating Earth science to policy- and decision-makers in support of the creation and funding of long-term strategies in ever-changing political and economic environments. In Canada, these challenges are further exacerbated for educational proponents as their sectors report to provincial and territorial Ministries of Education which have minimal geoscience teaching in their education programs (geosciences are not even designated as a teachable in Canada). It was suggested that educators and organizations collaborate with government departments (such as the Geological Survey of Canada and Provincial and Territorial geological surveys) who are well situated to influence policy development. For instance, the Pan-Canadian geoscience strategy, which does not include research-granting councils and universities, lists geoscience outreach to the public and decisions makers as a priority. The EuroGeoSurveys strategy, which supports the new Geological Service of Europe project, has similar aims for promoting geoscience and education outreach (EuroGeoSurveys 2022).

Creating Long-Term Strategies and Solutions

John Ludden commented in his presentation that Earth scientists can provide ample evidence of global issues (e.g. the climate emergency) but that they tend to move on to identifying the next issue hoping that engineers will come up with solutions. This led to discussion invoking several newer geoscience programs as examples of how this mindset might be shifting. For example, several cross-disciplinary programs throughout Canada are attempting to develop methods for mitigating the impacts of climate change. They include collaborations between scientists, engineers, and policy-makers across industry, government, and academia in the fields of carbon capture and sequestration, groundwater mapping, geothermal, critical minerals for green energy, hydrogen storage, geohazards, coastal erosion and other topics. Even with these programs, Earth scientists need to do better at engaging other disciplines in order to develop more meaningful solutions to the global climate emergency.

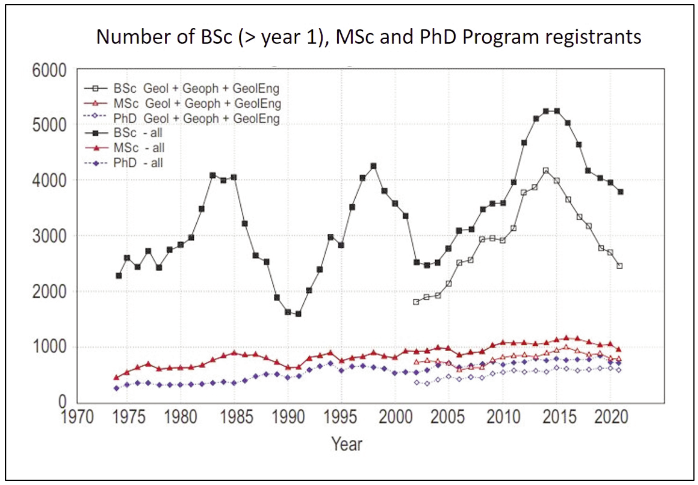

Figure 5. The number of geoscience students in Canadian universities from 1974 to 2021 (courtesy of the Council of Chairs of Canadian Earth Science Departments; cccesd.acadiau.ca/). The solid symbols include all students in their respective programs (BSc, MSc and PhD), the hollow symbols include the students in geology + geophysics + geological engineering fields minus the environmental sciences students. This separation was started in 2002. Note that there has been a drop of 1700 (42%) in 2021 from 4200 undergraduate geoscience students in 2014.

Attracting the Next Generation into Earth Sciences

Significant concern was expressed at the panel discussion regarding the lack of students enrolled in current post-secondary Earth science programs, especially in Canada. This is going to cause problems in the not-so-distant future as it will lead to workforce challenges that will inhibit tackling climate-change issues. This does not only represent shortages of geologists, but also a lack of Earth scientists with data processing expertise and knowledge of environmental issues. At the same time, qualified geoscientists are required to support mineral exploration and the petroleum industry, especially as these industries also contribute to the development of solutions to tackle climate change such as carbon sequestration and storage as well as critical mineral resource identification and extraction.

According to panelists and audience members, many Canadian, Australian, and European Earth science departments report decreased enrollment (e.g. see Fig. 5 for Canadian data) as the new generation looks to environmental science and geography to tackle climate change while viewing geology only in terms of mineral and petroleum exploration. This makes attracting and retaining students in geoscience programs difficult. The University of Toronto was put forward as an example of a successful Canadian post-secondary institution which has not seen a decline in geoscience enrollment. Their geology program is designed to connect to more popular, related fields such as environmental science, and employs an Earth-system science approach. This multi-faceted strategy has attracted a wider range of students, and helped to keep the geoscience program numbers steady, and may provide a template for other universities to follow.

Having good, engaging instructors in first-year geology courses may also help to attract students from other disciplines. Another useful approach may be to get children interested in the Earth sciences well before post-secondary education, preferably before Grade 5 when many children have already developed math and science anxieties (e.g. Friesen 2009). Both initiatives may help bolster future enrollments. Encouraging further discussions regarding geoscience enrollment is necessary for the development and implementation of strategies aimed at increasing student participation in Earth sciences.

Relevancy and Communication with the General Public Through Education and Outreach

A lack of capacity is partly caused by the challenge of making Earth sciences more relevant to students and to society in general. Geologists understand the importance of what we do, but how do we effectively communicate that to students or people lacking an Earth science background, so they understand and support the geosciences? Other organizations, such as IGCP, are working on this issue. The IGCP's focus on geoscience education and its strategic position in UNESCO are assets that should be capitalized on. It is, however, limited by funding challenges. Half of the current IGCP projects involve social connections to local communities and all projects require an outreach component.

It was expressed during the panel discussion that Earth science projects would benefit from increased engagement with the public and Indigenous communities. Promoting and facilitating citizen science are effective ways of involving local communities. UNESCO Global Geoparks are important for demonstrating the applications of geosciences to the public. Ongoing funding for the IGCP Geoparks program, and the creation and maintenance of these parks, are important for facilitating interactions with and communications between scientists and society, while preserving these unique geoheritage sites. Furthermore, panels, committees, commissions, task forces etc., should strive for increased representation, the inclusion of early career researchers, and the involvement of non-geologists such as social scientists and geographers. Museums are key in communicating science with the public and attracting children into the sciences, yet museums also face financial struggles, especially at the provincial level in Canada.

Future Direction of the Earth Sciences

Geoscientists know that "*the present is the key to the past*" but John Ludden asked if, given the current climate emergency, Earth sciences should focus solely on the present and abandon 'deep time' to work towards solutions for imminent issues. The panel and audience members discussed this question at length and the consensus was that there is still value to be gained from the deep past, particularly with respect to mass extinction events and climatic variations. There is a need to better understand mass extinctions, what causes them, how to define and recognize them, their repercussions for life on Earth, and how the Earth recovered from past mass extinctions. Studying the deep time record of climate change may help us to better determine the long-term effect our species is having on the planet and give insights into the reality we are facing (the rates, causes, tipping points, etc., that relate to climate change).

Internal and External Geoscience Communication

The challenges facing the scientific community, specifically the Earth sciences, will require us to strengthen the ties between our various disciplines, and also with other sciences and the various fields of engineering. We are all in this together and only through working together can we develop meaningful strategies and solutions to tackle pressing issues. Specifically, Earth scientists need to cooperate with other disciplines including industry, engineering, biology, geography, and socioeconomics. Goals should include improving communications, timely sharing of data and research, and involving these other disciplines in Earth science organizations, panels, and committees. It was mentioned that Canadian geoscientists need to support and collaborate more with students and researchers from under-represented, under-funded countries on targeted, meaningful projects for the benefit of everyone. Broader volunteer-based participation by Canadians in IUGS, IGCP and other international endeavours will be crucial in the coming decades to stay connected, build synergies, and integrate between various disciplines, genders, and cultural diversities.

Funding

Funding is always a major concern to any researcher, and challenges associated with a lack of funding were a common theme during the panel discussion. As scientists, we have ideas for future projects and collaborations, but funding these undertakings is a challenge. A lack of consistent funding also exacerbates the issue of attracting the next generation of geoscientists; students will not come without funding. It would be ideal if a program (national, international, or a combination of both) with ample funding was created that supported academics and government researchers to pursue the recommendations outlined in the Hutton Series. Such a program would fund student projects on climate change, attracting candidates into the program. The question still remains though: where does this money come from? Geoscience research and solutions are expensive so there is a need to find ways to make these programs more affordable and prioritization will require rigorous cost-benefit analyses. This will attract people to the geosciences, contribute to effective societal change, and increase the relevancy of the Earth sciences. Funding is a complex, ongoing problem and requires the involvement and support of science agencies such as the Natural Sciences and Engineering Research Council of Canada (NSERC). NSERC has identified to "*mobilize knowledge on a global scale*" through support for the development of international partnerships as a priority in its strategic plan (NSERC 2022).

UNESCO World Heritage and Global Geoparks Discussion Panel

Following the presentations on UNESCO World Heritage Sites and Global Geoparks during the second day of the symposium, a panel examined areas that are under-represented in Canada and challenges experienced when developing geoparks in the Canadian context. It was apparent from the discussions that Indigenous leadership, traditional knowledge, culture, and representation should be a requirement for future geoparks. The pros and cons of placing a global geopark in environmentally fragile areas, such as Canada's North, were also discussed. The potential negative impacts of increased traffic to these regions must be considered for aspiring geoparks. However, a geopark in the North would illustrate the impact of climate change (e.g. glacial retreat, the impacts of thawing permafrost on coastlines and infrastructures, etc.) while providing financial gains to northern communities through geotourism, and significant local employment opportunities. It was also pointed out that social scientists, especially geographers, and geoscientists would both benefit from improved collaboration and communication, especially with respect to identifying, developing, and maintaining UNESCO World Heritage Sites and Global Geoparks.

CLIFFS OF FUNDY GEOPARK FIELD TRIP

A three-day, post-conference field trip to the Cliffs of Fundy UNESCO Global Geopark (Nova Scotia), showcased this unique area. This geopark strives to support and promote the concept of "Two-Eyed Seeing" wherein Indigenous heritage and modern science are given equal consideration and respect. The field trip highlighted how the landscapes and seascapes of the region evolved, and how these features influenced the cultural, industrial, and agricultural heritage of the area. The field trip also provided insights into the process of establishing an UNESCO Global Geopark and touched on related topics including geoscience communication, UNESCO educational objectives, sustainable development with respect to mineral and energy resources, and geohazards associated with climate change and rising sea levels. The three intertwined pillars that form the identity of the Cliffs of Fundy Geopark (Mi'kmaw culture, highest tides, and sea cliffs) were explored in various stops throughout the park.

The Cliffs of Fundy Geopark is located within the territory of Kluskap (or Glooscap; Calder and Gloade 2016; Grant et al. 2022), named for the first human in Mi'kmaq lore (as detailed by the *Guide to 30 Geosites*). Highway 2 through the park is locally called the Glooscap Trail and the iconic painting of the Three Sisters (distinctive sea stacks along the Bay of Fundy coastline) by Gerald Gloade, a Mi'kmaw artist and current Program Development Officer for the Mi'kmawey Debert Project in Truro, greets visitors on a highway sign enroute to the Cliffs of Fundy Geopark, Nova Scotia (Fig. 2D). The Three Sisters figure prominently in the Glooscap legend where they played a trick on Glooscap when he was hunting moose. Glooscap punished the sisters by turning them into stone: the three prominent sea stacks located offshore (Calder 2017).

A key aspect of global geoparks is their cultural significance and involvement of local Indigenous communities. During the early stages in the process of designating the Cliffs of Fundy Geopark, community consultations with the Mi'kmaq Elders Advisory Council were held. Feedback from the Mi'kmaq community resulted in extending the eastern boundary of the park to include Mi'kmawey Debert (Calder 2018), which is a significant Indigenous archeological site that dates back 11,000 years to a time when the last continental glaciers were retreating (Cliffs of Fundy Geopark Society 2020). Other Mi'kmaq cultural highlights in the Cliffs of Fundy Geopark include sites of copper mining and weir fishing. The Mi'kmaq in the region mined copper locally which was widely traded across eastern North America centuries before it was 'discovered' by Samuel de Champlain (Hanley et al. 2022). Weir fishing, using inward water flow during high tides to direct the fish into the trap that are collected later during low tides, was a technique used by the Mi'kmaq for thousands of years (Bernard et al. 2015) and one weir is still used near Partridge Island.

The highest tides on Earth occur in the Bay of Fundy due to the shape of the bay combined with the resonance of 13.3 hours along the Gulf of Maine–Bay of Fundy system, which is similar to the period of the main tides in the open Atlantic Ocean (Piper and Pe-Piper 2022). Nearly as much water as the combined discharge of all the rivers of the world (Dai and Trenberth 2002) pours through the Minas Passage at average current speeds of 12 km/hour at a million m^3/sec (Karsten et al. 2008) twice daily with every tide. Modelling estimates that an array of turbines through the Minas Passage could generate 2000 megawatts, enough to power two million homes (Karsten et al. 2011); however the strong currents and suspended sediment continue to damage infrastructure (Piper and Pe-Piper 2022). Tidal bores moving upstream may also be visible. The tide schedule is important to consider when planning a visit along the Bay of Fundy, including to the Cliffs of Fundy Geopark.

The Cliffs of Fundy Geopark is defined by spectacular sea cliffs that were sculpted by the tides. These cliffs record evidence for the assembly and separation of the supercontinent Pangea. The cliffs are composed of rocks that include Paleozoic metasedimentary rocks, Triassic magmatic rocks that formed during the breakup of Pangea and the initiation of the Atlantic Ocean, and Mesozoic shales that contain evidence of the Triassic–Jurassic mass extinction event. Zeolites are abundant in the cliffs and include stilbite (the provincial mineral of Nova Scotia; Fig. 2H), mesolite, analcime and natrolite, with rare heulandite, laumontite, chabazite and thomsonite (Pe-Piper and Miller 2002). Flint, copper, basalt, and hematite were collected and used by the Mi'kmaq for tools, jewelry, and ceremonial purposes (Mi'kmawey Debert Cultural Centre 2014).

CONCLUSION

The authors hope that the symposium held in Halifax and the ensuing connections made between people, ideas, strategies, initiatives, and projects summarized in this paper will form a modest seed from which a new generation of Canadian geoscience diplomacy for the world will emerge and grow into more potent global geoscience solutions. Canadian geoscientists have contributed significantly to IUGS, to numerous IGCP programs, and to initiatives that link geological survey organizations across the world. Nevertheless, more collaboration is needed to address the enormous challenges, notably climate change, that are now facing humanity. While geoscientists recognize the important contributions that our discipline can contribute to the global green transition, panel discussions during the symposium emphasized that improved education-outreach-communication programs are critical for conveying these contributions to the general public. Geoparks, such as the Cliffs of Fundy, combined with museums, are powerful communication platforms for engaging society, including children and their families, and inspiring the geoscientists of the future.

ACKNOWLEDGEMENTS

We would like to acknowledge the presenters for the symposium who provided invaluable insights into their experiences and projects related to IUGS, IGCP, and UNESCO Geoparks. We would also like to thank the panelists and audience for the panel discussions. These discussions identified several key areas of focus for further exploration. The authors would also like to thank the local organizing committee for the GAC-MAC-IAH-CNC-CSPG 2022 conference. Thanks are also owed to Leith MacLeod (GSC) for creating the background maps for the figures, to Marie-Claude Williamson (GSC) for her internal review of the manuscript, and to Andy Kerr for his edits and suggestions. This paper is NRCan contribution no. 20230036.

REFERENCES

Adiyaman Lopes, Ö., 2022, IGCP's outreach for 50 years: evolution from east-west male researcher collaboration to global outreach with gender equality and a perspective for a sustainable future for our planet (Abstract): GAC-MAC-IAH-CNC-CSPG 2022 Halifax Meeting, 2022, Abstracts, Volume 45: Geoscience Canada, v. 49, p. 62, https://doi.org/10.12789/geocanj.2022.49.188.

Berger, A., 2022, Episodes and AGID – Two ventures with Canadian roots (Abstract): GAC-MAC-IAH-CNC-CSPG 2022 Halifax Meeting, 2022, Abstracts, Volume 45: Geoscience Canada, v. 49, p. 73, https://doi.org/10.12789/geocanj.2022.49.188.

Bergquist, B., Fernandez, L., Vega, C., Szponar, N., Gerson, J., Nason, K., and Bernhardt, E., 2022, A new program aimed at understanding impacts of artisanal and small-scale gold mining in the Amazon (IGCP Project 696), (Abstract): GAC-MAC-IAH-CNC-CSPG 2022 Halifax Meeting, 2022, Abstracts, Volume 45: Geoscience Canada, v. 49, p. 73–74, https://doi.org/10.12789/geocanj.2022.49.188.

Bernard, T., Rosenmeier, L.M., and Farrell, S.L., (*Editors*), 2015, Mi'kmawe'l Tan Telikina'muemk: Teaching about the Mi'kmaq: The Confederacy of Mainland Mi'kmaq, Truro, NS, 218 p. Available at: https://www.mikmaweydebert.ca/home/wp-content/uploads/2015/06/Mikmawel_Tan_Telikinamuemk_Final_Online.pdf.

Boggs, K., O'Connor, K., Pavelka, J., and Nowlan, G., 2022, The Mackenzie Delta; A potential UNESCO Global Geopark for the future (Abstract): GAC-MAC-IAH-CNC-CSPG 2022 Halifax Meeting, 2022, Abstracts, Volume 45: Geoscience Canada, v. 49, p. 77, https://doi.org/10.12789/geocanj.2022.49.188.

Brink, J., 2022, Head-Smashed-In Buffalo Jump: A UNESCO World Heritage Site in the Porcupine Hills of southwestern Alberta, Canada (Abstract): GAC-MAC-IAH-CNC-CSPG 2022 Halifax Meeting, 2022, Abstracts, Volume 45: Geoscience Canada, v. 49, p. 80, https://doi.org/10.12789/geocanj.2022.49.188.

Calder, A., 2017, Cliffs of Fundy eyes Geopark status: The Chronicle Herald, 10 December 2017 newspaper publication, Retrieved October 18, 2022 from https://www.mikmaweydebert.ca/2017/12/cliffs-of-fundy-eyes-geopark-status/.

Calder, J., and Nowlan, G., 2022, UNESCO Global Geoparks in Canada: Their growth, potential, and challenges (Abstract): GAC-MAC-IAH-CNC-CSPG 2022 Halifax Meeting, 2022, Abstracts, Volume 45: Geoscience Canada, v. 49, p. 83, https://doi.org/10.12789/geocanj.2022.49.188.

Calder, J.H., 2018, Island at the Centre of the World: The Geological Heritage of Prince Edward Island: Acorn Press, 96 p.

Calder, J.H., and Gloade, G., 2016, Seeing a Geopark through Indigenous and geological eyes: The Fundy Rift, home of Kluscap: 7th International UNESCO Conference on Global Geoparks, Torquay, England, September 2016.

Caron, J.-B., 2022, The Willner Madge Gallery Dawn of Life: Exposing the last four billion years of life on Earth at the Royal Ontario Museum (Abstract): GAC-MAC-IAH-CNC-CSPG 2022 Halifax Meeting, 2022, Abstracts, Volume 45: Geoscience Canada, v. 49, p. 84–85, https://doi.org/10.12789/geocanj.2022.49.188.

Chi, G., Fayek, M., Delaney, G., Potter, E., Xue, C., Nie, F., Xu, D., Li, Z., Li., Z., Yi, L., Jin, R., Chen, Y., Song, H., and Xu, Z., 2022, Canada – China collaborative research on uranium deposits: A retrospection and vision for the future (Abstract): GAC-MAC-IAH-CNC-CSPG 2022 Halifax Meeting, 2022, Abstracts, Volume 45: Geoscience Canada, v. 49, p. 86–87, https://doi.org/10.12789/geocanj.2022.49.188.

Cliffs of Fundy Geopark Society, 2020, Cliffs of Fundy UNESCO Global Geopark: Guide to 30 Geosites, Nova Scotia, Canada, Retrieved from: https://storymaps.arcgis.com/stories/4fe5ddb9093a46eb920df5234773e8fd.

Dai, A., and Trenberth, K.E., 2002, Estimates of freshwater discharge from continents: Latitudinal and seasonal variations: Journal of Hydrometeorology, v. 3, p. 660–687, https://doi.org/10.1175/1525-7541(2002)003<0660:EOFDFC>2.0.CO;2.

Derbyshire, E., (*Editor*), 2012, Tales set in stone: 40 years of the International Geoscience Programme (IGCP): UNESCO Digital Library, Paris, France, 140 p.

Dingwall, P., Weighell, T., and Badman, T., 2005, Geological World Heritage: A global Framework: The World Conservation Union (IUCN), Protected Area Programme, 52 p. Available at: https://portals.iucn.org/library/sites/library/files/documents/Rep-2005-009.pdf.

EuroGeoSurveys, 2022, Launch of a "Geological Service for Europe" project: EuroGeoSurveys News release September 1, 2022. Retrieved October 30th, 2022, https://egsnews.eurogeosurveys.org/?p=1339.

Fedoroff, N.V., 2009, Science diplomacy in the 21st century: Cell, v. 136, p. 9–11, https://doi.org/10.1016/j.cell.2008.12.030.

Friesen, S., 2009, What did you do in school today? Teaching effectiveness framework: A framework and rubric: Canadian Education Association, Toronto, ON, 18 p. Retrieved from: galileo.org/cea-2009-wdydist-teaching.pdf.

Grant, C., Calder, J., Piper, D., Pe-Piper, G., and Leslie, L., 2022, Telling the story of the Cliffs of Fundy UNESCO Global Geopark, Nova Scotia: Linking geoheritage, Indigenous heritage and culture: GAC-MAC-IAH-CNC-CSPG Joint Annual Meeting, Halifax, May 2022, Field Trip Guidebook – B3, Atlantic Geoscience Society, Special Publication Number 61, 122 p. Available at: https://atlanticgeosciencesociety.ca/wp-content/uploads/2022/10/B3-Cliffs-of-Fundy.pdf.

Hanley, J., Terekhova, A., Drake, P., Cottreau Robins, K., Lewis, R., Suttie, B., and Boucher, B., 2022, Geochemical provenance of copper in pre-contact artifacts on the Maritime Peninsula, Eastern Canada: Determining source using laser ablation inductively coupled plasma-mass spectrometry, *in* Holyoke, K.R., and Hrynick, M.G., *eds.,* The Far Northeast: 3000 BP to Contact: University of Ottawa Press, ON, p. 219–258, https://doi.org/10.2307/j.ctv2kzv0n0.11.

Harrison, J.M., 1978, The roots of IUGS: Episodes, v. 1, p. 20–23, https://doi.org/10.18814/epiiugs/1978/v1i1/005.

Henderson, C., 2022, The Permian System: A collaborative effort directed by the International Union of Geological Sciences (IUGS), the International Commission on Stratigraphy (ICS) and the Subcommission on Permian Stratigraphy (SPS) (Abstract): GAC-MAC-IAH-CNC-CSPG 2022 Halifax Meeting, 2022, Abstracts, Volume 45: Geoscience Canada, v. 49, p. 121, https://doi.org/10.12789/geocanj.2022.49.188.

Hill, P.R., Lebel, D., Hintzman, M., Smelror, M., and Thorleifson, H., 2020, The changing role of Geological Surveys: Introduction, *in* Hill, P.R., Lebel, D., Hitzman, M., Smelror, M., and Thorleifson, H., *eds.,* The Changing Role of Geological Surveys: Geological Society, London, Special Publications, v. 499, p. 1–15, https://doi.org/10.1144/SP499-2020-19.

Histon, K., Kölbl-Ebert, M., and Vaccari, E., 2022, Organizing the Geological Sciences: Retreading the path from international congresses to scientific union: International Union of Geological Sciences (IUGS), E-Bulletin Issue 188, 7 p. Retrieved from: https://www.inhigeo.com/anniversaries/Histon_K.,_Koelbl-Ebert_M.,_Vaccari_E._IUGS_founded_60_years_ago.pdf.

IGCP. International Geoscience Programme, 2020, IGCP 2020 call for proposals: Division of Ecological and Earth Sciences, UNESCO, 3 p. Available at: https://en.unesco.org/sites/default/files/1_igcp_2020_call_for_project_proposal.pdf.

IUGS. International Union of Geological Sciences, 2019, Earth Science for the Global Community: International Union of Geological Sciences (IUGS), 2019 Edition, 6 p. Available at: https://www.iugs.org/_files/ugd/f1fc07_eb51eba6b35443d981f10478bf27f931.pdf.

IUGS. International Union of Geological Sciences, 2022, The First 100 IUGS Geological Heritage Sites: International Geosciences Program IGCP 731 (2021–2023), 153 p. Available at: https://iugs-geoheritage.org/videos-pdfs/iugs_first_100_book_v2.pdf.

Karsten, R., Greenberg, D., Tarbotton, M., Culina, J., Swan, A., O'Flaherty-Sproul, M., and Corkum, A., 2011, Assessment of the potential of tidal power from Minas Passage and Minas Basin: Acadia University, Report No. 300-170-09-11, 64 p. Available at: https://tethys.pnnl.gov/publications/assessment-potential-tidal-power-minas-passage-minas-basin.

Karsten, R.H., McMillan, J.M., Lickley, M.J., and Haynes, R.D., 2008, Assessment of

tidal current energy in the Minas Passage, Bay of Fundy: Proceedings of the Institution of Mechanical Engineers, Part A: Journal of Power and Energy, v. 222, p. 493–507, https://doi.org/10.1243/09576509JPE555.
Kerr, A., and Wylezol, P., 2022, The Cabox aspiring geopark on the scenic west coast of Newfoundland: Where the earth sciences revolution first resolved the tectonic revolutions of the distant past (Abstract): GAC-MAC-IAH-CNC-CSPG 2022 Halifax Meeting, 2022, Abstracts, Volume 45: Geoscience Canada, v. 49, p. 134, https://doi.org/10.12789/geocanj.2022.49.188.
Knoll, A.H., Walter, M.R., Narbonne, G.M., and Christie-Blick, N., 2004, A new Period for the Geologic Time Scale: Science, v. 305, p. 621–622, https://www.science.org/doi/pdf/10.1126/science.1098803.
Knoll, A.H., Walter, M.R., Narbonne, G.M., and Christie-Blick, N., 2006, The Ediacaran Period: a new addition to the geologic time scale: Lethaia, v. 29, p. 13–30, https://doi.org/10.1080/00241160500409223.
Kuiper, Y.D., Barr, S.M., Haissen, F., Montero, P.G., and Belkacim, S., 2022, The International Geoscience Programme (IGCP): An example and a fiftieth anniversary perspective (Abstract): GAC-MAC-IAH-CNC-CSPG 2022 Halifax Meeting, 2022, Abstracts, Volume 45: Geoscience Canada, v. 49, p. 139, https://doi.org/10.12789/geocanj.2022.49.188.
Laflamme, M., and Schiffbauer, J., 2022, Subdividing the Ediacaran (Abstract): GAC-MAC-IAH-CNC-CSPG 2022 Halifax Meeting, 2022, Abstracts, Volume 45: Geoscience Canada, v. 49, p. 140, https://doi.org/10.12789/geocanj.2022.49.188.
Lebel, D., and Bobrowsky, P., 2022, Canadian contributions to global geosciences: A few key highlights and future outlook (Abstract): GAC-MAC-IAH-CNC-CSPG 2022 Halifax Meeting, 2022, Abstracts, Volume 45: Geoscience Canada, v. 49, p. 144, https://doi.org/10.12789/geocanj.2022.49.188.
Lebel, D., and Hill, P., 2020, Epilogue: The rhymes musings and riddles of the International Community of Geological Surveys (IOGS), *in* Hill, P., Lebel, D., Smelror, M., Hintzman, M., and Thorleifson, H., *eds.,* The Changing Role of Geological Surveys: Geological Society, London, Special Publications, v. 499, p. 283–294, https://doi.org/10.1144/SP499-2020-61.
Lesher, C.M., and Barnes, S-J., 2022, IGCP Projects 161-336-427-479: Genesis and localization of magmatic Ni-Cu-PGE deposits (Abstract): GAC-MAC-IAH-CNC-CSPG 2022 Halifax Meeting, 2022, Abstracts, Volume 45: Geoscience Canada, v. 49, p. 146, https://doi.org/10.12789/geocanj.2022.49.188.
Ludden, J., 2022, Geosciences for the next decade (Abstract): GAC-MAC-IAH-CNC-CSPG 2022 Halifax Meeting, 2022, Abstracts, Volume 45: Geoscience Canada, v. 49, p. 151, https://doi.org/10.12789/geocanj.2022.49.188.
McKeever, P., and Narbonne, G., 2022, Geological World Heritage – A revised global framework for the application of criterion (viii) of the World Heritage Convention and a comparison with UNESCO Global Geoparks (Abstract): GAC-MAC-IAH-CNC-CSPG 2022 Halifax Meeting, 2022, Abstracts, Volume 45: Geoscience Canada, v. 49, p. 161, https://doi.org/10.12789/geocanj.2022.49.188.
McKeever, P.J., and Narbonne, G.M., 2021, Geological World Heritage: A revised global framework for the application of criterion (viii) of the World Heritage Convention: The World Conservation Union (IUCN), 118 p. Available at: https://doi.org.10.2305/IUCN.CH.2021.12.en.
Mi'kmawey Debert Cultural Centre, 2014, Wa'so'q [video]: Vimeo. Available at: https://vimeo.com/87139846.
Narbonne, G., 2022, IGCP sedimentary and paleontological projects: 50 years of evolution from "stratigraphic correlation" to "deep-time global change", with a perspective for the future (Abstract): GAC-MAC-IAH-CNC-CSPG 2022 Halifax Meeting, 2022, Abstracts, Volume 45: Geoscience Canada, v. 49, p. 170, https://doi.org/10.12789/geocanj.2022.49.188.
Nature Reviews Earth and Environment Editorial, 2021, Geoscience on the chopping block: Nature Reviews Earth and Environment, v. 2, p. 587, https://doi.org/10.1038/s43017-021-00216-1.
NSERC. Natural Science and Engineering Research Council, 2022, NSERC 2030: Discovery. Innovation. Inclusion: NSERC Strategic Plan, 45 p. Retrieved October 30, 2022, https://www.nserc-crsng.gc.ca/_doc/NSERC2030/Strategic-Plan_PlanStrategique_en.pdf.
Pe-Piper, G., and Miller, L., 2002, Zeolite minerals from the North Shore of the Minas Basin, Nova Scotia: Atlantic Geology, v. 38, p. 11–28, https://doi.org/10.4138/1252.
Pilarczyk, J., Brain, M., Green, A., Hein, C., Lau, A., and Ramos, N., 2022, From cores to code: IGCP 725's plan to bridge the gaps between geology, process, and numerical modelling to improve forecasts of coastal change (Abstract): GAC-MAC-IAH-CNC-CSPG 2022 Halifax Meeting, 2022, Abstracts, Volume 45: Geoscience Canada, v. 49, p. 183, https://doi.org/10.12789/geocanj.2022.49.188.
Piper, D.J.W., and Pe-Piper, G., 2022, The Story in the Rocks of the Cliffs of Fundy: leanpub, 105 p. Available from: https://leanpub.com/story_in_the_rocks.
Raymond, J., Blessent, D., Alcaraz, M., Malo, M., Daniele, L., and Somma, R., 2022, Geothermal resources for energy transition: Past, present and future of IGCP Group 636 (Abstract): GAC-MAC-IAH-CNC-CSPG 2022 Halifax Meeting, 2022, Abstracts, Volume 45: Geoscience Canada, v. 49, p. 189, https://doi.org/10.12789/geocanj.2022.49.188.
UNESCO World Heritage Centre, 2019, Operational guidelines for the implementation of the World Heritage Convention: UNESCO World Heritage Center, 10 July 2019, Paris, France, 177 p. Available at: https://whc.unesco.org/en/guidelines/.

Received July 2023
Accepted as revised November 2023

GEOLOGICAL ASSOCIATION OF CANADA (2023–2024)

Corporate Members

PLATINUM

Memorial University

GOLD

AngloAmerican

Northwest Territories Geological Survey

SILVER

Royal Tyrrell Museum

Yukon Geological Survey

British Columbia Geological Survey

NICKEL

University of Waterloo

GEOSCIENCE CANADA AND THE GEOLOGICAL ASSOCIATION OF CANADA ARE GRATEFUL TO THE CANADIAN GEOLOGICAL FOUNDATION FOR THEIR FINANCIAL SUPPORT OF THIS JOURNAL

Canadian Geological Foundation / Fondation Géologique du Canada

GAC-MAC: FIELD GUIDE SUMMARY

Brandon 2024: GAC–MAC–PEG Joint Annual Meeting Field Trips

Chris Couëslan

Manitoba Geological Survey
360-1395 Ellice Avenue
Winnipeg, Manitoba, R3G 3P2, Canada
E-mail: Chris.Coueslan@gov.mb.ca

BRANDON 2024 FIELD TRIPS OVERVIEW

Are you ready for an unforgettable geological experience? Join us at the 2024 GAC-MAC annual meeting, partnered with the 10th International Symposium on Granitic Pegmatites (PEG), and hosted at beautiful Brandon University, at the heart of the continent. A plethora of exciting symposia, special sessions, and short courses are planned, along with six field trips led by experts from various organizations. Delegates can pick from one pre-conference, one syn-conference, and four post-conference field trips that range from day trips to multi-day geological adventures. Get ready to immerse yourself in central Canada geology and discover breathtaking landscapes in the company of colleagues and fellow enthusiasts!

Pre-Conference Field Trip

Participants will be led by Chris Couëslan on a four-day field trip exploring "*Stratigraphy, ore deposits, and metamorphism in the Thompson Nickel Belt, Manitoba*". Extensive outcrops of almost continuous Ospwagan Group stratigraphy will be examined at two open pit mines in the Thompson area (Fig. 1). Sulphidic horizons within the Ospwagan Group are interpreted as the source of sulphur for magmatic Ni-Cu ore systems, and are the ore horizons for the three largest mines that have operated in the Thompson Nickel Belt. Styles of mineralization were strongly controlled by ductile deformation during high-grade metamorphism, the effects of which will also be observed in outcrop. Time will be spent looking at styles of mineralization in drillcore from the Thompson mine area in the northern part of the belt, and from the past-producing Manibridge mine area in the south. An underground tour is being planned for the Thompson mine, which has been in continuous production since 1961. The field trip will depart from Winnipeg on the morning of May 16th and finish in Brandon on the evening of May 19th.

Syn-Conference Field Trip

A lunch and field trip sponsored by Cypher Environmental will discuss "*Better mine haul roads using environmentally responsible techonology*". Following a lunch and learn session at Brandon University, Todd Burns will lead an afternoon excursion to visit a haulage road in the Brandon area that is stabilized using clay-rich soil blended with organic catalysts and ordinary aggregate (Fig. 2). The electronic bonding of clay minerals combined with basic construction protocols results in roads that require very little maintenance and provide numerous environmental

Figure 1. Headframe and outcrops of Archean gneiss overlooking the past-producing Pipe II open pit mine near Thompson, Manitoba. Photo: C. Couëslan.

Geoscience Canada, v. 50, https://doi.org/10.12789/geocanj.2023.50.205 pages 313–315

Figure 2. Curries Landing haul road near Brandon, Manitoba after stabilization using clay-rich soil and organic catalysts. Photo: Cypher Environmental.

benefits including reduced dust production. This event will take place during the conference proceedings.

Post-Conference Field Trips

Attached to the 10th International Symposium on Granitic Pegmatites is an excursion visiting "*Pegmatites of the Cat Lake–Winnipeg River (MB) and Separation Rapids (ON) Pegmatite Fields*" that will be led by several field trip leaders from provincial surveys, academia, and industry. This four day field trip will explore the regional setting, emplacement controls, and mineralogy of lithium pegmatites in outcrops of the Cat Lake–Winnipeg River and Separation Rapids pegmatite fields of Manitoba and northwestern Ontario. Site visits are planned for the Eagle, FD no. 5, Big Mack, and Big Whopper pegmatites. In addition, a visit to the world-class Tanco pegmatite will include a tour of the spodumene mill and underground workings, and examination of drillcore (Fig. 3). A paragenetic sample suite of the Tanco pegmatite, collected by Petr Černý, will be viewed at the University of Manitoba. This field excursion will be a round trip that starts in Winnipeg on the morning of May 23rd and ends in Winnipeg the evening of May 26th.

A joint, one and a half day field trip by the Canadian Sedimentological Research Group, Paleontological Division of the GAC, and the Canadian Society of Vertebrate Paleontology investigating "*Life in the Western Interior Seaway: A field trip to the Cretaceous escarpment in Morden, Manitoba*", will be led by Ricardo Silva, Kirstin Brink, and Adolfo Cuetara. The excursion will focus on the globally significant sedimentary successions of the Upper Cretaceous in the Morden-Miami area of Southern Manitoba. In addition to discussion-filled stops exploring the Cretaceous formations, there will also be a visit and dining experience at the Canadian Fossil Discovery Center where examples of Campanian fossils including plesiosaurs, giant turtles, toothless sharks, flightless birds, plants, and 'Bruce' the mosasaur are on display (Fig. 4). Bruce, a *Tylosaurus Pembinesis* mosasaur, was found in 1974 and holds the Guinness World Record as the largest publicly displayed mosasaur. Along the way, participants will learn about the local indigenous and settler history of the area and take a brief look at Pleistocene–Holocene shoreline and lake deposits of Lake Agassiz. The trip will depart from Brandon on the afternoon of May 22nd and finish in Winnipeg the evening of the 23rd.

Figure 3. Underground mining operations at the Tanco Li-Cs-Ta mine, southeastern Manitoba. Photo: T. Martins.

Kyle Reid will lead participants on a four day exploration of the "*Volcanic stratigraphy, hydrothermal alteration and metamorphism associated with VMS deposits in the Flin Flon–Snow Lake mining camp*". The Flon Flon greenstone belt is one of the largest Paleoproterozoic volcanogenic massive sulphide (VMS) districts in the world. The excursion will begin by examining the stratigraphy of the Flin Flon arc assemblage, where the relatively low metamorphic grade has preserved volcanic textures and structures in rocks spatially associated with the Flin Flon ore bodies (Fig. 5). This will be followed by a day focussing on the volcanic stratigraphy of the Snow Lake arc assemblage and the syn-volcanic hydrothermal alteration systems that developed in association with the Chisel–Lalor VMS deposits, which were affected by middle amphibolite-facies metamorphic conditions during the ca 1.8 Ga Trans-Hudson orogeny. This excursion will depart from Brandon on the morning of May 23rd and end in Winnipeg the evening of May 26th.

A one day "*Field trip to PADCOM's potash mine and Gambler First Nation*" is jointly sponsored by the Manitoba Prospectors and Developers Association, Gambler First Nation, and the Potash and Agri Development Corporation of Manitoba (PADCOM). The excursion will be led by Michelle Nicolas and MaryAnn Mihychuk and will begin with a visit to Gambler First Nation, approximately 130 km northwest of Brandon. A

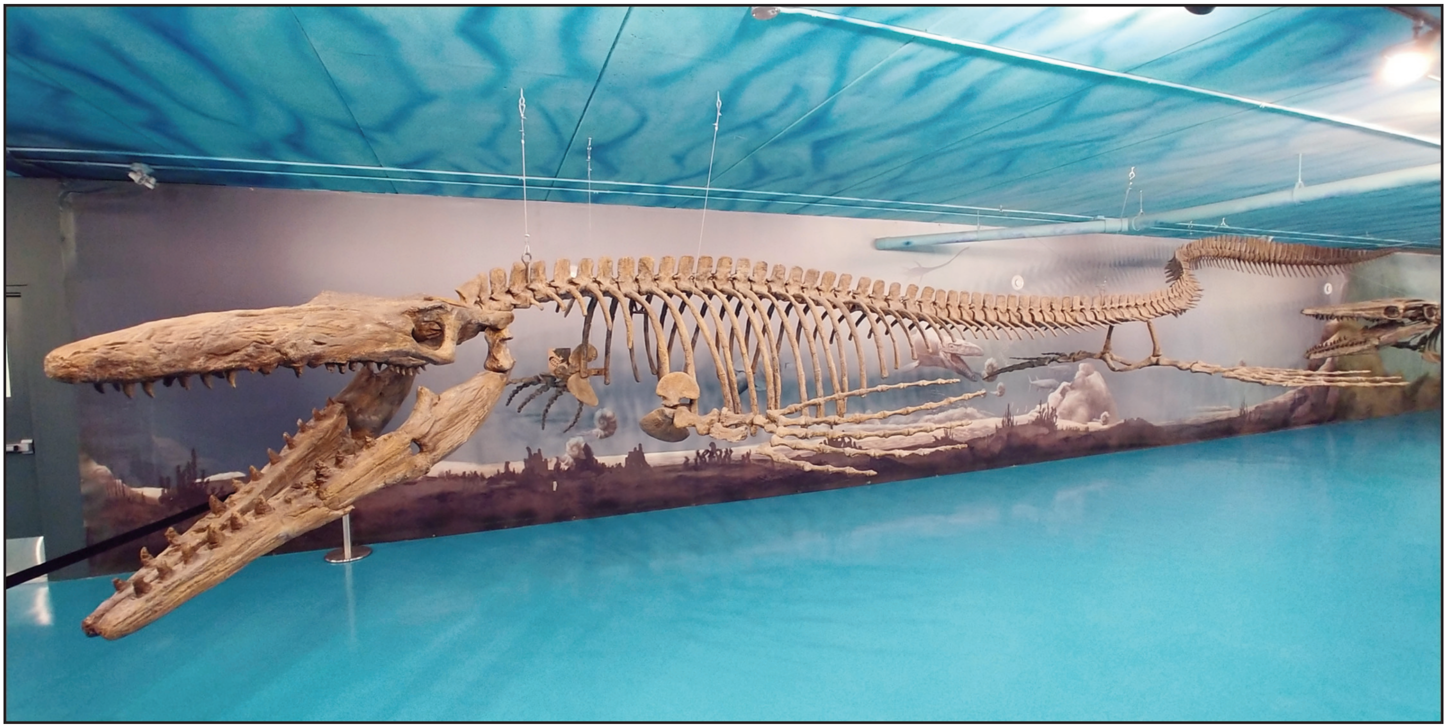

Figure 4. The Canadian Fossil Discovery Centre in Morden, Manitoba, is home to many marine fossils of the Upper Cretaceous including 'Bruce' the mosasaur. Photo: Canadian Fossil Discovery Centre.

Figure 5. Pillowed basalt of the Flin Flon arc assemblage near Flin Flon, Manitoba. Photo: C. Couëslan.

brief history of the First Nation will be followed by an outline of their businesses and relationship/partnership with PADCOM. A feast will be provided by Gambler First Nation before the trip continues to the first, and so far only, potash mine in Manitoba. The mine tour will focus on the polythermic selective solution process used by the operator, PADCOM, and will include a discussion of their partnership and revenue sharing agreements with Gambler First Nation. The field excursion will be a round trip out of Brandon on May 23rd.

We hope that there is something that appeals to everyone in the field trip listing for the 2024 GAC-MAC-PEG joint annual meeting! For full details on the technical program, travel, and accommodation information, please visit: *event.fourwaves.com/gacmac2024/*.

BRANDON UNIVERSITY
DEPARTMENT OF GEOLOGY

AND

NMMA
NORTHERN MANITOBA MINING ACADEMY

INVITE YOU TO THE

GAC-MAC ANNUAL MEETING

AND

THE 10TH SYMPOSIUM ON GRANITIC PEGMATITES

Please join us for a full program of
- scientific presentations
- workshops and short courses
- field trips
- special events.

Brandon University, May 19-22 2024 - see you there!

GEOSCIENCE CANADA

JOURNAL OF THE GEOLOGICAL ASSOCIATION OF CANADA
JOURNAL DE L'ASSOCIATION GÉOLOGIQUE DU CANADA

2023 VOLUME 50 GSCNA7 50 239-316
PRINT EDITION ISSN 0315-0941
ONLINE EDITION ISSN 1911-4850